Characterisation of human co-culture systems for applications in bone tissue engineering

Dissertation zur Erlangung des Grades
„Doktor der Naturwissenschaften“

am Fachbereich Biologie
der Johannes Gutenberg-Universität

Renate Magdalene Ostertag
geborene Rehlich am 09. September 1982
in Bielefeld

September 10, 2013

Dekan:

1. Berichterstatter:

2. Berichterstatter:

Tag der mündlichen Prüfung: 06.09.2013

Für meine Familie

Luck is where preparation meets opportunity.

Randy Pausch

Contents

Abbreviations

Introduction
1.1. Preface . . . 2
1.2. Bone - A skeletal organ . . . 2
1.2.1. Function, properties and structure . . . 3
1.2.2. Formation and degradation . . . 5
1.2.3. Bone tissue engineering . . . 7
1.3. Blood vessels - Growth in development and disease . . . 9
1.3.1. Function, physiology and structure . . . 9
1.3.2. Formation of blood vessels . . . 11
1.3.3. Regulation of angiogenesis . . . 12
1.3.4. Co-culture systems . . . 15
1.4. Aim of this study . . . 18

Material and Methods
2.1. Materials . . . 21
2.1.1. Instruments and microscopes . . . 21
2.1.2. Consumables . . . 22
2.1.3. Chemicals . . . 22
2.1.4. Buffers . . . 24
2.1.5. Solutions and cell culture media . . . 25
2.1.6. Enzymes . . . 26
2.1.7. Antibodies . . . 26
2.1.8. Oligonucleotides . . . 27
2.1.9. Kit systems . . . 27
2.1.10. Primary cells and cell lines . . . 28
2.1.11. Software . . . 28
2.2. Methods . . . 29
2.2.1. Isolation of primary human endothelial cells . . . 29
2.2.1.1. Isolation of HUVEC . . . 29
2.2.1.2. Isolation of HDMEC . . . 29
2.2.1.3. Isolation of HPMEC . . . 31
2.2.1.4. Isolation of OEC . . . 31
2.2.1.5. Isolation of pOB . . . 32
2.2.2. Cell culture . . . 32
2.2.2.1. Coating of cell culture surfaces . . . 33
2.2.2.2. Cell passage and cell seeding . . . 33
2.2.2.3. Cryoconservation and thawing of cells . . . 34
2.2.2.4. Cell number quantification . . . 34
2.2.2.5. Transfection of SaOS-2 . . . 34
2.2.2.6. Cell treatment with growth factors . . . 35
2.2.2.7. 2-D co-cultures on cell culture plastic . . . 35

2.2.2.8. 2-D co-cultures with flexiPERM chamber . . . 35
2.2.2.9. 3-D culture in collagen type I gel matrix . . . 36
2.2.2.10. 3-D culture in fibrin gel matrix . . . 36
2.2.3. Cytotoxicity assays . . . 37
2.2.3.1. Calcein-AM cell viability assay . . . 37
2.2.3.2. Viability test with WST-1 . . . 37
2.2.4. Protein biochemical methods . . . 38
2.2.4.1. ELISA . . . 38
2.2.4.2. EIA . . . 39
2.2.4.3. Immunofluorescent staining of cell components . . . 39
2.2.4.4. Antibody array human angiogenesis . . . 40
2.2.4.5. Protein quantification by BCA assay . . . 40
2.2.4.6. DNA quantification in cell lysates . . . 41
2.2.4.7. Quantification of ALP activity . . . 41
2.2.4.8. Quantification of mineralisation with alizarin red . . . 42
2.2.4.9. Quantification of Collagen . . . 42
2.2.4.10. Quantification of Calcium . . . 42
2.2.4.11. FACS . . . 43
2.2.4.12. SDS-PAGE . . . 43
2.2.4.13. Western blot . . . 44
2.2.4.14. TCA precipitation of proteins . . . 45
2.2.4.15. Albumin depletion from cell culture medium . . . 45
2.2.4.16. Mass spectroscopy . . . 46
2.2.5. Molecular genetic techniques . . . 47
2.2.5.1. Isolation and quantification of DNA . . . 47
2.2.5.2. Isolation and quantification of RNA . . . 48
2.2.5.3. cDNA-synthesis via RT-PCR . . . 48
2.2.5.4. Polymerase chain reaction . . . 49
2.2.5.5. Cloning of podoplanin into pEGFP-N1 vector . . . 50
2.2.5.6. Cell characterisation by PCR . . . 51
2.2.5.7. Quantitative real-time polymerase chain reaction . . . 51
2.2.6. Statistical analysis . . . 52

Results

3.1. Characterisation of human osteoblasts . . . 54
3.1.1. Human primary osteoblasts . . . 54
3.1.1.1. pOB growth and morphology . . . 54
3.1.1.2. Osteogenic differentiation and matrix mineralisation . . . 55
3.1.2. Human osteosarcoma cell lines . . . 56
3.1.2.1. MG-63 . . . 57
3.1.2.2. Cal-72 . . . 57
3.1.2.3. SaOS-2 . . . 58
3.1.3. Effects of media on osteoblast growth and differentiation . . . 58
3.1.4. Comparison of osteosarcoma cell lines expressing GFP . . . 62
3.2. Characterisation of endothelial cells . . . 65
3.2.1. HDMEC . . . 65
3.2.2. HUVEC . . . 66
3.2.3. Umbilical artery endothelial cells . . . 66
3.2.4. Lymphatic and vascular populations of endothelial cells . . . 66
3.3. Angiogenesis-inducing potential of osteoblasts in co-culture with EC . . . 68

3.3.1. Angiogenesis in 2-dimensional co-cultures . . . 68
3.3.2. 3-D co-cultures of endothelial cells and osteoblasts . . . 71
3.3.3. Angiogenic effects of osteoblast cell culture medium supernatants . 72
3.3.4. Transcriptional analysis of angiogenesis-related factors in osteosarcoma cell lines . . . 78
3.3.5. Effects of bFGF on angiogenesis . . . 80
3.3.6. Release of HGF and VEGF in osteosarcoma cell lines . . . 82
3.3.7. Correlation between HGF and endostatin . . . 84
3.3.8. Effects of podoplanin on angiogenic potential of osteoblasts . . . 84
3.3.8.1. Cloning and transfection of SaOS-2 cells with podoplanin 85
3.3.8.2. Podoplanin expressing SaOS-2 cells . . . 87
3.4. Mass spectroscopy on used media supernatants . . . 89
3.4.1. Gel-electrophoretic separation of cell culture supernatants . . . 89
3.4.2. Mass spectroscopy . . . 90

Discussion
4.1. Characterisation of co-culture components . . . 92
4.1.1. Human primary osteoblast characterisation . . . 93
4.1.2. Osteosarcoma cell line characterisation . . . 95
4.1.3. Comparison of osteoblast cell lines expressing GFP . . . 100
4.1.4. Primary human endothelial cells . . . 103
4.2. Angiogenesis in co-culture systems . . . 104
4.2.1. Comparison of angiogenic effects in co-culture systems . . . 105
4.2.2. Angiogenic potential of osteoblast cell culture supernatants . . . 106
4.2.3. Angiogenic effects of lymphatic and vascular populations . . . 107
4.3. Screening for angiogenesis-inducing factors . . . 109
4.3.1. Translational analysis . . . 110
4.3.2. Transcriptional analysis . . . 111

Summary

Zusammenfassung

Appendix
A.1. FACS analysis . . . II
A.2. Effects of osteoblast cell culture medium supernatants on angiogenesis . . . V
A.3. Effects of medium supernatants with basic fibroblast growth factor (bFGF) on angiogenesis . . . X
A.4. Transcriptional analysis of angiogenesis-related factors . . . XI
A.5. Mass spectroscopic analysis . . . XIII

References

List of Figures

List of Tables

Abbreviations

All units derivate, if not aberrant marked, from SI base units (ISO/IEC 80000-1). Unit prefixes like m, µ, n, p or f represent milli, micro, nano, pico or femto and serve accordingly to DIN1301 to generate parts from the dimension unit. Chemical elements are not listed here. Numerical indices in elemental formula indicate the molar ratio.

ALP	alkaline phosphatase
ANG	angiopoietin
ANGPTL3	angiopoietin-like 3
ANOVA	analysis of variance
APC	allophycocyanin
APS	ammonium persulfate
ATCC	American Type Culture Collection, Rockville, USA
BCA	bicinchoninic acid
bFGF	basic fibroblast growth factor
β-ME	β-mercaptoethanol
BSA	bovine serum albumin
°C	degree Celsius
CD	cluster of differentiation
CDH5	cadherin 5
cDNA	complementary deoxyribonucleic acid
CDS	coding DNA sequence
CM	collagen matrix
CMV	cytomegalovirus
COL18A1	collagen alpha-1(XVIII) chain
Ct	cycle threshold
CXCL6	chemokine (C-X-C motif) ligand 6
CXCL10	C-X-C motif chemokine 10
D	dimension
Da	dalton
DAPI	4',6-diamidino-2-phenylindole
DMSO	dimethyl sulfoxide
DMEM	Dulbecco's modified eagle medium
DNA	desoxyribonucleic acid
dNTP	desoxyribonukleosidtriphosphate
DTT	dithiothreitol
EC	endothelial cells
ECBM	endothelial cell basal medium
ECGM	endothelial cell growth medium
ECGS	endothelial cell growth supplement

ECL	enhanced chemiluminescence
EDTA	ethylenediaminetetraacetic acid
EGTA	ethylene glycol tetraacetic acid
EIA	enzyme immunoassay
ELISA	enzyme-linked immunosorbent assay
EREG	epiregulin
F-12	nutrient mixture F-12
FACS	fluorescence-activated cell sorting
FCS	fetal calf serum
FD	fold difference
FGF	fibroblast growth factor
FITC	fluorescein isothiocyanate
Flt	fms-related tyrosine kinase
GFP	green fluorescent protein
GSH	glutathion
h	hours
HA	hydroxyapatite
HCAEC	human coronary arterial endothelial cells
HCMEC	human cardiac microvascular endothelial cells
HDMEC	primary human dermal microvascular endothelial cells
HEPES	4-(2-hydroxyethyl)-1-piperazineethanesulfonic acid
HGF	hepatocyte growth factor
HPMEC	primary human pulmonary microvascular endothelial cells
HPSE	heparanase
HRP	horseradish peroxidase
HUVEC	primary human umbilical vein endothelial cells
ICAM-1	intercellular adhesion molecule 1
IGF-1	insulin-like growth factor 1
IGF-2	insulin-like growth factor 2
IL6	interleukin-6
IL8	interleukin-8
IL17	interleukin-17
JAG1	jagged 1
kb	kilobase
KDR	kinase insert domain receptor
LB	lysogeny broth
LEP	leptin
LPS	lipopolysaccharide
M	molar concentration defined as $mol \cdot l^{-1}$
MALDI	Matrix-assisted laser desorption/ionization
MCS	multiple cloning site
MDK	midkine
MetOH	methanol
min	minutes
MEE	monoethyl ester
OD	optical density
OEC	outgrowth endothelial cells
o-PD	o-Phenylenediamine dihydrochloride
PBS	phosphate-buffered saline

PCR	polymerase chain reaction
PDGF	platelet-derived growth factor
PEG	polyethylene glycol
PE	phycoerythrin
PECAM	platelet endothelial cell adhesion molecule
P/S	penicillin/streptomycin
PFA	paraformaldehyde
PlGF	placental growth factor
PIPES	piperazine-N,N-bis(2-ethanesulfonic acid)
pNPP	para-nitrophenylphosphate
pNP	para-nitrophenol
PMSF	phenylmethanesulfonylfluoride
pOB	primary osteoblasts
qPCR	quantitative real-time polymerase chain reaction
RNA	ribonucleic acids
RIPA	radioimmunoprecipitation assay
rpm	rounds per minute
RT-PCR	reverse transcription polymerase chain reaction
sdH_2O	sterile distilled water
s	seconds
SDS	sodium dodecyl sulfate
SD	standard deviation
SDS-PAGE	sodium dodecyl sulfate polyacrylamide gel electrophoresis
TBE	tris-borate-EDTA
TCA	trichloroacetic acid
TE	tris-EDTA
TEK	angiopoietin-1 receptor
TEM	transmission electron microscopy
TEMED	tetramethylethylenediamine
TFPI	tissue factor pathway inhibitor
TGF-α	transforming growth factor alpha
TGF-β	transforming growth factor beta
THBS1	thrombospondin 1
TIMP	TIMP metallopeptidase inhibitor
TNF	tumour necrosis factor
TOF	time of flight
Tris	tris(hydroxymethyl)aminomethane
UV	ultra violet
VEGF	vascular endothelial growth factor
VEGFR	vascular endothelial growth factor receptor
vol.-%	percent of volume
vWF	von Willebrand factor
WST-1	2-(4-Iodophenyl)-3-(4-nitrophenyl)-5-(2,4-disulfophenyl)-2H-tetrazolium
***x*g**	gravitation defined as $m \cdot s^{-2}$

Introduction

1.1. Preface . . . 2
1.2. Bone - A skeletal organ . . . 2
1.2.1. Function, properties and structure . . . 3
1.2.2. Formation and degradation . . . 5
1.2.3. Bone tissue engineering . . . 7
1.3. Blood vessels - Growth in development and disease . . . 9
1.3.1. Function, physiology and structure . . . 9
1.3.2. Formation of blood vessels . . . 11
1.3.3. Regulation of angiogenesis . . . 12
1.3.4. Co-culture systems . . . 15
1.4. Aim of this study . . . 18

1.1 Preface

For successful integration of bone tissue engineering constructs into patients, adequate supply of oxygen and nutrients is critical. Due to the important role of angiogenesis in bone formation, remodelling and regeneration, vascularisation of bone tissue engineering constructs has been a key research focus during the last decade. Several approaches have been proposed using host vasculature as a mechanism to vascularise engineered implants. Previous strategies have included the use of endothelial cells, osteoblasts, co-culture systems and additional treatment of the engineered constructs with growth factors or morphogens.

The current study focuses on angiogenesis in the context of bone tissue engineering using co-culture systems of human endothelial cells and primary osteoblasts as well as osteosarcoma cell lines. Co-culture models offer further insight into the underlying mechanisms of bone vascularisaton and could also help to identify factors that stimulate angiogenesis and promote the vascularisation process in therapeutic approaches. In the following sections general background of fundamentals in bone tissue engineering, bone formation and blood vessel formation, current co-culture approaches and vascularisation strategies will be provided with an emphasis on potential applications in bone tissue engineering.

1.2 Bone - A skeletal organ

For the repair and regeneration of bone defects by bone tissue engineering, a basic understanding of the constitution of bone is needed. A typical bone is part of the human endoskeleton and is built around a matrix containing inorganic and organic compounds. The inorganic component makes up approximately two-thirds of the bone matrix and consists primarily of hydroxyapatite (HA) (calcium hydroxyphosphate) and calcium carbonate (Biltz and Pellegrino, 1977; Detsch et al., 2008). The organic bone matrix is predominantly composed of type I collagen fibres but also has ground

substance containing protein belonging to several different protein families, incuding proteoglycans and glycoproteins. Proteins in bone matrix undergo extensive posttranslational modifications (for example phosphorylation or sulfation) (Robey et al., 1993). Only two per cent of the total bone mass is composed of cells (Martini et al., 2011).

The combination of inorganic and organic compounds gives the bone remarkable properties. Bone is hard and lightweight with significant elasticity, giving it a number of mechanical and metabolic functions. In isolation, calcium salts are hard but rather fragile, while collagen fibres are stronger but in contrast relatively flexible (Viguet-Carrin et al., 2006). Their combination in bone, with minerals surrounding the collagen fibres, results in a strong, somewhat flexible organ that is highly resistant to fractures (Viguet-Carrin et al., 2006). These properties mean, that bone can compete with the best steel-reinforced concrete. In essence, the collagen fibres in bone act like the steel reinforcing rods, and the mineralised matrix acts like concrete (Martini et al., 2011). However, in some musculoskeletal conditions (including maxillofacial syndrome, orthopaedic trauma, osteoporosis and bone cancer) therapies are required using tissue engineering constructs for implantation that mimic bone properties and are linked to the host vasculature.

1.2.1 Function, properties and structure

The skeletal system is comprised of skeletal bone as well as cartilage, ligaments, and other connective tissues that stabilise and interconnect the bones. The major functions of the skeletal system are given in Table 1.1.

Table 1.1: Primary functions of the skeletal system (Martini et al., 2011; Klinke et al., 2009)

Function	Description
Mechanical support and protection	The skeletal system provides mechanical support and protection for internal organs in the body. Joints, muscles and tendons determine movement capabilities.
Metabolic depot and organ	Bone marrow is involved in haematopoiesis. Bones store minerals, fat, growth factors and hormones, and have a role in phosphate metabolism.

Two types of bone can be distinguished: *compact bone*, also called *cortical bone*, which is relatively solid and dense, and *cancellous* or *trabecular bone* that consists of an open network of osseous tissue. Depending on the location and skeletal requirements, compact or cancellous bone tissue predominates within a single bone (for example the femur, a typical long bone with an extended tubular shaft dominated by compact bone tissue). Cancellous bone is more active in terms of growth, calcium homeostasis and haematopoiesis, whilst compact bone is known to be more static having a greater role in providing mechanical strength (Yaszemski et al., 1996). As well as containing calcified intercellular material, the bone matrix contains bone cells, so-called osteocytes, within lacunae. The lacunae are typically organised around blood vessels that penetrate the bony matrix (Martini et al., 2011).

A major compound of this three dimensional internal network is mineralised osseous tissue, which gives bone its rigidity. Additional tissue types in bone, such as marrow, nervous tissue, blood vessels and endosteum, fulfill other needs both at a local level for the single bone and on a wider scale for the body as a whole, like haematopoiesis, blood transport and bone maintenance. Formed bone tissue is a relatively hard yet lightweight material. The midshaft of a typical human femur has an estimated longitudinal tensile strength of 133.0 MPa (Reilly and Burstein, 1975), which is comparable to cast iron (ASTM A-48 G1800). Longitudinal compressive strength has been demonstrated to be 193.0 MPa the magnitude of which is even more evident when it is transformed to 19 300 $^{N}/_{cm^2}$. In contrast, the longitudinal shear strength of a human femoral midshaft resists only 51.6 MPa (Turner et al., 2001). Thus a typical bone resists higher compressive forces, than torsional or pulling forces. This significant degree of elasticity is due to the presence and organisation of collagen fibres in bone.

For a better understanding of the properties of bone, a closer look at the structure and cell-mediated bone formation is needed. A profile of a long bone as an example of a typical bone is given in Figure 1.1. In order to provide the technical properties mentioned above, an extensive vasculature is required to supply the incorporated cells, which in turn

allow for growth and maintenance of the bone. Bone is externally covered by periosteum, a dense connective tissue, which generates new bone material thus playing a key role in bone growth and repair. Bone tissue is highly vascularised, even the so called, compact bone tissue (Figure 1.1B). Organisation of osteons and lamellae in compact bone forms distinct complexes, which are well regulated. The orientation of collagen fibres in adjacent lamellae of each osteon forms a series of nested cylinders around a central canal (Figure 1.1C) (Martini et al., 2011).

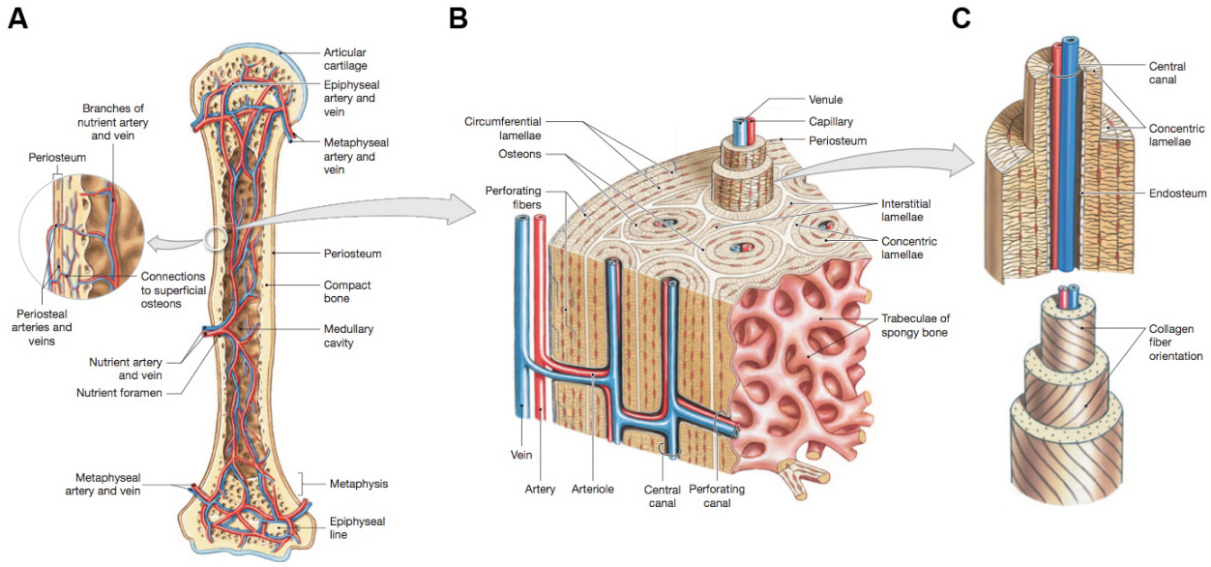

Figure 1.1: **Structure and blood supply of a mature long bone (Martini et al., 2011)** **A** Longitudinal profile included blood supply of a mature bone. **B** Organisation of osteons and different lamellae in compact bone. **C** Orientation of collagen fibres in adjacent lamellae, which are responsible for bone characteristics.

1.2.2 Formation and degradation

Bone formation involves a series of complex and highly regulated events, like mineralisation of extracellular matrix proteins, and is tightly orchestrated by cells which specifically maintain the integrity of the bone (LeGeros, 2002). The formation of new bone directly from mesenchymal tissue occurs during embryogenesis and is known as intramembranous bone formation (Campbell and Kaplan, 1992). It begins with differentiation of

osteoprogenitor cells into an osteoblast lineage. Ossification requires adequate vascularisation to form cancellous bone. When bone density is sufficient, the cancellous bone is remodelled, which involves both bone resorption by osteoclasts and bone formation by osteoblasts until the optimal structure is achieved. For the formation of long bone ossification occurs by endochondral bone formation and in fracture repair also by intramembranous ossification. Undifferentiated mesenchymal cells condense and differentiate into rapidly proliferating chondrocytes (Chung et al., 2004), and when the cartilage framework becomes ossified the chondrocytes stop proliferating and become hypertrophic. The hypertrophic chondrocytes finally undergo apoptosis. Osteoblasts surround the mineralised cartilage matrix to form a bone collar, the precursor of cortical bone, which then is invaded by vasculature carrying osteoblasts and cartilage-degrading chondroclasts. Cancellous bone is then formed from primary spongiosa.

Bone tissue is under a continuous process of remodelling (Cohen, 2006) by osteogenesis and osteolysis, which are in turn mediated by osteoprogenitor cells, osteoblasts, osteocytes and osteoclasts (Figure 1.2). Many growth factors such as transforming growth factor alpha (TGF-α), transforming growth factor beta (TGF-β) and fibroblast growth factor (FGF) are abundant in bone tissue and involved in these processes (Zambonin et al., 2000; Mackie et al., 1998).

The osteoprogenitor cells are involved in growth and repair of bones (Figure 1.2A). These cells mature to (pre)osteoblasts under the influence of calcitriol, glucocorticoids, prostaglandins and growth factors like TGF-α and FGF (Widdermann, 2004; Dodds et al., 1994; Mundy et al., 1995; Tsai et al., 2000; Ibbotson et al., 1986). Osteoblasts are mononuclear cells involved in bone matrix formation (Figure 1.2B). These cells produce osteoid, a type I collagen matrix. After type I collagen, osteocalcin is the most abundant secreted protein in bone (Carpenter et al., 1998; Puchacz et al., 1989). It can bind hydroxyapatite as well as calcium and is a marker for osteogenic maturation (Nakamura et al., 2009). However, this marker is not osteoblast-specific as it is also expressed in fibroblasts (Newberry et al., 1996).

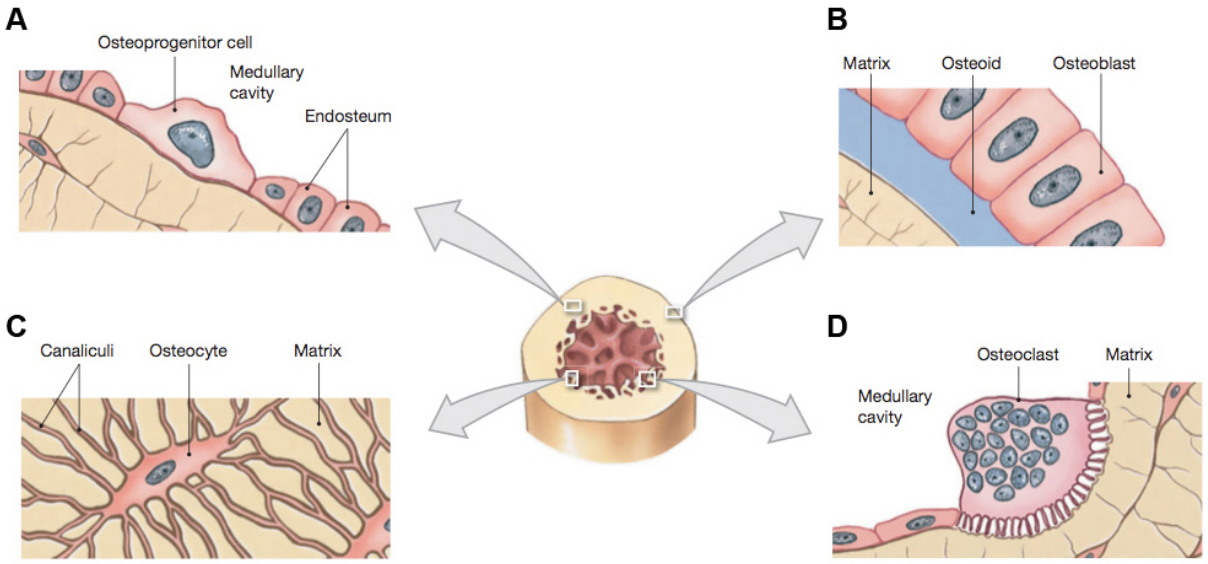

Figure 1.2: **Types of bone cells (Martini et al., 2011)**
A Osteoprogenitor cells are stem cells that maturate to osteoblasts. **B** Osteoblasts are involved in the formation of organic matrix. **C** Osteocytes are mature bone cells that maintain the bone matrix. **D** Osteoclasts secrete acids and enzymes to dissolve bone matrix.

When osteoblasts are embedded in their secreted matrix, they become osteocytes, inactive osteoblasts, or bone-lining cells or they undergo programmed cell death (Dallas and Bonewald, 2010). The osteocytes are derived from osteoblasts and do not divide during their entire lifetime of 50 years (Knothe Tate et al., 2004). Osteocytes are active in spaces called lacunae and canaliculi and function to maintain the bone matrix (Figure 1.2C). Osteoclasts are derived from haematopoietic origin and constitute the main class of cells that are able to resorb bone (Walker, 1973) (Figure 1.2D). Osteoclasts are derived from myeloid progenitors through a progression that involves the fusion of mononuclear precursor cells under the influence of cytokine receptor activator of NF-κB ligand (RANKL) (Jacome-Galarza et al., 2011). Osteocalcin is involved in osteoclast differentiation (Glowacki et al., 1991).

1.2.3 Bone tissue engineering

The repair and regeneration of large bone defects caused by trauma and disease is an important topic in regenerative medicine. Current standard treatment is either the

transplantation of natural bone tissue from the patient (autograft) (Brown and Cruess, 1982; Laurencin et al., 1999) or the transplantation of tissue from a different individual to the patient (allograft) (Burg et al., 2000). However, the use of autografts is restricted because of donor shortages and complications including infection, pain and donor morbidity (Gitelis and Saiz, 2002) while the application of allografts has its own set of limitations, for instance it carries a high risk of immune rejection.

A potential alternative to natural bone transplantation is being studied in the field of bone tissue engineering, which focusses on the development of biological substitutes for bone fragments that restore function to a bone defect using the natural healing response of the body. Cells, signalling molecules or growth factors, and scaffolds made from either natural materials or synthetic polymers are used to generate a construct, with the aim of implanting it in the patient (Albert et al., 2006; Rueger et al., 1998; Schieker et al., 2004). However, since bone tissue is a highly vascularised and dynamic system with a complex construction (Caplan and Goldberg, 1999), the vascularisation of engineered constructs with the host vasculature is necessary for successful and optimal scaffold integration into the patient. The supply of the engineered cell-containing constructs with nutrients and oxygen by diffusion is limited to 100–200 µm around a capillary. Thus, establishing a functional vascular network in the engineered constructs is the major challenge in the field of bone tissue engineering and regenerative medicine.

Several different strategies for vascularisation of engineered bone tissue constructs have been developed in the last decade. Some aim to improve the scaffold architecture (Lovett et al., 2009; Santos et al., 2008), whereas others target the delivery of angiogenesis-inducing growth factors (Geiger et al., 2005; Gu et al., 2004; Zisch et al., 2003). It has been shown that vascularisation is enhanced by prevascularisation of scaffolds using different cell types and co-culture systems (Rivron et al., 2008; Rouwkema et al., 2006; Kaigler et al., 2003). For example, the use of endothelial cells in co-culture with osteoblasts is a promising strategy to establish a functional vascular network in tissue engineering constructs (Kaigler et al., 2003; Fuchs et al., 2007).

1.3 Blood vessels - Growth in development and disease

Blood vessels are part of the circulating blood transport system that supplies tissues and organs with nutrients and oxygen, eliminates waste and provides immune cells with broad access to sites of endogenous and exogenous perturbations (Tsaryk et al., 2012). The vascular system is generated early during embryonic development and also pervades bone tissue (Starr and McMillan, 2011) as well as nervous and cartilaginous tissues.

1.3.1 Function, physiology and structure

Blood vessels are versatile and multifunctional, having many metabolic properties (Figure 1.3). Besides blood flow, these include regulation of platelet adherence, modulation of vascular tone and regulation of immune and inflammatory responses (Sumpio et al., 2002).

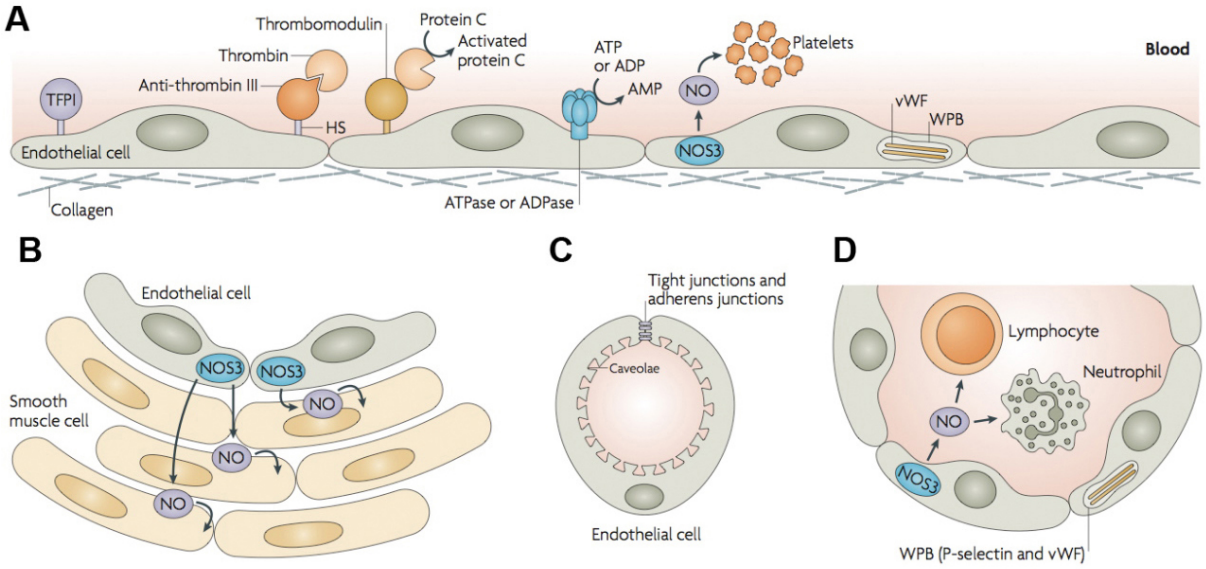

Figure 1.3: **Functions of resting endothelial cells (Pober and Sessa, 2007)**
A Endothelial cells inhibit coagulation of the blood by binding and displaying tissue factor pathway inhibitor (TFPI) which blocks the actions of the factor-VIIa–tissue-factor complex. **B** Arterial endothelial cells have a major role in regulating blood flow by controlling the tone of smooth muscle cells in the medial vessel wall layer. **C** Capillary endothelial cells are the principal regulators of trans-endothelial extravasation of plasma proteins. They form intercellular junctions, closing off the paracellular pathway between the cells. The extent of this barrier varies among different tissues. **D** Venular endothelial cells form the principal site of leukocyte trafficking from the blood into the tissues. Efficient recruitment of leukocytes requires activation of endothelial cells.

Blood is transported in the vessel lumen, which is lined by endothelial cells. The primary essential function of the endothelium is to maintain vessel wall partial permeability whilst sealing the circulatory system (Cines et al., 1998). Additionally, the blood vessels may be lined with pericytes and smooth muscle cells, which stabilise the vessels and can suppress proliferation of endothelial cells as well as promote their survival (Tsaryk et al., 2012). In total around $1 \cdot 10^{13}$ vascular endothelial cells contribute to this 1 kg organ.

The developmental pathway of endothelial cells is still being discussed (Choi et al., 1998), but it is agreed that they derive from blast-like bipotential cells, called hemangioblasts. It is well known, that there is strong phenotypic variation between endothelial cells in different parts of the vascular tree. Furthermore, there are variations in the responses generated by endothelial cells to the same stimulus (Sumpio et al., 2002). Cell responses to stimuli can vary significantly between the individual donors, even when the cells were obtained from the same part of the vasculature.

Endothelial cells in the lymphatic system differ from blood vessel derived endothelial cells in a number of ways. Some markers (such as platelet endothelial cell adhesion molecule (PECAM)-1 or cluster of differentiation (CD)34) are present in all endothelial cells, whereas others are more specific, for example vascular endothelial growth factor receptor (VEGFR)-3 (fms-related tyrosine kinase (Flt)-4) is primarily expressed in lymphatic endothelial cells (Ruoslahti and Rajotte, 2000). Podoplanin is also reported to be a specific marker for lymphatic endothelium (Breiteneder-Geleff et al., 1999). As mentioned previously, bone tissue is highly vascularised with two different types of vessels. Periosteal blood vessels are integrated within growing bone tissue close to the bone surface. In secondary ossification vessels sprout into the epiphysis. As well as this vessel network, a secondary lymphatic network can be found in the periosteum to support a large number of osteons (Martini et al., 2011).

1.3.2 Formation of blood vessels

The process of postnatal formation of blood vessels from existing vessels is called angiogenesis. In contrast, vasculogenesis describes the formation of new blood vessels from angioblasts during embryogenesis (Risau, 1997). Both processes seem to be coupled and act together during blood vessel formation (Hristov et al., 2007). Angiogenesis naturally occurs in growth and development, the menstrual cycle and in wound healing. It also plays an important role in several pathologies, including cancer, rheumatoid arthritis, eye diseases, obesity, asthma, diabetes, multiple sclerosis, endometriosis, bacterial infection, autoimmune disease, stroke and ulcers (Carmeliet, 2005). Furthermore, angiogenesis is essential in bone formation, remodelling and regeneration.

Vasculogenesis, which occurs during embryonic development, begins with the differentiation of angioblasts from mesoderm and the formation of a primitive blood vessel plexus (Risau and Flamme, 1995). Further differentiation of angioblasts into endothelial cells leads to aggregates, known as blood islands, which form a lumen and subsequently a primary capillary plexus by fusion with each other (Risau and Flamme, 1995). Vasculogenesis is directly followed by angiogenesis.

Angiogenesis begins in the endothelium of postcapillary venules and forms new vascular networks by capillary sprouting (Klinke et al., 2009; Carmeliet, 2000a). In response to an angiogenic stimulus, pericytes detach from blood vessels and degrade the vessel membrane. Growth factors induce detachment of endothelial cells from the extracellular matrix and promote new vessel formation primarily coordinated by tip-cells. Subsequently, neighbouring cells (stalk cells) proliferate and contribute to the formation of the vessel lumen. This crosstalk between tip and stalk cells is mediated by the Notch signalling pathway (Blanco and Gerhardt, 2013). The endothelial cells return to a quiescent state once the new vessel connects with an existing vessel. Finally, pericytes are recruited and new basal membrane is formed (Carmeliet and Jain, 2011).

Understanding the process of blood vessel formation is essential for developing our knowledge and therapeutic options for several diseases (Unger et al., 2007). For

sophisticated bone tissue engineering approaches, differentially regulated angiogenesis is desirable. Whilst, a number of promoting and inhibitory factors of angiogenesis are known, others are still being discussed, thus a complete and detailed understanding of the angiogenic process in bones has still not been fully elucidated.

1.3.3 Regulation of angiogenesis

Regulation of angiogenesis is part of an intensive clinical research effort as angiogenesis plays a critical role in tumour growth and a number of other pathologies (Cook and Figg, 2010) and it is also important for bone tissue engineering (Unger et al., 2007; Meijer et al., 2007). Adequate supply of oxygen and nutrients is essential for tumour survival (Ferrara et al., 1998; Hanahan and Folkman, 1996) and for integration of engineered tissue constructs into the body (Awwad et al., 1986). Tumours induce blood vessel formation by secretion of several growth factors that stimulate sprouting of endothelial cells in surrounding tissue (Wang et al., 2010; Ricci-Vitiani et al., 2010). Angiogenesis is a highly regulated process, which is under the control of different growth factors, cytokines, chemokines and adhesion molecules (Table 1.2).

Table 1.2: A selection of the most important angiogenic factors

Factor	**Mechanism**	**Reference**
Angiopoietins	Vessel stabilisation	(Satoh et al., 2008)
bFGF	Proliferation stimulator	(Kuhn et al., 2012; Globus et al., 1989) (Montero et al., 2000)
FGF	Proliferation and differentiation stimulation	(Stegmann, 1999)
TGF-β	Extracellular matrix production	(Petito et al., 2013)
PDGF	Smooth muscle cell recruitment	(Heldin, 1992; Hannink and Donoghue, 1989)
VEGF	Binds tyrosine kinase receptors	(Holmes et al., 2007)
VEGFR	Acts on several signalling pathways	(Cook and Figg, 2010; Schlaeppi et al., 1997) (Akeno et al., 2002)

The main angiogenic inducers are vascular endothelial growth factor (VEGF), bFGF, hepatocyte growth factor (HGF), tumour necrosis factor (TNF)-α and angiopoietins (Folkman, 1995). Inhibitors of angiogenesis include prolactin, angiostatin and endostatin. One of the most important and well-documented inducers of angiogenesis is

VEGF, which acts as a signal protein for capillary sprouting. The VEGF family includes VEGF-A, VEGF-B, VEGF-C, VEGF-D and placental growth factor (PlGF) that bind to three types of VEGF receptors (Ferrara and Alitalo, 1999). VEGF (synonym VEGF-A) is released by a number of different cell types, including macrophages, fibroblasts and osteoblasts (Diegelmann and Evans, 2004). It stimulates cellular responses (for example it induces endothelial cell sprouting) by binding to VEGFR-2, a tyrosine kinase receptor. This has clinical relevance, as tumours can be targeted using anti-angiogenic tyrosine kinase inhibitors (Gotink and Verheul, 2010), blocking the action of VEGF and its receptors (Neufeld et al., 1999). Recent studies have shown that angiogenesis is inhibited by blocking VEGF signalling pathways, which consequently reduces tumour growth (Kim et al., 1993). Approved tyrosine kinase inhibitors that block the signalling cascade through VEGF receptors include sorafenib (Nexavar®), sunitinib (Sutent®), pazopanib (Votrient®) and vandetanib (Zactima™). Endothelial cells also express VEGF, which is important for vessel maintenance. It is regulated by TGF-β, a major cytokine released from bone tissue (Chim et al., 2013). The secretion of VEGF in different cell types is also induced by hypoxia during wound healing (Fraisl et al., 2009; Ratcliffe, 1981; Steinbrech et al., 2000).

Other relevant angiogenic growth factors include members of the FGF protein family. A number of its members are involved in angiogenesis, early stage embryonic development and wound healing. They induce angiogenesis directly through the activation of endothelial cells via FGF receptors and indirectly by stimulating other cells to produce angiogenic factors (Tsaryk et al., 2012). The most recently described member of this protein family, FGF23, is responsible for phosphate metabolism and is secreted by osteoblasts and osteoclasts in response to calcitriol (Kolek et al., 2005; Prie and Friedlander, 2010). FGF as well as TGF-β-1 are abundant in bone tissue (Zambonin et al., 2000; Mackie et al., 1998). Since tumours have an increased FGF level, its inhibition is a valuable anti-angiogenic tumour therapy in cancer research (Folkman, 1996). Recent osteoblast and osteoclast related studies have shown that FGF-6 may regulate bone metabolism (Bosetti et al., 2010), but this requires further research.

An important angiogenic factor from the FGF protein family is bFGF, which has pleiotropic effects. It is expressed by fibroblasts, osteoblasts and a number of other cell types (Chim et al., 2013; Klein et al., 1993). In osteoblasts, bFGF production is induced in response to prostaglandins and TGF-β (Beck and D'Amore, 1997). It acts as both an autocrine and paracrine factor, that stimulates cell proliferation and angiogenesis-related growth factor expression in endothelial cells (Seghezzi et al., 1998).

Another key player in angiogenesis is hepatocyte growth factor (HGF), which acts primarily on endothelial cells as a paracrine growth factor (Yamada et al., 2013). In the literature, there are reports that HGF has a central role in angiogenesis, tissue regeneration and tumour growth (Porta et al., 2013). It is secreted by osteoblasts and, in cooperation with cell-associated cytokines, is responsible for stem cell-stimulating activities of osteogenic cells (Taichman et al., 2001). HGF regulates cell growth and motility by stimulating mitogenesis (Zambonin et al., 2000; Kimoto et al., 2012; Jin et al., 2004). It also increases osteopontin expression in human osteoblasts through several signalling pathways (including PI3K and AKT) and promotes invasiveness and progression of osteosarcoma by autocrine receptor c-MET (Chen et al., 2012; Rochet et al., 1999).

Besides the stimulation of angiogenesis, inhibition is essential *in vivo* for vascular haemostasis and is therefore also a focus of cancer research. Endostatin, a fragment of collagen, is believed to interact with α_5-integrins and inhibit integrin-dependent endothelial cell functions, such as cell proliferation and migration (Rehn et al., 2001). As an endogenous inhibitor of angiogenesis, it is thought to interfere with the growth factors bFGF and VEGF. In general, endostatin regulates many signalling pathways via multiple targets, including TNFα and AP-1 (Abdollahi et al., 2004). Endostatin also blocks VEGF-mediated signalling by direct interaction with kinase insert domain receptor (KDR) (Kim et al., 2002). Due to its wide-ranging actions, endostatin is currently intensively studied in clinical trials.

Other relevant proteins involved in angiogenesis inhibition are matrix metalloproteinases. Although they are key factors in normal physiological cell processes like tissue connections or development, unregulated activities of matrix metalloproteinases are involved in numerous pathologies, especially tumour cell metastasis (Brew et al., 2000). The family of tissue inhibitors of metalloproteinases consists of four homologous proteins (TIMP-1 to TIMP-4) that are thought to be metastasis suppressors. TIMP-2 directly inhibits proliferation of endothelial cells and is therefore designated as an interesting prospect in cancer research (Fiedler et al., 2001). Within the TIMP metallopeptidase inhibitor (TIMP) protein family, TIMP-2 is unique, due to its ability to inhibit protease activity in tissues undergoing extracellular matrix remodelling (Kai et al., 2002).

The combination of different angiogenic factors can have diverse effects in different cell types (Nishishita and Lin, 2004). It has been shown that in smooth muscle cells, TGF-β down-regulates angiopoietin (ANG)-1 expression, which is induced by PDGF stimulation and is necessary for pericyte recruitment in newly formed blood vessels. In endothelial cells, ANG-1 or TGF-β stimulation decreases PDGF expression. The combination of both TGF-β and ANG-1 results in a dramatically greater downregulation of PDGF. Thus, regulation of gene expression can be very complex and unpredictable. For maintenance of vascular homeostasis, up or down-regulation of gene expression is essential. *In vitro* co-cultures can provide further insights into important factors involved in angiogenesis and mechanisms.

1.3.4 Co-culture systems

Co-culture systems of endothelial cells with osteoblasts as a 'drug delivery' system are an exciting strategy for angiogenesis-related research as well as for the *in vitro* study of prevascularisation of tissue engineering constructs (Bishop et al., 1999; Kirkpatrick et al., 2011; Unger et al., 2007). The co-cultivation of endothelial cells and osteoblasts gives an insight into cell growth and proliferation processes that are relevant for repairing large bone defects using bone tissue engineering (Liu et al., 2012). While co-cultures

of endothelial cells and osteoblasts undergo angiogenesis and osteogenesis, monocultures of endothelial cells show no formation of micro-capillary structures (Hofmann et al., 2008; Guillotin et al., 2008). Additionally, co-cultivation of these cell types seems to have positive effects on the osteoblastic differentiation of the osteoblasts (Qu and von Schroeder, 2006; Stains and Civitelli, 2005). The main issue in angiogenesis research is the choice of an appropriate system (Staton et al., 2009). The use of transfected cell lines in co-culture systems allows *in vitro* analysis of the precise contribution of single genes to the angiogenic process (Balconi et al., 2000).

In previous studies, endothelial cells in monoculture and in co-culture with osteoblasts have been shown to form lumen containing micro-capillary structures by self-assembly and without the addition of any angiogenic stimulants (Unger et al., 2007). Moreover, the addition of VEGF did not induce any further formation of such structures. Compared to monoculture, the life span of endothelial cells *in vitro* was increased by the co-cultivation with osteoblasts (Unger et al., 2007). Pre-formed microcapillary structures *in vitro* remain stable for at least two weeks after implantation in immunodeficient mice and anastomose with the host vasculature (Unger et al., 2010). In another study, outgrowth endothelial cells (OEC) were co-cultured with osteoblasts and formation of lumina as well as tight junctions was observed (Fuchs et al., 2007). Furthermore, the formation of micro-capillary structures coincided with the production of mineralised matrix by osteoblasts (Fuchs et al., 2009).

Since co-culture systems have a high degree of complexity, several parameters need to be considered before starting any angiogenesis-related study (Kirkpatrick et al., 2011). The choice of cell line is important and depends on the system and experimental question being addressed. A comparative study of primary endothelial cells and cell lines *in vitro* revealed significant differences in expression of the endothelial phenotype (Unger et al., 2002). Furthermore, the level of osteoblast differentiation in primary osteoblasts and osteosarcoma cell lines has effects on the expression profile of osteoblasts as well as the co-cultured endothelial cells (Kirkpatrick et al., 2011).

However, while endothelial cells are well described in the literature (Jaffe et al., 1973; Hewett and Murray, 1996; Bishop et al., 1999; Donovan et al., 2001; Albelda and Buck, 1990), osteosarcoma cell lines are poorly characterised in terms of angiogenesis-inducing potential. For example, the molecular composition of osteosarcoma extracellular matrix is unknown but is thought to have a characteristic labelling profile (Pautke et al., 2004).

For blood vessel-related research *in vitro*, primary human umbilical vein endothelial cells (HUVEC), primary human dermal microvascular endothelial cells (HDMEC) and OEC are commonly used on account of their ready availability and potent pro-angiogenic activity (Bouis et al., 2001; Unger et al., 2004; Kirkpatrick et al., 2011). Interactions between cells in co-culture systems are mediated by several factors. Various molecules that are involved in the growth and differentiation of endothelial cells and osteoblasts, including adhesion proteins and growth factors, can influence cells in co-culture. In a spheroid 3-D co-culture model of human primary osteoblasts and HUVEC, a bi-directional influence of the cells on osteogenic and angiogenic gene expression has been shown (Stahl et al., 2004; Kirkpatrick et al., 2011).

In addition to cellular components of co-culture systems, the cell culture media and seeding logistics (relative cell number, etc.) need to be considered. Furthermore, the potential need of cells to have dynamic mechano-stimulation can be addressed by the use of bioreactors (Hutmacher and Singh, 2008; Khetani and Bhatia, 2006) or rotating culture systems. Finally, one should consider whether to use a 2-D or 3-D initial cell seeding on a scaffold or matrix (Kirkpatrick et al., 2011; Fuchs et al., 2007).

In order to understand interactions between endothelial cells and osteoblasts in bone tissue engineering, angiogenesis research is essential. *In vitro* models can provide deep insights into co-regulation and facilitate identification of factors involved in angiogenesis (Vailhe et al., 2001). For reproducible results, established and well-characterised cell lines are needed.

1.4 Aim of this study

The involvement of endothelial cells in inflammation and angiogenesis confers a pivotal role in tumour suppression and the integration of bone tissue engineering constructs. For example, drug delivery in vascularised tumours could be better directed and improved. Because of the important role of angiogenesis in bone formation, remodelling and regeneration, the vascularisation of bone tissue engineering constructs is critical. The prevascularisation of a scaffold can accelerate the healing response and integration of implants (Kirkpatrick et al., 2011). Osteoblasts influence these processes by stimulation of endothelial cells to form new blood vessels *in vivo* and vessel-like structures *in vitro*. However, the effects that osteoblasts have on angiogenesis may result either from cell-cell interactions or from cell signalling processes in the extracellular matrix.

The aim of this study was to demonstrate the relevance of the choice of cell types and cell characteristics in multicellular *in vitro* co-culture systems. This study focussed on the characterisation of endothelial cells and osteoblasts and their potential to induce angiogenic processes. It also aimed to identify signal molecules that might be involved in angiogenesis induction. Therefore, important components of the co-culture systems were analysed to assess their effects on the endothelial cells and the formation of micro-capillary structures.

In the initial experiments primary osteoblasts and several osteosarcoma cell lines (MG-63, Cal-72 and SaOS-2) were analysed. These cells were characterised with respect to growth and morphology, osteogenic differentiation and matrix mineralisation markers as well as protein expression levels. Additionally, the effects of green fluorescent protein (GFP)-transfection on osteosarcoma cell lines for cell visualisation were studied. The results were compared with the potential of the cells to induce angiogenesis in 2-D and 3-D co-cultures with endothelial cells.

The second part of the co-culture studies was to carry out an analysis with endothelial cells, which are very well characterised in the literature. The cells were verified after isolation based on expression of endothelial cell markers and the ratio of lymphatic

and vascular sub-populations was analysed. Also, the effect of the lymphatic endothelial cell marker podoplanin on angiogenesis in co-culture systems was investigated.

The third part of the co-culture studies consisted of examining cell culture medium composition for its effect on angiogenesis. In order to gain a better understanding of the influence of osteoblasts on angiogenesis, optimal medium conditions for the co-cultures were determined, since both cell types require different media in monoculture. Furthermore, changes of the medium composition (especially by secretion of factors) by the cells in mono- and co-cultures were analysed. Important factors that induce or inhibit angiogenesis are secreted by different cell types and include bFGF, HGF, VEGF and endostatin. Other possible angiogenesis-related factors were determined by transcriptional analysis and mass spectroscopy.

Material and Methods

2.1. Materials . . . 21
2.1.1. Instruments and microscopes . . . 21
2.1.2. Consumables . . . 22
2.1.3. Chemicals . . . 22
2.1.4. Buffers . . . 24
2.1.5. Solutions and cell culture media . . . 25
2.1.6. Enzymes . . . 26
2.1.7. Antibodies . . . 26
2.1.8. Oligonucleotides . . . 27
2.1.9. Kit systems . . . 27
2.1.10. Primary cells and cell lines . . . 28
2.1.11. Software . . . 28
2.2. Methods . . . 29
2.2.1. Isolation of primary human endothelial cells . . . 29
2.2.1.1. Isolation of HUVEC . . . 29
2.2.1.2. Isolation of HDMEC . . . 29
2.2.1.3. Isolation of HPMEC . . . 31
2.2.1.4. Isolation of OEC . . . 31
2.2.1.5. Isolation of pOB . . . 32
2.2.2. Cell culture . . . 32
2.2.2.1. Coating of cell culture surfaces . . . 33
2.2.2.2. Cell passage and cell seeding . . . 33
2.2.2.3. Cryoconservation and thawing of cells . . . 34
2.2.2.4. Cell number quantification . . . 34
2.2.2.5. Transfection of SaOS-2 . . . 34
2.2.2.6. Cell treatment with growth factors . . . 35
2.2.2.7. 2-D co-cultures on cell culture plastic . . . 35
2.2.2.8. 2-D co-cultures with flexiPERM chamber . . . 35
2.2.2.9. 3-D culture in collagen type I gel matrix . . . 36
2.2.2.10. 3-D culture in fibrin gel matrix . . . 36
2.2.3. Cytotoxicity assays . . . 37
2.2.3.1. Calcein-AM cell viability assay . . . 37
2.2.3.2. Viability test with WST-1 . . . 37
2.2.4. Protein biochemical methods . . . 38
2.2.4.1. ELISA . . . 38
2.2.4.2. EIA . . . 39
2.2.4.3. Immunofluorescent staining of cell components . . . 39
2.2.4.4. Antibody array human angiogenesis . . . 40
2.2.4.5. Protein quantification by BCA assay . . . 40
2.2.4.6. DNA quantification in cell lysates . . . 41
2.2.4.7. Quantification of ALP activity . . . 41
2.2.4.8. Quantification of mineralisation with alizarin red . . . 42
2.2.4.9. Quantification of Collagen . . . 42
2.2.4.10. Quantification of Calcium . . . 42
2.2.4.11. FACS . . . 43
2.2.4.12. SDS-PAGE . . . 43
2.2.4.13. Western blot . . . 44
2.2.4.14. TCA precipitation of proteins . . . 45
2.2.4.15. Albumin depletion from cell culture medium . . . 45
2.2.4.16. Mass spectroscopy . . . 46
2.2.5. Molecular genetic techniques . . . 47
2.2.5.1. Isolation and quantification of DNA . . . 47
2.2.5.2. Isolation and quantification of RNA . . . 48
2.2.5.3. cDNA-synthesis via RT-PCR . . . 48
2.2.5.4. Polymerase chain reaction . . . 49
2.2.5.5. Cloning of podoplanin into pEGFP-N1 vector . . . 50
2.2.5.6. Cell characterisation by PCR . . . 51
2.2.5.7. Quantitative real-time polymerase chain reaction . . . 51
2.2.6. Statistical analysis . . . 52

2.1 Materials

2.1.1 Instruments and microscopes

Table 2.3: Instruments and microscopes

Instrument	Model	Company
Analytical Balance	A120S	Sartorius, Göttingen, Germany
Autoclave		Heraeus, Hanau, Germany
Balance	LC420	Sartorius, Göttingen, Germany
Biological Safety Cabinet	HeraSafe KS 12	Heraeus, Hanau, Germany
Centrifuge	Megafuge 1.0	Kendro, Langenselbold, Germany
Cooling centrifuge	S403	Eppendorf, Hamburg, Germany
Deep Freezer	HeraFreeze	Heraeus, Hanau, Germany
Digital Camera		Olympus, Hamburg, Germany
Digital Camera	DC 300 F	Leica, Wetzlar, Germany
Electrophoresis apparatus	Mini-PROTEAN	Bio-Rad, Hercules, USA
FACSCalibur		BD Biosciences, Pharmingen, Belgium
Fluorescent microplate reader	GENios Plus	Tecan, Crailsheim, Germany
Fluorescence microscope	Biorevo BZ-9000	Keyence, Neu-Isenburg, Germany
Freezer -20°C		Siemens, München, Germany
Heating block	Dri-Block DB-20	Techne, Burlington, UK
Heating block	Thermomixer 5436	Eppendorf, Hamburg, Germany
Incubator	HeraCell 150	Heraeus, Hanau, Germany
Inverted fluorescence microscope	Leica DM IRBE	Leica, Wetzlar, Germany
Laser scanning confocal microscope	Leica DM RE	Leica, Wetzlar, Germany
Liquid nitrogen tank	MVE Cryosystem 6000	German-Cryo, Jüchen, Germany
Liquid nitrogen tank	Cryo 1°C	Nalgene, Rochester, UK
Luer forceps		Aesculap, Tuttlingen, Germany
Magnet	MPC-1	Dynal, Hamburg, Germany
Magnetic stirrer	IKAMAG RET-GS	IKA-Labortechnik, Staufen, Germany
MALDI LTQ Orbitrap XL		Thermo Scientific, Dreieich, Germany
Microcentrifuge	SD	Roth, Karlsruhe, Germany
Microcentrifuge	Biofuge Pico	Heraeus, Hanau, Germany
Microplate reader	Multiscan Plus MK II	Titerscan, Huntsville, USA
Nano Drop	ND-1000	NanoDrop, Wilmington, USA
Neon Transfection System		Invitrogen, Carlsbad, Germany
Neubauer cell counting chamber		Marienfeld, Germany
PCR Cycler	Gene PCR System 9700	Applied Biosystems, Foster City, USA
pH meter	InoLab 730	WTW, Weilheim, Germany
Plate centrifuge	Biofuge Stratos	Heraeus, Hanau, Germany
Plate washer	Hydro Control	Tecan, Männedorf, Switzerland
Power supply	PowerPac HC	Bio-Rad, Hercules, USA
Real-time PCR cycler	7300	Applied Biosystems, Foster City, USA
Refridgerator 4°C		Bosch, München, Germany
Roll mixer	Assistent RMS	Karl Hecht, Sondheim, Germany
Sterilizer		Heraeus, Hanau, Germany
Shaker	Reax3	Heidolph, Schwabach, Germany
Shaker	Unimax1010	Heidolph, Schwabach, Germany
Ultrasound water bath	Sonorex TK52	Bandelin, Berlin, Germany
UV table		Bachofer, Waibingen, Germany
Vacuum Pump	Vacusafe Comfort	Integra Biosciences, Fernwald, Germany
Vortex		VWR International, Darmstadt, Germany
Water bath	SW-20C	Julabo, Seelbach, Germany
Wide-mouth bottles 250ml		Nalgene, Rochester, UK

2.1.2 Consumables

Table 2.4: Consumables

Material	Company
15 ml High Clarity PP Conical Tubes (17x120mm)	BD Falcon, NJ, USA
50 ml Cell Star Tubes	Greiner bio-one, Tuttlingen, Germany
Bioreactor for 3G5 hypridoma cells	CELLine CL1000, IBSINTEGRA Biosciences, Chur, Schweiz
Cell Strainer 40 µm and 100 µm Nylon	BD Falcon, Heidelberg, Germany
Coverslips (25x40 mm and 18x18 mm)	Menzel, Braunschweig, Germany
Coverslips (ø 15 mm and ø 18 mm)	Roth, Karlsruhe, Germany
Cryo tubes	Nalgene, Rochester, UK
Cytodex microcarrier beads	GE Healthcare, Uppsala, Sweden
Examination gloves, latex	Semper med, Wien, Austria
Examination gloves, nitrile	Igefa, Ahrensfelde, Germany
FlexiPERM chamber	Greiner bio-one, Tuttlingen, Germany
Gelmount mounting media	Biomedia
HTS Transwell 0,4 µm #3378 Polyester membranes	Costar/Corning Life sciences, Amsterdam, Netherlands
Hyperfilm, ECL	Amersham Pharmacia Biotech, Freiburg, Germany
Ibidi µ-slides	Ibidi, Martinsried, Germany
Laboratoryfilm, Parafilm	Pechiney Plastic Packaging, Chicago, USA
LabTek II CC2-treated glass chamber slide	Nunc, Roskilde, Denmark
Maxisorb 96-wells plates	Nunc, Roskilde, Denmark
Microplates (non-sterile, flat-bottom, 96-well)	Greiner bio-one, Tuttlingen, Germany
Object slides	Mentel, Braunschweig, Germany
Optical adhesive film (qPCR)	Applied Biosystems, Foster City, USA
PCR reaction tubes	Applied Biosystems, Foster City, USA
Pipette tips (10, 100, 1000 µl)	Greiner, Soligen, Germany
Pipettes (2, 5, 10, 25 ml)	Greiner, Soligen, Germany
Protran Nitrocellulose Transfer Membrane	Schleicher & Schuell, Dassel, Germany
qPCR optical 96-well reaction plates	Applied Biosystems, Foster City, USA
Scalpels	Braun, Tutlingen, Germany
Syringe filter 0,2 µm	Thermo Scientific, Dreieich, Germany
Terralin liquid	Pharmacy, Universitätsmedizin Mainz, Germany
Thermanox coverslips (12 mm)	Roth, Karlsruhe, Germany
Tissue culture dishes (ø 3.5 cm, ø 6 cm, ø 10 cm)	Greiner bio-one, Tuttlingen, Germany
Tissue culture flask (12.5 cm^2)	BD Falcon, NJ, USA
Tissue culture flask (25.0 and 75.0 cm^2)	TPP, Trasadingen, Switzerland
Tissue culture plates (6-, 24-, 48- and 96-well)	TPP, Trasadingen, Switzerland
Tissue culture plates (12-well)	Greiner bio-one, Tuttlingen, Germany
Tubes (1.5 ml and 2.0 ml)	Eppendorf, Hamburg, Germany
Tubes (15 ml and 50 ml)	BD Falcon, Heidelberg, Germany
Whatman 3 mm filter paper	Schleicher & Schuell, Dassel, Germany

2.1.3 Chemicals

Table 2.5: Chemicals

Chemical	Company
1-Butanol	Merck, Darmstadt, Germany
2-Propanol	Fluka, Basel, Switzerland
10 vol.-% β-mercaptoethanol	Dako Hamburg, Germany
40 % Acrylamide/Bisacrylamide solution, 19:1	Bio-Rad, Hercules, USA
Acetone	Sigma-Aldrich, St. Louis, USA
Acetic acid	Roth, Karlsruhe, Germany
Agar-100 resin	PLANO, Germany
Agarose	AppliChem, Darmstadt, Germany
AlexaFluor 594 phalloidin	Invitrogen, Carlsbad, Germany
APS	Bio-Rad, Hercules, USA
sdH_2O	Braun, Meslingen, Germany

Continued on the following page

Table 2.5 – Continued from the previous page

Chemical	Company
bFGF	Sigma-Aldrich, St. Louis, USA
Blocking reagent	Roche, Freiburg, Germany
BSA	Sigma-Aldrich, St. Louis, USA
$CaCl_2$ x $2H_2O$	Sigma-Aldrich, St. Louis, USA
Calcein AM	Molecular Probes, Carlsbad, Germany
CH_3COOH	Merck, Darmstadt, Germany
Ciprobay 200	Bayer, Leverkusen, Germany
Citric acid	Sigma-Aldrich, St. Louis, USA
Collagen type I	ICN Biomedicals, Eschwege, Germany
Coomassie Blue G250	Sigma-Aldrich, St. Louis, USA
Crystal violet	Merck, Darmstadt, Germany
DAPI (Hoechst)	Sigma-Aldrich, St. Louis, USA
dimethyl sulfoxide	Sigma-Aldrich, Germany
dNTP mix	Qiagen, Hilden, Germany
DTT	ICN Biomedicals, Eschwege, Germany
Dynabeads CD31	Dynal, Hamburg, Germany
ECL Western Blotting Detection Reagents	Amersham Pharmacia Biotech, Freiburg, Germany
EDTA	Sigma-Aldrich, St. Louis, USA
EGTA	Sigma-Aldrich, St. Louis, USA
ethanol	AppliChem, Darmstadt, Germany
FCS	Sigma-Aldrich, St. Louis, USA
Fibrinogen	Fluka, Basel, Switzerland
Fibronectin	Roche, Freiburg, Germany
Ficoll solution	Sigma-Aldrich, St. Louis, USA
Formalin	Sigma-Aldrich, St. Louis, USA
Fungizone	Gibco, Karlsruhe, Germany
Gelatine	Sigma-Aldrich, St. Louis, USA
GenCarrier-1 Cell Transfection Reagent	Epoch Biolabs, Sugar Land, USA
GlutaMax^{TM} (100x)	Gibco, Carlsbad, Germany
Glycerol	Sigma-Aldrich, St. Louis, USA
Glycine	Roth, Karlsruhe, Germany
GSH-MEE	Calbiochem, Darmstadt, Germany
H_2O_2	Merck, Darmstadt, Germany
HNO_3	Fisher Scientific, United Kingdom
H_2SO_4	Merck, Darmstadt, Germany
H_3PO_4	Merck, Darmstadt, Germany
HCL	Merck, Darmstadt, Germany
HEPES	Sigma-Aldrich, St. Louis, USA
Hoechst 33342	Sigma-Aldrich, St. Louis, USA
Hydrochloric acid	Merck, Darmstadt, Germany
Isopropanol	Fluka, Basel, Switzerland
KCl	Calbiochem, Darmstadt, Germany
KOH	Merck, Darmstadt, Germany
L-glutathione reduced	Sigma-Aldrich, St. Louis, USA
LPS	Sigma-Aldrich, St. Louis, USA
MetOH	AppliChem, Darmstadt, Germany
$MgCl_2$ x $6H_2O$	Merck, Darmstadt, Germany
Na_2HPO_4	Roth, Karlsruhe, Germany
NaCl	Roth, Karlsruhe, Germany
NaOH	Roth, Karlsruhe, Germany
n-butanol	Fluka, Basel, Switzerland
Nonfat dried milk powder	AppliChem, Darmstadt, Germany
o-PD tablet	Roche, Freiburg, Germany
PBS	Gibco, Carlsbad, Germany
PBS (10x sterile solution)	Sigma-Aldrich, St. Louis, USA
PEG	Sigma-Aldrich, St. Louis, USA
PKH26	Sigma-Aldrich, St. Louis, USA
P/S (each 10,000 U/ml)	Gibco, Carlsbad, Germany
PFA (3.7 vol.-% in CS-buffer)	Merck, Darmstadt, Germany
PIPES	Sigma-Aldrich, St. Louis, USA
PMSF	Sigma-Aldrich, St. Louis, USA
Ponceau S solution	Sigma-Aldrich, St. Louis, USA
Power SYBR Green	Applied Biosystems, Foster City, USA
Precision Plus Protein Standards Dual Color	Bio-Rad, Hercules, USA
Precision Plus Protein Standards Western Color	Bio-Rad, Hercules, USA
Precision StrepTactin-HRP Conjugate	Bio-Rad, Hercules, USA

Continued on the following page

Table 2.5 – Continued from the previous page

Chemical	Company
Protease Inhibitors Cocktail	Sigma-Aldrich, St. Louis, USA
Random Primer, $d(N)_x$	New England Biolabs, Frankfurt am Main, Germany
RotiLoad-1 loading buffer	Roth, Karlsruhe, Germany
SDS	Serva, Heidelberg, Germany
Sodium deoxycholate	Sigma-Aldrich, St. Louis, USA
Sodium heparin	Sigma-Aldrich, St. Louis, USA
Substrate reagents	R&D Systems, Wiesbaden, Germany
Sucrose	Serva, Heidelberg, Germany
Supplement Mix	PromoCell, Heidelberg, Germany
TEMED	Bio-Rad, Hercules, USA
Tris	Roth, Karlsruhe, Germany
Tris-HCl 1M	Sigma-Aldrich, St. Louis, USA
Triton X-100	Sigma-Aldrich, St. Louis, USA
Tween 20	Serva, Heidelberg, Germany
VEGF	Gibco, Carlsbad, Germany

2.1.4 Buffers

Table 2.6: Buffers

Buffer	Composition	Used for (company)
Bradford reagent	50 mg Coomassie Blue G250 25 ml ethanol 50 ml H_3PO_4 adjusted to 1.0 l with sdH_2O	Visualisation of proteins
Buffy coat buffer	0.5 % FCS 0.4 % 20 mM EDTA adjusted with PBS	OEC isolation
Cacodylat/HCl	150 mM NaCacodylat 1 mM $CaCl_2$ 0.5 mM $MgCl_2$ pH 7.2 adjusted with HCl	TEM
Blocking solution	5 % Milk powder PBS 0.2 % Tween 20	Western blot
CM buffer	0.26 M $NaHCO_3$ 0.2 M HEPES 0.04 N NaOH	Reconstitution buffer for collagen gel matrix
CS	0.1 M PIPES 1 mM EGTA 4 % PEG 0.4 % NaOH pH 7.2	Solvent buffer for paraformaldehyde
Laemmli Stock	30 g Tris 144 g Glycine adjust to 1 l with sdH_2O	Laemmli Stock for SDS-PAGE
SDS-PAGE running buffer	200 ml Laemmli Stock 5 ml 20 % SDS adjust to 1 l with sdH_2O	Running buffer for SDS-PAGE
SDS-PAGE transfer buffer	100 ml Laemmli Stock 250 ml MetOH adjust to 1 l with sdH_2O	Transfer buffer for SDS-PAGE

Continued on the following page

Table 2.6 – Continued from the previous page

Buffer	Composition	Used for (company)
PBS	20x stock solution 160.0 g NaCl 4.0 g KCl 4.0 g KH_2PO_4 adjusted to 1.0 l with sdH_2O	Wash buffer for ELISA, Western blot
RIPA buffer	50 mM Tris-HCl pH 7.4 150 mM NaCl 1 mM EDTA 1 % Sodium deoxycholate 0.1 % SDS 1 % Triton X-100 1 mM PMSF	Lysis of cells and tissues
SDS transfer buffer	25 mM Tris-HCl, pH 8.0 100 mM Glycine 25 % MetOH	Western blot
Sodium citrate 10x stock	1 M citric acid 2 M Na_2HPO_4	CAM-EIA
Stripping buffer	10 ml PBS 70 µl β-ME 2 % SDS	Western blot
Substrate solution	5 ml Sodium citrate 10x stock 45 ml sdH_2O 1 tablet o-PD (20 mg) 20 µl H_2O_2	CAM-EIA
TBE buffer	Tris borate EDTA	DNA agarose gels
TE buffer	100 mM Tris-HCl pH 8.0 10 mM EDTA pH 8.0	
Umbilical cord buffer	900 ml sdH_2O 100 ml HEPES 10x 1 % P/S 1 % ciprobay 1 % fungizone	HUVEC isolation
BSA-Tris buffer	Tris 1.0 % BSA	ELISA

2.1.5 Solutions and cell culture media

Table 2.7: Solutions and cell culture media

Chemical	Company
DMEM	Sigma-Aldrich, St. Louis, USA
DMEM/F-12 (1:1) (1x) and GlutaMax^{TM}	Gibco, Carlsbad, Germany
EBM2	Lonza, Köln, Germany
ECBM and supplements	PromoCell, Heidelberg, Germany
ECGM and supplements	Lonza, Köln, Germany
EGM2 BulletKit supplements	Lonza, Köln, Germany
Medium 199	Sigma-Aldrich, St. Louis, USA

2.1.6 Enzymes

Table 2.8: Enzymes

Enzyme	Company
BamHI	Fermentas, St. Leon-Rot, Germany
Collagenase type I	Worthington, Lakewood, UK
Dispase	Gibco, Carlsbad, Germany
EcoRI	Fermentas, St. Leon-Rot, Germany
Proteinkinase K	Sigma-Aldrich, St. Louis, USA
RNaseA	Roche, Freiburg, Germany
RNase-Free DNase	Qiagen, Hilden, Germany
Streptavidin HRP	R&D Systems, Wiesbaden, Germany
Streptavidin-biotinylated HRP complex	Amersham Pharmacia Biotech, Freiburg, Germany
Thrombin	Sigma-Aldrich, St. Louis, USA
Trypsin	Gibco, Carlsbad, Germany
Trypsin-EDTA (1x)	Gibco, Carlsbad, Germany
Versene	Gibco, Carlsbad, Germany

2.1.7 Antibodies

Table 2.9: Antibodies

Antibody	Source	Dilution	Company
Alexa 488 anti-mouse IgG	goat	1:1000	Invitrogen, Carlsbad, Germany
Alexa 488 anti-rat IgG	goat	1:1000	Invitrogen, Carlsbad, Germany
Alexa 488 anti-rabbit IgG	donkey	1:1000	Invitrogen, Carlsbad, Germany
Alexa 488 anti-goat IgG	donkey	1:1000	Invitrogen, Carlsbad, Germany
Alexa 546 anti-mouse IgG	goat	1:1000	Invitrogen, Carlsbad, Germany
Alexa 546 anti-rabbit IgG	goat	1:1000	Invitrogen, Carlsbad, Germany
Alexa 594 anti-rabbit IgG	donkey	1:1000	Invitrogen, Carlsbad, Germany
Alexa 594 anti-goat IgG	donkey	1:1000	Invitrogen, Carlsbad, Germany
Anti-D2-40	mouse	1:20	Covance, Princeton, USA
Anti-CD31 FITC conjugate	mouse	1:40	Chemicon, Billerica, USA
Anti-CD31	mouse	1:50	Dako, Glostrup, Danmark
Anti-E-selectin	mouse	1:2000	Bender MedSystems, Vienna, Austria
Anti-ICAM-1	rabbit	1:1000	Cell Signaling, Danvers, USA
Anti-ICAM-1	mouse	1:400	Bender MedSystems, Vienna, Austria
Anti-VE-Cadherin	mouse	1:100	BD Biosciences, Pharmingen, Belgium
Anti-vWF	rabbit	1:8000	Dako, Glostrup, Danmark
Anti-mouse IgG biotinylated	goat	1:1000	Amersham Pharmacia Biotech, Freiburg, Germany
Anti-mouse IgG HRP linked	sheep	1:2000	Amersham Pharmacia Biotech, Freiburg, Germany
Anti-mouse IgG HRP linked	rabbit	1:400	Dako, Glostrup, Danmark
Anti-rabbit IgG HRP linked	donkey	1:3000	Amersham Pharmacia Biotech, Freiburg, Germany
Anti-rabbit IgG HRP linked	goat	1:5000	Jackson ImmunoResearch, Suffolk, UK
ELISA antibodies	see Table 2.11		R&D Systems, Wiesbaden, Germany

2.1.8 Oligonucleotides

Table 2.10: Oligonucleotides

Primer	Sequence
18s 3'	5'-GGCATCGTTTATGGTCGGAA-3'
18s 5'	5'-AGCGAAAGCATTTGCCAAGA-3'
Actin 3'	5'-TACGCCAACACAGTGCTGTCT-3'
Actin 5'	5'-TGCATCCTGTCGGCAATG-3'
E-selectin 3'	5'-CCCGTGTTTGGCACTGTGT-3'
E-selectin 5'	5'-GCCATTGAGCGTCCATCCT-3'
GAPDH 3'	5'-ATGGGGAAGGTGAAGGTCG-3'
GAPDH 5'	5'-TAAAAGCAGCCCTGGTGACC-3'
HIF-1α 3'	5'-GCAAGCCCTGAAAGCG-3'
HIF-1α 5'	5'- GGCTGTCCGACTTTGA-3'
ICAM-1 3'	5'-CGGCTGACGTGTGCAGTAAT-3'
ICAM-1 5'	5'-CACCTCGGTCCCTTCTGAGA-3'
IL-8 3'	5'-TGGCAGCCTTCCTGATTTCT-3'
IL-8 5'	5'-TTAGCACTCCTTGGCAAAACTG-3'
VEGF 3'	5'-CGAGGGCCTGGAGTGTGT-3'
VEGF 5'	5'-CCGCATAATCTGCATGGTGAT-3'
Podoplanin 3'	5'-ATGCTGACTCCGCTCG-3'
Podoplanin 5'	5'-TTAGGGCGAGTACCTTC-3'
podoplaninEcoRI	5'-ATTAAGAATTCATGCTGACTCCGCTCG-3'
podoplaninBamHI	5'-TATTATGGATCCTTAGGGCGAGTACCTTC-3'

2.1.9 Kit systems

Table 2.11: Kit systems

Kit	Company
Albumin and IgG Depletion Kit	Qiagen, Hilden, Germany
BCA Protein Assay Kit	Pierce, Rockford, USA
Calcium OCP Fluid	MTI-diagnostics, Idstein, Germany
DNA Damage Quantification Kit	BioVision, Mountain View, USA
DNeasy Blood & Tissue Kit	Qiagen, Hilden, Germany
Human Angiogenesis Proteome Profiler Antibody Array Kit	R&D Systems, Wiesbaden, Germany
Human VEGF DuoSet ELISA Kit	R&D Systems, Wiesbaden, Germany
Human bFGF DuoSet ELISA Kit	R&D Systems, Wiesbaden, Germany
Human IGF-1 DuoSet ELISA Kit	R&D Systems, Wiesbaden, Germany
Human HGF DuoSet ELISA Kit	R&D Systems, Wiesbaden, Germany
Human endostatin DuoSet ELISA Kit	R&D Systems, Wiesbaden, Germany
MinElute Reaction Cleanup Kit	Qiagen, Hilden, Germany
NanoOrange Protein Quantification Kit	Molecular Probes, Carlsbad, Germany
Neon Transfection Kit	Invitrogen, Carlsbad, Germany
Omniscript RT Kit	Qiagen, Hilden, Germany
Osteogenesis Quantification Kit	Chemicon International, Temecula, USA
Proteo Mass MALDI Calibration Kit for LT QXL	Thermo Scientific, Dreieich, Germany
Qiagen Plasmid Mini Kit	Qiagen, Hilden, Germany
Qiaquick Gel Extraction Kit	Qiagen, Hilden, Germany
Quanti-iT PicoGreen dsDNA	Invitrogen, Carlsbad, Germany
Rapid DNA Ligation Kit	Roche, Freiburg, Germany
RNeasy Mini Kit	Qiagen, Hilden, Germany
Sircol Soluble Collagen Kit	Biocolor, Carrickfergus, UK
SuperScript II Reverse Transcriptase	Invitrogen, Carlsbad, Germany
SYBR Green PCR Master Mix	Applied Biosystems, Foster City, USA
WST-1 Cell Proliferation Assay	Roche, Freiburg, Germany

2.1.10 Primary cells and cell lines

Table 2.12: Bacteria, primary cells and cell lines

Cell type abbreviation	Source
E. coli XL1-Blue	Stratagene
HUVEC	primary human umbilical vein endothelial cells (HUVEC) from umbilical cord
HDMEC	primary human dermal microvascular endothelial cells (HDMEC) from juvenile foreskin
HPMEC	primary human pulmonary microvascular endothelial cells (HPMEC) from lung tissue
OEC	outgrowth endothelial cells (OEC) from blood buffy coat
pOB	primary osteoblasts (pOB) from cancellous bone fragments
MG-63	human osteosarcoma cell line purchased from ATCC
Cal-72	human osteosarcoma cell line purchased from DSMZ
SaOS-2	human osteosarcoma cell line purchased from ATCC
ST1	human pulmonary endothelial cell-derived cell line (Krump-Konvalinkova et al., 2001)

2.1.11 Software

Table 2.13: Software

Used for	Software	Version	Developer	System
Sequence analysis	ApE - A plasmid Editor	1.17	*M. Wayne Davis*	Mac OS X
	MacVector	11.0.4	MacVector Inc.	
	Serial Cloner	2.1	Serial Basic	
	VectorNTI Advance	11	Invitrogen	Windows 7
	GNCPro		Qiagen (SABiosciences, 2013)	Online
Primer design	Oligo	7.54	Molecular Biology Insights, Inc.	Mac OS X
	Primer Premier	5.00	Premier Biosoft International	Windows 7
Statistical data analysis	Prism	5.0c	GraphPad Software Inc.	Mac OS X
	Quantity One	4.6.3	Bio-Rad	Windows7
	Excel	2010	Microsoft	
Image processing	Photoshop	CS4/5	Adobe	Mac OS X
	FITS Liberator	2.2/3.0	ESA/ESO/NASA	
FACS analysis	FACS Calibur	2.1	BD Biosciences	Mac OS X
	Cell Quest Pro	2.1	BD Biosciences	
qPCR software	7300 Real Time PCR System	1.4	Applied Biosystems	Windows 7
Microscope software	BZ-9000 Analyzer		Keyence	Windows 7
	BZ-9000 Viewer		Keyence	
	LCS		Leica Microsystems	
	QWin		Leica Microsystems	

2.2 Methods

2.2.1 Isolation of primary human endothelial cells

2.2.1.1 Isolation of HUVEC

Primary human umbilical vein endothelial cells (HUVEC) were isolated according to Jaffe et al. (1973) from fresh umbilical cords which were obtained from the GPR Clinic, Rüsselsheim. Soon after birth the cord was cropped from the placenta and kept at 4°C in a sterile bottle containing umbilical cord buffer (Table 2.6) until further processing. The umbilical cord was cleaned with 70 % ethanol and cut at both ends to remove areas with clamp marks. At both ends of the vein a plastic needle was inserted and fixed with a clamp. The umbilical vein was rinsed with 4-(2-hydroxyethyl)-1-piperazineethanesulfonic acid (HEPES). Eventually occurring defects were fixed with clamps. After cleaning, the vein was filled with 5 ml of a collagenase type I (0.1 %) and HEPES mixture (1:1 (v/v)) for enzymatic tissue dissociation. The umbilical vein was sealed with clamps and incubated at 37°C. After 20 min, the umbilical cord was softly massaged for 1 min to loosen endothelial cells. The enzyme-cell suspension was collected in a sterile 50 ml tube and the vein was rinsed with phosphate-buffered saline (PBS) to a final volume of 50 ml. The cells were then centrifuged (1200 rpm, 5 min), resuspended in M199 (containing 20 % FCS, 1 % P/S, 2 mM GlutaMax^{TM}, ECGS (1:2000), sodium heparin (1:2000)) and seeded on a 0.2 % gelatine-coated T25 cell culture flask.

The cells were cultivated in an atmosphere of 5 % CO_2, 95 % humidity and 37°C (Section 2.2.2) until reaching confluence (passage 0). They were passaged in 1:3 ratio on a gelatine-coated cell culture flask (passage 1). When reaching confluence again, the cells were passaged in 1:3 ratio or frozen as described in Section 2.2.2.3 (passage 2).

2.2.1.2 Isolation of HDMEC

Primary human dermal microvascular endothelial cells (HDMEC) were isolated from juvenile foreskin (Kirkpatrick et al., 2002). After disinfection with 70 % ethanol, the foreskin was washed with PBS. Connective tissue was removed and the dermis was cut into 2x2 mm pieces before incubation in 2.36 U/ml dispase at 4°C overnight. The enzymatic

reaction was stopped by the addition of 2 ml 20 % FCS. Epidermis was removed from the dermis and the pieces were washed in PBS. Afterwards, the foreskin was digested with 5 ml versene and 80 µl 2.5 % trypsin at 37°C for 2 h under moderate shaking. Enzymatic reaction was stopped by addition of 40 ml 20 % FCS. The pieces were transferred into a glass petri dish and squeezed with the flat side of a sterile plastic syringe. The tissue suspension was filtered (100 µm) into a fresh 50 ml tube and centrifuged (1200 rpm, 5 min). The cell pellet was resuspended in 12 ml endothelial cell basal medium (ECBM) with Supplement-Mix and 1 % P/S, seeded onto a T75 cell culture flask pre-coated with gelatine (passage 0) and cultivated (Section 2.2.2). Unattached cells and remaining tissue particles were removed the next day by changing the medium. Continuous medium change was performed every 3-4 days.

When confluence was reached endothelial cells were purified using Dynabeads conjugated with antibody against CD31. 8 to 16 µl Dynabeads suspension were washed with PBS in a tube fixed to a magnet. Subsequently the Dynabeads were resuspended in 5 ml PBS with 0.1 % bovine serum albumin (BSA) and added to the cell culture. Beads were incubated with the cells at 37°C for 20 min. After 10 min, the binding of the beads to endothelial cells was controlled microscopically. Medium was discarded and cells were detached with 1 ml of 25 % trypsin/ethylenediaminetetraacetic acid (EDTA) solution. The cells were resuspended in PBS with 10 % FCS and transferred into a 15 ml tube fixed to a magnet. After 1 min of incubation, cells labelled with CD31-Dynabeads were located at the side of the tube closest to the magnet. The liquid was discarded and cells were resuspended in 3 ml PBS with 0.1 % BSA. The cells were mixed in the tube on a roll mixer at 4°C for 10 min and separated by the magnet before repeating the resuspension step. This washing step was performed three times before HDMEC were sieved through a 40 µm filter. HDMEC were resuspended in 12 ml ECBM with supplement-mix and 1 % P/S, and seeded onto a gelatine-coated cell culture flask (passage 1).

HDMEC were grown to confluence, passaged 1:3. After 4 h a second CD31 separation was performed (passage 2). When HDMEC reached confluence, the cell culture medium was changed to endothelial cell growth medium (ECGM) (containing 15 % FCS, 1 % P/S, sodium heparin (10 µg/ml), bFGF (2.5 ng/ml)). Cells were passaged in 1:3 ratio or cryo conserved (Section 2.2.2.3).

2.2.1.3 Isolation of HPMEC

Primary human pulmonary microcascular endothelial cells (HPMEC) were isolated from lung tissue (Carley et al., 1992).

2.2.1.4 Isolation of OEC

OEC were isolated from human peripheral blood buffy coats which were obtained from the Transfusionszentrale, University Medical Center, Mainz (Fuchs et al., 2007). Buffy coat is the middle fraction between plasma and erythrocytes of a blood density gradient centrifugation. It mostly contains leuco- and monocytes.

OEC were separated by diluting the blood 1:2 with buffycoat buffer (Table 2.6), overcoating carefully 15 ml of ficoll solution (specific density: 1.077 g/ml) with 35 ml of the mixture and centrifuging (400 xg without brake, 35 min) at room temperature. The sedimentation equilibrium state in combination with formation of a density gradient led to separation of erythro- and granulocytes at the bottom of the tube, monocytes as a white interphase (buffy coat) and blood plasma and thrombocytes above the interphase (Figure 2.4). Buffy coat containing monocytes was carefully transferred into a fresh tube and mixed with 50 ml of PBS. The suspension was centrifuged (400 xg, 10 min), supernatant was discarded and the pellet was washed three times with PBS. With the last washing step, 1 ml of the cell suspension was used to count the cells. Meanwhile, 24-well cell culture plates were prepared by coating with collagen type I (10 µg/ml) for 1 h at 37°C (Section 2.2.2.1). The cells were then resuspended in EBM2 with EGM2 BulletKit supplements, 5 % FCS und 1 % P/S and plated onto the previously coated 24-well plates (5 x 10^6 cells per well). Cell culture medium was refreshed three times

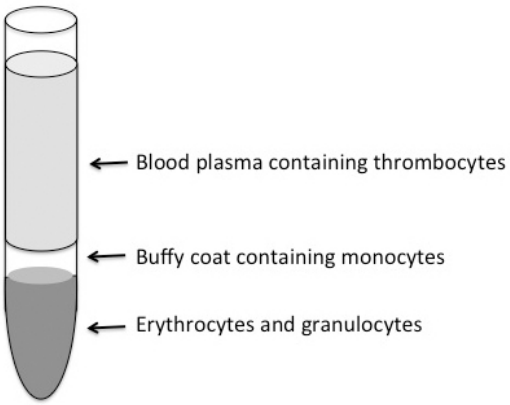

Figure 2.4: **Density gradient centrifugation of human peripheral blood**
Scheme of density gradient centrifugation of human peripheral blood with the different phases. For OEC isolation the buffy coat phase was used.

a week. After three to four weeks, single colonies of OEC appeared, showing typical bouldering morphology. They were combined 28 days after isolation and plated onto fibronectin coated (10 µg/ml) 24-well cell culture plates. When the cells reached confluence they were passaged 1:2 several times until the needed cell amount was reached. The cells were used between passage 8 and 18.

2.2.1.5 Isolation of pOB

pOB were isolated from human cancellous bone fragments of healthy donors according to Annaz et al. (2004) and Hoffmann et al. (2003). Bone fragments were obtained from Orthopedics, University Medical Center, Mainz. Bone fragments were cleaned with sterile PBS/1 % P/S in glass petri dishes and cut into pieces. The pieces were put into a 50 ml tube with PBS and washed by shaking the tube vigorously. The supernatant was discarded. This step was repeated until the supernatant was limpid and did not show any tissue or blood residues. Subsequently the bone parts were placed in sterile 6-well plates, each well carrying 3 pieces. Wells were filled with 2 ml Dulbecco's modified eagle medium (DMEM)/nutrient mixture F-12 (F-12) (containing 1 % P/S, 20 % FCS). Cells were cultivated (Section 2.2.2), medium was changed daily and cell proliferation was monitored twice a week by microscopic analysis (passage 0).

When the cell layer was confluent the medium was discarded and cells were detached with 1 ml 25 % trypsin/EDTA solution for one minute at 37°C. The enzymatic reaction was stopped by the addition of DMEM/F-12 (containing 1 % P/S, 20 % FCS). Detached cells were pooled in a 50 ml tube, separated from the bone residues by filtration (40 µm nylon) and transferred into a T75 cell culture flask (4 confluent wells per T75, passage 1). Medium was changed twice a week and the DMEM/F-12 (containing 1 % P/S, 20 % FCS) was substituted by DMEM/F-12 (containing 1 % P/S, 10 % FCS, 2 % GlutaMax^{TM}).

2.2.2 Cell culture

All cells mentioned in this study were grown under standard cell culture conditions with 5 % CO_2 and 95 % humidity at 37°C. Cells were handled in sterile conditions using biological safety cabinet. For 2-D cell culture the culture surface was coated. Prior to

experiments, cells were grown in standard culture conditions until confluence and used in the needed cell density after being counted in a Neubauer cell counting chamber.

2.2.2.1 Coating of cell culture surfaces

Extracellular membrane proteins like gelatine, fibronectin or collagen increase and improve the adhesion of endothelial cells to the culture surface. Therefore flasks, plates, LabTeks, transwell filter membranes and petri dishes were coated prior to cell seeding. For the coating of culture surfaces, they were incubated for 1 h at 37°C with gelatine (0.2 %), rat tail collagen type-I (12.12 µg/cm^2) and fibronectin (5 µg/ml) diluted in PBS.

2.2.2.2 Cell passage and cell seeding

Cells were grown (in case of endothelial cells on coated) tissue culture flasks and plates. When cells reached 90 - 100 % confluence they were detached and seeded on a fresh culture surface. Used cell culture medium was discarded and cells were washed once with PBS. For detaching the cells, they were incubated with 0.5 ml of 25 % trypsin/EDTA solution at 37°C for 2 min. The enzymatic reaction was stopped by the addition of 5 ml 10 % FCS. Cells were transferred in 1:3 to 1:5 ratio in the respective cell culture medium (Table 2.14). For experiments, cells were counted and seeded at the needed cell density. Some angiogenesis experiments were performed with endothelial cells and used osteoblast medium supernatants. For this, the medium

Table 2.14: Cell culture media for different cell types

Cell type	Medium	Passage
HDMEC	ECGM 15 % FCS 1 % P/S bFGF (1:500) sodium heparin (1:5000)	1:3; ≤ passage 3
HCMEC	ECGM 15 % FCS 1 % P/S bFGF (1:500) sodium heparin (1:5000)	1:4; ≤ passage 35
HPMEC	ECGM 15 % FCS 1 % P/S bFGF (1:500) sodium heparin (1:5000)	1:4; ≤ passage 35
HUVEC	M199 15 % FCS 1 % P/S ECGS (1:2000) sodium heparin (1:2000)	1:3; ≤ passage 3
OEC	EBM2 5 % FCS 1 % P/S EGM2 BulletKit supplements	1:3; ≤ passage 18
pOB	DMEM 10 % FCS 1 % P/S 1 % GlutaMax^{TM} sodium heparin (1:2000)	1:3; ≤ passage 12
Cal-72 MG-63 SaOS-2	DMEM 10 % FCS 1 % P/S 1 % GlutaMax^{TM} sodium heparin (1:2000)	1:3; ≤ passage 35

supernatants were centrifuged (1200 rpm, 5 min) to remove possible contamination with dead cells and mixed 1:1 with fresh cell culture medium. Cells were grown in standard cell culture conditions (Section 2.2.2).

2.2.2.3 Cryoconservation and thawing of cells

For cryoconservation of cells, cell culture medium was discarded and the cells were washed with PBS before being trypsinised with 0.5 ml trypsin/EDTA in 37°C for 2 min. The enzymatic reaction was stopped by the addition of 5 ml 10 % FCS. Cells were pelleted by centrifugation (1200 rpm, 5 min) and re-suspended in cell culture medium containing 10 % dimethyl sulfoxide (DMSO). Portions of 1.8 ml were transferred into cryo tubes. The cryo tubes were stored at -80°C and put into a fluid nitrogen tank the next day. For defrosting, the cells were thawed in a water bath at 37°C, transferred into a coated culture flask and supplemented with fresh cell culture medium. Medium was changed after the cells attached to the culture surface.

2.2.2.4 Cell number quantification

Relative cell number was determined by Neubauer cell counting chamber. The chamber was prepared by cleaning the polished surface and coverslip. The coverslip was placed over the counting surface and 10 µl of the cell suspension was introduced into one well. The cells in the counting grid were counted. If needed, the cell suspension was diluted to avoid overlapping particles or cell clusters. Each square has an area of 1/25 mm^2 and depth of 0.1 mm. For calculation of total cells per ml the following equation was used:

$$cells\ per\ ml = counts\ per\ grid \cdot 10000 \tag{2.1}$$

2.2.2.5 Transfection of SaOS-2

SaOS-2 were transfected using Neon Transfection System. A 24-well cell culture plate was prepared by adding 500 µl DMEM (containing 10 % FCS, 1 % P/S, 1 % GlutaMax^{TM}, sodium heparin (1:2000)) per well. Trypsinised and centrifuged cells were resuspended in PBS and counted. 1.7 million cells were centrifuged (1200 rpm, 2 min) and resuspended

Table 2.15: SaOS-2 transfection

voltage	duration	repeats
1200 V	40 ms	1 x
1300 V	10 ms	3 x
1100 V	40 ms	1 x
1300 V	20 ms	2 x
1400 V	10 ms	1 x
1200 V	30 ms	2 x

in 285 µl solution R. Cells were transferred to a 1.5 ml tube containing 15 µg plasmid desoxyribonucleic acid (DNA) in not more than 15 µl liquid. A microporation tube was filled with 3 ml of solution E and the cells/DNA mixture was soaked into the microporator pipette before being placed in the pipette station. Microporation pulse conditions were set according to Table 2.15 and applied 4 times each on fresh cells/DNA mixture. Samples were seeded into 24-well cell culture plates and incubated for 10 days changing medium every third day.

2.2.2.6 Cell treatment with growth factors

For growth factor experiments, co- and monocultures of endothelial cells and osteosarcoma cell lines were treated with different growth factor concentrations (Table 2.16). For monocultures, endothelial cells were seeded in collagen type I gel matrix (Section 2.2.2.9). Cell culture medium was supplemented with the growth factor in appropriate concentration. At different time points, the cells were detected by Calcein-AM staining (Section 2.2.3.1).

Table 2.16: Growth factor concentrations

Growth factor	Used concentration
VEGF	5 ng/ml, 50 ng/ml, 200 ng/ml
bFGF	1 ng/ml, 10 ng/ml, 100 ng/ml
IGF-1	2 ng/ml, 20 ng/ml, 200 ng/ml
IGF-2	2 ng/ml, 20 ng/ml, 200 ng/ml

2.2.2.7 2-D co-cultures on cell culture plastic

For co-cultivation of endothelial cells and osteoblasts, both cell types were trypsinised and counted before 168000 endothelial cells and 26000 osteoblasts were seeded onto precoated petri dishes. The cells were supplied with 2 ml ECBM (containing 15 % FCS, 1 % P/S, sodium heparin (10 µg/ml), bFGF (2.5 ng/ml)) and cultured for 7, 14, 21 and 28 days before being visualised by immunofluorescent staining (Section 2.2.4.3).

2.2.2.8 2-D co-cultures with flexiPERM chamber

Co-cultures of endothelial cells and osteoblasts in flexiPERM chambers were performed in petri dishes. One flexiPERM ring was put onto one petri dish before cell culture surface was coated with gelatine. Meanwhile, cells were trypsinised and counted. First,

25000 endothelial cells were seeded in the middle of the flexiPERM chamber, then 100000 osteoblasts were seeded outside the flexiPERM ring and coated with ECBM (containing 15 % FCS, 1 % P/S, sodium heparin (10 µg/ml), bFGF (2.5 ng/ml)). After 4-5 h cells were adherent and the flexiPERM chambers could be removed carefully. Co-culture was kept for 21 days, changing medium every 3-4 days.

2.2.2.9 3-D culture in collagen type I gel matrix

Confluent cells were used for 3-D cultures in collagen type I gel matrix. The cells were trypsinised and cell number was estimated in a Neubauer cell counting chamber. On a 48-well plate, 150 µl of collagen type I gel matrix were used per well with a total cell number of 175000. The appropriate amount of cells per experiment was centrifuged in a sterile tube (1200 rpm, 5 min). Meanwhile the collagen gel matrix mixture was prepared. 50 % sterile distilled water (sdH_2O), 30 % collagen type I and 10 % M199 (10x) were mixed before 10 % collagen matrix (CM) buffer (10x) was added. The solution was mixed carefully until the colour changed from yellow to red/brown and kept on ice until being used. The pelleted cells were resuspended in collagen type I gel matrix solution and 150 µl were seeded in each well of a 48-well plate. The plate was incubated for 20 min at 37°C until a stable gel was formed. The wells were carefully covered with 300 µl of 37°C pre-warmed cell culture medium.

Some angiogenesis experiments were performed with endothelial cells in the collagen gel matrix and used osteoblast medium supernatants. The medium supernatants were centrifuged (1200 rpm, 5 min) to remove a possible contamination with dead cells and mixed 1:1 with fresh ECGM (containing 15 % FCS, 1 % P/S, sodium heparin (10 µg/ml), bFGF (2.5 ng/ml)). At different time points the angiogenic effects were documented by phase contrast microscopy and Calcein-AM staining (Section 2.2.3.1).

2.2.2.10 3-D culture in fibrin gel matrix

For 3-D cultures in fibrin gel matrix fibrinogen (20 mg/ml) and thrombin (200 U/ml) solutions were prepared in advance. The fibrinogen solution contained 4.5 g fibrinogen diluted in 255 ml ECBM medium without supplements. The mixture was dissolved at

37°C for 4 h with gentle shaking every 30 min. The solution was filtered (0.2 µm) and stored in aliquots at -20°C. 10000 Units of thrombin were dissolved in 50 ml ECBM supplemented with 0.1 % BSA, filtered (0.2 µm) and stored in aliquots at -20°C. Confluent cells were used for 3-D cultures in fibrin gel matrix. The cells were trypsinised (Section 2.2.2.2) and counted. On a 48-well plate, 150 µl of fibrin gel matrix were used per well with a total cell number of 175000. The appropriate amount of cells per experiment was centrifuged in a sterile tube (1200 rpm, 5 min). Cell pellets were resuspended in ECBM supplemented with 10 U/ml thrombin and 110 µl per well were seeded on a 48-well plate. 40 µl fibrinogen solution were added and kept at room temperature for 10 min.

2.2.3 Cytotoxicity assays

2.2.3.1 Calcein-AM cell viability assay

For determination of cell viability Calcein-AM cell viability assay was used. Cell culture medium was supplemented with 1 mM Calcein-AM and incubated at 37°C for 15 min. Viable cells were detected by fluorescence microscopy. In viable cells with intact membrane, internalised Calcein-AM is hydrolysed by an endogenous esterase into fluorescent calcein. The fluorescence was monitored by Leica IBRE microscope with a 485 nm excitation filter and 530 nm emission filter system.

2.2.3.2 Viability test with WST-1

The 2-(4-Iodophenyl)-3-(4-nitrophenyl)-5-(2,4-disulfophenyl)-2H-tetrazolium (WST-1) cell proliferation assay is based on the formation of formazan after cleavage of a tetrazolium salt by mitochondrial dehydrogenases in viable cells. The formazan level produced by viable, metabolically active cells following the addition of WST-1 can be quantified by the absorption of light at a monochromatic wavelength of λ=450 nm. The absorption is proportional to the number of living cells.

10000 cells were seeded per well in a 96-well plate and grown until 90 % confluence. Cell culture medium was removed and cells were washed twice with HEPES buffer supplemented with 0.2 % BSA. A mixture of cell culture medium and WST-1 was prepared (100 µl medium and 10 µl WST-1 stock solution per well), 120 µl were added per well

and incubated at 37°C. After 60 min 100 µl of the supernatant was transferred to a new 96-well plate and the absorption was measured at λ=450 nm in a microplate reader. For the calculation of the percent viability the blank (no cells with medium and WST-1 stock solution) was subtracted from all measured values.

2.2.4 Protein biochemical methods

2.2.4.1 ELISA

The enzyme-linked immunosorbent assay (ELISA) was used for analysis of factors released by cells into the cell culture medium supernatants. Cells were grown in co- and monocultures on petri dishes. The used cell culture medium was collected and stored at -80°C or used directly for ELISA.

Released growth factors in cell culture medium were quantified using NUNC Maxisorp 96-well plates coated with 100 µl primary capture antibody (4 µg/ml diluted in tris(hydroxymethyl)aminomethane (Tris) buffer with 1 % BSA) at room temperature on a shaker (50 rpm) overnight. The plates were washed subsequently with PBS containing 0.05 % Tween 20. Blocking was performed with 100 µl BSA at room temperature for 1 h followed by another washing step. 100 µl of the diluted medium supernatants (dilution dependent on cell types and amount of cells in Tris with 1 % BSA) and standards were added to the wells. The plates were incubated at 37°C for 2 h to allow antibody binding. Standard dilutions are listed in Table 2.17. The plates were washed three times with PBS containing 0.05 % Tween 20. Biotinylated detection antibodies were first diluted in Tris buffer with 1 % BSA (20 ng/ml) before 100 µl of them were added to each well and incubated for 2 h. The plates were washed again three times with PBS containing 0.05 % Tween 20. For the detection of antibody-antigen complexes, 100 µl working dilution of streptavidin-HRP (1:200 in Tris buffer with 1 % BSA) were added to the wells and incubated for 1 h. After another wash step with PBS containing 0.05 % Tween 20, 100 µl of substrate solution (mixture

Table 2.17: ELISA standard dilutions

Growth factor	Standard stock solution	Dilution range
VEGF	110 ng/ml	62.5 - 2000 pg/ml
bFGF	80 ng/ml	31.25 - 1000 pg/ml
Endostatin	150 ng/ml	125 - 4000 pg/ml
HGF	480 ng/ml	125 - 8000 pg/ml
IGF-1	110 ng/ml	62.5 - 2000 pg/ml

of H_2O_2 and tetramethylbenzidine) were added and incubated for 20 min at room temperature. The reaction was terminated by addition of 50 µl 2 N H_2SO_4. The optical density (OD) was measured at $\lambda = 450$ nm with the wavelength correction at 540 nm. Based on dilutions of medium supernatants and standard curves, the concentrations of different cytokines were calculated.

2.2.4.2 EIA

Detection of intercellular adhesion molecule 1 (ICAM-1) and E-selectin expression in fixed cells was done by enzyme immunoassay (EIA). Cell culture medium was discarded and cells were fixed in 3.7 % paraformaldehyde (PFA) for 15 min. After being washed with PBS, the binding sites were saturated with 10x diluted blocking reagent with 1 % H_2O_2 to deplete the activity of endogeneous peroxidases at 37°C for 30 min. The primary antibody was diluted in blocking reagent and incubated with the samples at 37°C for 30 min with gentle shaking. Samples were subsequently washed three times with PBS supplemented with 0.025 % Tween 20. Biotinylated secondary antibody was added to washed samples and incubated at 37°C for 30 min with gentle shaking. After three more washing steps with PBS supplemented with 0.025 % Tween 20, samples were incubated with biotinylated streptavidin-HRP at 37°C for 1 h with gentle shaking. Samples were then washed six more times with PBS supplemented with 0.025 % Tween 20. The colourimetric reaction was initiated by addition of substrate solution and incubation at 37°C for 20 min, and terminated by addition of 3 M HCl. The mixture was transferred to a fresh 96-well microplate and OD was measured at $\lambda = 492$ nm. A mixture of substrate and stop solution served as blank.

2.2.4.3 Immunofluorescent staining of cell components

Immunofluorescent staining was performed using primary and secondary antibodies listed in Table 2.18. At the end of a 2-D experiment the cell culture medium was aspirated and cells were fixed in 3.7 % PFA for 15 min. Subsequently, the samples were washed three times with PBS and permeabilised by addition of 0.1 % Triton X-100 in PBS and incubation for 5 min. Afterwards, 4 wash steps with PBS (5 min each) were performed. Primary

Table 2.18: Antibodies for immunofluorescent staining

Antibody	Source	Dilution
Alexa 488 anti-mouse	goat	1:1000
Alexa 488 anti-rabbit	donkey	1:1000
Alexa 546 anti-mouse	goat	1:1000
Alexa 546 anti-rabbit	goat	1:1000
Alexa 594 anti-rabbit	donkey	1:1000
Anti-CD31	mouse	1:50
Anti-D2-40	mouse	1:20
Anti-E-selectin	mouse	1:2000
Anti-ICAM-1	rabbit	1:1000
Anti-ICAM-1	mouse	1:400
Anti-VE-Cadherin	mouse	1:100
Anti-vWF	rabbit	1:8000

or isotype control antibody (or phalloidin, dilution 1:40) was incubated with the cells in PBS containing 1 % BSA for 1 h at room temperature. Again, samples were washed four times with PBS for 5 min. Cells were incubated with fluorescently labelled secondary antibody in PBS with 1 % BSA for 1 h at room temperature in darkness. Cells were washed twice with PBS and cell nuclei were stained with 0.5 µg/ml 4',6-diamidino-2-phenylindole (DAPI) for 5 min. Finally, samples were washed and covered with mounting medium and glass coverslips. Before microscopical examination, samples were stored at 4°C. Fluorescence microscope and laser scanning confocal microscope (Leica DMRE) were used for detection and image capture.

2.2.4.4 Antibody array human angiogenesis

Soluble protein expression of angiogenesis-related proteins in different cell types was measured by an antibody array kit containing capture antibodies which are spotted in duplicates on a nitrocellulose membrane. The membranes were blocked with 2 ml array buffer 7 for 1 h at room temperature. Medium supernatants of Cal-72, MG-63 and SaOS-2 cultures were diluted 3:1 with array buffer 4 before 15 µl of a cocktail of biotinylated detection antibodies were added. The nitrocellulose membrane was incubated with the sample mixture over night at 4°C. Present protein/antibody complexes were bound by their cognate immobilised capture antibody on the membrane. Unbound material was washed away twice with wash buffer before the membrane was incubated with streptavidin-horseradish peroxidase (HRP) detection reagents for 30 min at room temperature. Chemiluminescence was detected, the light at each spot is proportional to the amount of protein bound.

2.2.4.5 Protein quantification by BCA assay

Protein concentration in media supernatants and cell lysates was measured by bicinchoninic acid (BCA) protein assay kit. It detects the reduction of Cu^{2+} to Cu^{+} in proteins that are present in alkaline environment by BCA which forms a violet BCA-Cu^{+} complex

with Cu^{+}. Proteins were extracted from cells by lysis with radioimmunoprecipitation assay (RIPA) buffer supplemented with fresh phenylmethanesulfonylfluoride (PMSF) and protease inhibitor cocktail for 10 min on ice. Lysates were centrifuged (1200 rpm, 5 min) at 4°C. The supernatants were used directly or stored at -20°C until usage. Lysed samples and BSA standards were diluted in PBS and transferred 25 µl each to a 96-well microplate. 200 µl of working reagent were added per well and incubated at 37°C for 30 min in darkness. The OD was measured at $\lambda = 550$ nm in a microplate reader and protein concentration was calculated from BSA standards.

2.2.4.6 DNA quantification in cell lysates

Quantification of DNA in cell cultures was done using Quanti-iT PicoGreen assay. PicoGreen is a fluorochrome that intercalates with double stranded DNA and changes absorption at $\lambda = 485$ nm proportional to the amount of DNA. Cells were first trypsinised, pelleted and resuspended in sdH_2O. They were deep frozen at -80°C and thawed before incubation for 15 min in an ultrasonic water bath to open the cell membranes. For quantification 28 µl sample were mixed with 100 µl tris-EDTA (TE) buffer in a 96-well microplate. PicoGreen solution was diluted 1:200 before 72 µl were added to each sample and incubated at room temperature for 10 min gently shaking in darkness. OD was measured at $\lambda = 485$ nm in a microplate reader. DNA concentration was calculated by DNA standard curve.

2.2.4.7 Quantification of ALP activity

Analysis of the osteogenic differentiation level was done by quantification of alkaline phosphatase (ALP) activity in cell culture supernatants. Colorless para-nitrophenylphosphate (pNPP) changes conformation to yellow para-nitrophenol (pNP) by ALP mediated dephosphorylation. 60 µl of a substrate solution containing 0.2 % pNPP, 1 M diethanolamin and 0.5 mM $MgCl_2$, pH 9.8 was mixed with 20 µl sample and standard in a 96-well microplate incubated at 37°C for 30 min before 80 µl stop solution (0.2 mM EDTA in aqueous NaOH (pH 8.0)) were added. OD was measured at $\lambda = 405$ nm in a microplate reader. ALP activity was calculated by comparison to the standard curve.

2.2.4.8 Quantification of mineralisation with alizarin red

Mineralisation of cell cultures was quantified by osteogenesis assay kit which uses alizarin red to bind crystalline calcium. The complex can be detected photometrically. Cell culture medium was aspirated from 2-D experiments, cells were fixed in 3.7 % PFA for 15 min and washed three times with PBS. 500 µl alizarin red solution were added and incubated at room temperature for 20 min. Cells were washed with sdH_2O until the colour cleared out and lysed with 400 µl 10 % acetate at room temperature for 30 min. The lysates were transferred into 1.5 ml tubes, vortexed and incubated at 85°C for 10 min in a heat block before being cooled on ice. To avoid clumps the samples were centrifuged (1200 rpm, 5 min), supernatants were transferred into fresh 1.5 ml tubes and neutralised with 150 µl 10 % ammonium hydroxide. Standard samples were diluted in ARS dilution buffer. 150 µl of all samples and standards were transferred into a 96-well microplate and OD was measured at $\lambda = 405$ nm in a microplate reader.

2.2.4.9 Quantification of Collagen

Collagen was quantified with Sircol soluble collagen assay. Cells were trypsinised, pelleted and resuspended in 1 ml pepsin (0.1 mg/ml 0.5 M acetic acid). The mixture was incubated at 4°C over night before 100 µl acid neutralising reagent was added. Further 200 µl cold isolation and concentration reagent were added and incubated at 4°C over night. Samples were centrifuged (maximum speed, 10 min), pellets were mixed with 1 ml dye reagent and incubated for 20 min at room temperature. After another centrifugation step (maximum speed, 10 min), 750 µl ice cold acid salt wash reagent were added to the pellet. Samples were centrifuged again (maximum speed, 10 min) before the pellets were drained carefully. 250 µl alkali reagent were added to blanks, standards and samples and vortexed until the dye dissolved. 200 µl of each mixture were transferred to a 96-well microplate. OD was measured at $\lambda = 555$ nm in a microplate reader.

2.2.4.10 Quantification of Calcium

Calcium was quantified by calcium OCP assay. 20 µl cell culture medium and standards were mixed with 120 µl reagent 1 and 120 µl reagent 2 in a 96-well microplate and

incubated for 5 min at room temperature with gentle shaking. OD was measured at $\lambda = 578$ nm in a microplate reader. Calcium amount was normalised to the amount of DNA and calculated by comparison to the standard as follows:

$$\delta A(sample)/\delta A(standard) \cdot 10 = mg/ml \tag{2.2}$$

2.2.4.11 FACS

The fluorescence-activated cell sorting (FACS) method allows analysing multiple factors in cell cultures on a single cell basis. Besides simple cell counting, different extracellular and intracellular molecules can be stained with antibodies linked to fluorescein isothiocyanate (FITC), phycoerythrin (PE) or allophycocyanin (APC) and quantified. Antibody isotypes served as controls and for definition of measurement parameters. Directly marked antibodies and corresponding isotypes are listed in Table 2.19. For each measurement 6000 - 10000 counts per approach were detected. Cells were trypsinised, pelleted and resuspended in 1 ml 3.7 % PFA. After incubation at room temperature for 15 min, cells were centrifuged (1200 rpm, 5 min) and resuspended in 100 µl PBS with 1 % BSA to saturate unspecific bonds. 10 µl antibody or corresponding isotype were added to each sample and incubated at 4°C for 20 min before 1 ml PBS was added. Samples were pelleted (8000 rpm, 5 min), resuspended in 350 µl PBS and transferred into FACS tubes. Measurement and analysis was done with Cell QuestPro and Prism GraphPad.

Table 2.19: FACS antibodies and isotypes

Antibody	Isotype control
CD146-PE	Mouse IgG1-PE
CD34-FITC	Mouse IgG2a-FITC
CD31-APC	Mouse IgG1-ABC

2.2.4.12 SDS-PAGE

Cell culture medium supernatants and protein extracts were separated by SDS-PAGE according to molecular weight (Laemmli, 1970). Polyacrylamide gels consisted of 10 % resolving and 4 % stacking gel. Resolving gel solution was cast between two glass plates and overlayed with n-butanol to ensure optimal polymerisation by a protecting layer against aerial oxygen. n-Butanol was removed and stacking gel solution was cast on top of the resolving gel. Pipetting scheme and buffer composition are given in Table 2.20.

Table 2.20: SDS-PAGE buffer and gel composition for two gels

buffer	composition		resolving gel 10 %	stacking gel 4 %
R-buffer	Tris pH = 8.8	1.5 M	2.50 ml	-
S-buffer	Tris pH = 6.8	0.5 M	-	2.50 ml
bis-/acrylamide	acrylamide bis-acrylamide	29.2 % 0.8 %	3.33 ml	1.33 ml
SDS Stock	SDS	10.0 %	0.1 ml	
APS	APS	10.0 %	60.0 µl	80.0 µl
TEMED	TEMED	6.63 M	5.0 µl	10.0 µl
sdH_2O			4.0 ml	6.0 ml
sample buffer	glycerol β-ME SDS bromophenol blue Tris	10.0 % 5.0 % 2.0 % 0.012 % 62.5 mM		

A comb was inserted between the glass plates in order to get wells after polymerisation. Samples were diluted if necessary, mixed 1:4 with loading buffer and denatured at 95°C for 5 min before being loaded to the wells of the stacking gel. Electrophoresis was carried out in sodium dodecyl sulfate (SDS) running buffer at 25 mA per gel. After electrophoretic separation the polyacrylamide gel was transferred into ethanol acetic acid with coomassie G250 staining solution (Table 2.21) for chemical precipitation and protein staining. The gel was incubated in the staining solution for 1 h with gentle shaking. Unbound coomassie dye was removed by washing the gel in sdH_2O.

Table 2.21: Acrylamide gel staining solution

Solution	Component	Concentration
Staining solution	Ethanol	30.0 %
	Acetic acid	10.0 %
	Coomassie brilliant blue G250	0.10 %

2.2.4.13 Western blot

For protein analysis by western blot, proteins were transferred to a nitrocellulose membrane after sodium dodecyl sulfate polyacrylamide gel electrophoresis (SDS-PAGE). The membrane, gel and six sheets of filter paper were equilibrated in SDS transfer buffer (Table 2.6) and stacked in layers. The gel was put on top of the membrane and covered with three sheets of wet filter paper from each side. The stack was covered with wet sponges and put vertically into the PROTEAN Mini transfer chamber orientating the membrane to the anode. The chamber was cooled with ice to reduce thermic development, and filled

with SDS transfer buffer. Transfer of proteins from the gel to the membrane was carried out for 1 h at 350 mA. Protein transfer was controlled by Ponceau S staining, which was rinsed out with PBS. Unspecific binding sites were saturated by incubation of the membrane in blocking solution (Table 2.6) at room temperature for 1 h. Incubation with primary antibody diluted in blocking solution was done at room temperature for 2 h or at 4°C over night. Subsequently the membrane was washed twice with PBS containing 0.2 % Tween 20 for 5 min to remove unbound antibody and incubated with correspondent HRP linked secondary antibody at room temperature for 2 h. After three more washing steps with PBS containing 0.2 % Tween 20 for 5 min each, the antibody bound to the protein of interest was detected with enhanced chemiluminescence (ECL) detection reagents and high performance chemiluminescent film. For analysis of the same membrane with another antibody, it was stripped twice in stripping buffer (Table 2.6) at room temperature for 20 min to remove previous antibodies. Antibody binding procedure was repeated with the needed antibody.

2.2.4.14 TCA precipitation of proteins

Proteins from medium supernatants were precipitated by trichloroacetic acid (TCA) precipitation. Samples were mixed 4:1 with 100 % TCA and incubated for 10 min at 4°C. They were pelleted by centrifugation (maximum speed, 5 min) and washed with ice cold acetone supplemented with bromophenolblue until the colour indicated a neutral pH. Samples were dried in a heat block to remove acetone and used for SDS-PAGE.

2.2.4.15 Albumin depletion from cell culture medium

Albumin depletion from cell culture medium was performed by passing the supernatants through an affinity resin comprising antibodies against albumin, covalently attached to an inert sepharose matrix. The columns were equilibrated twice with 0.5 ml of dilution buffer by gravity flow. The diluted samples (1:4 in PBS) were applied to the column and incubated for 5 min at room temperature with gentle shaking. The colums were centrifuged (500 xg, 10 s) and washed twice with 100 µl PBS, always collecting the flow-through which was used for SDS-PAGE.

2.2.4.16 Mass spectroscopy

Protein identification was performed by mass spectroscopic analysis (Matrix-assisted laser desorption/ionization (MALDI)-time of flight (TOF)) in the Augenklinik, University Medical Centre, Mainz. Cell culture medium supernatants were segmented by SDS-PAGE. Proteins were fragmented, ionised and analysed regarding their relative molecular mass. Proteins can be identified by characteristic peptide fingerprints. Medium supernatants were used for SDS-PAGE and segmented by cutting each lane of the gel into the same number of pieces. Each piece was incubated for 5 min in 300 µl of 50 mM $NH_4(CO_3)_2$ by shaking at room temperature. Supernatants were discarded and samples were dried in a speedvac for 1 h at 37 °C. These wash steps were repeated three times or more until all coomassie blue staining was washed out.

Rehydration was done by incubation for 1 h at 56 °C in 100 µl 10 mM DTT in 100 mM $NH_4(CO_3)_2$ solution. Supernatants were discarded and gel pieces were incubated in 100 µl of a 100 mM $NH_4(CO_3)_2$ buffered 55 mM 2-iodoacetamide solution for 45 min in darkness. These steps were repeated three times to ensure a quantitative removal of disulfide bonds. For restriction samples were incubated in 50 µl of 1 % trypsine solution buffered in 50 mM $NH_4(CO_3)_2$ first for 45 min on ice, then for 16 h at 37 °C. After incubation, all supernatants were collected and incubated with the solutions listed in Table 2.22 (Shevchenko et al., 2006). Supernatants were concentrated by speedvac to a volume of 20±5 µl and incubated with 5 µl of 0.4 % trifluoroacetic acid. The C_{18} matrix of a 10 µl ZipTip pipette tip was activated by pipetting 3 times 10 µl of 100 % trifluoroacetic acid. Peptides were bound to the matrix by pipetting 20 times. The matrix was washed three times with 0.1 % trifluoroacetic acid solution. Elution was done by pipetting three times 5 µl of aquous 60 % acetonitrile solution. Samples were kept in -80 °C until measurement.

Table 2.22: Elution buffers for trypsin restriction of gel samples

Solution	Chemical	Concentration
A	$NH_4(CO_3)_2$	25 mM
B	formic acid	5 %
	acetonitrile	50 %
C	acetonitrile	100 %

Ionisation of peptide fragments was done on α-cyano-4-hydroxycinnamic acid matrix. This matrix is the standard for small peptides and laser with 337 and 355 nm wavelengths. The use of a reflector flight tube enhanced signal selectivity (Lottspeich et al., 2008). The

α-cyano-4-hydroxycinnamic acid matrix was prepared on the carrier plate by pipetting the samples on the plate before mixing them with 2 µl of a 0.2 % α-cyano-4-hydroxycinnamic acid solution (50 % acetonitrile and 0.2 % trifluoroacetic acid). The mixture was dried at 37 °C and analysed in a MALDI LTQ Orbitrap XL spectrometer (Thermo Scientific). Calibration was done by Proteo Mass MALDI Calibration Kit for LT QXL and LTQ hybrids (200 - 4000 Da). Mass spectroscopic measurement was done by shooting each spot 10 times with 25 µJ. The impulse responses were filtered for significant signals and fragmented by collision-induced dissociation.

2.2.5 Molecular genetic techniques

2.2.5.1 Isolation and quantification of DNA

Genomic DNA was isolated using DNeasy Blood and Tissue Kit. Cell pellets obtained after trypsinisation were resuspended in 200 µl PBS and ribonucleic acids (RNA) were digested by addition of 20 µl RNase A (10 mg/ml) for 2 min. Subsequently, 20 µl proteinase K and 200 µl buffer AL were added and samples were incubated at 70°C for 10 min to open the cell membranes. DNA was precipitated by 200 µl of 100 % ethanol. The mixture was applied onto the DNeasy Mini spin column and centrifuged (8000 rpm, 1 min). Membrane-bound DNA in the column was washed with 500 µl buffer AW1 and centrifuged (8000 rpm, 1 min). It was washed with 500 µl buffer AW2 and centrifuged (14000 rpm, 3 min). DNA was eluted from columns by 50 µl TE buffer (1 min at 8000 rpm).

The DNA concentration was measured with a NanoDrop ND1000 spectrophotometer. 1 µl eluted DNA was used to determine DNA concentration. Absorptions at the wavelengths $\lambda = 260$ nm and $\lambda = 280$ nm were measured to investigate the purity of samples. Pure DNA has an absorption quotient ($OD_{260/280}$) of 1.8. Water was used as blank and for synchronisation of the NanoDrop system. The concentration of DNA was calculated by the NanoDrop software as follows:

$$c[g/ml] = OD_{260nm}/extinction\ coefficient \cdot layerthickness \tag{2.3}$$

An extinction coefficient of 1 equals 50 ng $\cdot$ µL^{-1} DNA. The DNA was stored at -20°C.

2.2.5.2 Isolation and quantification of RNA

RNA isolation was carried out using the RNeasy Mini Kit from Qiagen. The kit was used according to recommendations by the manufacturer. Cell pellets obtained after trypsinisation were lysed with RLT buffer containing β-mercaptoethanol (β-ME) (10 µl per 1 ml buffer). If not processed immediately the cell lysates were stored at -80°C. RNA was precipitated with 1 volume of 70 % ethanol and loaded onto an RNeasy spin column. The samples were centrifuged (8000 rpm, 15 s). 350 µl RW1 buffer were added to the column and centrifuged again (8000 rpm, 15 s). DNA bound to the membrane was digested for 15 min with DNase I. 350 µl RW1 buffer was added to the column and centrifuged (8000 rpm, 15 s). The membrane was subsequently washed twice with RPE buffer (centrifugation at 8000 rpm, 15 s, 2 min) and dried by centrifugation (8000 rpm, 1 min). RNA was eluted in 30 µl RNase-free sdH_2O by centrifugation (8000 rpm, 1 min).

Quantification of RNA concentration was done photometrically using a NanoDrop ND1000 spectrophotometer. 1 µl eluted RNA solution was used to determine the RNA concentration. Absorptions at wavelengths $\lambda = 260$ nm and $\lambda = 280$ nm were measured to determine purity of samples. Pure RNA has an absorption quotient ($OD_{260/280}$) of 2.0. Water was used as blank and to synchronise the NanoDrop system. The concentration of RNA was calculated by NanoDrop software as follows:

$$c[g/ml] = OD_{260nm}/extinction\ coefficient \cdot layerthickness \tag{2.4}$$

An extinction coefficient of 1 equals 40 ng $\cdot$ µL^{-1} RNA. RNA was directly used for cDNA synthesis or stored at -80°C.

2.2.5.3 cDNA-synthesis via RT-PCR

1 µg RNA was reverse transcribed into complementary deoxyribonucleic acid (cDNA) using Omni-Script reverse transcription polymerase chain reaction (RT-PCR) Kit. Sample volume was adjusted to 10 µl and 2 µl random primers (0.1 µg/µl) were added to RNA. 8 µl of a mastermix containing 2 µl buffer (10×), 2 µl 0.1 M DTT, 2 µl dNTP Mix (5 mM each)

Table 2.23: RT-PCR scheme and program

Pipetting scheme	RT-PCR program
x µl RNA (1 µg) 2 µl 10x buffer 2 µl dNTP mix (5 mM/dNTP) 2 µl oligo dT Primer (10 µM) 1 µl RNAse inhibitor (10 U/µl) 1 µl Omniscript adjust to 20 µl with H_2O	synthesis: 37°C, 1 h inhibition: 70°C, 15 min storage: -20°C

were added to each sample. The reaction was carried out at 42°C for 50 min. It was stopped by heating the samples to 70°C for 15 min. The pipetting scheme is depicted in Table 2.23. After RT-PCR samples were stored at -20°C.

2.2.5.4 Polymerase chain reaction

After RNA isolation and cDNA synthesis expression of different genes in various cell types was studied by the polymerase chain reaction (PCR). Different gene-specific oligomers were designed with ApE and the genescript.com homepage, checked by BLAST NCBI (Altschul et al., 1990) and purchased from Eurofins MWG Operon. Primers are listed in Table 2.10. PCR was done using the Taq PCR core kit, according to the pipetting scheme and PCR program in Table 2.24. After PCR amplification the reaction mixture was diluted with sample buffer. DNA fragments were separated by gel electrophoresis on a 2 % agarose gel containing 0.02 % ethidium bromide (80 Volt for 1 h in 1 % tris-borate-EDTA (TBE)-buffer).

Table 2.24: Pipetting scheme and PCR program

Pipetting scheme	template (diluted 1:20 in sdH_2O) buffer (10x) dNTP mix (5 mM each dNTP) forward primer (1:10) reverse primer (1:10) Taq polymerase (10 U/µl) sdH_2O	2 µl 2.5 µl 0.5 µl 2.5 µl 2.5 µl 0.125 µl 14.875 µl	
PCR program	94°C	2 min	1 cycle
	94°C 60°C 72°C	30 s 30 s 30 s	35 cycles
	72°C	10 min	1 cycles
	4°C	until being used or storage at -20°C	

For size determination of DNA fragments a 1 kilobase (kb) marker was used. Due to the intercalation of ethidium bromide into DNA double helices electrophoretically separated fragments can be visualised and monitored by ultra violet (UV) light. Images were obtained with a digital camera and colours were inverted by Adobe Photoshop CS5.

2.2.5.5 Cloning of podoplanin into pEGFP-N1 vector

Podoplanin was cloned into pEGFP-N1 vector with type II restriction enzymes. The construct was used to transfect SaOS-2 cells (Section 2.2.2.5). The gene was amplified by PCR from HDMEC using the primers *podoplaninEcoRI* and *podoplaninBamHI*. It was run on agarose gel electrophoresis and extracted from the gel using Qiaquick Gel Extraction Kit according to protocol to clean it from buffer salts. For optimisation of the site-directed integration of the podoplanin gene into the expression vector a sub-cloning process was applied. The gene was cloned into pJET1.2/blunt sub-cloning vector (Table 2.25) by ligation and transformation into chemically competent *E. coli* XL1-Blue.

Table 2.25: Blunt-end subcloning

20 µl preparation	
element	**volume**
10x blunting buffer	2 µl
50 ng PCR product	up to 7 µl
blunting enzyme	1 µl
sdH_2O	up to 18 µl
T4 DNA ligase	1 µl
pJET1.2/blunt vector [50 ng/µl]	1 µl

Ligation was done for 30 min at room temperature according to Table 2.27. The ratio of purified PCR product to pJET1.2/blunt vector was 1:4 to ensure an optimal transformation result. For heat shock transformation, 50 µl of chemically competent *E. coli* XL1-Blue were incubated with 25 fmol of the construct for 20 min on ice. After 45 s of heat shock at 42°C, the samples were resuspended in 200 µl lysogeny broth (LB)-medium and incubated for 90 min at 37°C with shaking.

Table 2.26: Restriction

20 µl preparation		**Thermal cycle conditions**		
element	**volume [µl]**	**process**	**temperature [°C]**	**time [min]**
10x FastDigest buffer	2	Incubation	37	5 - 60
DNA [1 µg]	1 - 5	Inactivation	80	2
sdH_2O	15 - 11	Cooling	4	∞
FastDigest EcoRI	1			
FastDigest BamHI	1			

The selection of successfully transformed bacteria was ensured by an ampicillin resistance gene on the pJET1.2/blunt vector. Samples were put on LB-agar petri dishes containing ampicillin and incubated at 37°C for 16 h. Only clones which carried the vector with integrate in the multiple cloning site (MCS) were able to grow. A double selection was performed by a gene that encodes for β-lactamase on the pJET1.2/blunt vector. It allowed selection of clones which were positively transformed. A lethal gene flanking the MCS permitted differentiation between clones which carried an integrate and those that

did not. The clones were screened by PCR. Positive clones were cultivated and plasmids were purified by Qiagen Plasmid Mini Kit. Podoplanin-carrying pJET1.2 plasmids and pEGFP-N1 vector were then restricted by EcoRI and BamHI (Table 2.26).

The enzymatically digested samples were cleaned, using MinElute Reaction Cleanup Kit. Ligation was done by incubation for 30 min at room temperature according to Table 2.27. Chemically competent *E. coli* XL1-Blue were transformed by heat shock transformation with the construct. 50 µl of competent *E. coli* XL1-Blue were incubated with 25 fmol of the construct for 20 min on ice. After 45 s of heat shock at 42°C, the samples were resuspended in 200 µl LB-medium and incubated for 90 min at 37°C with shaking. Selection of successfully transformed bacteria was ensured by a kanamycin resistance gene on the pEGFP-N1 vector. The samples were put on a LB-agar petri dish containing kanamycin and incubated at 37°C for 16 h. Positive transformation was tested by colony PCR. The plasmids of positive clones were purified using the Qiagen Plasmid Mini Kit, sequenced by the Sanger sequencing method and used for transfection of SaOS-2 cells (Section 2.2.2.5).

Table 2.27: Ligation

20 µl preparation	
element	**volume [µl]**
2x reaction buffer	10
podoplanin	2
sdH_2O	6
pEGFP-N1 vector [50 ng]	1
T4 DNA Ligase [5 $U \cdot l^{-1}$]	1

2.2.5.6 Cell characterisation by PCR

Cells were characterised using PCR. They were grown to confluence, washed with PBS and detached by the addition of RLT buffer (RNeasy Mini Kit from Qiagen) with 10 % β-ME. RNA was isolated and transcribed to cDNA. Cell and gene specific primers were used for the characterisation of cells by PCR.

2.2.5.7 Quantitative real-time polymerase chain reaction

The quantitative real-time polymerase chain reaction (qPCR) method was done using SYBR Green DNA-binding fluorescent dye. For one reaction 3.75 ng cDNA were used. 12.5 pmol of each 3´ and 5´ primers were mixed with cDNA and the volume was adjusted to 12.5 µl with sdH_2O. 12.5 µl SYBR Green mastermix were added, resulting in a total volume of 25 µl. qPCR was performed in triplicate for each cDNA sample.

PCR amplification was carried out in an Applied Biosystems 7300 Real-Time PCR System. The reaction conditions were 10 min at 95°C, followed by 40 amplification cycles (15 s at 95°C and 1 min at 60°C). At the end, DNA dissociation was performed by slow elevation of the temperature from 60°C to 95°C. After each PCR cycle the amount of SYBR Green that intercalated into the double helix of the DNA was measured and plotted. As endogeneous standard, different unregulated genes were used dependent on experimental setup. Data were analysed with SDS software to obtain cycle threshold (Ct) values.

Relative gene expression was determined with the ΔΔCt method using 18s RNA as endogenous control. Briefly the Ct value of the endogenous control was subtracted from the Ct value of the gene studied to obtain the ΔCt value. ΔCt of the control sample was subtracted from ΔCt of the experimental sample to obtain the ΔΔCt value. Relative expression was calculated with the formula $2^{-\Delta\Delta Ct}$. Data are presented as means of relative expression, error bars indicate 95 % confidence interval. For statistical analysis one-way analysis of variance (ANOVA) for independent samples was performed on ΔΔCt values (Yuan et al., 2006). To take into account possible differences in PCR efficiencies data were additionally analysed with the REST method (Pfaffl, 2004) using LinRegPCR Software (Ramakers et al., 2003) to determine efficiencies of single PCR reactions.

2.2.6 Statistical analysis

All experiments were repeated at least three times. Results are presented as means with standard deviation (SD). Statistical analysis was carried out with Microsoft Excel and GraphPad Prism software. Where possible, results were normalised to the amount of DNA or cells. If possible, the student t-test was applied to test hypotheses.

Results

3.1. Characterisation of human osteoblasts . . . 54
3.1.1. Human primary osteoblasts . . . 54
3.1.1.1. pOB growth and morphology . . . 54
3.1.1.2. Osteogenic differentiation and matrix mineralisation . . . 55
3.1.2. Human osteosarcoma cell lines . . . 56
3.1.2.1. MG-63 . . . 57
3.1.2.2. Cal-72 . . . 57
3.1.2.3. SaOS-2 . . . 58
3.1.3. Effects of media on osteoblast growth and differentiation . . . 58
3.1.4. Comparison of osteosarcoma cell lines expressing GFP . . . 62
3.2. Characterisation of endothelial cells . . . 65
3.2.1. HDMEC . . . 65
3.2.2. HUVEC . . . 66
3.2.3. Umbilical artery endothelial cells . . . 66
3.2.4. Lymphatic and vascular populations of endothelial cells . . . 66
3.3. Angiogenesis-inducing potential of osteoblasts in co-culture with EC . . . 68
3.3.1. Angiogenesis in 2-dimensional co-cultures . . . 68
3.3.2. 3-D co-cultures of endothelial cells and osteoblasts . . . 71
3.3.3. Angiogenic effects of osteoblast cell culture medium supernatants . . . 72
3.3.4. Transcriptional analysis of angiogenesis-related factors in osteosarcoma cell lines . . . 78
3.3.5. Effects of bFGF on angiogenesis . . . 80
3.3.6. Release of HGF and VEGF in osteosarcoma cell lines . . . 82
3.3.7. Correlation between HGF and endostatin . . . 84
3.3.8. Effects of podoplanin on angiogenic potential of osteoblasts . . . 84
3.3.8.1. Cloning and transfection of SaOS-2 cells with podoplanin . . . 85
3.3.8.2. Podoplanin expressing SaOS-2 cells . . . 87
3.4. Mass spectroscopy on used media supernatants . . . 89
3.4.1. Gel-electrophoretic separation of cell culture supernatants . . . 89
3.4.2. Mass spectroscopy . . . 90

3.1 Characterisation of human osteoblasts

Prior to co-culture experiments, the cell phenotypes had to be characterised. This was important to ensure that only well characterised cell types were used, to identify any contaminating cells and to enable reliable conclusions to be drawn from the experiments. For cell characterisation experiments, cells were counted after isolation and used after confluency was reached. Important features used to characterise human osteoblasts were cell morphology, protein expression and potential to induce the formation of micro-capillary structures in co-culture systems.

3.1.1 Human primary osteoblasts

For the characterisation of pOB from cancellous bone fragments the aforementioned parameters were analysed. In addition, osteogenic differentiation and matrix mineralisation were assessed, as these are also important characteristics of pOB. The osteoblastic markers, ALP, collagen and calcium, are parameters for osteogenic differentiation as well as matrix mineralisation, thus these markers were used for cell characterisation of pOB.

3.1.1.1 pOB growth and morphology

The morphology of pOB in *in vitro* culture was largely similar between different bone fragment donors and growth conditions. However, variation was seen in growth rates, dependent on the donor, origin of the bone fragments and growth conditions. In turn, these parameters were dependent on the age, health condition and disease history of the donor as well as variations in cell culture handling. Before reaching confluence, the

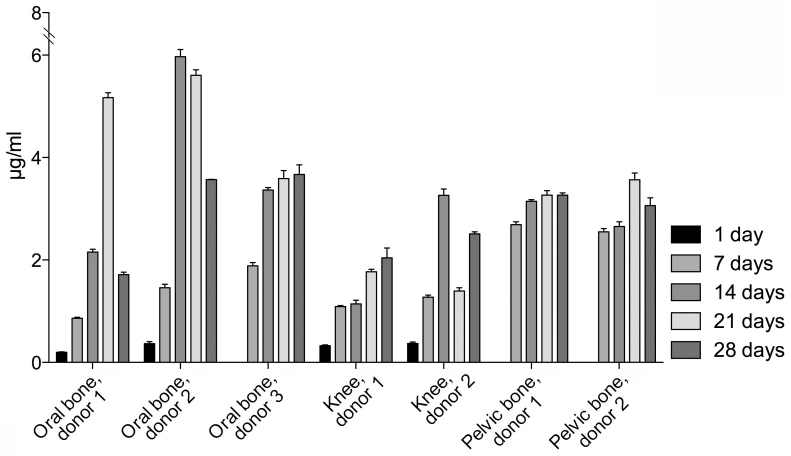

Figure 3.5: **DNA quantification in pOB cultures**
DNA quantification in monocultures of pOB from oral bone, knee and pelvic bone after 1, 7, 14, 21 and 28 days in DMEM.

typical morphology of pOB was cuboidal with a large central nucleus. A confluent monolayer of pOB showed a slightly different morphology with cells having a more polygonal appearance (data not shown).

pOB from different donors demonstrated different growth rates. Growth rates in monocultures of pOB from different donors were measured by DNA quantification over time. Each sample in the experiment began with the same number of confluent cells. The results showed that cell samples from some donors grow fastest between day 14 and day 21 (oral bone donor 1) whereas others grow fastest between day 7 and day 14 (oral bone donor 2 and knee donor 2) (Figure 3.5). Whilst the amount of DNA remained stable after 28 days in cultures from most of the pOB donors, it decreased in oral bone donor 1 and 2.

3.1.1.2 Osteogenic differentiation and matrix mineralisation

pOB from different donors and origins of bone fragments varied in the expression of osteogenic differentiation markers and matrix mineralisation. This is examined by comparing cells with respect to the activity of ALP and the amount of collagen and calcium produced at different time points (1, 7, 14, 21 and 28 days) in DMEM medium (Figure 3.6). Mineralisation of the cell monolayer was analysed at the same time points. All data were normalised to the amount of DNA in the cell cultures.

The results showed a lower ALP activity in pOB from pelvic bone than in pOB from knee and oral bone. One pOB donor from oral bone showed considerably less ALP activity than the other donors. In pOB from oral bone the peak ALP activity was between day 14 and 21 while knee pOB had increased activity at day 28 of the cell culture. The amount of collagen in oral bone pOB culture increased at day 21. In contrast, the amount of collagen increased in pelvic bone pOB culture at day 28. Knee pOB produced the lowest levels of collagen except for donor 2, which showed a peak in the amount of collagen at day 28, similar to pelvic bone pOB. The amount of calcium produced by the cells also illustrated differences between the different sources and donors. The two donors of oral bone pOB produced higher levels of calcium than the third donor, that showed a lower amount of calcium similar to pelvic bone pOB. The cells from knee bone had an increased calcium level at day 28 of cell culture. The highest calcium level of oral bone pOB appeared

between day 14 and 21 and it subsequently dropped at day 28. The mineralisation levels of the cell layers were similar in pOB from knee and pelvic bone in all donors. In contrast, the oral bone pOB showed strong differences in mineralisation between the donors. Donor 1 had peak mineralisation at day 21 while donor 2 reached saturation at day 14. Oral bone pOB from donor 3 showed the highest level of mineralisation at day 28.

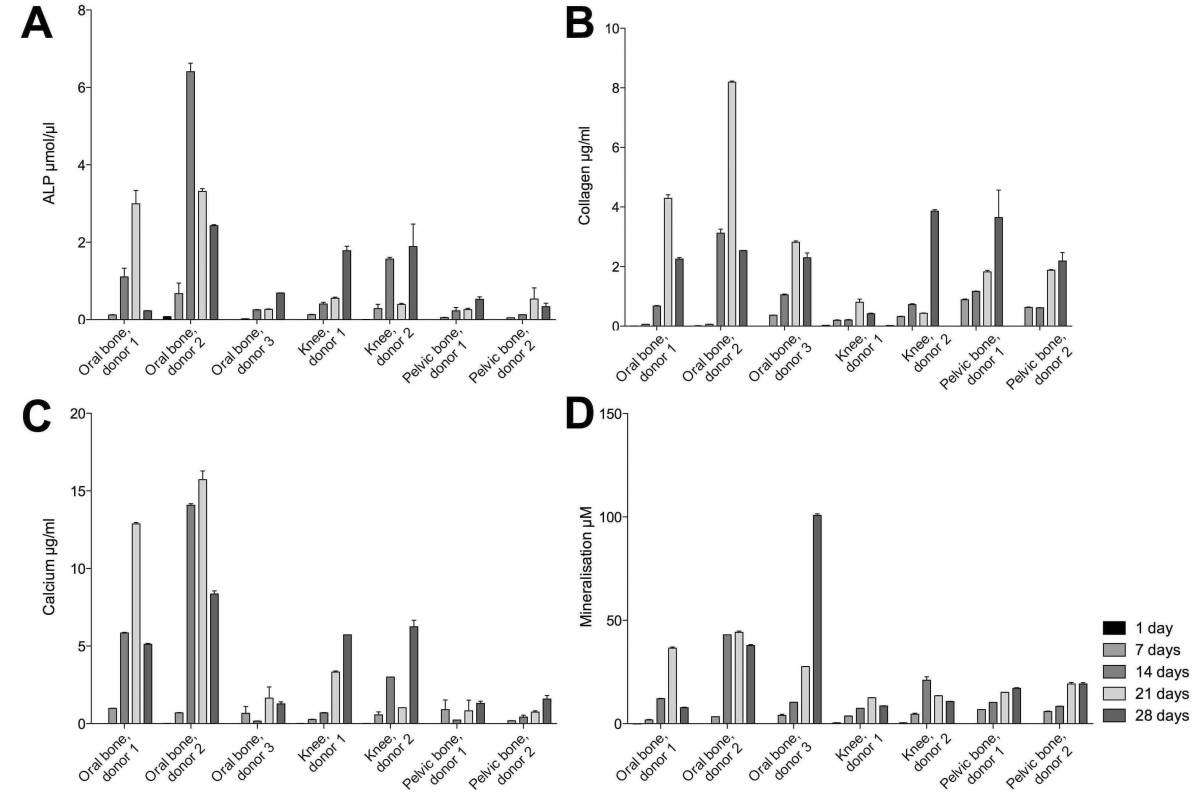

Figure 3.6: **Quantification of osteogenic differentiation markers in pOB cultures**
Quantification of osteogenic differentiation markers (**A** ALP activity, **B** collagen, **C** calcium) and **D** matrix mineralisation in monocultures of pOB from oral bone, knee and pelvic bone after 1, 7, 14, 21 and 28 days in DMEM. All data were normalised to the amount of DNA.

In summary, the pOB from different origin of bone fragments and donors differed with respect to growth rates and osteogenic differentiation markers. The results revealed no predictable tendencies between the cells and culture durations.

3.1.2 Human osteosarcoma cell lines

The osteosarcoma cell lines, MG-63, Cal-72 and SaOS-2, have osteoblast-like cell morphology. In monolayer culture they have a similar morphology to spindle-shaped fibroblasts and exhibited multilayer growth when confluence is exceeded. After several passages,

the morphology changed to a flat cell body with radial branches (data not shown). Unhealthy or dying cells detached and appeared spheroidal.

MG-63, Cal-72 and SaOS-2 were obtained from different biological resource centres. Before being used in studies, the confluent cells were passaged once and cultured for a further 3 to 4 days. In a prior study (Günther, 2009), each cell line was transfected with GFP, and cloned. This allows tracking and identification in cultures with mixed cell types. For the characterisation of osteosarcoma cell lines, the same parameters were analysed as for the pOB. In addition to osteogenic differentiation and matrix mineralisation markers, various growth factors were also examined.

3.1.2.1 MG-63

The MG-63 cell line is derived from an osteogenic sarcoma of a 14-year-old male child (Heremans et al., 1978). Cells of the MG-63 line have a typical osteoblast-like morphology, that changes with confluence of the monolayer from a spindle-like cell profile to a flat cell body with radial branches. The GFP-transfected cell line exibited a similar morphology (data not shown). Results for ALP activity, collagen and calcium production and matrix mineralisation of the cell monolayer are described in Section 3.1.3 (Figure 3.7). In the standard cell culture medium (DMEM) MG-63 cells exhibited an increasing ALP activity over time, reaching a peak at day 21. The collagen and calcium production as well as matrix mineralisation also increased over time with the highest levels reached on day 28.

3.1.2.2 Cal-72

The Cal-72 cell line was isolated from an osteosarcoma of the knee obtained from a 10-year-old boy (Rochet et al., 1999). Cal-72 cells showed a typical osteoblast-like cell morphology that changed with confluence of the monolayer from a spindle-like cell profile to a flat cell body. The cell morphology was similar in the GFP-transfected cells (data not shown). Results for ALP activity, collagen and calcium production and matrix mineralisation of the cell monolayer are described in Section 3.1.3 (Figure 3.7). Cal-72 cells showed a very low ALP activity in DMEM over time. Maximum collagen production was reached on day 14, and decreased from day 21 to 28. Cal-72 produced calcium from day 14, reaching

a peak at day 21. The matrix mineralisation of Cal-72 increased until day 14 and remained at this level until day 28.

3.1.2.3 SaOS-2

Similar to the other osteosarcoma cell lines mentioned above, SaOS-2 cells also exhibited the typical osteoblast-like morphology. The appearance of SaOS-2 cells also changed with confluence of the monolayer from a spindle-like cell profile to a flat cell body. The GFP-transfected SaOS-2 exhibited a similar cell morphology to the SaOS-2 cells (data not shown). Results for ALP activity, collagen and calcium production and matrix mineralisation of the cell monolayer are described in Section 3.1.3 (Figure 3.7). In DMEM, SaOS-2 cells demonstrated an increasing level of ALP activity over time. Maximum collagen production was reached on day 21. SaOS-2 cells produced calcium from day 14, reaching a peak at day 21. Matrix mineralisation of the cell layer increased from day 7 to day 28.

3.1.3 Effects of media on osteoblast growth and differentiation

Standard cell culture of osteoblasts differs from cell culture of endothelial cells with respect to the medium used. Osteoblasts are cultured in DMEM, while endothelial cells need ECGM for cell proliferation and viability. Since ECGM is used for co-cultures of endothelial cells and osteoblasts, the osteogenic differentiation markers and matrix mineralisation were compared in both media with the osteosarcoma cell lines and pOB. All data were normalised to the quantification of DNA in the cell cultures.

In osteosarcoma cell lines the activity of ALP and the production of collagen, calcium and matrix mineralisation was measured at different time points (1, 7, 14, 21 and 28 days) in DMEM and ECGM (Figure 3.7). The ALP activity showed significant differences ($p < 0.05$) between both media in all cell lines. For Cal-72 and MG-63 cells the differences were detected after 21 and 28 days of cell culture, respectively. In SaOS-2 cell culture, the media made a significant difference to ALP activity after 28 days. The ALP activity was higher in ECGM than in DMEM for Cal-72 and MG-63 cells. SaOS-2 cells showed significantly higher ($p < 0.001$) ALP activity in DMEM.

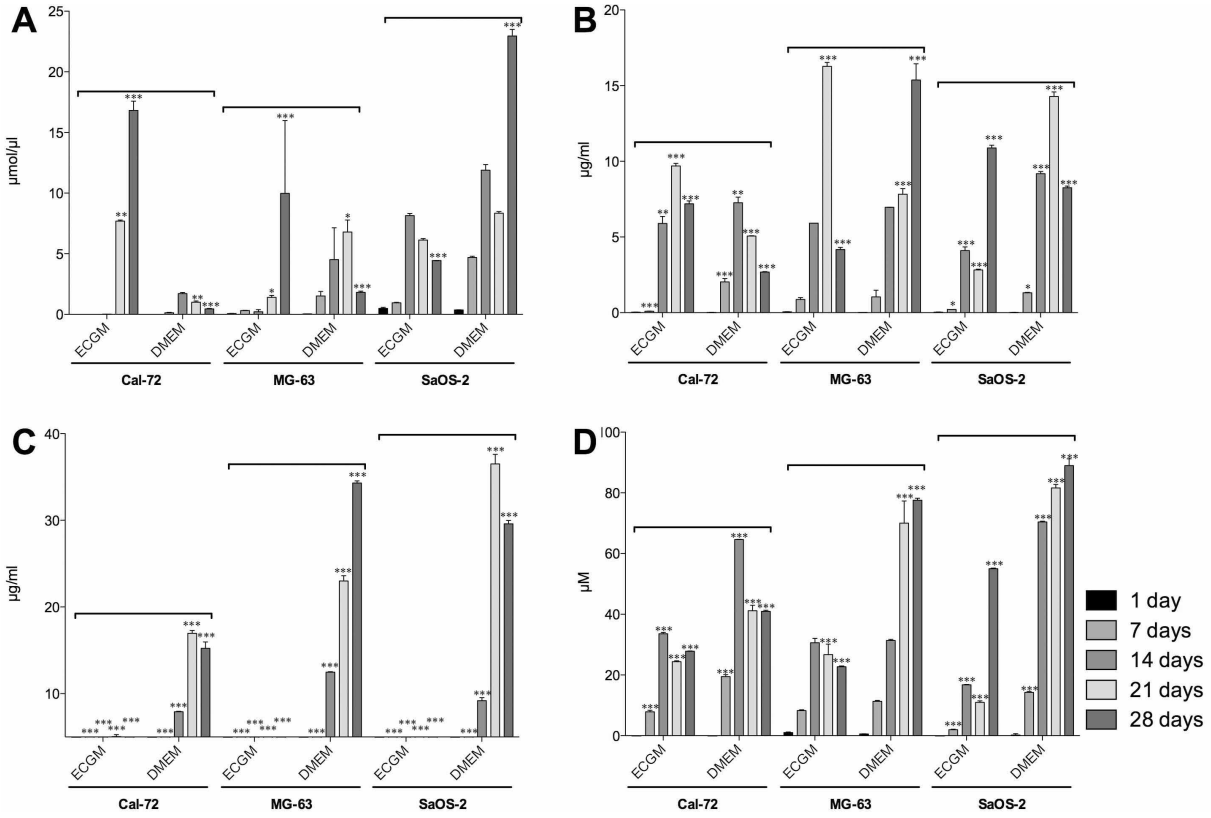

Figure 3.7: **Quantification of osteogenic differentiation markers in osteosarcoma cell lines** Quantification of osteogenic differentiation markers (**A** ALP activity, **B** collagen, **C** calcium) and **D** matrix mineralisation in monocultures of osteosarcoma cell lines after 1, 7, 14, 21 and 28 days in DMEM and ECGM. All data were normalised to the amount of DNA and analysed by two-way ANOVA (*: p value < 0.05, **: p value < 0.01, ***: p value < 0.001).

The amount of collagen produced was significantly different for DMEM and ECGM in all osteosarcoma cell lines. In Cal-72 cell culture, the collagen expression was significantly higher ($p < 0.01$) in DMEM than in ECGM at day 7 and day 14 time points. On day 21 and 28 of the cell cultures, the amount of collagen increased in ECGM compared to DMEM.

MG-63 cells showed significant differences between both media after 21 and 28 days. After 21 days, the amount of collagen was higher in ECGM while it was higher in DMEM after 28 days of cell culture. For SaOS-2 cells, significant differences could be seen at all time points. The cells had a tendency to produce more collagen in DMEM than ECGM until day 21. After 28 days, the collagen production in ECGM was higher. The amount of calcium produced by the cells in both media showed highly significant differences at all time points. All cell lines had increased calcium production in DMEM compared to

very small amounts produced in ECGM. This may have been due to different medium composition. The matrix mineralisation of the osteosarcoma cell lines was significantly different between the media. In all cell lines, mineralisation was higher in DMEM than ECGM at the majority of the measured time points.

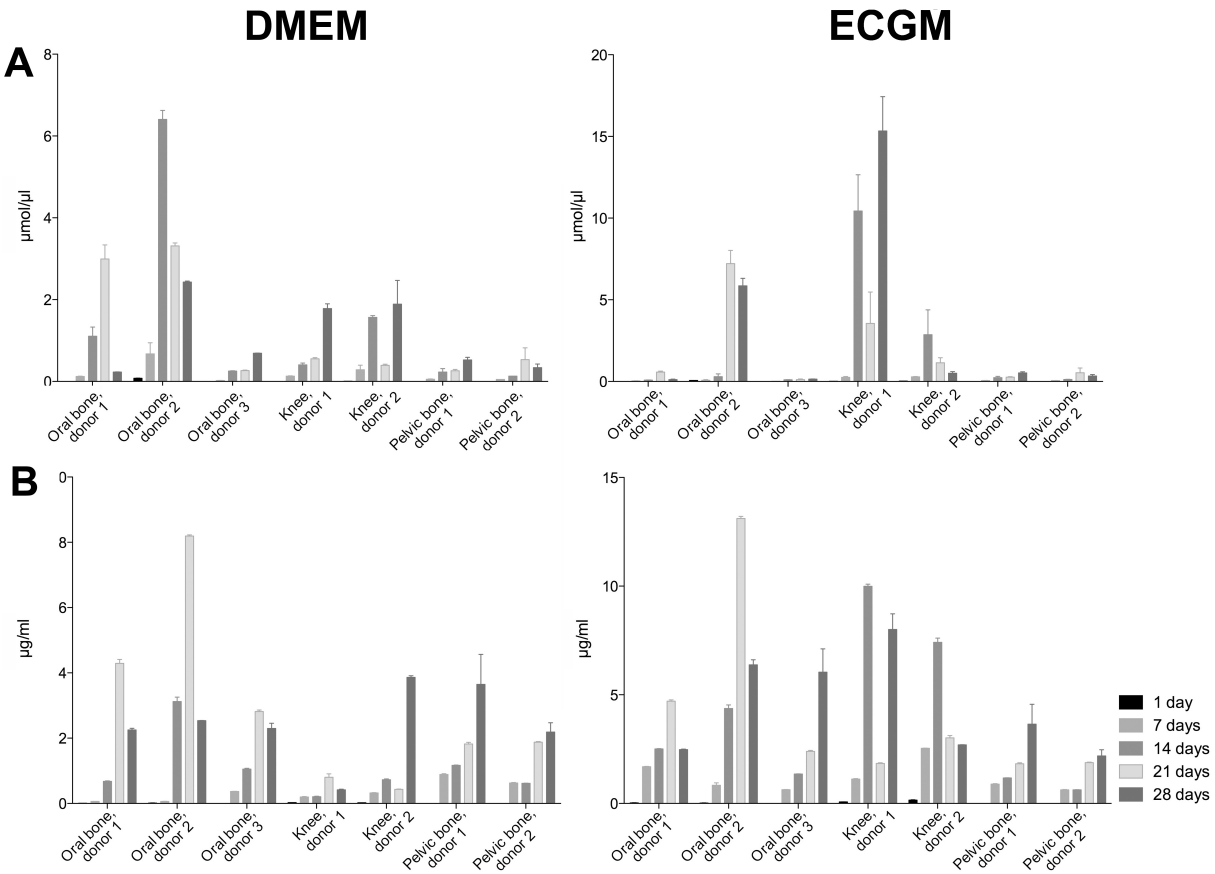

Figure 3.8: **ALP activity and collagen quantification in pOB cultures**
Quantification of **A** ALP activity and **B** collagen in monocultures of of pOB after 1, 7, 14, 21 and 28 days in DMEM and ECGM. All data were normalised to the amount of DNA.

In pOB the activity of ALP and the production of collagen, calcium and matrix mineralisation was also measured at different time points (1, 7, 14, 21 and 28 days) in DMEM and ECGM (Figures 3.8 and 3.9). The activity of ALP in both media differed, dependent on the donor and source of osteoblasts. In DMEM, oral bone donors 1 and 2 as well as both knee donors had a higher ALP activity after 21 and 28 days of culture than the other pOB. In ECGM, only oral bone donor 2 and knee donor 1 had detectable ALP activity. The levels of ALP activity differed between media from 2 to 7 mol/l in DMEM and 5 to 15 mol/l in ECGM. The amount of collagen produced differed in knee pOB.

Donor 1 showed a low level of collagen production at all time points in DMEM while donor 2 expressed an increased collagen level at day 28 in DMEM and at day 14 and 28 in ECGM. The levels of collagen production differed between the media from 1 to 8 µg/ml in DMEM and 1 to 14 µg/ml in ECGM.

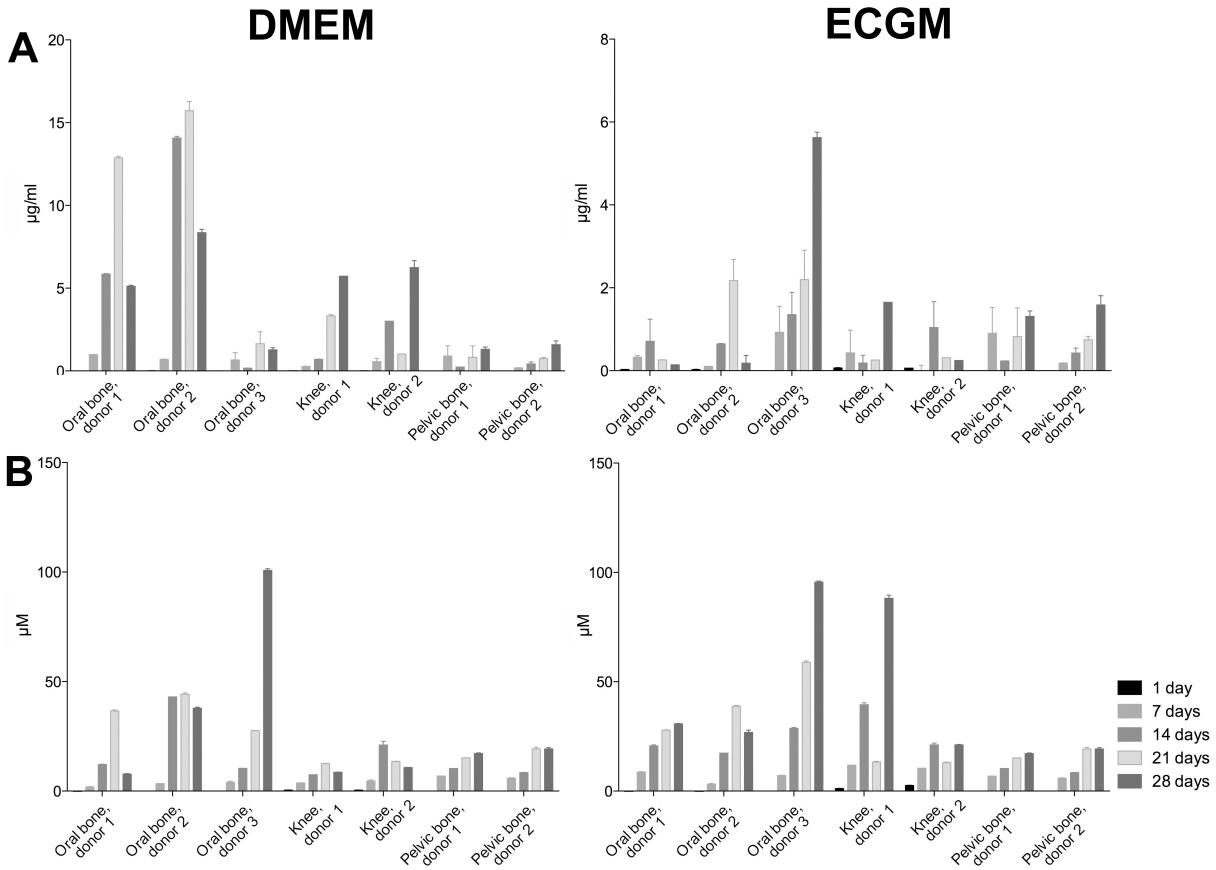

Figure 3.9: **Calcium and matrix mineralisation quantification in pOB cultures**
Quantification of **A** calcium and **B** matrix mineralisation in monocultures of pOB after 1, 7, 14, 21 and 28 days in DMEM and ECGM. All data were normalised to the amount of DNA.

In contrast to ALP activity and collagen production, the amount of calcium in DMEM was higher than in ECGM. Concentrations of calcium differed from 1 to 17 µg/ml in DMEM and 1 to 6 µg/ml in ECGM. The highest calcium levels were reached by oral bone and knee donors 1 and 2 in DMEM. These cells showed less calcium production in ECGM. In contrast, in oral bone donor 3 cell culture an increasing amount of calcium was measured in ECGM over time while these cells showed nearly no calcium production in DMEM. The mineralisation of pOB cell layers was almost homogeneous in both media. Only knee donor 1 mineralised more in ECGM after 14 and 28 days than in DMEM.

In summary, the results showed significant differences in osteosarcoma cell lines cultured in ECGM or DMEM. With respect to ALP activity Cal-72 and MG-63 showed higher levels in ECGM than in DMEM whereas SaOS-2 cells showed higher ALP activity in DMEM. All cell lines produced more calcium and mineralised matrix in DMEM compared to ECGM. For pOB from different origin of bone fragments and donors, the results for osteogenic differentiation markers in both media differed with no predictable tendencies between the cells and cell cultures durations.

3.1.4 Comparison of osteosarcoma cell lines expressing GFP

In addition to morphological comparison, GFP-expressing and parental osteosarcoma cell lines were compared with respect to viability, proliferation, growth factor release and ALP activity. This was carried out before GFP-expressing osteosarcoma cell lines were used for co-culture experiments to determine whether both cell lines exhibited similar characteristics.

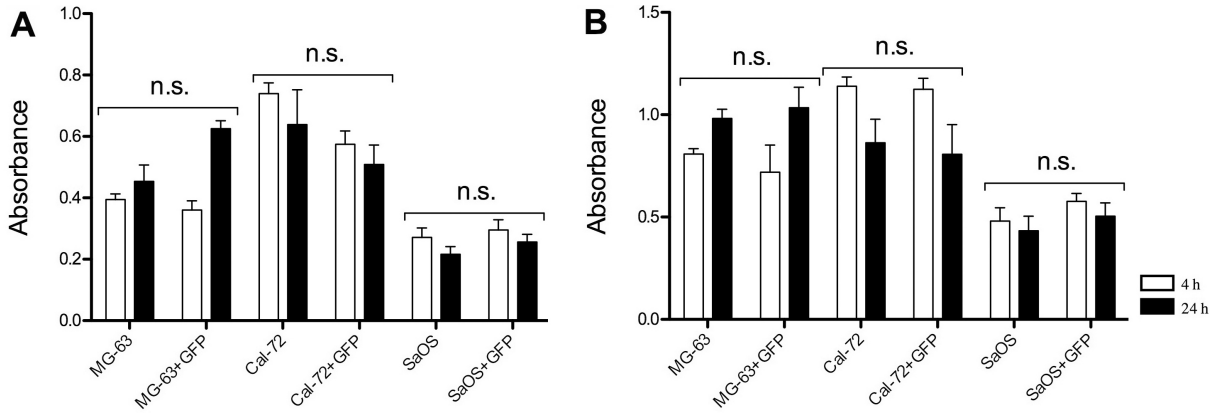

Figure 3.10: **WST-1 assay on osteosarcoma cell line cultures**
WST-1 assay on GFP-expressing and normal osteosarcoma cell line cultures at 4 and 24 hours. The experiment was set up using **A** 10000 cells and **B** 20000 cells. Student's t-test analysis showed no significant differences (n.s., $p < 0.05$) between GFP-expressing and normal cell lines.

WST-1 assay was used as a tool to study cell viability and proliferation. The experiment was set up using 10000 cells and 20000 cells for each cell line and subsequently analysed at 4 and 24 hours. The results demonstrated no significant difference in terms of cell viability and proliferation ($p < 0.05$) between GFP-expressing and normal cell lines (Figure 3.10). However, a comparison of different cell lines showed SaOS-2 cells had lower proliferation rates than MG-63 and Cal-72 cells.

In order to compare GFP-expressing and parental osteosarcoma cell lines, osteogenic differentiation markers and matrix mineralisation were quantified. The activity of ALP and the production of collagen, calcium and matrix mineralisation were measured at different time points (1, 7, 14, 21 and 28 days) in GFP-expressing and parental osteosarcoma cell line cultures (Figure 3.11). All data were normalised to the amount of DNA in the cell cultures and analysed using Student's t-test.

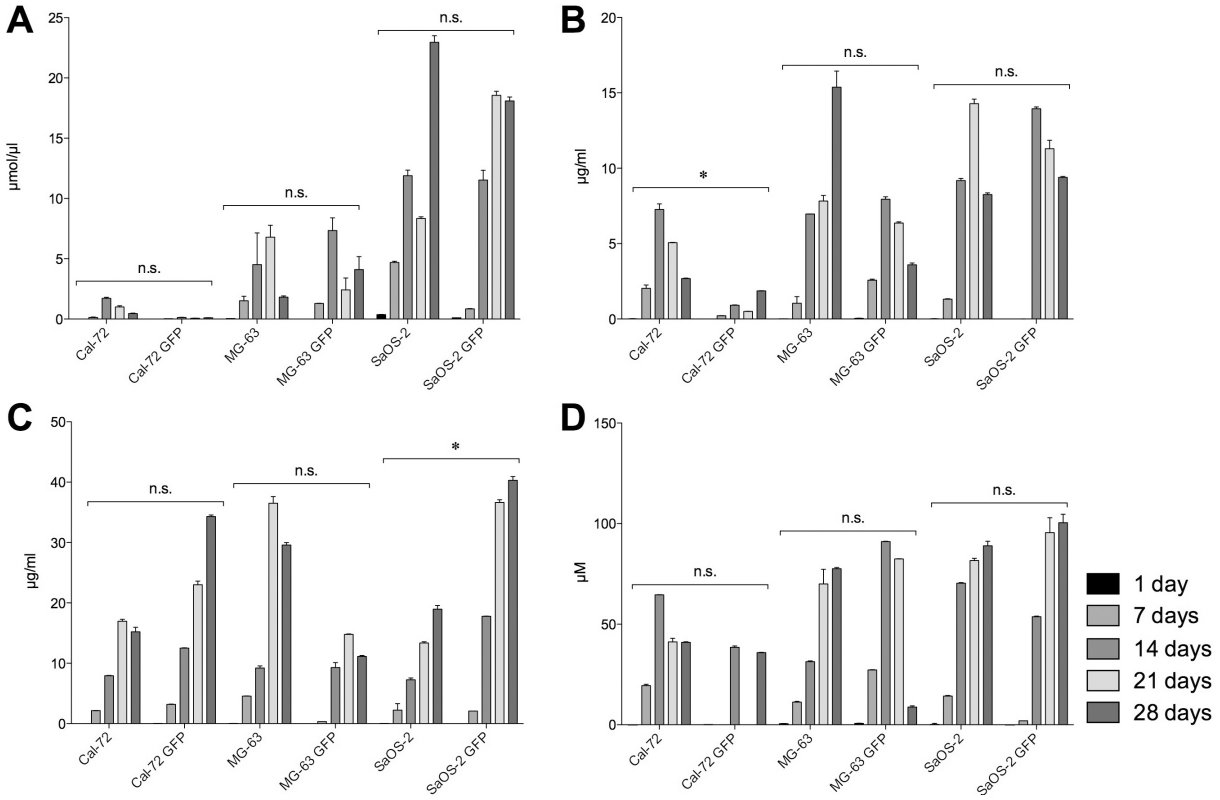

Figure 3.11: **Quantification of osteogenic differentiation markers in GFP-expressing and normal osteosarcoma cell lines**
Quantification of osteogenic differentiation markers (**A** ALP activity, **B** collagen, **C** calcium) and **D** matrix mineralisation in monocultures of GFP-expressing and normal osteosarcoma cell lines after 1, 7, 14, 21 and 28 days in DMEM. All data were normalised to the amount of DNA. Significant differences ($p < 0.05$) are marked with (*), not significant results are labeled (n.s.).

No significant differences were found between GFP-expressing and parental osteosarcoma cell lines for ALP activity. Comparing the different cell lines with each other, SaOS-2 cells showed greater ALP activity compared to Cal-72 and MG-63, and MG-63 had greater activity than Cal-72. With respect to collagen production, GFP-expressing Cal-72 cells showed a significant decrease in production compared to normal Cal-72 cells. MG-63 and SaOS-2 cells showed no significant differences in their GFP-expressing counterparts.

Calcium production in Cal-72 and MG-63 was not significantly different when comparing GFP-expressing and normal cell lines. In contrast, GFP-expressing SaOS-2 cells produced significantly more calcium than normal SaOS-2 cells. No significant difference was found in matrix mineralisation between GFP-expressing and parental osteosarcoma cell lines.

As bFGF and VEGF are known to be involved in the formation of new blood vessels (Cross and Claesson-Welsh, 2001; Leung et al., 1989), both factors were quantified by ELISA in GFP-expressing and parental osteosarcoma cell lines (Figure 3.12). All data were normalised to the amount of DNA in the cell cultures.

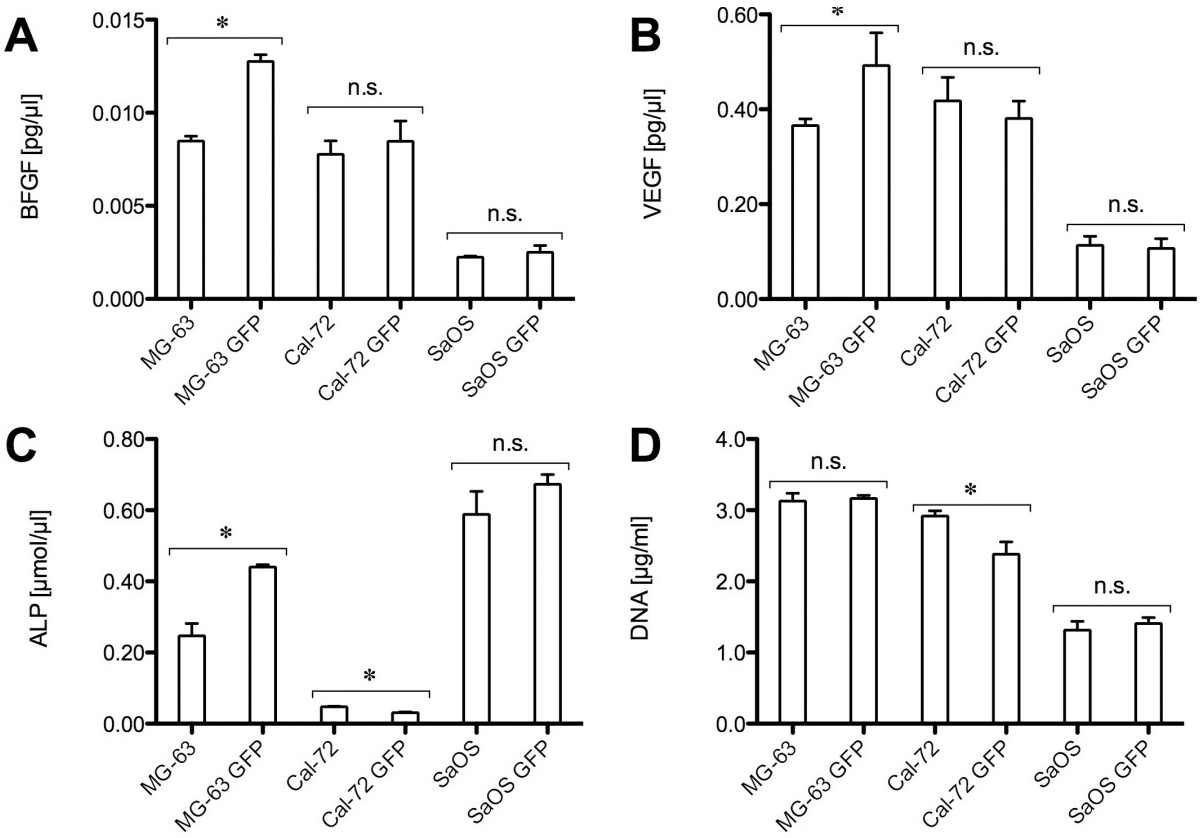

Figure 3.12: **Quantification of growth factors, ALP and DNA in GFP-expressing and normal osteosarcoma cell lines**
Quantification of **A** bFGF, **B** VEGF, **C** ALP activity and **D** DNA by ELISA in GFP-expressing and normal osteosarcoma cell line cultures after 14 days in DMEM. All data were normalised to the amount of DNA showing significant (*: $p < 0.05$) and not significant results (n.s.).

A significant difference in the release of bFGF and VEGF was found between GFP-expressing and parental MG-63 cells. GFP-expressing MG-63 produced more bFGF and VEGF than normal MG-63. The other two cell lines showed no significant change

in the release of the growth factors. Comparing the cell lines, SaOS-2 cells were found to secrete considerably less bFGF and VEGF than MG-63 and Cal-72 cell lines. Significant alterations in ALP activity between GFP-expressing and normal cells were found in MG-63 and Cal-72 cell lines. The GFP-expressing MG-63 cell line had more active ALP than normal MG-63, while GFP-expressing Cal-72 cell line showed lower amounts of active ALP than parental Cal-72 cells.

In summary, GFP-expressing and normal osteosarcoma cell lines showed no significant differences with respect to cell viability and proliferation, ALP activity and matrix mineralisation. In terms of collagen production, GFP-expressing Cal-72 cells showed decreased amounts compared to normal Cal-72 cells, while MG-63 and SaOS-2 cells showed no differences compared to their GFP-expressing counterparts. GFP-expressing SaOS-2 cells produced significantly more calcium than normal SaOS-2 cells, while Cal-72 and MG-63 showed no differences when comparing GFP-expressing and normal cell lines. Results from growth factor quantification revealed that GFP-expressing MG-63 produced more bFGF and VEGF than normal MG-63, while the other two cell lines showed no change in the release of the growth factors.

3.2 Characterisation of endothelial cells

For a better understanding of co-culture systems, it was necessary to characterise endothelial cells, as they are also part of co-culture experiments for the study of angiogenesis. For cell characterisation experiments all cells were used in passage 2 once confluence was reached. Important features used to characterise human endothelial cells were cell morphology, expression of endothelial cell specific markers and micro-capillary formation in co-culture systems.

3.2.1 HDMEC

HDMEC are commonly used in *in vitro* studies and are thus very well characterised in the literature (Unger et al., 2002; Richard et al., 1998). The cells form a density-inhibited

monolayer with cobblestone-like morphology and exhibit a number of unique cell-specific characteristics, such as the expression of von Willebrand factor (vWF), CD31 and CD34. The cells have been previously described and characterised as cells with typical endothelial characteristics (Unger et al., 2002). For verification, after isolation the cells were analysed by control staining with CD31 (data not shown). The isolated HDMEC formed a density-inhibited monolayer with clear cell-cell contacts.

3.2.2 HUVEC

HUVEC are well characterised in the literature (Unger et al., 2002) and commonly used in *in vitro* studies. Similar to HDMEC, HUVEC form a density-inhibited monolayer with cobblestone-like morphology and express a number of endothelial-specific markers, such as vWF, CD31 and CD34 (Unger et al., 2002). After isolation the cells were verified by control staining with CD31 and analysed for the formation of the typical density-inhibited monolayer with clear cell-cell contacts (data not shown).

3.2.3 Umbilical artery endothelial cells

Umbilical artery endothelial cells are rarely described in the literature as isolation of HUVEC is more efficient and alternative arterial endothelial cells can be readily purchased (HCAEC) (Wei et al., 2013). As endothelial cells they have similar characteristics as HDMEC and HUVEC. Umbilical artery endothelial cells also form a density-inhibited monolayer with cobblestone-like morphology and exhibit a number of endothelial cell specific characteristics, such as the expression of vWF, CD31 and CD34. Once isolated a control stain with CD31 antibody was performed to verify the identity of the cells (data not shown). Microscopic analysis demonstrated that the isolated umbilical artery endothelial cells formed the typical density-inhibited monolayer with clear cell-cell contacts.

3.2.4 Lymphatic and vascular populations of endothelial cells

Depending on the source, endothelial cells may show two types of morphology within one population (Figure 3.13). In monolayer culture lymphatic endothelial cells form clusters

within vascular endothelial cells. The lymphatic endothelial cells exhibit the lymphatic cell marker D2-40 in addition to the endothelial cell marker CD31. Therefore they can be detected and distinguished from vascular endothelial cells by D2-40 immunofluorescent staining.

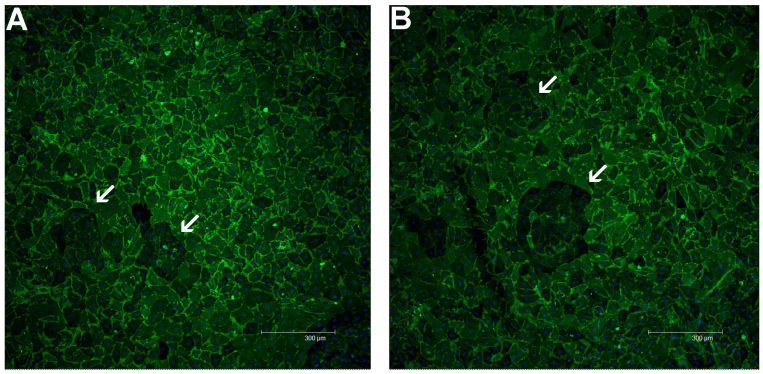

Figure 3.13: **HDMEC monolayer**
HDMEC monolayer (**A,B**) with different cell morphologies within one population, stained with CD31 after 21 days. Cell clusters are marked (↙). Cells were visualised by fluorescence microscopy.

The ratio between D2-40 positive and D2-40 negative cells was revealed by FACS analysis and showed differences between endothelial cells from different sources (Figure 3.14). In HUVEC no D2-40 positive cells were detected, while all other endothelial cell types expressed differing levels of the lymphatic marker. Oral mucosa endothelial cells had the lowest ratio of lymphatic to vascular endothelial cells. HDMEC and HCMEC showed similar D2-40 positive fractions. Cultures of HPMEC had an average of approximately 30 % lymphatic cells, but there was high deviation between donors. The highest ratio between lymphatic and vascular endothelial cells was found in ST1 and OEC.

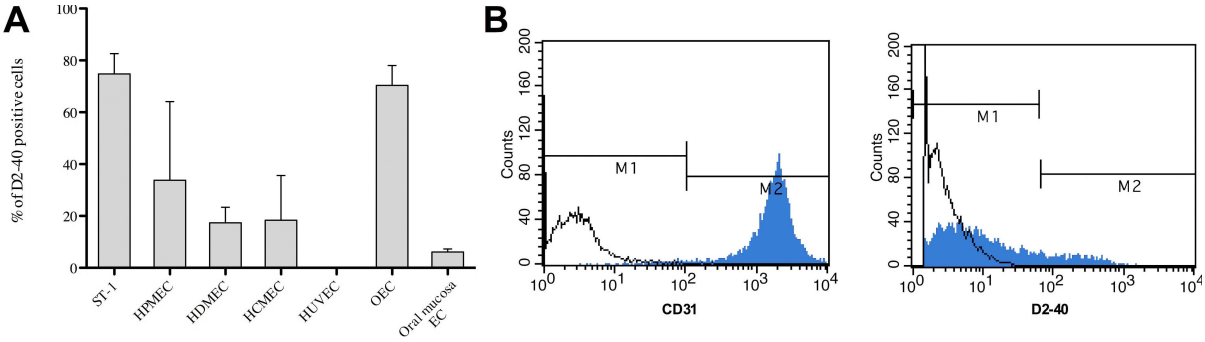

Figure 3.14: **Endothelial cell types and ratio of D2-40 positive to D2-40 negative cells**
A D2-40 positive cells in per cent. Cell origins are described in Table 2.12. **B** Histrogram plot of HDMEC; the complete list of histograms can be found in the appendix (Section A.1)

3.3 Angiogenesis-inducing potential of osteoblasts in co-culture with EC

One of the main functions of endothelial cells is the formation of new blood vessels. This process is important physiologically, for wound healing, and pathologically, it plays a central role in tumour growth. To analyse how osteoblasts can affect this specific function of endothelial cells, osteoblasts and endothelial cells were used in different co-culture systems. The co-culture systems varied in terms of cell combination, surface or scaffold. Furthermore, variable co-culture duration and medium composition were used in co-culture systems. The effects of media, growth factors and cell types on the formation of micro-capillary structures were assessed as a measure of angiogenesis. Immunofluorescent staining and microscopic analysis were used to detect the formation of angiogenic structures in co-cultures. Changes in gene and protein expression of the co-cultured cells were detected by qPCR and ELISA methods.

3.3.1 Angiogenesis in 2-dimensional co-cultures

The formation of micro-capillary structures by endothelial cells can be stimulated by the addition of pOB or osteosarcoma cell lines to endothelial cell cultures. Different osteoblast-like cells (pOB from oral bone, osteosarcoma cell lines) were compared regarding their angiogenesis-inducing potential. In 2-D co-cultures not all of the osteoblast-like cells showed the same angiogenesis-inducing potential. In this study, co-cultures of HDMEC with primary osteoblasts or osteosarcoma cell lines (Cal-72, MG-63 and SaOS-2) were performed over 21 and 28 days. The cultures were analysed by immunofluorescent staining with CD31 antibody and microscopic analysis.

Cal-72 and MG-63 demonstrated the strongest potential to stimulate endothelial cells to form micro-capillary structures (Figure 3.15A,B). The endothelial cells in these co-cultures showed elongated morphology, connecting each other by the formation of branches. Primary osteoblasts from most donors also had a strong tendency to induce angiogenesis, but formed shorter structures than Cal-72 and MG-63 (Figure 3.15D). In contrast, the co-cultures with SaOS-2 cells showed no formation of micro-capillary structures

in 2-D co-cultures with HDMEC (Figure 3.15C). As a negative control for these experiments, HDMEC were cultured in monoculture, without other cell types. The control showed no formation of micro-capillary structures.

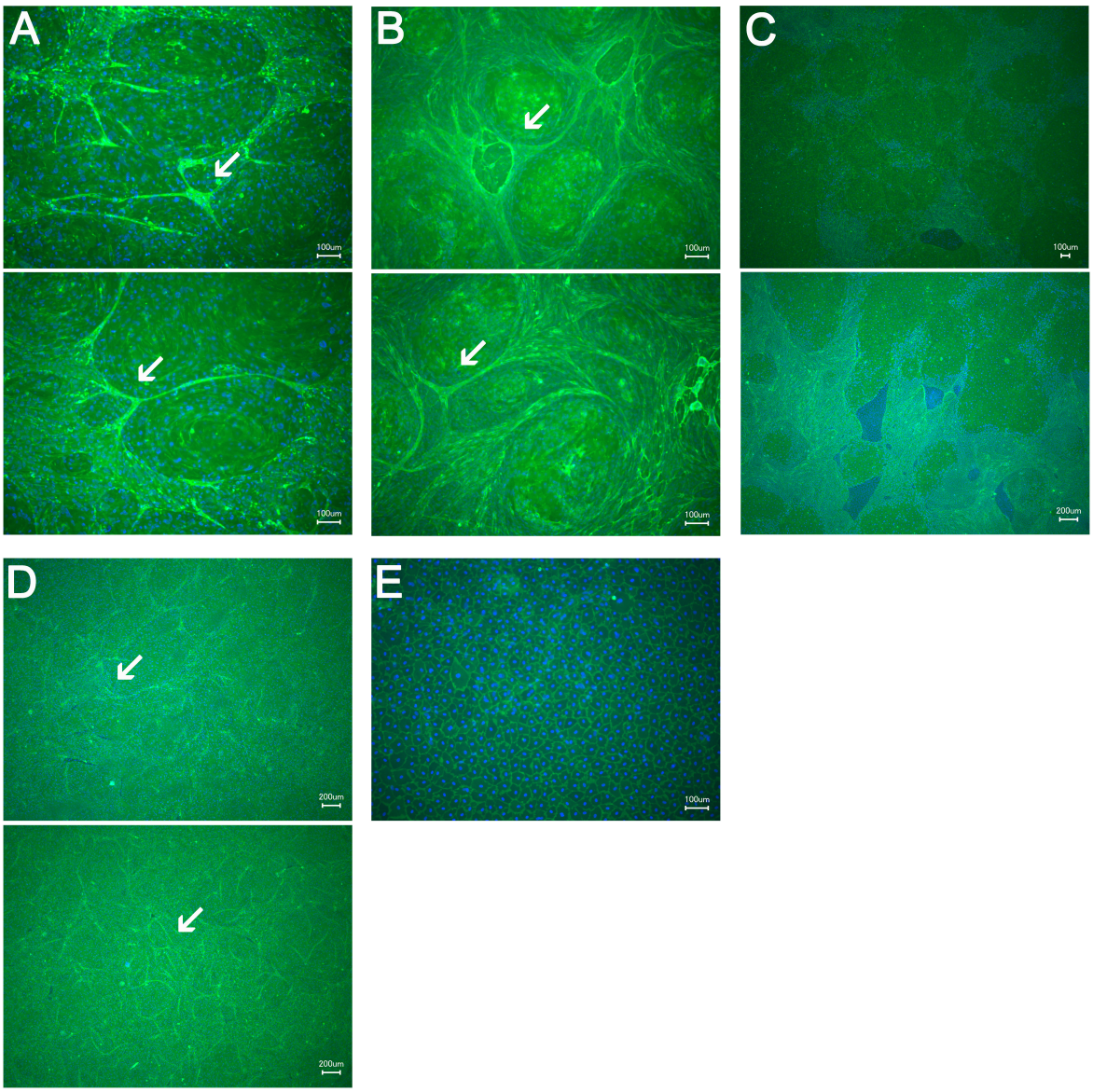

Figure 3.15: **2-D co-culture of HDMEC and osteoblasts**
2-D co-culture of HDMEC and osteoblasts (**A** Cal-72, **B** MG-63, **C** SaOS-2, **D** pOB) and **E** HDMEC monoculture after 21 days forming structures (↙). Cells were immunostained (CD31 antibody (green), DAPI (blue)) and monitored by laser scanning confocal microscopy.

GFP-expressing osteosarcoma cell lines showed similar results (Figure 3.16). GFP-expressing SaOS-2 cells showed no formation of micro-capillary structures in 2-D co-cultures with HDMEC (Figure 3.16C). Cal-72 and MG-63 demonstrated the strongest potential to stimulate endothelial cells to form micro-capillary structures (Figure 3.16A,B).

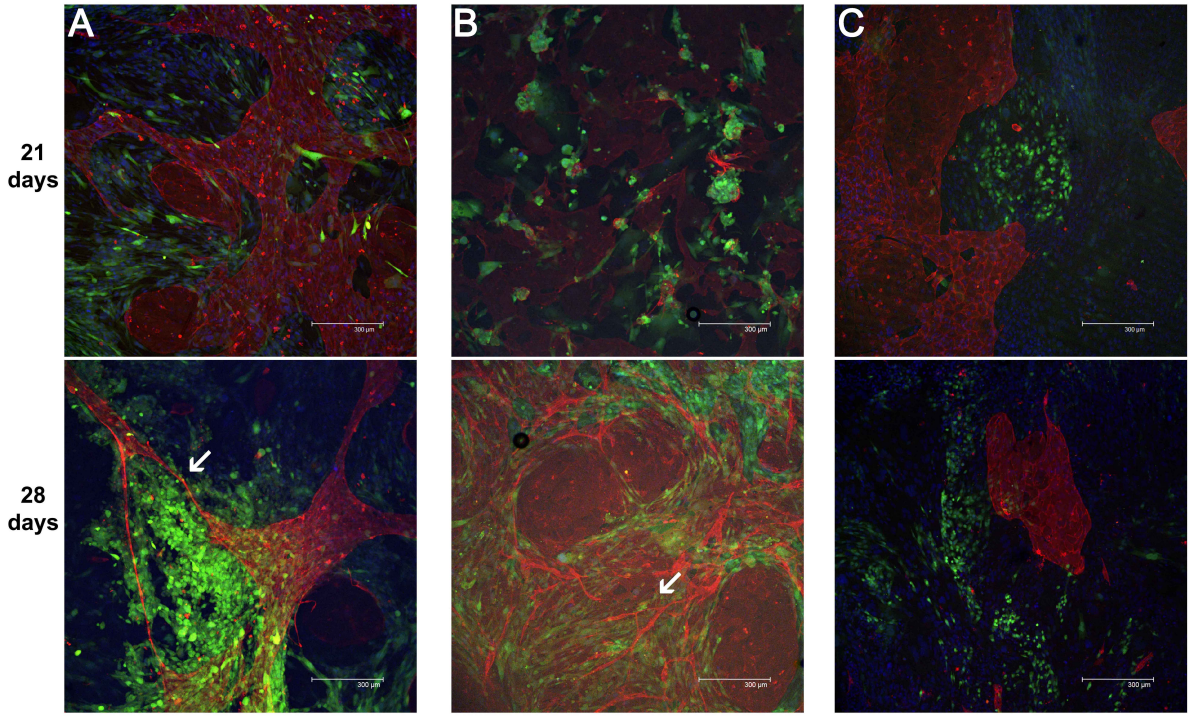

Figure 3.16: **2-D co-culture of HDMEC and GFP-expressing osteosarcoma cell lines**
2-D co-culture of HDMEC and GFP-expressing osteosarcoma cell lines (**A** Cal-72 GFP, **B** MG-63 GFP, **C** SaOS-2 GFP) after 21 and 28 days forming structures (↙). Cells were immunostained (CD31 antibody (red), DAPI (blue)) and monitored by laser scanning confocal microscopy.

2-D co-cultures of osteosarcoma cell lines with HUVEC and umbilical artery endothelial cells showed similar results as with HDMEC (Figure 3.17). Cal-72 and MG-63 cells demonstrated the strongest potential to induce the formation of micro-capillary structures compared to other osteoblast-like cells (Figure 3.17A,B). HUVEC have an elongated morphology, connecting each other by the formation of branches. The immunostained co-cultures showed that SaOS-2 cells did not induce angiogenesis in HUVEC or in umbilical artery endothelial cell co-cultures (Figure 3.17C).

In HUVEC, the formation of micro-capillary structures reached a point of plateau after 21 days. However, the co-cultures with umbilical artery endothelial cells showed enhanced formation of micro-capillary structures between 21 and 28 days.

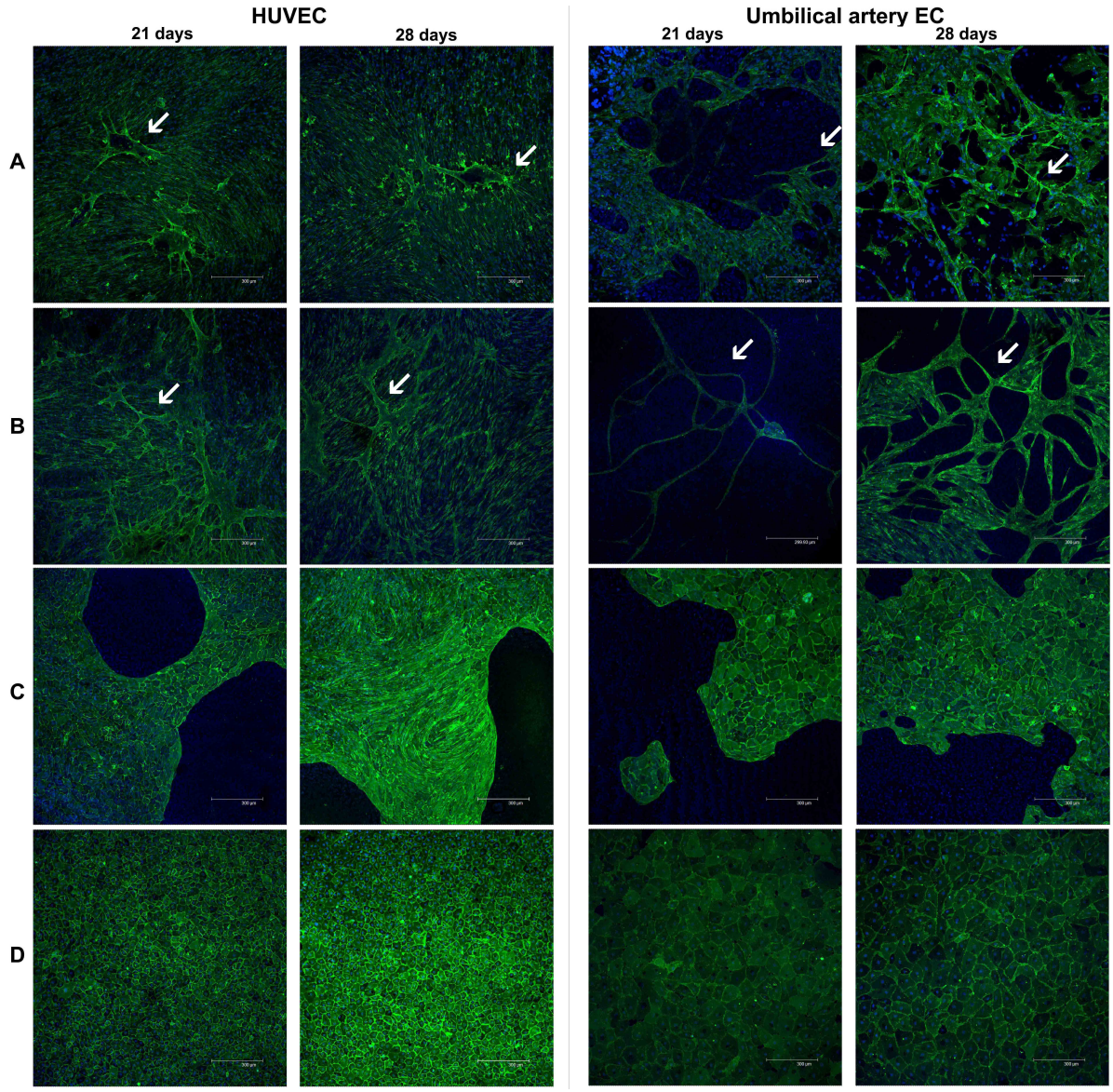

Figure 3.17: **2-D co-culture of umbilical endothelial cells with osteosarcoma cell lines**
2-D co-culture of HUVEC/umbilical artery endothelial cells and osteosarcoma cell lines (**A** Cal-72, **B** MG-63, **C** SaOS-2) and **D** monoculture controls after 21 and 28 days forming structures (↙). Cells were immunostained (CD31 antibody (green), DAPI (blue)) and monitored by confocal microscopy.

3.3.2 3-D co-cultures of endothelial cells and osteoblasts

Cells in 3-D co-cultures of endothelial cells with pOB or osteosarcoma cell lines may have different effects on the formation of micro-capillary structures compared to those in 2-D co-cultures. To determine whether the same occurs in 3-D co-cultures, pOB, osteosarcoma cell lines and endothelial cells were examined in a collagen gel and analysed in terms of the formation of micro-capillary structures. In 3-D co-cultures, not all osteoblast-like cells

showed the same angiogenesis-inducing potential. 3-D co-cultures of HDMEC with pOB or osteosarcoma cell lines (Cal-72, MG-63 and SaOS-2) were performed over 24 and 48 hours. The cultures were analysed by Calcein-AM staining and microscopy.

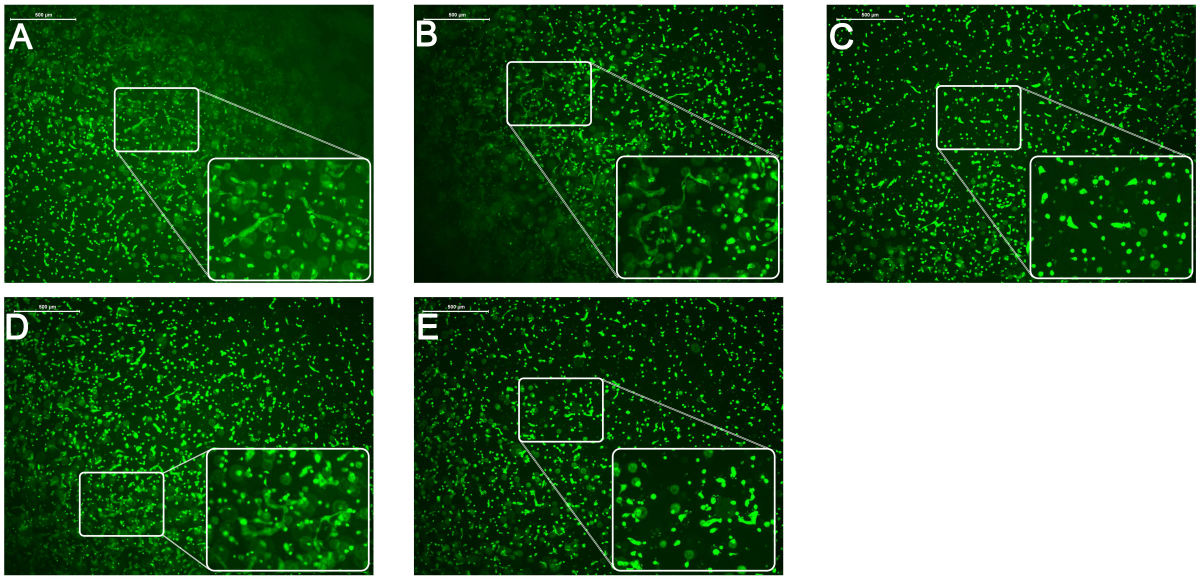

Figure 3.18: **Co-cultures of HDMEC and osteoblasts in collagen gel**
3-D co-culture of HDMEC and osteoblasts (**A** Cal-72, **B** MG-63, **C** SaOS-2, **D** pOB) and **E** HDMEC monoculture control in collagen gel after 24 hours (h) forming structures (↙). Cells were stained with Calcein-AM and visualised by fluorescence microscopy.

Cal-72 and MG-63 showed potential to form micro-capillary structures in 3-D co-cultures (Figure 3.18A,B). The cells in these co-cultures showed elongated morphology, connecting each other over distances. pOB from most donors also exhibited a strong angiogenesis-inducing potential (Figure 3.18D). As shown in the 2-D model, co-cultures with SaOS-2 cells did not show micro-capillary structure formation in 3-D cultures, similar to the negative control (Figure 3.18C,E).

3.3.3 Angiogenic effects of osteoblast cell culture medium supernatants

The difference observed between Cal-72 and MG-63 compared to SaOS-2 to induce angiogenesis may be due either to secretion of factors into the cell culture medium or direct cell-cell communication between the cells in co-cultures. In order to determine if one type of cell produces soluble factors that induce the formation of micro-capillary structures in

2-D and 3-D co-culture systems, endothelial cells were cultivated with cell culture medium supernatants of osteosarcoma cell lines. The supernatants were taken from monocultures 4 days after medium change and used for 2-D and 3-D cell culture experiments.

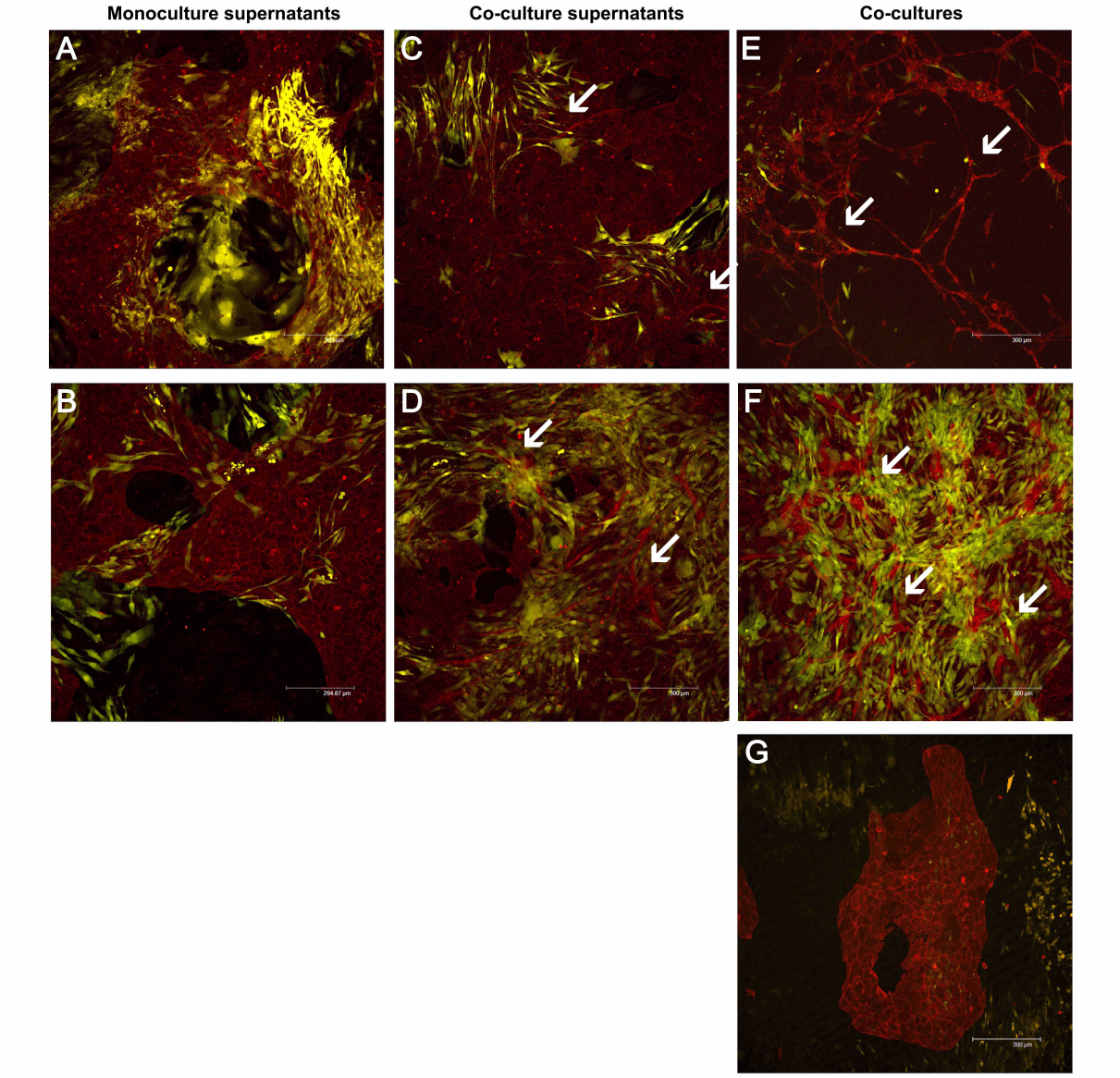

Figure 3.19: **HDMEC and SaOS-2 GFP co-cultures with medium supernatants**
Co-cultures of HDMEC and GFP-expressing SaOS-2 cells with cell culture medium supernatants from monocultures of **A** Cal-72 GFP, **B** MG-63 GFP and co-cultures of **C** HDMEC-Cal-72 GFP, **D** HDMEC-MG-63 GFP after 28 days forming structures (↙). Co-cultures of HDMEC and **E** Cal-72 GFP, **F** MG-63 GFP are positive and **G** HDMEC-SaOS-2 GFP negative controls. Cells were immunostained (CD31 antibody (red) and DAPI (blue)) and visualised by confocal microscopy.

In 2-D co-culture of HDMEC with GFP-expressing SaOS-2 cells no formation of microvessel structures was detected (Figure 3.19G). The addition of osteoblast cell culture medium supernatants from Cal-72 GFP and MG-63 GFP monocultures to HDMEC

and SaOS-2 GFP co-cultures resulted in no formation of micro-vessel structures (Figure 3.19A,B). In contrast, cell culture medium supernatants from co-cultures of HDMEC with GFP-expressing Cal-72 and MG-63 induced formation of micro-capillary structures (Figure 3.19C,D). The positive controls (co-cultures of HDMEC with GFP-expressing Cal-72 and MG-63) both resulted in clear formation of micro-vessel structures (Figure 3.19E,F).

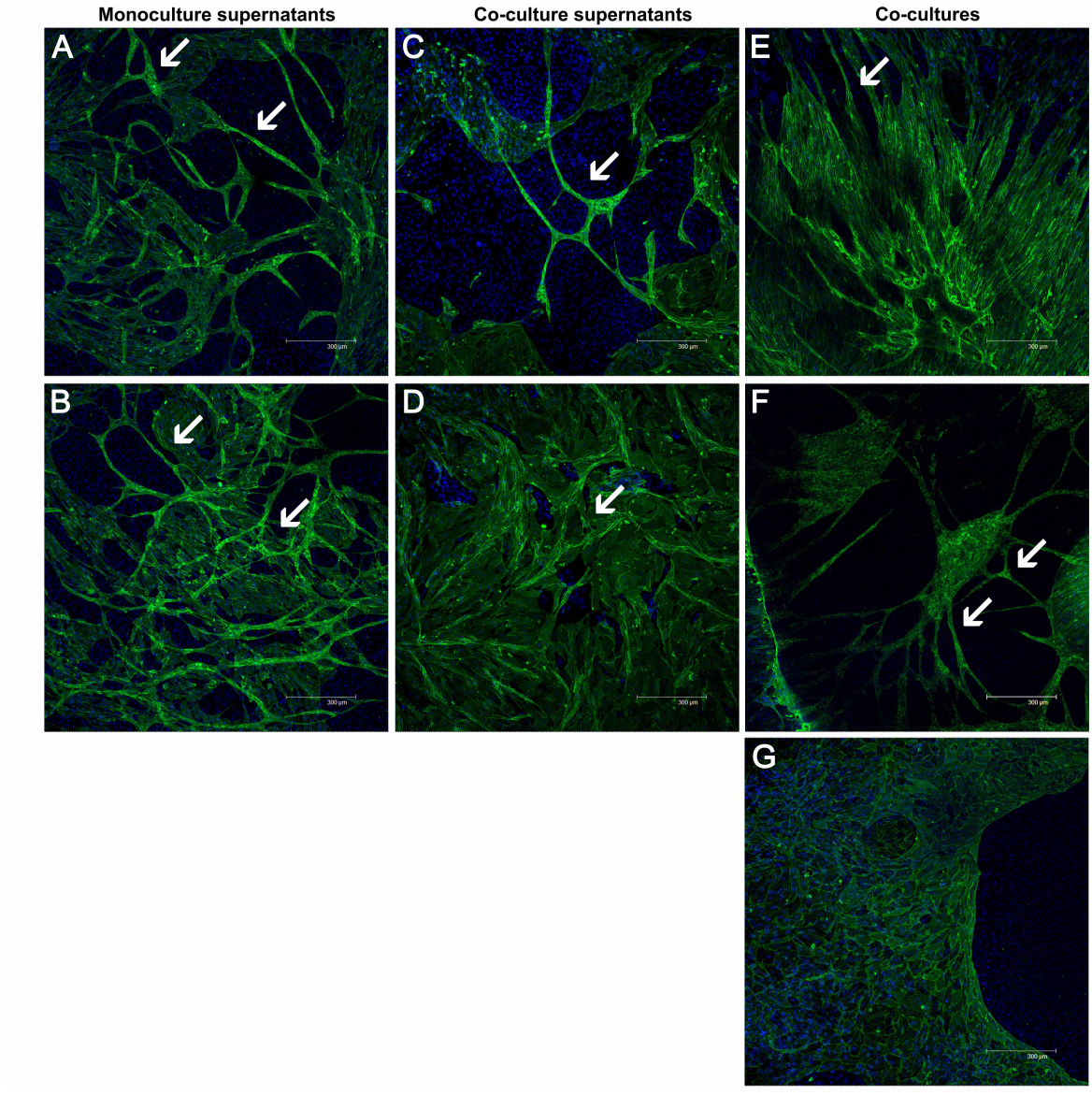

Figure 3.20: **HDMEC and SaOS-2 co-cultures with cell culture supernatants**
Co-cultures of HDMEC and SaOS-2 cells with medium supernatants from monocultures of **A** Cal-72, **B** MG-63 and co-cultures of **C** HDMEC-Cal-72, **D** HDMEC-MG-63 after 28 days forming structures (↙). Co-cultures of HDMEC and **E** Cal-72, **F** MG-63 are positive controls, co-culture of **G** HDMEC and SaOS-2 GFP is the negative control. Cells were immunostained (CD31 antibody (green) and DAPI (blue)) and visualised by laser scanning confocal microscopy.

In 2-D co-culture of HDMEC with parental SaOS-2 cells, the results were similar to HDMEC with GFP-expressing SaOS-2 cells. The addition of osteoblast cell culture medium supernatants from Cal-72 and MG-63 monocultures to a co-culture of HDMEC and SaOS-2 cells resulted in the formation of micro-capillary structures (Figure 3.20A,B). In addition, the cell culture medium supernatants from co-cultures of HDMEC with Cal-72 and MG-63 induced angiogenesis in HDMEC-SaOS-2 co-cultures (Figure 3.20C,D). All supernatant experiments resulted in similar elongation of endothelial cells and more or less cell-cell connections and branching endothelial cells in the co-cultures with SaOS-2 cells. The positive controls, HDMEC in co-culture with Cal-72 or MG-63, resulted in angiogenic structures (Figure 3.20E,F). The negative control, HDMEC in co-culture with SaOS-2 cells showed no formation of micro-capillary structures after 28 days (Figure 3.20G). Thus, factors in supernatants from Cal-72 and MG-63 can induce angiogenesis in co-culture of HDMEC with SaOS-2 cells.

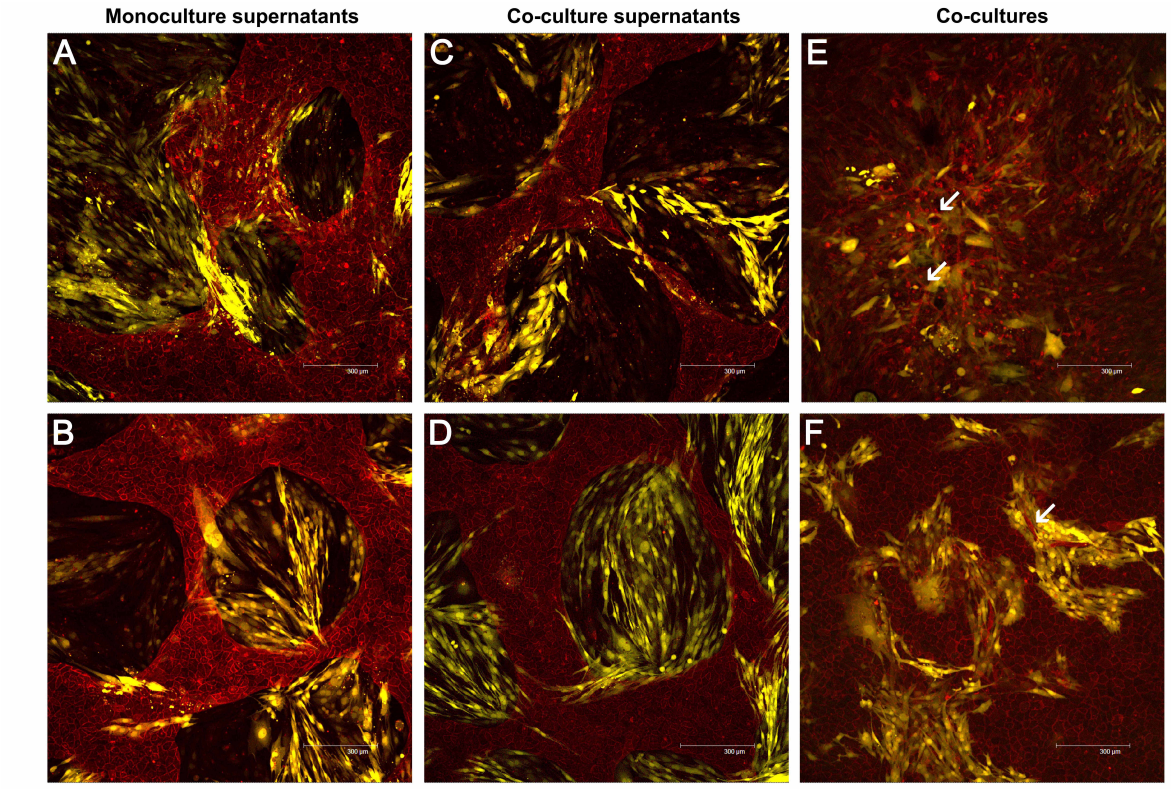

Figure 3.21: **HUVEC and SaOS-2 GFP co-cultures with medium supernatants**
Co-cultures of HUVEC and GFP-expressing SaOS-2 cells with medium supernatants from monocultures of **A** Cal-72 GFP, **B** MG-63 GFP and co-cultures of **C** HUVEC-Cal-72 GFP, **D** HUVEC-MG-63 GFP after 28 days forming structures (↙). Co-cultures of HUVEC and **E** Cal-72 GFP, **F** MG-63 GFP are positive controls. Cells were immunostained (CD31 antibody (red) and DAPI (blue)) and visualised by laser scanning confocal microscopy.

In 2-D co-culture of HUVEC with GFP-expressing SaOS-2 cells no formation of micro-capillary structures could be observed. The addition of osteoblast cell culture medium supernatants from Cal-72 GFP and MG-63 GFP monocultures to co-cultures of HUVEC and SaOS-2 GFP did not induce formation of micro-capillary structures (Figure 3.21A,B). In addition, cell culture medium supernatants from HUVEC in co-culture with Cal-72 GFP and MG-63 GFP did not lead to angiogenesis (Figure 3.21C,D). Only in the positive controls of HUVEC in co-culture with Cal-72 GFP and MG-63 GFP were micro-capillary structures detected (Figure 3.21E,F).

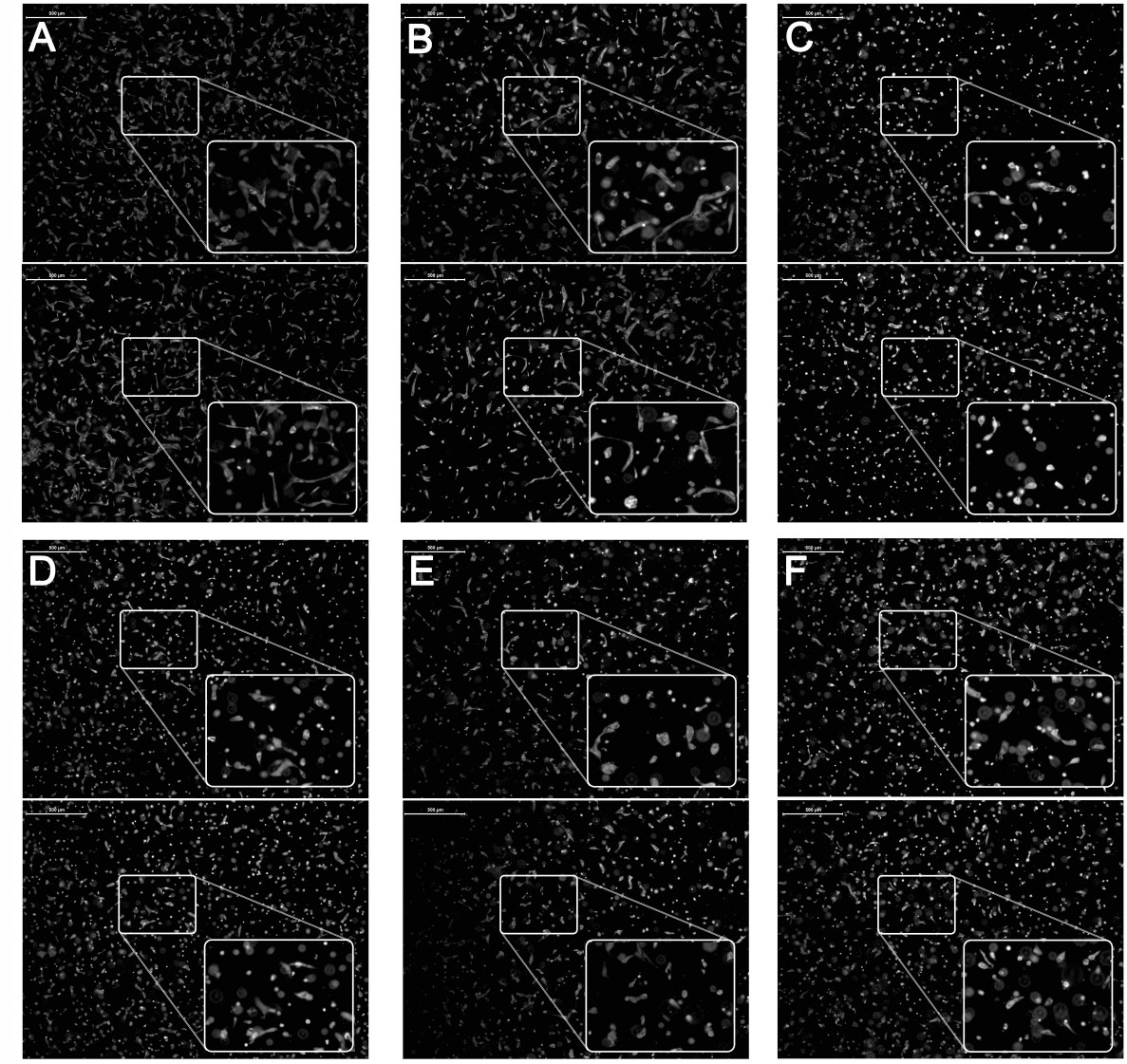

Figure 3.22: **HDMEC in collagen gel with medium supernatants**
3-D cultures of HDMEC in collagen gel with medium supernatants from **A** Cal-72, **B** MG-63, **C** SaOS-2, **D** and **E** pOB donors and **F** HDMEC monoculture control after 24 h. The cultures were stained with Calcein-AM and monitored by fluorescence microscope.

The 3-D experiments were performed with HDMEC monocultures for 24 hours in collagen gels and the addition of cell culture medium supernatants from osteoblasts after 4 days. The formation of micro-capillary structures in the cultures was observed. The results indicated that similar to the 2-D setups, cell-free supernatants from Cal-72 and MG-63 cells as well as two pOB donors were capable of inducing angiogenesis in HDMEC in collagen gels (Figure 3.22A,B,D,E). HDMEC exhibited micro-capillary structure morphology with some cell-cell connections in these cultures. SaOS-2 cells showed no formation of micro-capillary structures, similar to the negative control (Figure 3.22C,F).

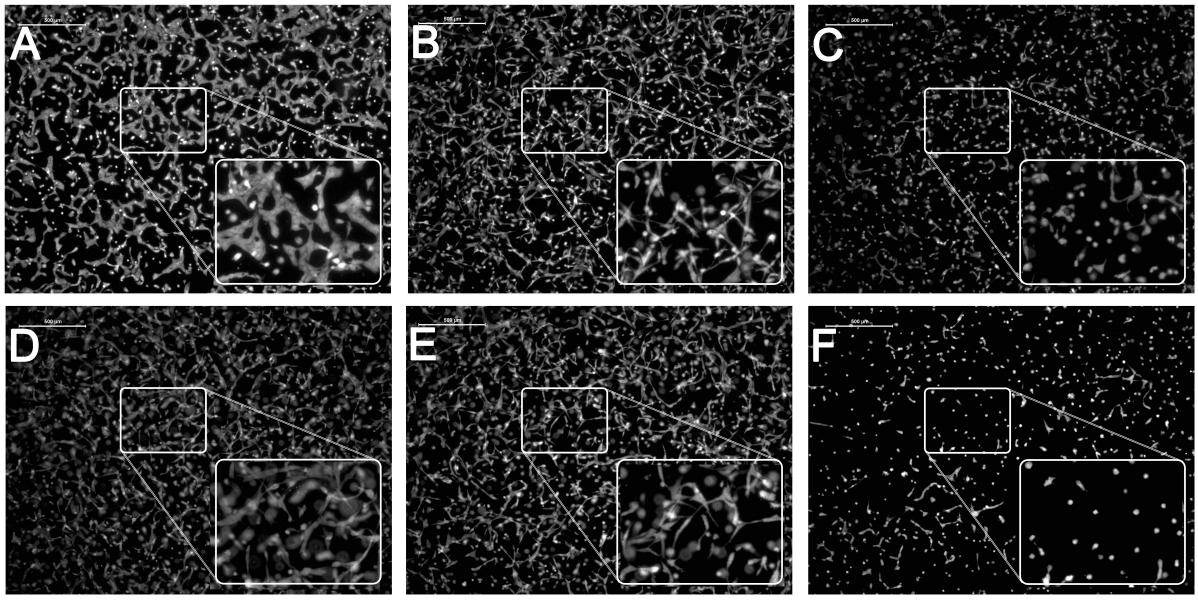

Figure 3.23: **HUVEC in collagen gel with medium supernatants**
3-D cultures of HUVEC in collagen gel with medium supernatants from **A** Cal-72, **B** MG-63, **C** SaOS-2, **D** and **E** pOB donors and **F** HUVEC monoculture control after 24 h. The cultures were stained with Calcein-AM and monitored by fluorescence microscope.

The 3-D experiments with HUVEC monocultures exhibited similar micro-capillary structure formation to HDMEC. Cal-72 and MG-63 cell culture medium supernatants had the potential to induce angiogenesis in HUVEC (Figure 3.23A,B). HUVEC cultures showed micro-capillary morphology with many cell-cell connections and branches. Furthermore, both pOB donors induced angiogenesis in these experiments (Figure 3.23D,E). Cell culture supernatants from SaOS-2 cells showed no potential to induce formation of micro-capillary structures, similar to the negative control (Figure 3.23C,F).

The results from medium supernatant experiments showed that SaOS-2 cells appear to

lack secretion of factors that lead to formation of micro-capillary structures. In contrast, medium supernatants from Cal-72 and MG-63 cultures resulted in formation of micro-capillary structures in both 2-D and 3-D cell culture experiments.

3.3.4 Transcriptional analysis of angiogenesis-related factors in osteosarcoma cell lines

In order to compare osteosarcoma cell lines with respect to angiogenesis-related gene transcription, qPCR was performed on Cal-72, MG-63 and SaOS-2 RNA. The results were compared and analysed for significant differences between Cal-72 and SaOS-2 as well as MG-63 and SaOS-2 (Figure 3.24) and Cal-72 and MG-63.

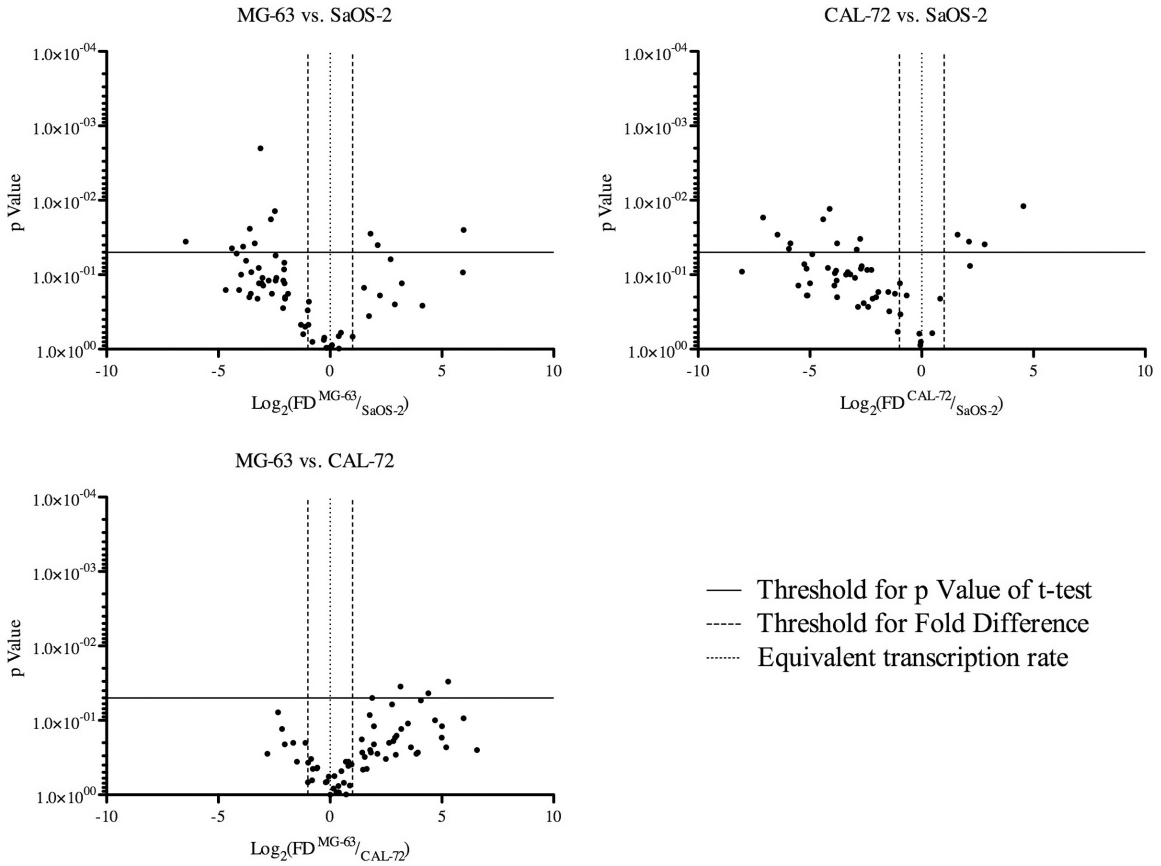

Figure 3.24: **Comparative results of qPCR on osteosarcoma cell lines**
Comparative results of qPCR on osteosarcoma cell lines (Cal-72, MG-63, SaOS-2). Abscissa: Log_2 of fold difference (FD) between osteosarcoma cell lines. Ordinate: p value. Margins: horizontal mark for p value = 0.05 (–), vertical dashed line (- - -) for two fold change in transcription and vertical dotted line (· · ·) for equilibrium in transcription. P values were estimated according to (Rudolf and Kuhlisch, 2008). Log_2FD were estimated according to (Biosystems, 2010). Housekeeping genes were determined with high expression stability and low $\Delta\Delta$Ct variation (Radonic et al., 2004; Vandesompele et al., 2002). Vulcano plots were generated according to (Tusher et al., 2001; Storey and Tibshirani, 2003).

Significant differences between qPCR results ($p < 0.05$) are summarised in Table 3.28. An intersection can be estimated by grouping the gene expression profiles in Cal-72 versus SaOS-2, and MG-63 versus SaOS-2. It can be seen that leptin (LEP), interleukin-6 (IL6), TNF, interleukin-8 (IL8), jagged 1 (JAG1) and cadherin 5 (CDH5) are upregulated in SaOS-2 cells, while VEGFA, TGF-α and TIMP-2 are significantly downregulated compared to MG-63 and Cal-72.

Table 3.28: Significant P-value results of qPCR on osteosarcoma cell lines
A complete list of p-values can be found in Appendix A.4.

MG-63 vs. SaOS-2			CAL-72 vs. SaOS-2			MG-63 vs. CAL-72		
Gene	Log_2FD	p Value	Gene	Log_2FD	p Value	Gene	Log_2FD	p Value
ANGPTL3	-3.60	0.024	ANGPTL3	-7.09	0.017	CXCL10	5.28	0.03
CDH5	-3.89	0.042	CDH5	-2.90	0.046	EREG	1.88	0.05
CXCL6	-3.12	0.002	COL18A1	-5.94	0.045	HPSE	4.40	0.043
IL6	-2.47	0.014	HPSE	-6.45	0.029	TGF-α	3.15	0.035
JAG1	-2.65	0.018	IL6	-2.75	0.033			
LEP	-6.46	0.036	JAG1	-4.12	0.013			
MDK	-3.37	0.038	LEP	-5.87	0.038			
TGF-α	5.97	0.025	MDK	-3.78	0.038			
TIMP-2	2.13	0.04	TEK	-4.41	0.018			
TNF	-4.39	0.044	TGF-α	2.82	0.039			
VEGFA	1.81	0.028	THBS1	4.55	0.012			
			TIMP-2	2.12	0.036			
			VEGFA	1.61	0.029			

In silico pathway interaction analysis was performed using GNCpro. A pathway and regulation network model based on the documented gene intersection in Cal-72 and MG-63 with respect to SaOS-2 cells is visualised in Figure 3.25.

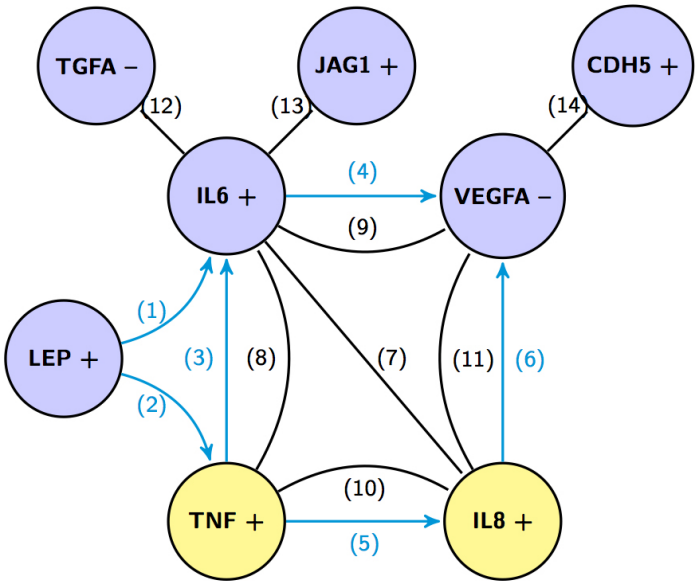

Figure 3.25: **Regulation network model in SaOS-2**
Pathway and regulation network model generated using GNCpro, based on significant (circles) and less significant (circles) key findings of qPCR. Upregulation (→) and unspecified regulation (—) are covered by literature (numbers in brackets correlating to Table 3.29), while upregulation (+) and downregulation (-) are covered by the results.

The model is enlarged by TNF and IL8 because of strong evidence for a coupled regulation. TNF and IL8 lack one measured value, thus calculation of a p-value was not possible. For angiopoietin-like 3 (ANGPTL3), midkine (MDK) and TIMP-2 it was not possible to determine a direct regulation network model. However, the result for VEGFA regulation is distinct.

Upregulation of VEGFA could occur in two ways: LEP → TNF → IL8 → VEGFA as well as LEP → IL6 → VEGFA (Table 3.29). But VEGFA expression was found to be reduced while CDH5 was up-regulated. For a better understanding of this inharmonious finding it may be important to recall the incapability of SaOS-2 cells to induce angiogenesis in an environment of decreased levels of VEGFA (Figure 3.12 and Sections 3.3.1 and 3.3.2).

Table 3.29: Pathway and regulation network references

Number	Connection	References
1	LEP – IL6	(Mattioli et al., 2005)
2	LEP – TNF	(Zarkesh-Esfahani et al., 2004; Mattioli et al., 2005)
3	TNF – IL6	(Ammit et al., 2002; Heyninck et al., 1999; Faggioli et al., 2004) (Alsalameh et al., 2003; Zhang et al., 2002; Morohoshi et al., 1996)
4	IL6 – VEGFA	(Huang et al., 2004; Wei et al., 2003; Borg et al., 2005)
5	TNF – IL8	(Luecke and Yamamoto, 2005; Lahav et al., 2002; Facchini et al., 2005) (Son et al., 2005; Lockwood et al., 2006; Boldrini et al., 2006) (Zhang et al., 2002; Nissen and Yamamoto, 2000; Becker et al., 1994) (Kazachkov et al., 2002; Fredriksson et al., 2003; Brunius et al., 2005) (Hirano et al., 2007; Xie and Gu, 2008)
6	IL8 – VEGFA	(Hellmuth et al., 2002; Li et al., 2008)
7	IL6 – IL8	(Theodoropoulos et al., 2006; Chen et al., 2005; Huang et al., 2006) (Landi et al., 2003)
8	IL6 – TNF	(Nieters et al., 2001; Pawlik et al., 2005; Theodoropoulos et al., 2006) (Zalewska et al., 2006; Kobayashi et al., 2005; Scapoli et al., 2007) (Guimaraes et al., 2007; Andersson et al., 2008; Landi et al., 2003) (de Sa et al., 2007; Chen et al., 2005; Tambur et al., 2006; Ross et al., 2004)
9	IL6 – VEGFA	(Yao et al., 2006; Borg et al., 2005; Ulbrich et al., 2008)
10	TNF – IL8	(Lu et al., 2005; Theodoropoulos et al., 2006; Chen et al., 2005) (Matheson et al., 2006; Landi et al., 2003; Williams et al., 2005) (Henriksen et al., 2004; Smit et al., 2003; Oltmanns et al., 2005) (Marcet et al., 2007; Zalewska et al., 2006; Baraldo et al., 2003)
11	IL8 – VEGFA	(Ulbrich et al., 2008)
12	IL6 – TGF-α	(Thiele et al., 2003)
13	IL6 – JAG1	(Sansone et al., 2007)
14	VEGFA – CDH5	(Ha et al., 2008; Gavard and Gutkind, 2006)

3.3.5 Effects of bFGF on angiogenesis

The results shown in Section 3.3.3 demonstrate a correlation between the composition of the medium supernatants from osteosarcoma cell line cultures and the formation of micro-capillary structures. Because bFGF is one component of standard supplemented endothelial cell culture medium ECGM and absent in osteoblast growth medium DMEM, studies were undertaken to analyse the effects when added to medium supernatants. Therefore, 20 ng/µl bFGF were added to the cell culture medium of osteosarcoma cell lines. In 3-D cultures with and without additional bFGF being added to HDMEC, micro-capillary structure formation was analysed by Calcein-AM staining and microscopic analysis.

The results showed that micro-capillary structures were formed in HDMEC with both cell culture media supernatants from Cal-72 and MG-63 irrespective of the presence

of bFGF (Figure 3.26A,B). In contrast, HDMEC cultured in DMEM supernatants from SaOS-2 cells with and without bFGF resembled the control showing no formation of micro-capillary structures (Figure 3.26C,D). HDMEC cultured in ECGM alone, showed strong formation of angiogenic structures, when supplemented with additional bFGF.

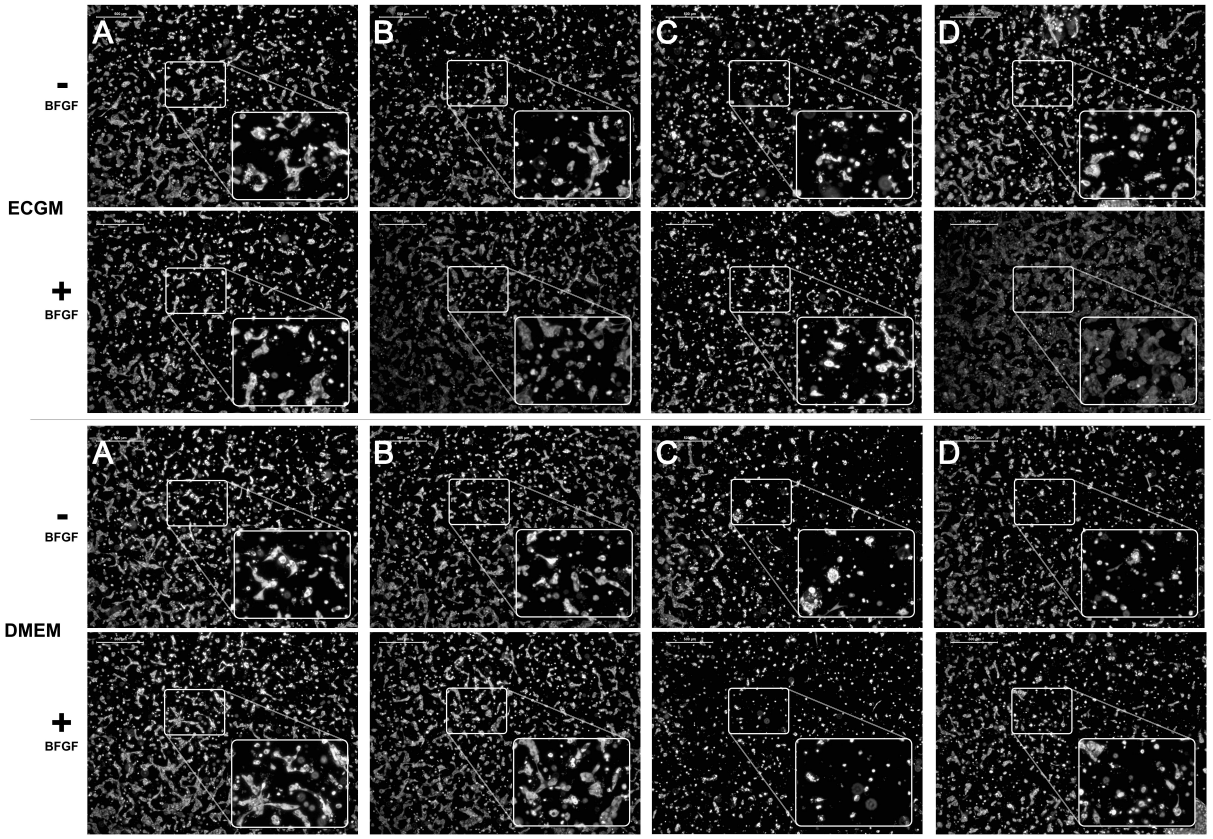

Figure 3.26: **3-D culture of HDMEC with medium supernatants and bFGF**
3-D collagen gel cultures of HDMEC with medium supernatants from **A** Cal-72, **B** MG-63, **C** SaOS-2 and the negative control **D** HDMEC supplemented with 20 ng/µl bFGF. Cultures were set up with ECGM and DMEM for 24 hours, stained with Calcein-AM and visualised by fluorescence microscope.

3-D monocultures of HUVEC in ECGM and DMEM showed no differences caused by the bFGF addition (Figure 3.27). With ECGM, HUVEC showed stronger formation of micro-capillary structures than with DMEM. The results showed that micro-capillary structures were formed in HUVEC with both cell culture media supernatants from Cal-72 and MG-63 (Figure 3.27A,B). In contrast, HUVEC cultured in supernatants from SaOS-2 cells with and without bFGF resembled the control showing no formation of micro-capillary structures (Figure 3.27C,D).

The 3-D monoculture of umbilical artery endothelial cells showed a slightly stronger

tendency to form micro-capillary structures with the addition of bFGF in both media of Cal-72 cell culture supernatants (data can be found in the Appendix A.3). All other samples showed weak to no formation of micro-capillary structures similar to the negative controls.

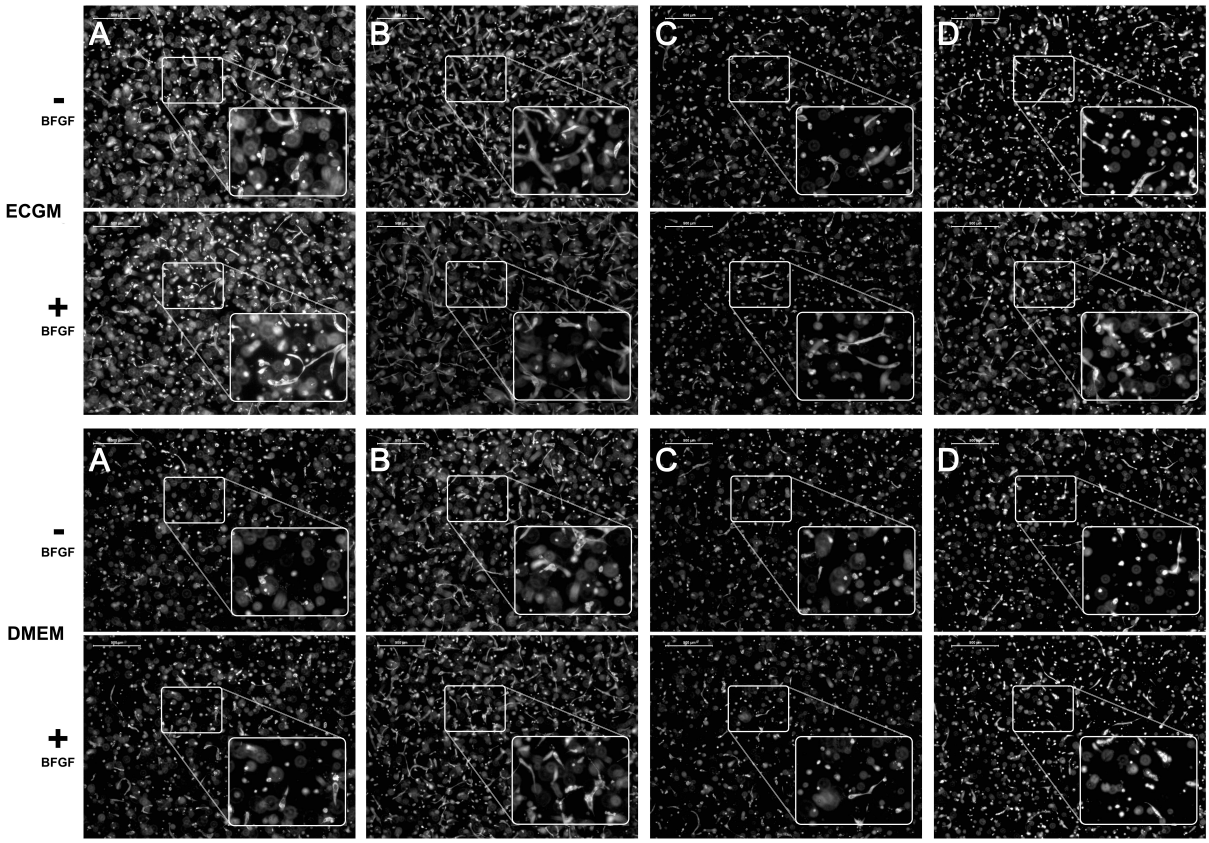

Figure 3.27: **3-D culture of HUVEC with medium supernatants and bFGF**
3-D collagen gel cultures of HUVEC with medium supernatants from **A** Cal-72, **B** MG-63, **C** SaOS-2 and the negative control **D** HUVEC supplemented with 20 ng/µl bFGF. Cultures were set up with ECGM and DMEM for 24 hours, stained with Calcein-AM and visualised by fluorescence microscope.

3.3.6 Release of HGF and VEGF in osteosarcoma cell lines

Cal-72 and MG-63 cells appear to secrete factors into their medium that are able to induce angiogenesis in endothelial cell monocultures as well as in endothelial cell co-cultures with SaOS-2 cells. Both VEGF and bFGF are known to be involved in angiogenesis (Cross and Claesson-Welsh, 2001; Leung et al., 1989). In Section 3.1.4, it was shown that Cal-72 and MG-63 cells secrete higher amounts of VEGF and bFGF than SaOS-2. However, the previously described experiments have shown that bFGF alone is not capable of inducing

micro-capillary structure formation. Therefore, VEGF production by osteosarcoma cell lines was examined. In addition, HGF production was also examined, as it has previously been reported to have a central role in angiogenesis (Porta et al., 2013). Both, HGF and VEGF from medium supernatants in 2-D and 3-D collagen gel monocultures, were quantified by ELISA at different time points. All data were analysed for significance ($p < 0.05$) and compared to the results of SaOS-2.

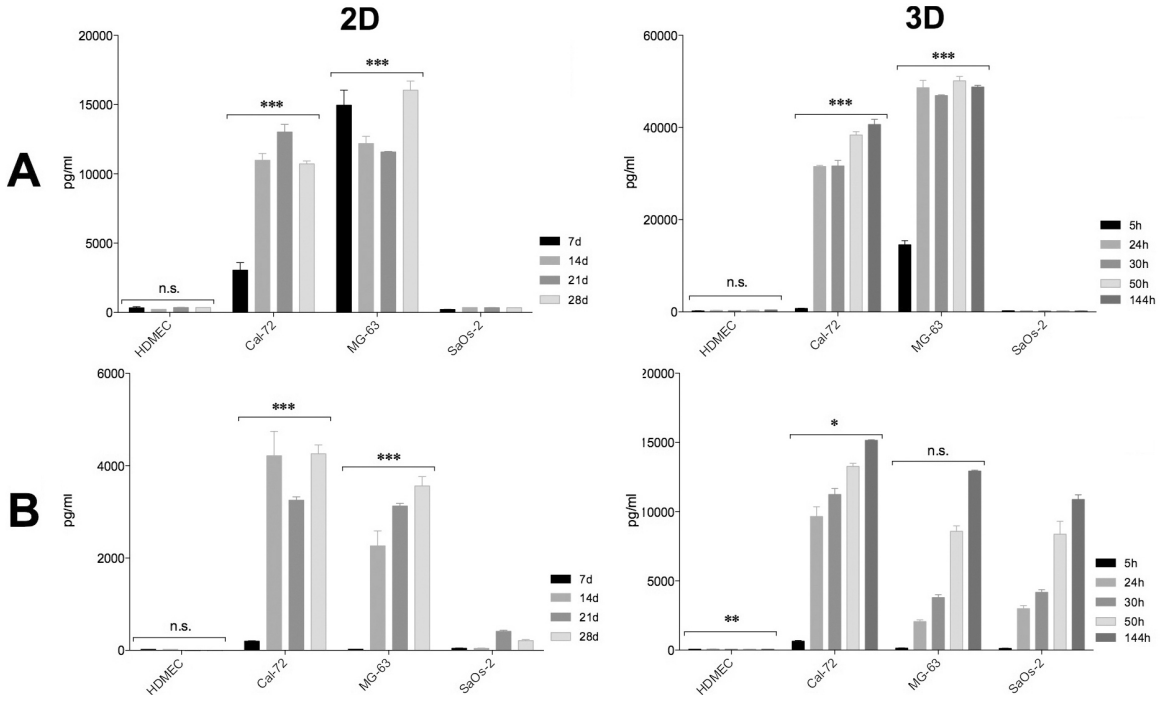

Figure 3.28: **Quantification of HGF and VEGF in medium supernatants**
ELISA quantification of **A** HGF and **B** VEGF in medium supernatants of 2-D and 3-D osteosarcoma cell line cultures at different time points. All data were normalised to the amount of DNA. One-way ANOVA (*: $p < 0.05$, **: $p < 0.01$, ***: $p < 0.001$) and Dunnett's test were applied and correlated with SaOS-2 cells.

In 2-D and 3-D cell cultures, HGF secretion by Cal-72 and MG-63 was significantly higher compared to SaOS-2 which secreted no HGF, similar to the HDMEC negative control (Figure 3.28). Significant VEGF release in Cal-72 and MG-63 2-D cell cultures was observed. No significant amount of VEGF was observed in SaOS-2 or HDMEC 2-D cell cultures. For 3-D cell cultures suprisingly, SaOS-2 cells exhibited VEGF at levels similar to MG-63 cells but significantly lower than Cal-72 cells. In contrast, HDMEC secreted a lower amount of VEGF compared to SaOS-2.

3.3.7 Correlation between HGF and endostatin

Endostatin is a known inhibitor of angiogenesis and is thus of interest to the pharmaceutical industry as a therapeutic inhibitor of endothelial cells (Fiedler et al., 2001). Since a higher quantity of HGF was found in Cal-72 and MG-63 compared to SaOS-2 cultures, endostatin was also quantified and correlated with the HGF results (Figure 3.29).

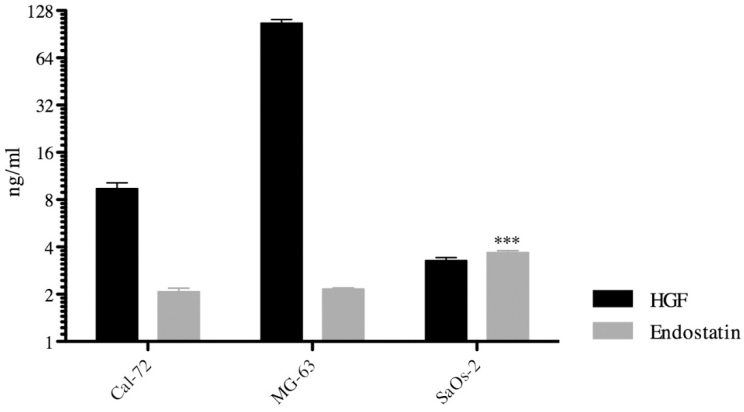

Figure 3.29: **Quantification of HGF and endostatin in medium supernatants**
Quantification of HGF and endostatin in medium supernatants of 7 day 2-D osteosarcoma cell line cultures by ELISA. All data were normalised to the amount of DNA. One-way ANOVA (***: $p < 0.001$) was applied.

Both targets were quantified by ELISA in medium supernatants from 2-D monocultures after 7 days. All data were analysed for significance ($p < 0.05$) and compared to the results of SaOS-2 cells. Again, HGF secretion by Cal-72 and MG-63 was significantly increased compared to SaOS-2 cells. In contrast, for endostatin, a significantly higher level was observed in SaOS-2 than in MG-63 and Cal-72 cells.

3.3.8 Effects of podoplanin on angiogenic potential of osteoblasts

The previously described populations of mixed lymphatic and vascular endothelial cells in the cell cultures (Section 3.2.4) may have had an effect on the formation of micro-capillary structures in these cell cultures. Therefore, the lymphatic and vascular endothelial cells were separated and re-combined and both used for angiogenesis experiments.

Separation and combination experiments of lymphatic and vascular fractions of endothelial cells (lymphatic endothelial cells alone, vascular endothelial cells alone, lymphatic and vascular endothelial cells combined) indicated a correlation between both fractions and the ability to form micro-capillary structures (Figure 3.30). It can be seen that lymphatic HDMEC form no micro-capillary structures in 2-D co-culture with pOB, while vascular HDMEC showed the formation of micro-capillary structures. The strongest

effects on the formation of micro-capillary structures was found in the combination of lymphatic and vascular HDMEC-fractions in co-culture with pOB. The results suggest that lymphatic endothelial cells increase the formation of micro-capillary structures in HDMEC. However, these cells have been shown not to be directly involved in angiogenesis. One possible factor causing initiation of micro-capillary structure formation may be podoplanin, the protein to which D2-40 antibody binds to.

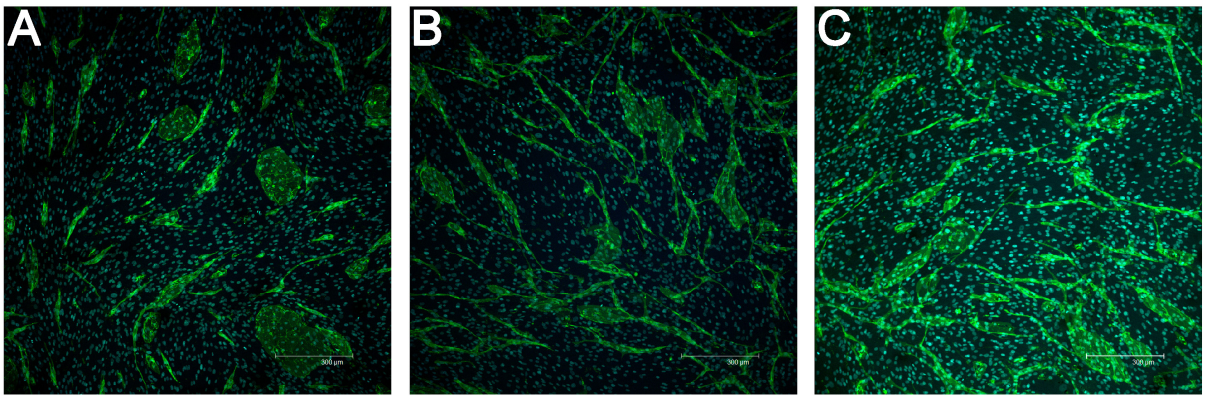

Figure 3.30: **2D co-cultures of HDMEC fractions with pOB**
Separated (**A** lymphatic, **B** vascular) and **C** combined (1:1) populations of HDMEC in 2D co-culture with pOB. Cells were stained with CD31 antibody and visualised by fluorescence microscope.

3.3.8.1 Cloning and transfection of SaOS-2 cells with podoplanin

In order to evaluate the role of podoplanin in the formation of micro-capillary structures, its coding DNA sequence (CDS) was transfected into SaOS-2 cells. SaOS-2 were previously shown to have no effect on angiogenesis in co-culture systems (Section 3.3). For better cloning efficiency, the blunt end PCR product was first cloned into pJET1.2/blunt subcloning vector before being transferred into pEGFP-N1. The final construct contained a stop-codon behind the podoplanin gene and was verified by colony PCR (Figure 3.31). The absence of substitutions or mutations was confirmed by DNA sequencing (data not shown). Podoplanin was cloned into a pEGFP-N1 vector before SaOS-2 cells were transfected with the construct. Successfully transfected cells were selected on a single cell basis and transfection was verified by immunofluorescent staining with D2-40 antibody and microscopic analysis.

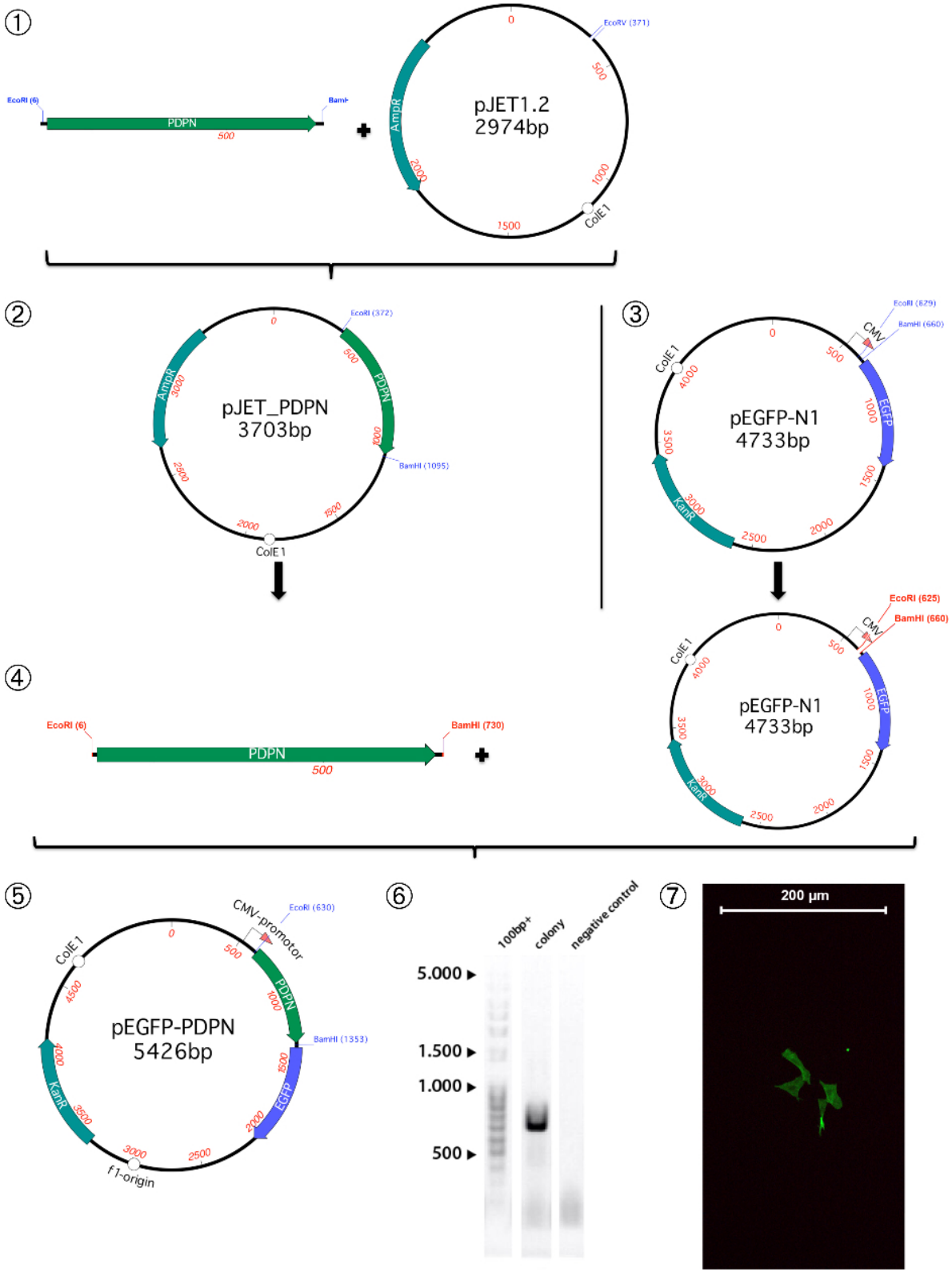

Figure 3.31: **Cloning of podoplanin into pEGFP-N1**
Cloning strategy and transfection of SaOS-2 cells with restriction sites (blue) and cleaved sticky end restriction sites (red). **1** Fusion of blunt end podoplanin PCR product and pJET1.2 sub-cloning vector. **2**, **3** Restriction of pJET-PDPN and pEGFP-N1. **4** Fusion of sticky end podoplanin gene with pEGFP-N1 vector. **5** Final construct pEGFP-PDPN. **6** Colony-PCR of positively transfected colony with negative control. **7** Podoplanin positive SaOS-2 cells stained with D2-40 antibody, visualised by fluorescence microscopy.

3.3.8.2 Podoplanin expressing SaOS-2 cells

As VEGF is known to be involved in the formation of new blood vessels (Cross and Claesson-Welsh, 2001; Leung et al., 1989), podoplanin-expressing and normal SaOS-2 cells were compared to pOB, Cal-72 and MG-63 for the production of VEGF. All data were normalised to the amount of DNA in the cell cultures and statistically analysed to identify significant differences ($p < 0.05$). Compared to untransfected SaOS-2 cells, transfected SaOS-2_PDPN showed a significant increase in VEGF production at both measured time points (Figure 3.32). Compared with pOB, Cal-72 and MG-63, the VEGF level was also significantly higher.

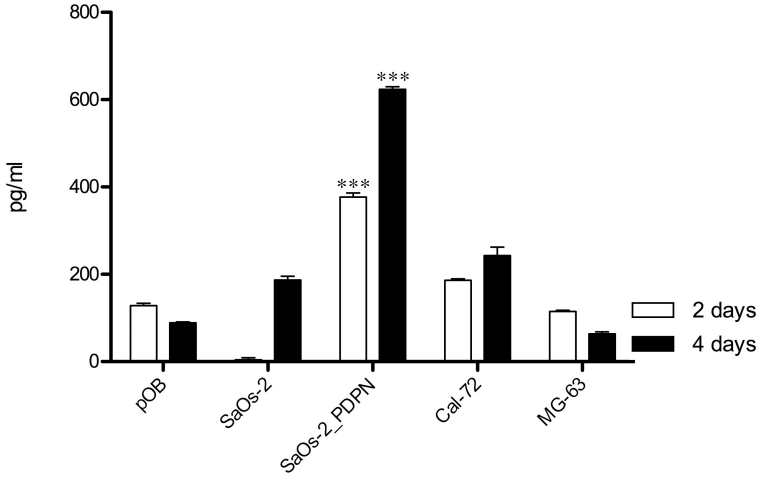

Figure 3.32: **VEGF quantification in osteoblasts and SaOS-2_PDPN**
VEGF quantification in pOB, SaOS-2, Cal-72, MG-63 and transfected SaOS-2_PDPN cell cultures after 2 and 4 days by ELISA. All data were normalised to the amount of DNA and analysed by two-way ANOVA (***: $p < 0.001$).

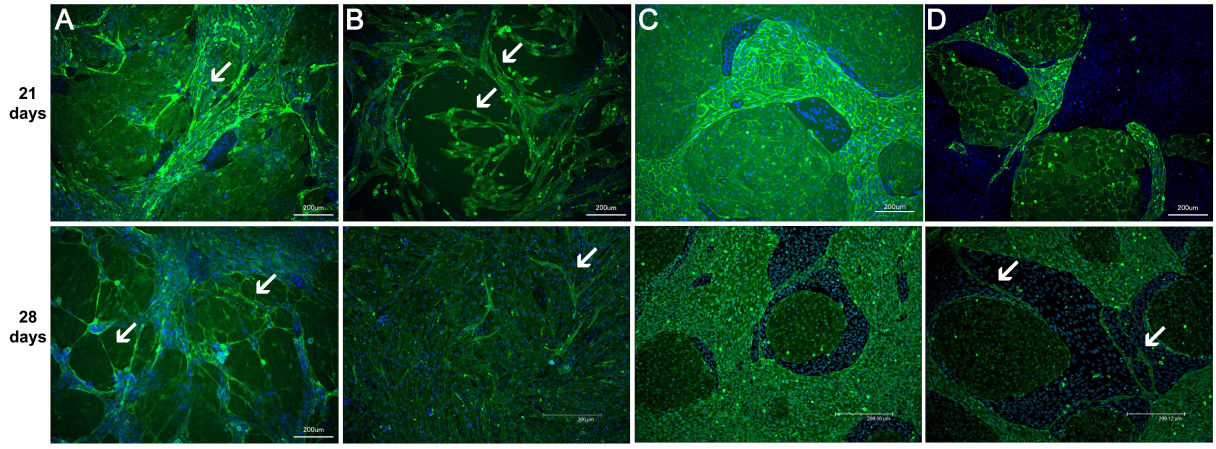

Figure 3.33: **2-D co-culture of HDMEC and SaOS-2_PDPN**
2-D co-culture of HDMEC and **A** Cal-72, **B** MG-63, **C** SaOS-2, and **D** SaOS-2_PDPN after 21 and 28 days with formation of vessel-like structures (↙). Cells were immunostained (CD31 antibody (green), DAPI (blue)) and monitored by laser scanning confocal microscopy.

As previously shown (Sections 3.3.1 and 3.3.2), the formation of micro-capillary structures *in vitro* can be stimulated by co-cultivation of endothelial cells with osteosarcoma cell lines. Because SaOS-2_PDPN showed upregulated VEGF levels, it was then determined whether these cells could stimulate angiogenesis. For comparison of transfected and untransfected SaOS-2 cells, 2-D and 3-D co-cultures with three HDMEC donors were performed for 48 hours, 21 and 28 days.

The results showed differences between transfected SaOS-2_PDPN and untransfected SaOS-2 in terms of the stimulation of angiogenesis (Figure 3.33). In 2-D co-culture, untransfected SaOS-2 cells showed no angiogenesis-stimulating potential while podoplanin positive SaOS-2_PDPN cells induced some micro-capillary structures after 28 days. As previously demonstrated, Cal-72 and MG-63 showed formation of micro-capillary structures in these experiments (Section 3.3).

In 3-D collagen gel co-culture of HDMEC with transfected SaOS-2_PDPN cells, micro-capillary structures formed after 48 hours (Figure 3.34). Untransfected SaOS-2 cells showed no angiogenesis-inducing potential. Cal-72 and MG-63 induced micro-capillary structure formation. HDMEC in 3-D monoculture was the negative control, showing no formation of micro-capillary structures.

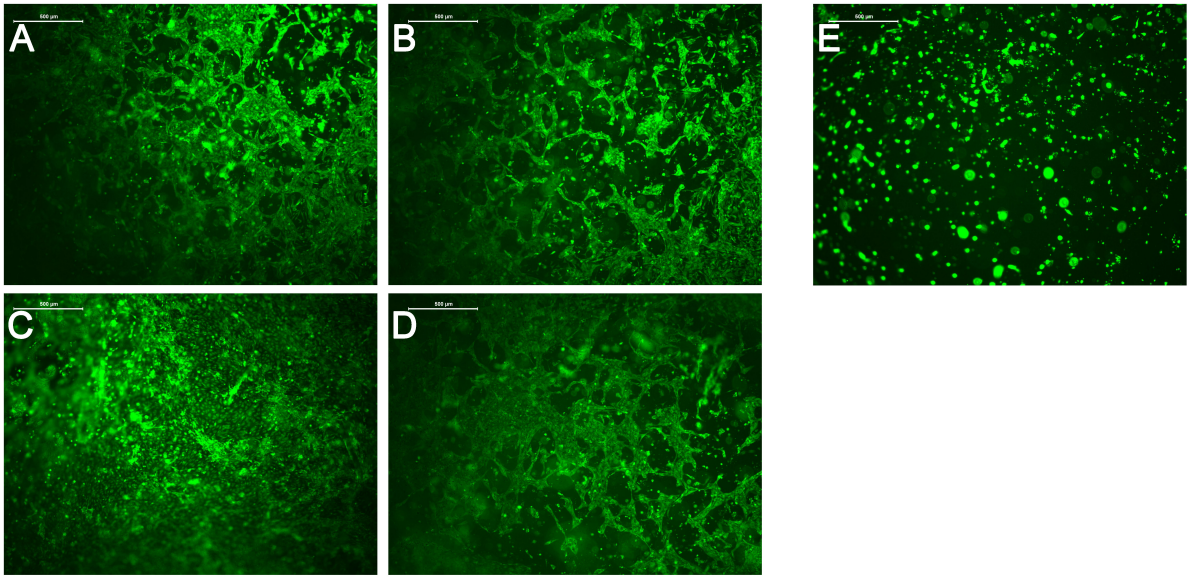

Figure 3.34: **3-D co-culture of HDMEC and SaOS-2_PDPN**
3-D co-culture of HDMEC and **A** Cal-72, **B** MG-63, **C** SaOS-2, and **D** SaOS-2_PDPN, and **E** HDMEC monoculture control in collagen gel after 48 hours. Cells were stained with Calcein-AM and monitored by fluorescence microscope.

3.4 Mass spectroscopy on used media supernatants

In order to detect differences in secreted protein expression between the osteosarcoma cell lines (Cal-72, MG-63, SaOS-2), medium supernatants were analysed by mass spectroscopy.

3.4.1 Gel-electrophoretic separation of cell culture supernatants

SDS-PAGE for separation of medium supernatants appears to have some disadvantages. One difficulty is that the potentially secreted signal peptides are highly diluted by the growth medium and therefore may be below the limits of detection. Thus, media supernatants were concentrated by TCA precipitation before being separated by SDS-PAGE (Figure 3.35A).

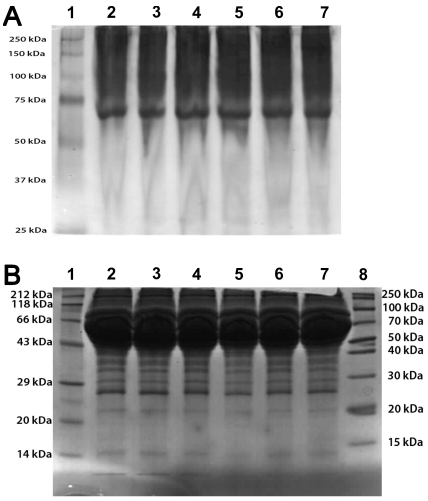

Number	Sample
1	Precision plus dual color
2	Cal-72 GFP ECGM
3	Cal-72 GFP DMEM
4	MG-63 GFP ECGM
5	MG-63 GFP DMEM
6	SaOS-2 GFP ECGM
7	SaOS-2 GFP DMEM

Number	Sample
1	Rotimark MW standard
2	Cal-72 GFP DMEM
3	Cal-72 GFP ECGM
4	MG-63 GFP DMEM
5	MG-63 GFP ECGM
6	SaOS-2 GFP DMEM
7	SaOS-2 GFP ECGM
8	Fermentas broad range

Figure 3.35: **SDS-PAGE of cell culture supernatants**
SDS-PAGE of medium supernatants (DMEM and ECGM) from Cal-72 GFP, MG-63 GFP and SaOS-2 GFP cultured 5 days. Cell culture medium supernatants were **A** TCA-precipitated and **B** albumin-depleted, 10 µl were loaded on 10% polyacrylamide gel.

However, the cell culture media contain serum albumin which is essential for cell proliferation and survival *in vitro*. Albumin is known to be a 'sticky' molecule capable of agglomerating other proteins (He and Carter, 1992; Kwok et al., 2007). With SDS-PAGE, albumin overlays all other signals. Therefore, a procedure was implemented to extract albumin from the media supernatants using an albumin depletion kit (Figure 3.35B). However, albumin remained the dominating signal in SDS-PAGE. It is well documented in the literature that albumin depletion is problematic (Andaç et al., 2012; Granger et al., 2005; Holewinski et al., 2013). There are some alternative methods that could be used, but as yet none of these promises complete albumin extraction. In addition, all approaches have disadvantages for mass spectroscopic analysis, either being too expensive, or by removing the agglomerated proteins leading to sample concentrations below the limits of detection.

3.4.2 Mass spectroscopy

The albumin-depleted samples from SDS-PAGE were used for mass spectroscopic analysis. In preparation for mass spectroscopy, the lanes were segmented and tryptically digested. For MALDI-TOF mass spectroscopic analysis, the amount of protein was quantified for each sample (Figure 3.36). MALDI-TOF is widely used for peptide analysis (Tanaka et al., 1988) and was accessible in the Ophthalmology Clinic, Mainz. The difficulties that emerged during SDS-PAGE with albumin overlapping all other signals continued to be an issue in MALDI-TOF spectra as well (Figure 3.37). Besides peaks that could be correlated to albumin, no other significant signals could be detected. The analysis was validated by a positive control sample.

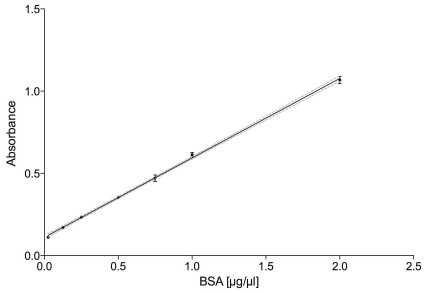

Number	c and dev [µg/µl]
1	6.521±0.0377
2	12.804±0.2673
3	13.150±0.2015
4	5.073±0.1134
5	5.413±0.1316
6	6.755±0.0252

Figure 3.36: **Quantification of the BSA standard sample**
The amount of protein was quantified for each sample before mass spectroscopic analysis was performed. The table shows an example of the measured segments after tryptical digestion.

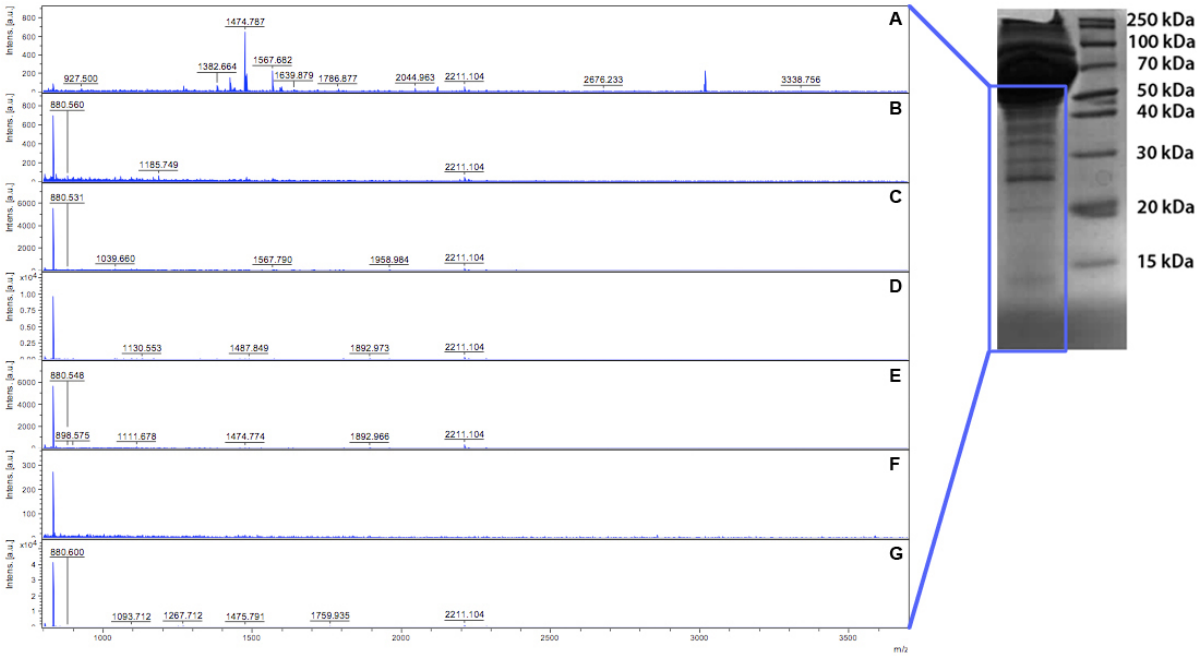

Figure 3.37: **Representative MALDI-TOF spectra**
Peptides in the region of interest below 50 kDa were seperated by SDS-PAGE, segmented into seven samples (A-G), digested tryptically and analysed by mass spectroscopy. One representative example of MALDI-TOF spectra is given above. Peptides above 50 kDa were also analysed (data not shown).

Discussion

4.1. Characterisation of co-culture components . . . 92
4.1.1. Human primary osteoblast characterisation . . . 93
4.1.2. Osteosarcoma cell line characterisation . . . 95
4.1.3. Comparison of osteoblast cell lines expressing GFP . . . 100
4.1.4. Primary human endothelial cells . . . 103
4.2. Angiogenesis in co-culture systems . . . 104
4.2.1. Comparison of angiogenic effects in co-culture systems . . . 105
4.2.2. Angiogenic potential of osteoblast cell culture supernatants . . . 106
4.2.3. Angiogenic effects of lymphatic and vascular populations . . . 107
4.3. Screening for angiogenesis-inducing factors . . . 109
4.3.1. Translational analysis . . . 110
4.3.2. Transcriptional analysis . . . 111

4.1 Characterisation of co-culture components

The successful integration of bone tissue engineering constructs in patients requires neovascularisation by the host blood vessels via angiogenesis. *In vitro* prevascularisation of scaffolds is a promising approach for bone tissue engineering and regenerative medicine. Human pOB from different tissues and osteosarcoma cell lines are commonly used alone or in combination with endothelial cells (Meyer and Wiesmann, 2006) to evaluate cell compatibility and their effects on the angiogenic potential of endothelial cells when cultured on biomaterials *in vitro*. Relevant parameters to assess biocompatibility of scaffolds for use in bone tissue replacement are adhesion of cells, replication, spread and survival of osteoblasts as well as the expression of osteoblastic markers such as ALP, osteocalcin, collagen, calcium and matrix mineralisation. It is hoped that the results from these studies will help to predict the outcome of the materials once implanted.

Human pOB from different tissues and different osteosarcoma cell lines vary in their potential to stimulate angiogenesis. In order to gain further insights into the ability of pOB from different tissues and osteosarcoma cell lines to induce angiogenesis in endothelial cells from different tissues, the cells were assessed in co-culture experiments with HDMEC and HUVEC. Since the co-culture conditions determine osteogenic and angiogenic outcome parameters (Ma et al., 2011), the determination of optimal co-culture conditions, such as culture medium and cell ratio is crucial (Grellier et al., 2009). The angiogenic effects of co-cultures in this study indicated differences between donors of pOB, osteosarcoma cell lines and types of endothelial cells, which will be discussed in the following sections.

For identification of factors that might be responsible for the aforementioned differences, the cellular co-culture components (primary osteoblasts from different tissues and three different osteosarcoma cell lines) were characterised in the first part of the study and examined for their ability to induce angiogenesis in HDMEC and HUVEC. Additionally, gene expression patterns of monocultures of primary osteoblasts from different tissues and the three osteosarcoma cell lines, Cal-72, MG-63 and SaOS-2, were assessed

and compared. The results showed significant differences between the cells in terms of production of angiogenesis-inducing and inhibiting factors, which will be discussed in the following sections.

4.1.1 Human primary osteoblast characterisation

Human pOB can be harvested from a variety of tissues and donors. The isolation methods are well established and range from enzymatic digestion with collagenase type II (Robey, 1995), to mechanical isolation, selectively collecting migrating osteoblasts (Jahn et al., 2010). Isolated pOB from cancellous bone display an osteoblastic phenotype (Beresford et al., 1984) with high levels of ALP activity, osteocalcin and calcium expression (Beresford et al., 1986) and matrix mineralisation (Jonsson et al., 1999). However, the origin of the bone tissue as well as the health, age and sex of the donor affect the osteoblastic phenotype of pOB *in vitro* by variations in the expression of osteogenic differentiation markers (Sutherland et al., 1995) and cytokines (Kamer et al., 2006). Also, donor dependent variations in cell proliferation (Malviya et al., 2009) and epigenetic imprints (Koch and Wagner, 2011) of pOB have been reported.

pOB are widely described with respect to osteogenic or angiogenic differentiation (Ma et al., 2011) in mono- and co-culture systems (Unger et al., 2011). The focus is mainly on the cell culture media, adhesion of cells, ALP activity or matrix mineralisation (Morike et al., 1995; Liu et al., 1997). The production of collagen and mineralised matrix is the major phenotypic characteristic of osteoblastic cells (Rodan et al., 1987). In addition, biological mineralisation is associated with elevated levels of ALP activity (Parfitt, 1976). The osteoblast phenotype is defined by the secretion of osteocalcin, collagen and calcium as well as the expression of ALP and matrix mineralisation (Metzger et al., 2013). These features indicate enhanced osteogenic differentiation (Villars et al., 2002; Kaigler et al., 2005; Villars et al., 2000).

In this study, pOB from multiple sources (bones and donors) were compared and analysed for variations in growth rates, osteogenic differentiation markers and the effects

of cell culture media on their characteristics. Additionally, the cells were used in co-cultures with endothelial cells for analysis of their potential to induce angiogenesis.

pOB were isolated from different donors of oral, knee and pelvic bones, established in cell culture and analysed at different time points. The growth of pOB was monitored by DNA quantification between day 1 and day 28 of cell culture. The results showed that pOB from pelvic bones in both donors come close to saturation density after 7 days of culture. pOB cultures from oral bone donor 3 were nearly at the saturation density after 14 days of culture, while the other donors had large quantities of DNA at day 21 and then decreased at day 28. pOB from knee donor 1 also showed an increasing DNA amount from time point to time point, while in the other donor culture the DNA quantity increased until day 14, it decreased at day 21, and then increased again until day 28.

The osteogenic differentiation markers, ALP, collagen, calcium and mineralised matrix were measured and compared between the pOB cell cultures from day 1 to day 28. Similar to the growth rates, the results show that pOB from pelvic bones in both donors produced comparable amounts of all osteogenic differentiation markers across the measured time points. Again, pOB from oral bone donor 3 differed from the other oral bone donors in that it showed increasing amounts of all markers over the culture time, while in the other donor cultures levels of all markers decreased after 14 or 21 days of culture. Analogous to the DNA amounts, knee donor 1 showed increasing amounts of osteogenic differentiation markers, while in the other donor cultures marker expression decreased after 14 days of culture, not increasing again until day 28.

These heterologous findings between the pOB source bones and donors may have been due to the differences in health, age and sex of the donors as described in previous studies (Sutherland et al., 1995; Malviya et al., 2009) and could be a source of difficulties encountered when trying to use pOB for biocompatibility studies of engineered scaffolds. Therefore, it is necessary to use one donor for each comparative experiment in biocompatibility studies and screen the scaffolds with multiple donors of pOB.

In this study it has also been demonstrated that the expression of osteogenic differentiation markers in pOB depends on the composition of the cell culture medium.

The cells demonstrated similar ALP activity in DMEM and ECGM, except for knee donor 1 which expressed higher amounts of ALP in ECGM. Collagen production was similar for cultures in both media, again except for knee donor 1 which expressed more collagen in ECGM than in DMEM. Calcium secretion in all pOB cultures was higher in DMEM than in ECGM. For matrix mineralisation the results have shown only slight differences between cultures in the two media, but knee donor 1 was found to produce more mineralised matrix in ECGM. In general, it has been shown that different media do not change the osteogenic differentiation of pOB significantly, depending on the source of bone and donor of the isolate.

The pOB were used for co-culture experiments in order to evaluate angiogenic effects on endothelial cells (HDMEC and HUVEC). pOB were used mainly as positive controls as they have a known positive influence on angiogenesis in co-cultures with endothelial cells (HDMEC and HUVEC). Negative effects of single pOB donors on angiogenesis could not be distiguished from variations between donors of primary endothelial cells.

4.1.2 Osteosarcoma cell line characterisation

The osteosarcoma cell lines Cal-72, MG-63 and SaOS-2 are widely described in the literature (Vohra et al., 2008) and commonly used in osteoblast function studies (Clover and Gowen, 1994; Bilbe et al., 1996; Rochet et al., 1999; Liu et al., 1997; Diaz-Rodriguez et al., 2009).

The osteosarcoma cell line, Cal-72, is derived from a tumor sample, extracted from the knee of a 10-year-old boy. It lacks the Y chromosome and exhibits morphological, immunohistochemical and molecular characteristics of osteoblasts. The phenotype appears to be closer to primary osteoblasts than other osteosarcoma cell lines (Rochet et al., 1999). Cal-72 cells have already been succesfully tested in bone bioengineering studies, for example on vertically aligned multi-walled carbon nanotubes where they changed their morphology depending on the nanopattern (Giannona et al., 2007).

Another osteosarcoma cell line, MG-63, is derived from an osteogenic sarcoma of

a 14-year-old male child and shows an abnormal karyotype with marker chromosomes similar to Cal-72 (Heremans et al., 1978). MG-63 cells express a similar integrin subunit profile to human pOB (Clover and Gowen, 1994). MG-63 have low level ALP activity (Rodan et al., 1987) and have previously been used for biomaterial studies on a 3-D scaffold of alginate gel combined with β-tricalcium phosphate (Florczyk et al., 2012).

The third human osteosarcoma cell line used in this study was SaOS-2 derived from a tumour sample from an 11-year-old girl (Fogh et al., 1977). The cells have a high level of osteoblastic differentiation (as highlighted by high levels of ALP activity) but very low angiogenesis-inducing potential compared to MG-63, which have low ALP expression levels (Clover and Gowen, 1994). SaOS-2 cells form a mineralised matrix which is one of the main phenotypic characteristics of osteoblasts (Rodan et al., 1987). SaOS-2 cells have previously been used in comparative biomaterial studies, showing a high degree of osteoblastic differentiation (Meikle et al., 2013). In terms of phenotypic stability, passage history should be considered as it has been shown to affect some phenotypic properties of SaOS-2 cells (Hausser and Brenner, 2005).

In previous studies, differences between SaOS-2 cells and the other osteosarcoma cell lines have been described. For example, the detachment of adherent cells from the extracellular matrix results in apoptosis (a process known as 'anoikis') (Frisch and Francis, 1994). SaOS-2 cells underwent significant apoptosis when adherence was prevented, while human osteosarcoma MG-63 cells were distinctly resistant to anoikis (Lin et al., 2008). Furthermore, SaOS-2 cells have been shown to produce no osteocalcin *in vitro* (Rodan et al., 1987) while pOB (Morike et al., 1995), Cal-72 and MG-63 (Rochet et al., 1999) cells do.

In this study, the osteosarcoma cell lines Cal-72, MG-63 and SaOS-2 were characterised and compared with respect to their osteoblastic differentiation and angiogenesis-inducing potential. Although these are cell lines which are expected to have similar phenotypes and effects in co-culture with endothelial cells, all three cell lines have shown significant differences in osteoblast differentiation markers and their potential to induce

angiogenesis in endothelial cells. A schematic overview of the characterisation results for Cal-72, MG-63 and SaOS-2 as found in this study is given in Figure 4.38.

The results for ALP activity differed significantly between the osteosarcoma cell lines. SaOS-2 cells showed strong expression of all osteoblastic differentiation markers, ALP, collagen, calcium and matrix mineralisation, thus indicating a high level of differentiation. In terms of ALP activity Cal-72 and MG-63 showed less osteoblastic differentiation than SaOS-2 cells, which is also documented in a previous study (Rodan et al., 1987). In addition, in terms of matrix mineralisation, the results here indicated a lower biological mineralisation by MG-63 than the other osteosarcoma cell lines. With respect to collagen and calcium production, all cell lines were comparable. All markers have the potential to influence cell adhesion, cell-cell communication in co-culture systems as well as the expression of other factors that might be relevant for the formation of micro-capillary structures in co-culture with endothelial cells.

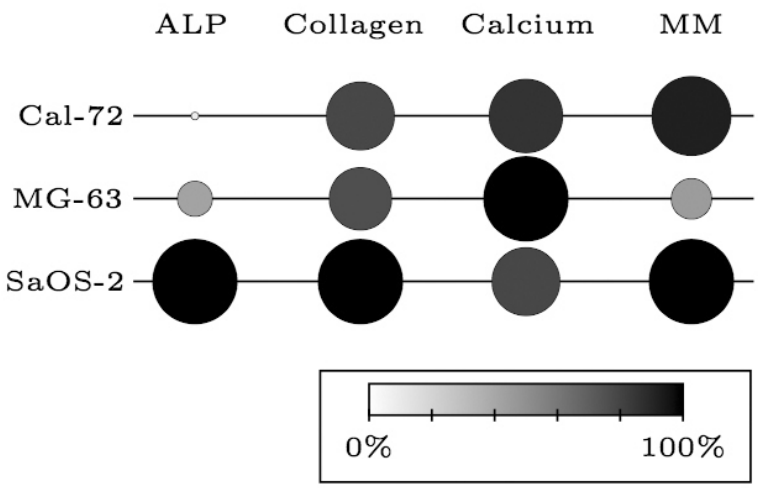

Figure 4.38: **Schematic overview of osteoblastic differentiation markers in human osteosarcoma cell lines**
Scaled characterisation results from Cal-72, MG-63 and SaOS-2 cell cultures at day 14. ALP, collagen, calcium and matrix mineralisation (MM) are related between the cell lines, the largest value is set 100 percent. Circle diameter and color are correlated to the relative percentage. Due to significant differences whithin pOB they were not included in this figure.

A comparative quantification of osteogenic differentiation markers in DMEM and ECGM was performed for the osteosarcoma cell line cultures between day 1 and day 28. The results for ALP indicate that Cal-72 have a higher ALP activity in ECGM than in DMEM while MG-63 and SaOS-2 show higher ALP activities in DMEM. Collagen production differed in both media for all cell lines depending on cell culture duration. All three osteosarcoma cell lines lacked calcium production in ECGM whereas in DMEM there were

high levels of calcium production. Matrix mineralisation, another osteoblastic property evaluated here, was higher in DMEM than in ECGM for all cell lines. To summarise, results indicated higher osteoblastic differentiation of Cal-72 cells in ECGM than in DMEM, followed by MG-63 and SaOS-2 cells. The lack of important compounds for osteoblast differentiation, such as calcium, in ECGM may be an explanation.

From the literature it is known that growth factors have variable effects on osteoblasts (Dodds et al., 1994; Mundy et al., 1995; Tsai et al., 2000). The growth factors, TGF-β and FGF, increase cell adhesion and proliferation of osteoblasts (Reyes-Botella et al., 2002). HGF, secreted by osteoblasts, also stimulates proliferation via the PI3K, Akt and AP-1 signaling pathways (Chen et al., 2012). It is a key player in angiogenesis, acting via stimulation of endothelial cells (Yamada et al., 2013). Cal-72 have been reported to express HGF and its receptor c-MET. This autokrine loop might contribute to the invasiveness of the tumor from which Cal-72 originated (Rochet et al., 1999). In addition, VEGF and bFGF are well known inducers of angiogenesis (Folkman, 1995).

VEGF is released by a number of different cell types, including osteoblasts, and acts as a signalling protein for capillary sprouting (Diegelmann and Evans, 2004). It stimulates cellular responses by binding to VEGFR-2, a tyrosine kinase receptor. VEGF is regulated by TGF-β, a major cytokine released from bone tissue (Chim et al., 2013). In addition, TGF-β initiates bFGF production in osteoblasts (Beck and D'Amore, 1997). bFGF acts as autocrine and paracrine factor that stimulates cell proliferation and angiogenesis-related growth factor expression in endothelial cells (Seghezzi et al., 1998). Cell proliferation and migration in endothelial cells is inhibited by endostatin (Rehn et al., 2001). It regulates many signalling pathways such as TNFα and AP-1, and is suggested to interfere with bFGF and VEGF (Abdollahi et al., 2004).

Since tumors induce blood vessel formation by the secretion of growth factors (Wang et al., 2010; Ricci-Vitiani et al., 2010), the osteosarcoma cell lines were characterised regarding their release of the growth factors VEGF, bFGF, HGF and the endothelial cell inhibitor endostatin. A schematic overview of the results from Cal-72, MG-63 and SaOS-2

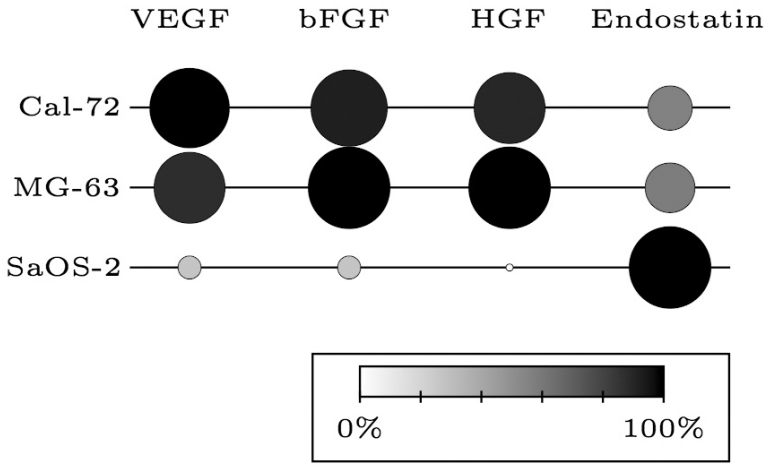

Figure 4.39: **Schematic overview of growth factors in human osteosarcoma cell lines**
Scaled characterisation results from Cal-72, MG-63 and SaOS-2 cell cultures at day 14. VEGF, bFGF, HGF and endostatin are related between the cell lines, the largest value is set 100 percent. Circle diameter and color are correlated to the relative percentage. Due to significant differences whithin pOB they were not included in this figure.

cultures in this study is given in Figure 4.39.

The osteosarcoma cell line cultures were analysed at different time points (between day 1 and day 28). The results of the growth factor quantification experiments are highly relevant when considering the effect of osteosarcoma cell lines on endothelial cells in co-culture systems and therefore biocompatibility of scaffolds. The results have shown that SaOS-2 cells secrete significantly less angiogenesis-inducing growth factors (VEGF, bFGF and HGF) than Cal-72 and MG-63 cells. VEGF is also known to retard the differentiation of osteoblasts in bone regeneration (Song et al., 2011), which might be an explanation for the decreased amounts of the osteoblast differentiation marker ALP in Cal-72 and MG-63 as mentioned above. Additionally, endostatin, which inhibits proliferation and migration in endothelial cells, is significantly increased in SaOS-2 cells compared to Cal-72 and MG-63 cells. These are very important findings for biocompatibility studies and scaffold vascularisation, as SaOS-2 cells have different effects than Cal-72 and MG-63.

Additionally, VEGF and HGF were analysed in 3-D cultures to assess permeability of the molecules through the collagen gel matrix. Analogous to the 2-D results, Cal-72 and MG-63 produced significantly higher amounts of HGF than SaOS-2 cells. VEGF levels also increased in Cal-72 and MG-63 compared to SaOS-2.

Bearing in mind results from growth factor quantification experiments, Cal-72 and MG-63 cells were expected to induce the formation of micro-capillary structures in co-

culture with endothelial cells *in vitro*, since VEGF, HGF and bFGF are known to have angiogenesis-inducing effects (Folkman, 1995; Yamada et al., 2013). In contrast, the angiogenesis-inducing potential of SaOS-2 cells in co-culture with endothelial cells was expected to be rather low. The results from co-culture experiments supported these assumptions, showing angiogenesis induction in co-cultures of Cal-72 and MG-63 with endothelial cells from different tissue sources and no angiogenesis in co-cultures of SaOS-2 with the same endothelial cells. These results are discussed further in Section 4.2.

To summarise, osteoblast differentiation markers indicated a lower osteoblastic differentiation level for Cal-72 and MG-63 than SaOS-2 cells. The results for pOB differed depending on the location of the bone from which osteoblasts were isolated, as well as on the donor, thus pointing to potential problems when using pOB for biocompatibility studies on engineered scaffolds. The medium composition also has strong effects on osteoblastic differentiation by providing important ions. Growth factor secretion by osteoblasts is essential for angiogenic activation of endothelial cells in co-culture systems. The osteosarcoma cell lines Cal-72 and MG-63 secrete higher amounts of angiogenic factors (VEGF, bFGF and HGF) than SaOS-2 cells and lower amounts of the angiogenic inhibitor, endostatin, in both 2-D and 3-D cultures.

4.1.3 Comparison of osteoblast cell lines expressing GFP

In this study, the osteosarcoma cell lines were also used in the GFP-transfected form (Günther, 2009) for co-culture experiments. The advantage of using GFP-expressing cells is that cells can be identified and tracked *in vitro* without additional staining. The GFP gene has been well documented to reliably produce fluorescent protein in heterologous cell systems without inducing cellular toxicity (Chalfie et al., 1994). To assure the comparability of the results to the parental osteosarcoma cell lines with GFP-expressing osteosarcoma cell lines, cells were also characterised regarding their morphology, cell viability and proliferation, as well as their osteoblast-like characteristics

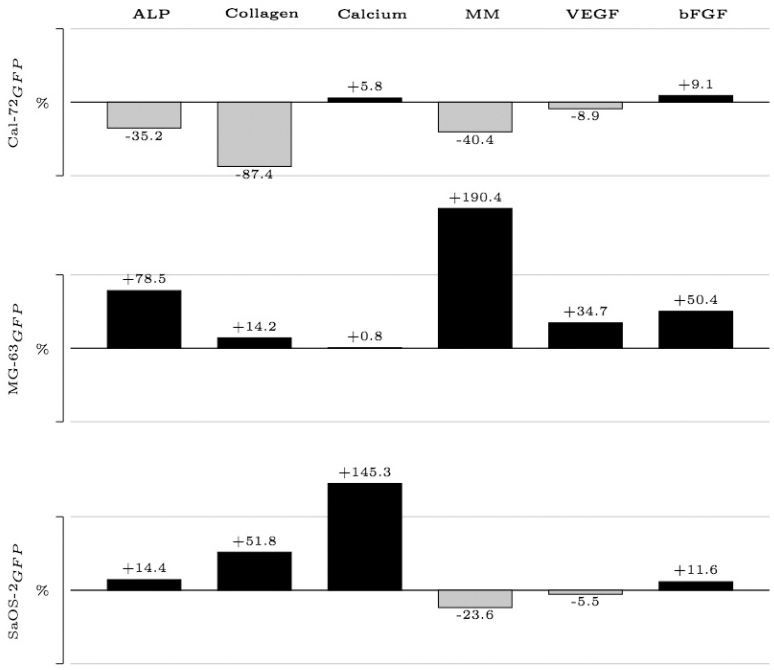

Figure 4.40: **Changes in key markers between GFP-expressing and parental osteosarcoma cell lines**
Increased expression rates (black), decreased rates (gray). Osteosarcoma cell lines were transfected by Günther (2009). Mean values from 14 day cell culture samples were used for comparison.

and compared with the untransfected cell lines. An overview of the differences is given in Figure 4.40.

The morphology of GFP-expressing osteosarcoma cell lines was observed by fluorescence microscopy and was found to resemble those of the normal osteosarcoma cell lines (Cal-72, MG-63 and SaOS-2). For SaOS-2 cells these results are also supported by previous literature (Morelli et al., 2007).

In terms of cell viability and proliferation, GFP-expressing and normal non-GFP-expressing osteosarcoma cell lines showed no significant differences. However, SaOS-2 cells with and without GFP were found to have reduced cell viability and proliferation than the other osteosarcoma cell lines, indicating a slower cell growth and proliferation *in vitro*. With respect to ALP, the GFP-expressing MG-63 cell line showed a nearly 80 % increase in ALP activity compared to non GFP-expressing MG-63, and changes of up to 35 % for Cal-72 and SaOS-2 cells. The results for GFP-expressing MG-63 revealed a significant increase in matrix mineralisation compared to normal MG-63. In terms of collagen production, the GFP-expressing Cal-72 cell line produced 87 % less collagen than the untransfected Cal-72 counterpart. Collagen production in GFP-expressing SaOS-2 cells was increased by 51 % compared to non-GFP-expressing SaOS-2 cells. The results for calcium quantification revealed significantly increased levels in the GFP-expressing SaOS-2 cells compared to the normal SaOS-2 cells. The observed differences in ALP activity,

collagen, calcium and matrix mineralisation between the cells might indicate different levels of osteoblastic differentiation. Further comparison of GFP-expressing and normal osteosarcoma cell lines was performed by the analysis of growth factors and co-cultures of those cell lines with endothelial cells.

The results showed that production of the angiogenesis-stimulating growth factors bFGF and VEGF was increased in GFP-expressing MG-63, while almost no changes were detected among the other cell lines. However, co-culture experiments of these cell lines with endothelial cells revealed no differences between GFP-expressing and normal cells. These findings indicate that the GFP transfection does not influence the angiogenic behaviour of the cells in the co-culture systems. Furthermore, SaOS-2 cells, which show no angiogenic behaviour of the cells in co-cultures, have been demonstrated to have a lower proliferation rate than Cal-72 and MG-63. This could be due to more factors then just bFGF and VEGF for stimulating angiogenesis in endothelial cells *in vitro* (Takahashi et al., 2005; Carmeliet, 2000b).

The GFP-transfected osteosarcoma cell lines showed stable GFP expression and similar cell viability and proliferation rates to the original Cal-72, MG-63 and SaOS-2 cell lines. The differences in expression of osteoblastic differentiation markers and growth factors may have been a result of the randomised integration site of the GFP gene into the host cell genome. The vector pEGFP-N1 used for transfection (Günther, 2009) is cut by restriction enzymes within the cell and randomly integrated into the genome (Yamaguchi et al., 2011; Stuchbury and Munch, 2010). Osteoblastic marker genes may have been affected by insertional mutagenesis as reported in previous literature (Cereseto and Giacca, 2004). Since the GFP-expressing osteosarcoma cell lines behave similarly to their parental cell line in co-culture systems, they are useful for visualisation of the GFP-labelled cells in *in vitro* studies.

4.1.4 Primary human endothelial cells

Primary human endothelial cells from different sources are one of the key elements of co-culture systems for the study of angiogenesis and vascularisation (Bishop et al., 1999; Donovan et al., 2001). In bone tissue engineering, a goal is to use endothelial cells for biomaterial colonisation to accelerate the healing response in patients. In previous studies it has been shown that vascularisation with the host vasculature occurs when co-cultures of endothelial cells and fibroblasts or osteoblasts are cultured on 3-D scaffolds and implanted after prevascularisation has occurred (Unger et al., 2010; Tremblay et al., 2005; Rouwkema et al., 2006; Dohle et al., 2011; Haq et al., 1992).

For the formation of micro-capillary structures, stability and differentiation of endothelial cells, extracellular matrix and growth factors are important (Donovan et al., 2001). In addition, the source of the endothelial cells may have effects on angiogenesis. Since the cells have been well characterised in the literature according to expression of specific markers, like vWF (Jaffe et al., 1973), PECAM (Albelda and Buck, 1990) and the VEGF-receptors, Flt-1 and KDR (Hewett and Murray, 1996), the isolated cells in this study were verified regarding these markers by immunofluorescent staining. All human endothelial cells used in this study express the endothelial cell specific marker PECAM, which was detected by CD31 staining in mono- and co-cultures. Endothelial cells were derived from juvenile foreskin (HDMEC), umbilical vein (HUVEC), umbilical artery, lung (HPMEC) and blood buffy coats (OEC).

In the present study, endothelial cells from all mentioned sources were analysed and compared in terms of their morphology and also to assess lymphatic subpopulations by immunofluorescent staining and FACS analysis using D2-40 antibody (Kahn and Marks, 2002). Depending on the origin of the tissue, vascular and lymphatic endothelial cells co-exist (Tammela et al., 2005) and indeed appeared together in the cell cultures of this study. The ratio of lymphatic and vascular endothelial cells in the cultures varied greatly. While the endothelial cell line ST-1 and OEC contained 75 to 80 % D2-40 positive cells, the ratio in HPMEC differed among the donors from 10 to 60 % D2-40 positive cells.

HDMEC and human cardiac microvascular endothelial cells (HCMEC) showed similar populations of lymphatic endothelial cells in the range of 15 to 35 %. The lowest ratio of lymphatic to vascular endothelial cells was found in oral mucosa endothelial cells. Only HUVEC were found to have no lymphatic population within cell cultures.

The mixed populations may have been due to the isolation methods employed, as this could have been a source of contaminating lymphatic endothelial cells. Only HUVEC were shown to consist solely of vascular endothelial cells. A probable explanation for this is that during the isolation of umbilical vein endothelial cells contact of the isolated cells with the lymphatic system is very unlikely. In contrast, in the isolation of HDMEC or HPMEC, for example, the co-isolation of lymphatic endothelial cells from the tissue is highly likely. The same applies to HCMEC, OEC and oral mucosa endothelial cells. Since the HPMEC derived cell line, ST-1 is pesumably a clone from a single cell, the lymphatic population might also derive from unstable immortalization or vascular endothelial cells changing their phenotype during *in vitro* cell culture.

4.2 Angiogenesis in co-culture systems

Vascularisation of bone tissue engineering constructs with the host vasculature is driven by angiogenesis. As described previously, *in vitro* prevascularisation of scaffolds is a promising approach for successful bone tissue engineering and regenerative medicine. Understanding the angiogenic processes in co-cultures is essential for optimisation of scaffold prevascularisation. Human pOB from different tissues and osteosarcoma cell lines are commonly used with endothelial cells in co-culture systems (Meyer and Wiesmann, 2006) in order to investigate cell compatibility and the effects on angiogenic potential *in vitro*.

In the present study, endothelial cells and osteoblasts were co-cultivated in 2-D and 3-D experiments to assess biomaterial colonisation and factors effecting angiogenesis. In designing co-culture experiments one must consider the question being asked and attempt to replicate, as far as possible, the physiological conditions (Takezawa, 2003).

Since it had been shown that pOB and the osteosarcoma cell lines, Cal-72, MG-63 and SaOS-2, differed in terms of osteoblastic differentiation level and growth factor expression, the cells were compared regarding their potential to induce angiogenesis in endothelial cells. The results of co-culture studies were verified by testing the cell culture medium supernatants for angiogenesis-inducing potential of the pOB and osteosarcoma cell lines.

4.2.1 Comparison of angiogenic effects in co-culture systems

In 2-D and 3-D co-cultures, angiogenesis was stimulated by the addition of primary osteoblasts or osteosarcoma cell lines to endothelial cell cultures. In 2-D co-culture systems, HDMEC and HUVEC from several donors were used to verify the results. For 3-D co-culture experiments only HDMEC were used, as these cells had previously been shown to have better stability in a collagen matrix than HUVEC.

In 2-D co-cultures, pOB appeared to have angiogenesis-inducing potential on HDMEC and HUVEC. However, the angiogenic effects were different between several donors, indicating in a similar manner to the results from pOB characterisation that the cell donor can affect culture characteristics. The donors differed in their osteogenic differentiation level, which may have determined the angiogenesis-inducing potential of the cells in 2-D co-cultures with HDMEC and HUVEC.

For the osteosarcoma cell lines, the results from 2-D co-culture experiments with HDMEC and HUVEC revealed angiogenic effects of Cal-72 and MG-63 but no detectable angiogenesis in SaOS-2 cell cultures. The results were the same for the GFP-expressing osteosarcoma cell lines. To correlate this with the characterisation results, the tendency of SaOS-2 cells to produce more osteogenic differentiation factors than Cal-72 and MG-63 and less angiogenesis-inducing growth factors resulted in the formation of fewer micro-capillary structures in 2-D co-cultures with HDMEC and HUVEC.

In 3-D co-cultures, pOB appeared to have similar angiogenesis-inducing potential in HDMEC and HUVEC as in 2-D co-culture experiments. The effects correlated with

characterisation results in that more micro-capillary structures were formed by less differentiated osteoblasts and fewer micro-capillary structures were formed by cells with greater osteogenic differentiation.

For the osteosarcoma cell lines, the results from 3-D co-culture experiments with HDMEC and HUVEC were analogous to those from 2-D co-culture experiments. Cal-72 and MG-63 induced the formation of micro-capillary stuctures in endothelial cells while SaOS-2 cells had no detectable angiogenic effects. Again the correlation of the co-culture results with those from cell characterisation revealed the tendency of SaOS-2 cells to produce more osteogenic differentiation markers than Cal-72 and MG-63 and less angiogenesis-inducing growth factors, thus resulting in formation of fewer micro-capillary structures in HDMEC and HUVEC.

It is known from the literature that VEGF retards differentiation of osteoblasts (Song et al., 2011). The high osteogenic differentiation level of SaOS-2 cells might result from the low level of VEGF in those cells, which may be a signal of cell aging or quiescence and lead to less angiogenic stimulation of endothelial cells. In addition, SaOS-2 cells produced high amounts of the endothelial cell inhibitor endostatin, which might also have been a contributory factor to the lack of angiogenesis in co-cultures.

4.2.2 Angiogenic potential of osteoblast cell culture supernatants

Besides secreted factors, cell-cell contacts between the cells may also contribute to induction of angiogenesis in endothelial cells (Kiran et al., 2011). Experiments with cell culture medium supernatants of osteoblasts on HDMEC and HUVEC were performed to exclude this possible explanation. The results verified that the angiogenesis-inducing factors are secreted and in this case no cell-cell contacts between osteoblasts and endothelial cells are necessarily involved in the process. Furthermore, the results have shown that collagen or other matrix components also have no effect on the formation of micro-capillary structures. These experiments were only carried out on osteosarcoma cell lines

due to their reliability compared to pOB, which showed strong variations between different donors.

In experiments with cell culture medium supernatants from osteosarcoma cell line monocultures, Cal-72 and MG-63 resulted in the formation of micro-capillary structures of HDMEC and weak angiogenic effects in HUVEC. In contrast, SaOS-2 cell culture medium supernatants did not induce angiogenesis in endothelial cells. Furthermore, these results were verified in 2-D co-cultures of endothelial cells with SaOS-2 cells. Alone, these co-cultures showed no formation of micro-capillary structures. However, when cell culture medium supernatants from Cal-72 or MG-63 are added to HDMEC and SaOS-2 co-cultures angiogenesis was initiated after 28 days of culture. From the literature it is known that endothelial cells stimulate osteoblasts to upregulate angiogenesis-inducing factors in co-cultures (Kirkpatrick et al., 2011). Therefore, the experiments were adjusted with regard to co-culture medium supernatants. Cell culture medium supernatants from co-cultures of endothelial cells with Cal-72 and MG-63 stimulated angiogenesis in co-cultures of HDMEC and SaOS-2 cells. However, the formation of micro-capillary structures was not as good as when HDMEC and Cal-72 or HDMEC and MG-63 were cultured together. This might be due to the dilution of used cell culture medium supernatants with fresh medium to provide enough nutrients for the cells.

However, the identity of the factors responsible for angiogenesis stimulation in co-cultures containing Cal-72 or MG-63, are not completely known. Therefore, the cell culture medium supernatants were studied for differences between the osteosarcoma cell lines, Cal-72, MG-63 and SaOS-2 using several analytical techniques. The results of these studies is discussed in Section 4.3.

4.2.3 Angiogenic effects of lymphatic and vascular populations

The previously described populations of lymphatic and vascular endothelial cells in cultures of primary endothelial cells were analysed for their angiogenic potential in co-culture with pOB. In this study, both populations have been shown to have different effects on the

formation of micro-capillary structures in co-cultures. Separation and combination experiments of lymphatic and vascular fractions of endothelial cells indicated that lymphatic endothelial cells may not be directly involved in angiogenesis. However, these cells are thought to strengthen the formation of micro-capillary structures in HDMEC co-cultures. The vascular endothelial cell fraction showed formation of micro-capillary structures in co-culture with pOB, whereas the lymphatic fraction did not result in angiogenesis in these studies.

The lymphatic endothelial cell marker and target for the D2-40 antibody, podoplanin, is different in the subpopulations of endothelial cells and was suggested as a possible factor involved in angiogenesis. It was proposed that podoplanin might be one mechanism of the angiogenesis-enhancing effects of lymphatic endothelial cells. Therefore, SaOS-2 cells, which alone had no angiogenic effect in co-cultures, were transfected with podoplanin.

Although the expression strength of the constitutive cytomegalovirus (CMV)-promoter can vary from cell type to cell type (Qin et al., 2010), positive transfection was detected by immunofluorescent staining. The event of gene silencing was unlikely, since strong expression was evident in microscopic evaluation of staining. In this study, the transfected cells (SaOS-2_PDPN) were analysed for the expression of the pro-angiogenic growth factor VEGF (Cross and Claesson-Welsh, 2001; Leung et al., 1989) and their ability to induce the formation of vessel-like structures. The results were compared with untransfected SaOS-2 cells as well as pOB, Cal-72 and MG-63.

It was demonstrated that transfected SaOS-2_PDPN secreted significantly higher amounts of VEGF than untransfected SaOS-2 cells as well as pOB, Cal-72 and MG-63. In addition, results from co-culture experiments with transfected SaOS-2_PDPN cells supported the suggestion that podoplanin might be involved in angiogenesis. However, the signalling cascade in which podoplanin might be involved or details of how it affects angiogenesis-related pathways are not yet known. Additionally, these first findings need to be verified in further experiments.

4.3 Screening for angiogenesis-inducing factors

In co-cultures, cells are in close apposition, thus allowing for intensive cell-cell communication (Santos et al., 2009; Pap et al., 2009). In the present study, cell-cell communication was investigated on translational and transcriptional levels with regard to angiogenesis-inducing factors. The osteosarcoma cell lines were compared in terms of gene expression and secretion of factors into the cell culture medium.

In the literature, the osteosarcoma cell lines, SaOS-2, Cal-72 and MG-63, have been widely used for different cancer and biomaterial studies. However these cells were not yet described and compared in terms of osteogenic differentiation, or expression of pro- or anti-angiogenic factors. It is known that SaOS-2 quickly reach a high level of osteogenic differentiation (Lamour et al., 2007), and this has been supported by the present study. These processes are regulated by Runt domain transcription factor (Schroeder et al., 2004). Additionally, the expression of pro-angiogenic VEGF in SaOS-2 can be stimulated in many ways by other growth factors (Goad et al., 1996).

It has previously been shown that some osteosarcoma cell culture medium supernatants, especially U2OS cells, are capable of inducing angiogenesis (Pignochino et al., 2009). These cells express functional tumour suppressor genes like p53 and pRb, while in more aggressive osteosarcoma cell lines, like SaOS-2 cells, these genes are mutated (Niforou et al., 2008). U2OS cells are also reported to have the lowest number of chromosomal variations and only 2 % of the cells have multipolar mitoses, probably due to the presence of functional p53 and pRb (Isfort et al., 1995). Besides U2OS, SaOS-2 cells are also commonly used and well established in our laboratory and were therefore used in the present study. Based on preliminary studies we suggested that there were significant differences between the osteosarcoma cell lines, Cal-72, MG63 and SaOS-2, on both translational and transcriptional level.

4.3.1 Translational analysis

Comparative translational analysis of angiogenesis-related markers was performed in this study to gain insights into the angiogenesis-inducing potential in the various osteosarcoma cell lines. For identification of potential peptide-based pro- and anti-angiogenic factors, cell culture supernatants from osteosarcoma cell line monocultures were analysed. Initially ELISA and protein arrays were used to quantify osteoblast differentiation markers (ALP, collagen, calcium), growth factors relevant for angiogenesis (VEGF, bFGF, HGF) and potential angiogenesis inhibitors (endostatin) in order to determine significant differences between Cal-72, MG-63 and SaOS-2 human osteosarcoma cell lines. ELISA and antibody arrays were chosen instead of western-blot analysis as they offer better cost-/time-effectiveness, and microplates allow for higher sample throughput.

As discussed previously and illustrated in Figure 4.39, the results revealed less angiogenesis-inducing growth factors VEGF, bFGF and HGF are produced in SaOS-2 cell culture medium supernatants than for Cal-72 and MG-63. In agreement with this, SaOS-2 cells did not induce the formation of micro-capillary structures in co-cultures. It is known that the combination of VEGF, bFGF and HGF has enhancing effects on the downstream signalling pathways AKT and ERK and induces proliferation and chemotaxis in endothelial cells (Sulpice et al., 2009; Cross and Claesson-Welsh, 2001). Therefore, further investigations into downregulation and other co-regulations of these growth factors in SaOS-2 cells are needed, some of which are described in Section 4.3.2.

Following these experiments, the effects of VEGF, bFGF and HGF were analysed by the exogenous application of these factors in the form of recombinant growth factors to the co-culture medium of SaOS-2 cells with endothelial cells. The recombinant proteins did not induce the formation of micro-vessel structures either in 2-D, or in 3-D experiments. Potential explanations for this could be that posttranslational modifications of the recombinant proteins, such as glycosylation, phosphorylation, hydroxylation, acetylation, methylation or ubiquitylation play an important role (Walsh, 2006) or that other factors, matrix proteins or as yet unknown factors are involved.

For identification of unknown angiogenic factors cell culture medium supernatants of Cal-72, MG-63 and SaOS-2 were compared using mass spectroscopic analysis. Critical hurdles were the removal of all cells from the supernatants as well as albumin, as albumin overlays all signals in SDS-PAGE being the most prominent protein in cell culture medium supernatant samples. Although the samples were carefully centrifuged and filtered with albumin-depletion columns, it was not possible to evaluate the results due to residual albumin. Besides peaks that could be correlated to albumin, no other significant signals could be detected. The analysis was validated by a positive control sample. As albumin-related problems arose during mass spectrometry, large-scale microarray analysis could be considered for further studies. However, issues may still arise as albumin is fairly 'sticky' thus cross-reaction and non-specific reactions are anticipated.

4.3.2 Transcriptional analysis

Following initial findings of differences between the osteosarcoma cell lines using translational analysis, a transcriptional analysis was performed in order to gain deeper insights into potential regulation of growth factors at the RNA level. These results were compared to current knowledge of interaction pathways.

The results from transcriptional analysis of the osteosarcoma cell lines revealed significant differences between when comparing Cal-72 and MG-63 with SaOS-2 cells. TGF-α and TIMP-2 genes appeared to be significantly downregulated in SaOS-2 cells compared to Cal-72 and MG-63 cells. In the literature, it is reported that TGF-α is upregulated in some cancers and responsible for the development of tubular structures (Greten et al., 2001). It is co-regulated with TIMP-2 (Siqueira et al., 2010) and involved in VEGF regulation through MEK and PI3K pathways (Chim et al., 2013; Wang et al., 2008).

Furthermore, the results showed up-regulation of JAG1 and CDH5, as well as IL6 in SaOS-2 cells compared to Cal-72 and MG-63 cells. This finding is contrary to current reports of IL6, IL8 and VEGF, which could point to disruptions in some growth

factor-regulating pathways in SaOS-2 cells. It is known that the pro-angiogenic and inflammatory chemokines, IL6 and IL8, are positively correlated with VEGF and tumour vasculature (Huang et al., 2004; Wei et al., 2003; Borg et al., 2005; Martin et al., 2009) and vice versa, with VEGF up-regulating IL6 and IL8 in endothelial cells (Hao et al., 2009). However, VEGF regulation is still not fully understood. Potential pathways which could be involved include PI3K, MAPK, STAT3 (Wei et al., 2003), AKT or ERK (Siqueira et al., 2010).

One factor that promotes VEGF-, bFGF- and HGF- mediated angiogenesis through enhancing VEGF-, bFGF- and HGF- induced growth of vascular endothelial cells is interleukin-17 (IL17) (Takahashi et al., 2005), which might be affected in SaOS-2 cells. This hypothesis needs further examination. Other as yet unknown regulation of angiogenesis-inducing growth factors might also be possible.

In conclusion, in future experiments further investigations into the downregulation and other regulation pathways of VEGF, bFGF and HGF in SaOS-2 cells are required. Further study of IL17 in osteoblasts and signalling cascades affected by podoplanin are also advisable. Furthermore, the possible role which matrix proteins and exosomes may play in the stimulation of micro-capillary structure formation in co-cultures of osteoblasts and endothelial cells is another interesting point for future experiments.

Summary

For the successful integration of bone tissue engineering constructs into patients, an adequate supply with oxygen and nutrients is critical. Therefore, prevascularisation of bone tissue engineering constructs is desirable for bone formation, remodelling and regeneration. Co-culture systems, consisting of human endothelial cells and primary osteoblasts (pOB) as well as osteosarcoma cell lines, represent a promising method for studying the mechanisms involved in the vascularisation of constructs in bone tissue engineering and could provide new insights into the molecular and cellular mechanisms that control essential processes during angiogenesis. The present study demonstrated the important components of co-culture systems with a focus on bone tissue replacement and the angiogenic effects of pOB and osteosarcoma cell lines on human endothelial cells. Furthermore, the studies emphasised an overall approach for analysis of signal molecules that are involved in the angiogenic activation of human endothelial cells by the regulation of VEGF-related pathways at the transcriptional and translational levels.

The osteosarcoma cell lines Cal-72, MG-63 and SaOS-2, as well as pOB from several donors, differed in their angiogenesis-inducing potential in 2-D and 3-D co-culture systems. SaOS-2 cells appeared to have a high osteogenic differentiation level with no detectable angiogenesis-inducing potential in co-culture with human endothelial cells. The angiogenic potential of the osteoblast-like cells is mainly correlated with the upregulation of essential angiogenic growth factors, such as VEGF, bFGF and HGF and the downregulation of the angiogenesis inhibitor, endostatin. However, other factors involved in angiogenic regulation were found to differ between SaOS-2 cells, compared to Cal-72 and MG-63. The present study focuses on VEGF pathway-effecting genes as key players in the regulation of angiogenesis. The levels of VEGF and VEGF-effecting genes, such as TGF-α and TIMP-2 are down-regulated in SaOS-2 cells. In contrast, direct regulators of VEGF, such as IL6, IL8 and TNF are strongly upregulated, which indicates disruptions in growth factor regulating pathways in SaOS-2 cells. Potential pathways, which could be involved include MEK, PI3K, MAPK, STAT3, AKT or ERK. Additional treatment of co-cultures with single growth factors did not accelerate or improve the angiogenesis-inducing potential of SaOS-2 cells. Knowledge of the detailed molecular mechanisms involved in angiogenesis control will hopefully allow improved approaches to be developed for prevascularisation of bone tissue engineering constructs.

Zusammenfassung

Für die erfolgreiche Integration von Knochenersatzmaterialien, ist die Versorgung mit Sauerstoff und Nährstoffen essentiell. Die Vaskularisierung dieser Materialien vor der Implantation in Patienten gilt als vorteilhaft für einen schnellen Anschluß des Implantats an das Gefäßsystem des peri-implantären Gewebes *in vivo*. Co-Kultur-Modelle aus humanen Endothelzellen und primären Osteoblasten (pOB), bzw. Osteosarcoma Zelllinien eignen sich für Vaskularisierungsstudien an Implantaten, können somit zur Verbesserung der Knochenregeneration beitragen und geben neue Einblicke in molekulare und zelluläre Mechanismen der Angiogenese.

In dieser Arbeit konnte gezeigt werden, dass die Charakteristika von Co-Kultur Komponenten einen entscheidenden Einfluss auf die Ausbildung von angiogenen Strukturen *in vitro* haben. So wurde sowohl auf Transkriptions- als auch auf Translations-Ebene nach Signal-Peptiden gesucht, die in Endothelzellen Angiogenese stimulieren und Einfluss auf die Regulation von Signalwegen haben könnten. Sowohl die Osteosarcoma Zell-Linien Cal-72, MG-63 und SaOS-2, als auch pOB von verschiedenen Spendern zeigten unterschiedlich ausgeprägte angiogene Wirkungen in 2-D und 3-D Co-Kultur Modellen. SaOS-2 Zellen, die sich am deutlichsten osteoblastär differenziert zeigten, konnte keine Angiogenese-induzierende Wirkung auf Endothelzellen nachgewiesen werden.

Das Angiogenese-induzierende Potential von osteoblastären Zellen ist abhängig von der Konzentration angiogener Faktoren, wie VEGF, bFGF und HGF sowie der Absenz von Angiogenese Inhibitoren, wie Endostatin. In dieser Arbeit wurden SaOS-2, Cal-72 und MG-63 Zellen bezüglich angiogener Faktoren untersucht und verglichen. So konnte nachgewiesen werden, dass die VEGF Menge in SaOS-2 erniedrigt ist und Gene, welche in die Regulation von VEGF-Signalwegen involviert sind, wie TGF-α und TIMP-2, in SaOS-2 herabreguliert sind. Ausserdem wurden direkte VEGF-Regulatoren, wie IL6, IL8 und TNF erhöht vorgefunden, was auf Störungen in Wachstumsfaktor-regulierenden Signalwegen in SaOS-2 deuten könnte. Potentiell involvierte Signalwege sind MEK, PI3K, MAPK, STAT3, AKT oder ERK. Zusätzlich konnte gezeigt werden, dass die monovariante Behandlung von Co-Kulturen mit Wachstumsfaktoren keinen Einfluss auf die fehlende angiogene Wirkung von SaOS-2 Zellen auf Endothelzellen hat. Ein besseres Verständnis der molekularen Kontrolle von Angiogenese könnte künftig zur verbesserten Vaskularisierung von Knochenersatzmaterialien führen.

Appendix

A.1. FACS analysis II
A.2. Effects of osteoblast cell culture medium supernatants on angiogenesis V
A.3. Effects of medium supernatants with bFGF on angiogenesis X
A.4. Transcriptional analysis of angiogenesis-related factors XI
A.5. Mass spectroscopic analysis XIII

A.1 FACS analysis

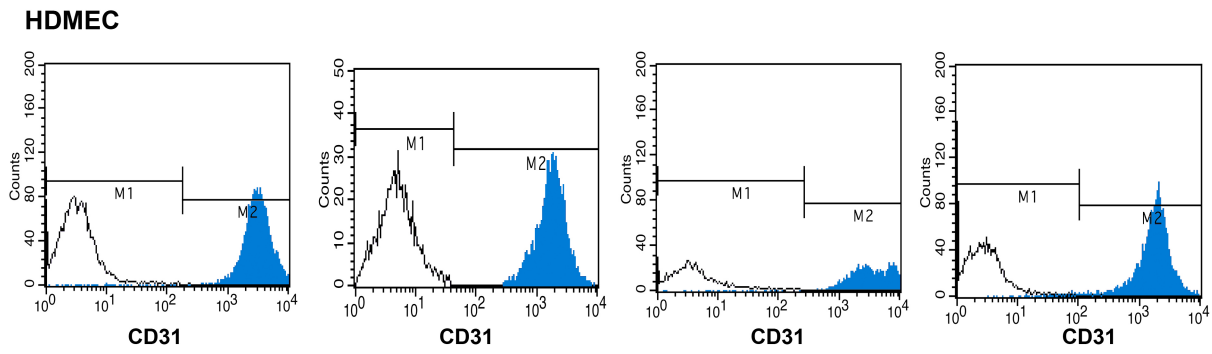

Figure A.41: **FACS analysis of CD31 in different HDMEC donors**
Histogram plots of confluent HDMEC monolayer cultures from different donors marked with CD31 antibody.

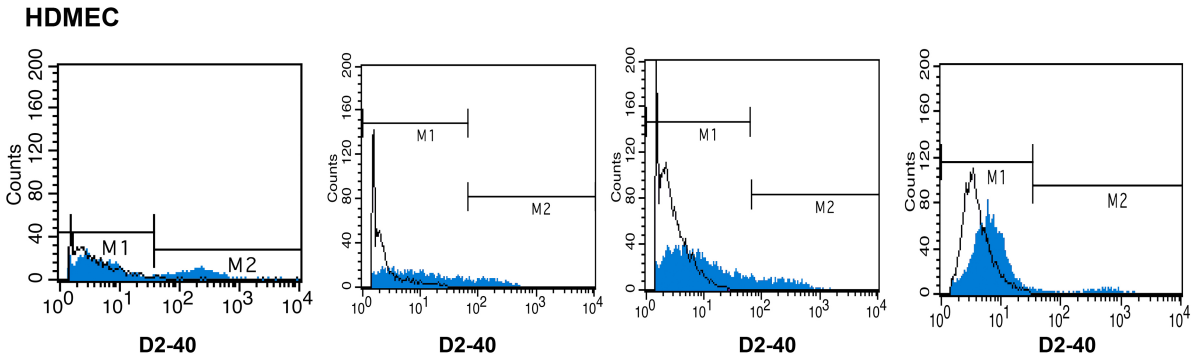

Figure A.42: **FACS analysis of CD31 and D2-40 in different HDMEC donors**
Histogram plots of confluent HDMEC monolayer cultures from different donors marked with CD31 and D2-40 antibody.

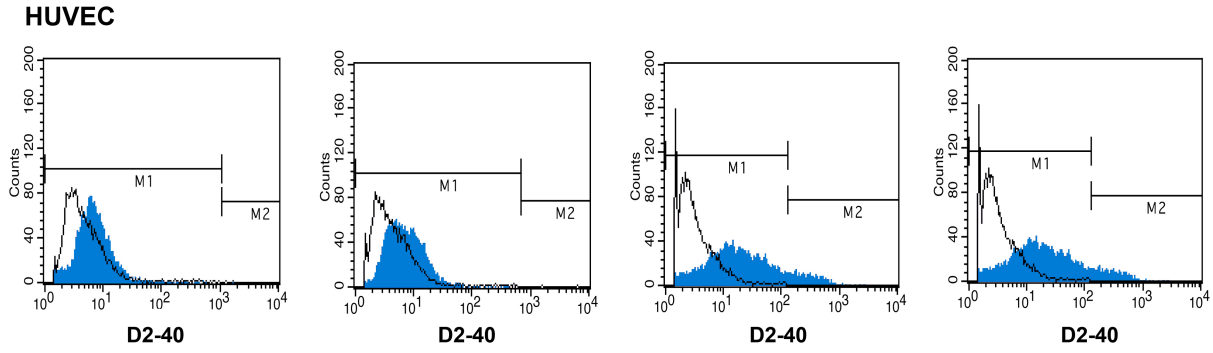

Figure A.43: **FACS analysis of D2-40 in different HUVEC donors**
Histogram plots of confluent HUVEC monolayer cultures from different donors marked with D2-40 antibody.

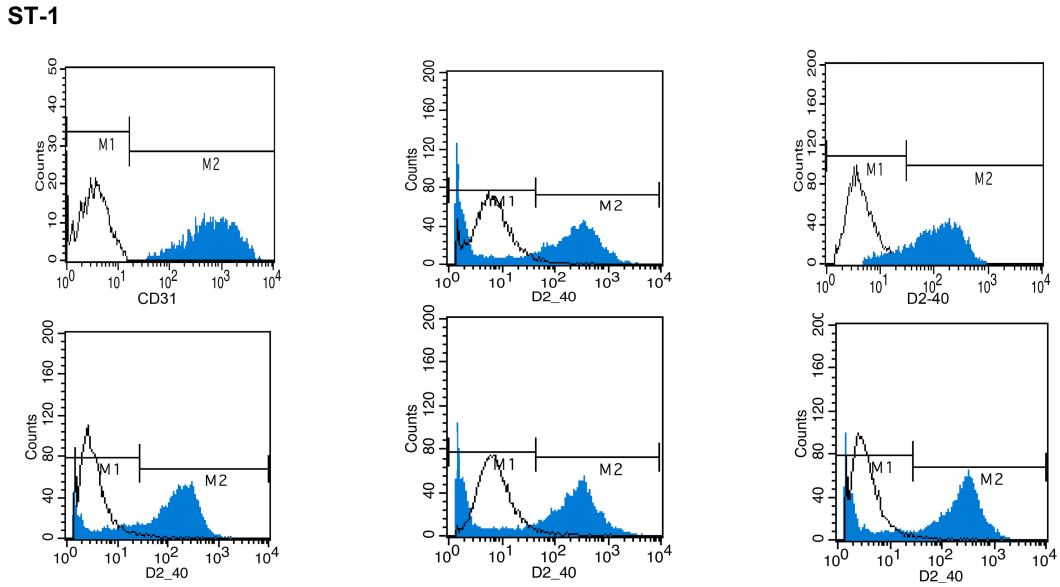

Figure A.44: **FACS analysis of CD31 and D2-40 in ST1 cultures**
Histogram plots of confluent ST1 monolayer cultures marked with CD31 and D2-40 antibody.

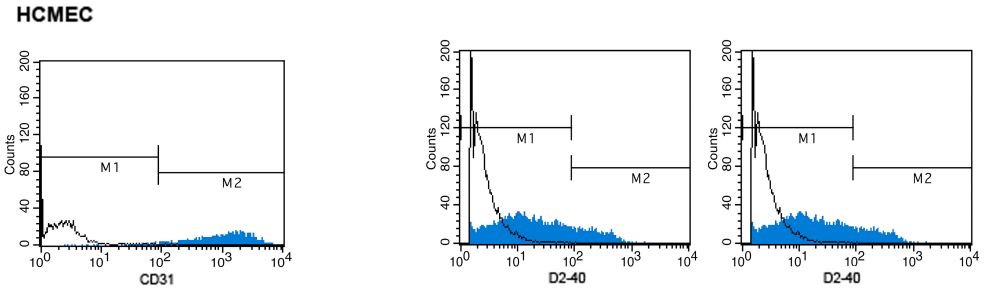

Figure A.45: **FACS analysis of CD31 and D2-40 in HCMEC cultures**
Histogram plots of different confluent HCMEC monolayer cultures marked with CD31 and D2-40 antibody.

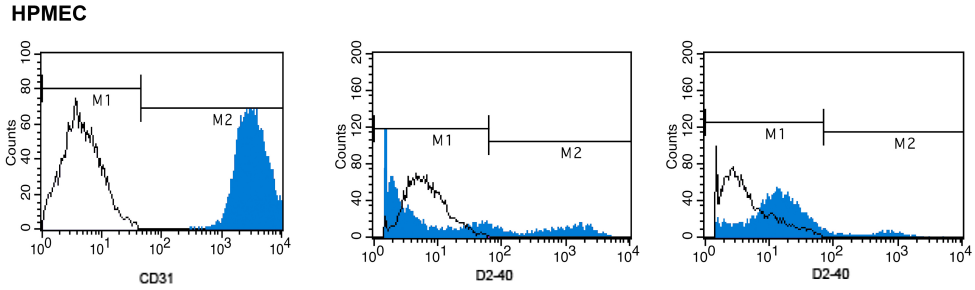

Figure A.46: **FACS analysis of CD31 and D2-40 in HPMEC cultures**
Histogram plots of different confluent HPMEC monolayer cultures marked with CD31 and D2-40 antibody.

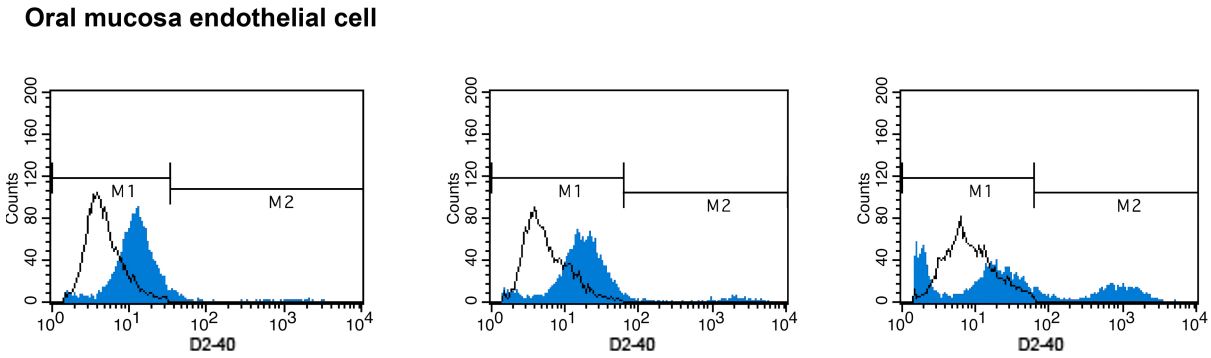

Figure A.47: **FACS analysis of D2-40 in oral mucosa endothelial cell cultures**
Histogram plots of different confluent oral mucosa endothelial cell monolayer cultures marked with D2-40 antibody.

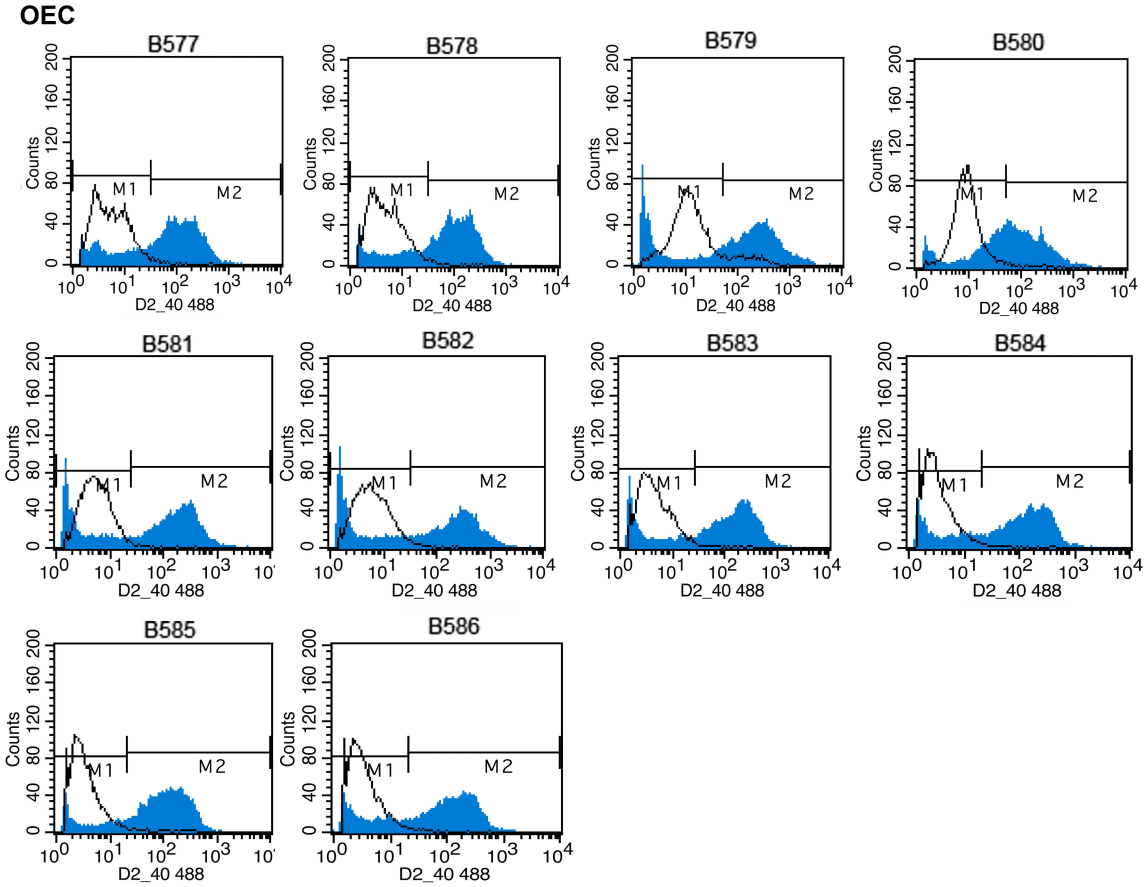

Figure A.48: **FACS analysis of D2-40 in OEC donors**
Histogram plots of confluent OEC monolayer cultures from different donors marked with D2-40 antibody.

A.2 Effects of osteoblast cell culture medium supernatants on angiogenesis

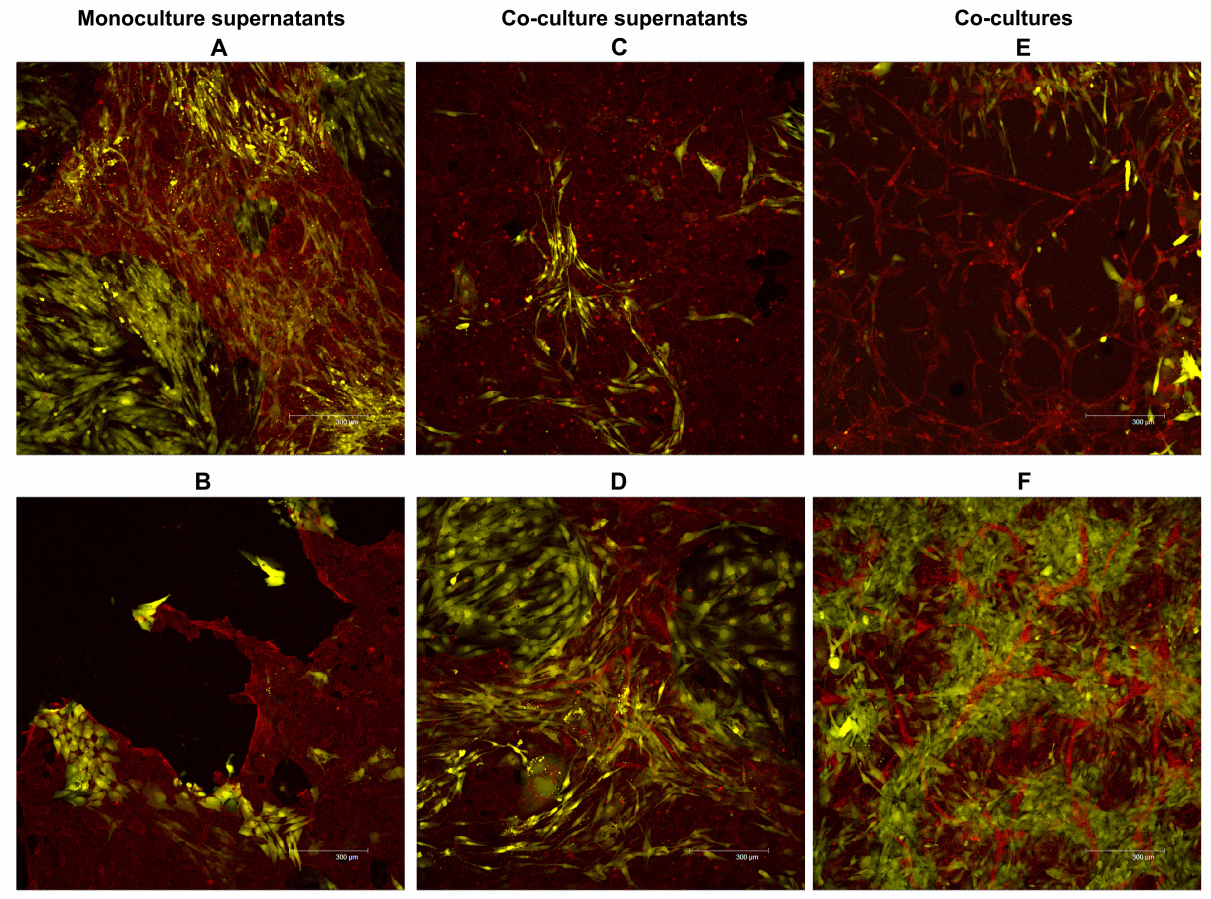

Figure A.49: **HDMEC and SaOS-2 GFP co-cultures with cell culture supernatants** Co-cultures of HDMEC and GFP-expressing SaOS-2 with cell culture medium supernatants from **A** Cal-72 GFP and **B** MG-63 GFP monocultures, and from **C** HDMEC-Cal-72 GFP and **D** HDMEC-MG-63 GFP co-cultures after 28 days. Positive controls are co-cultures of HDMEC with **E** Cal-72 GFP and **F** MG-63 GFP. Cells were immunostained with CD31 antibody (red) and DAPI (blue) and visualised by laser scanning confocal microscopy.

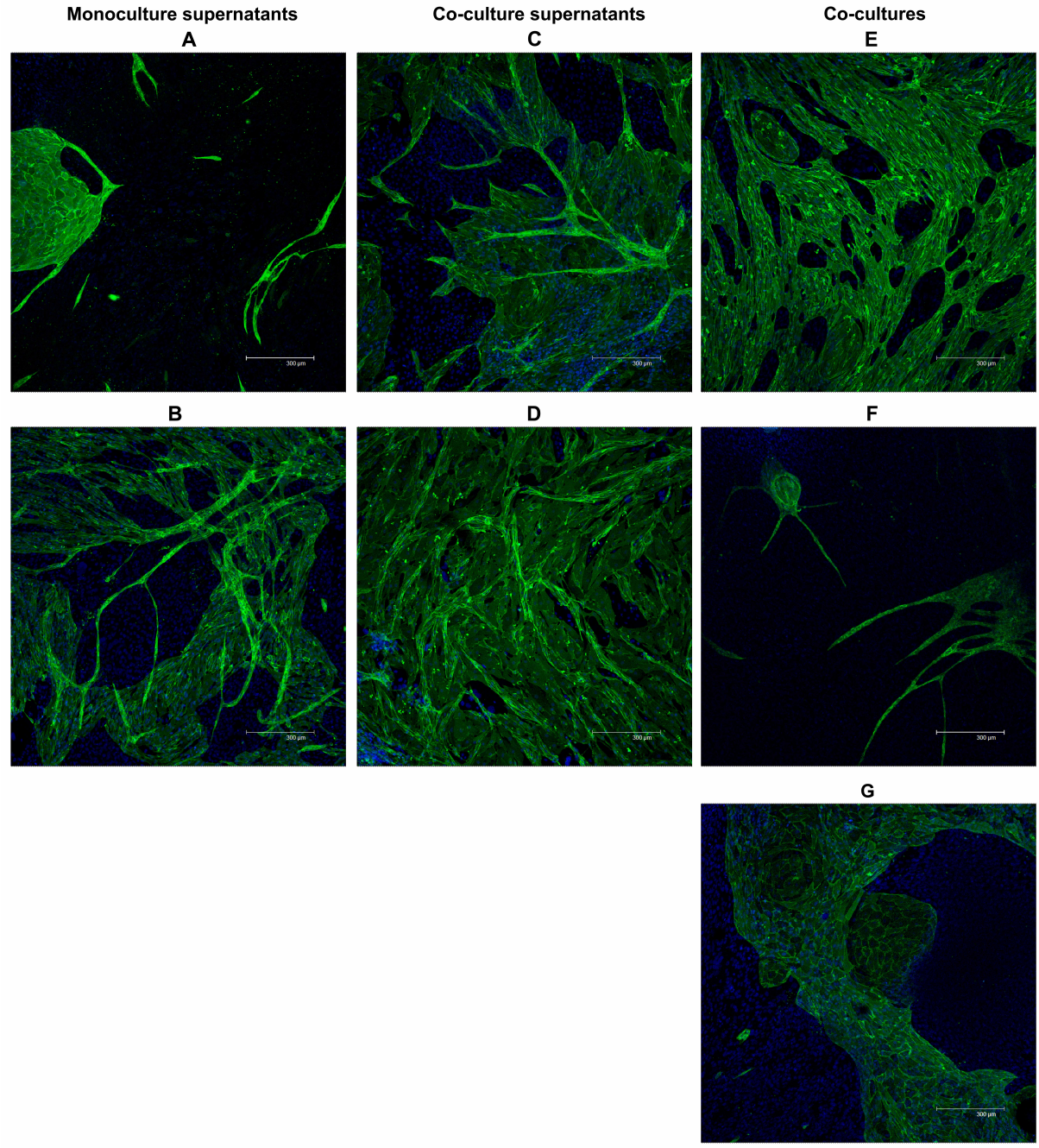

Figure A.50: **HDMEC and SaOS-2 co-cultures with cell culture supernatants**
Co-cultures of HDMEC and SaOS-2 with medium supernatants from **A** Cal-72 and **B** MG-63 monocultures, and from **C** HDMEC-Cal-72 and **D** HDMEC-MG-63 co-cultures after 28 days. Positive controls are co-cultures of HDMEC with **E** Cal-72 and **F** MG-63. The negative control **G** is a co-culture of HDMEC with SaOS-2. Cells were immunostained with CD31 antibody (green) and visualised by laser scanning confocal microscopy.

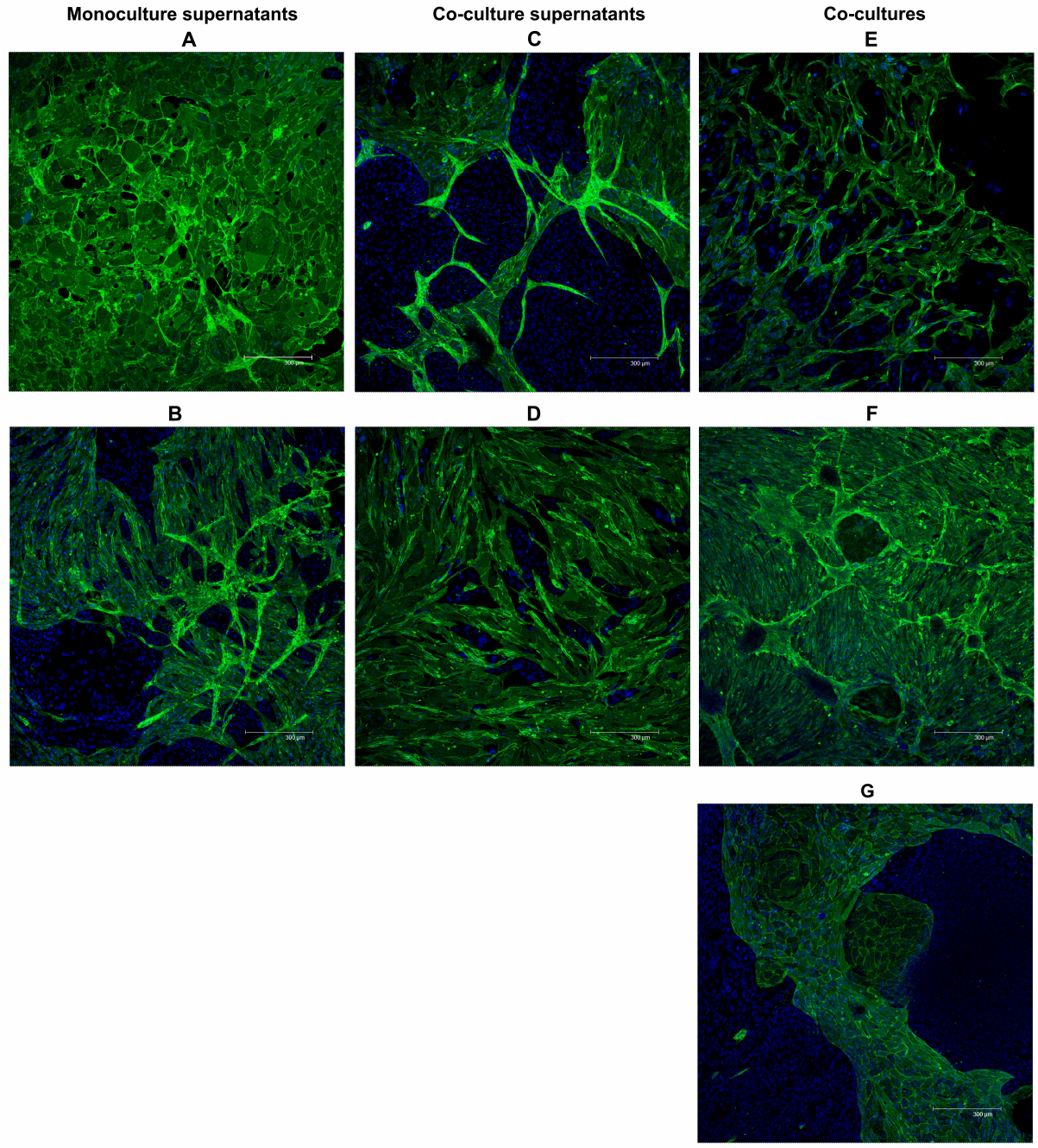

Figure A.51: **HDMEC and SaOS-2 co-cultures with cell culture supernatants**
Co-cultures of HDMEC and SaOS-2 with medium supernatants from **A** Cal-72 and **B** MG-63 monocultures, and from **C** HDMEC-Cal-72 and **D** HDMEC-MG-63 co-cultures after 28 days. Positive controls are co-cultures of HDMEC with **E** Cal-72 and **F** MG-63. The negative control **G** is a co-culture of HDMEC with SaOS-2. Cells were immunostained with CD31 antibody (green) and DAPI (blue) and visualised by laser scanning confocal microscopy.

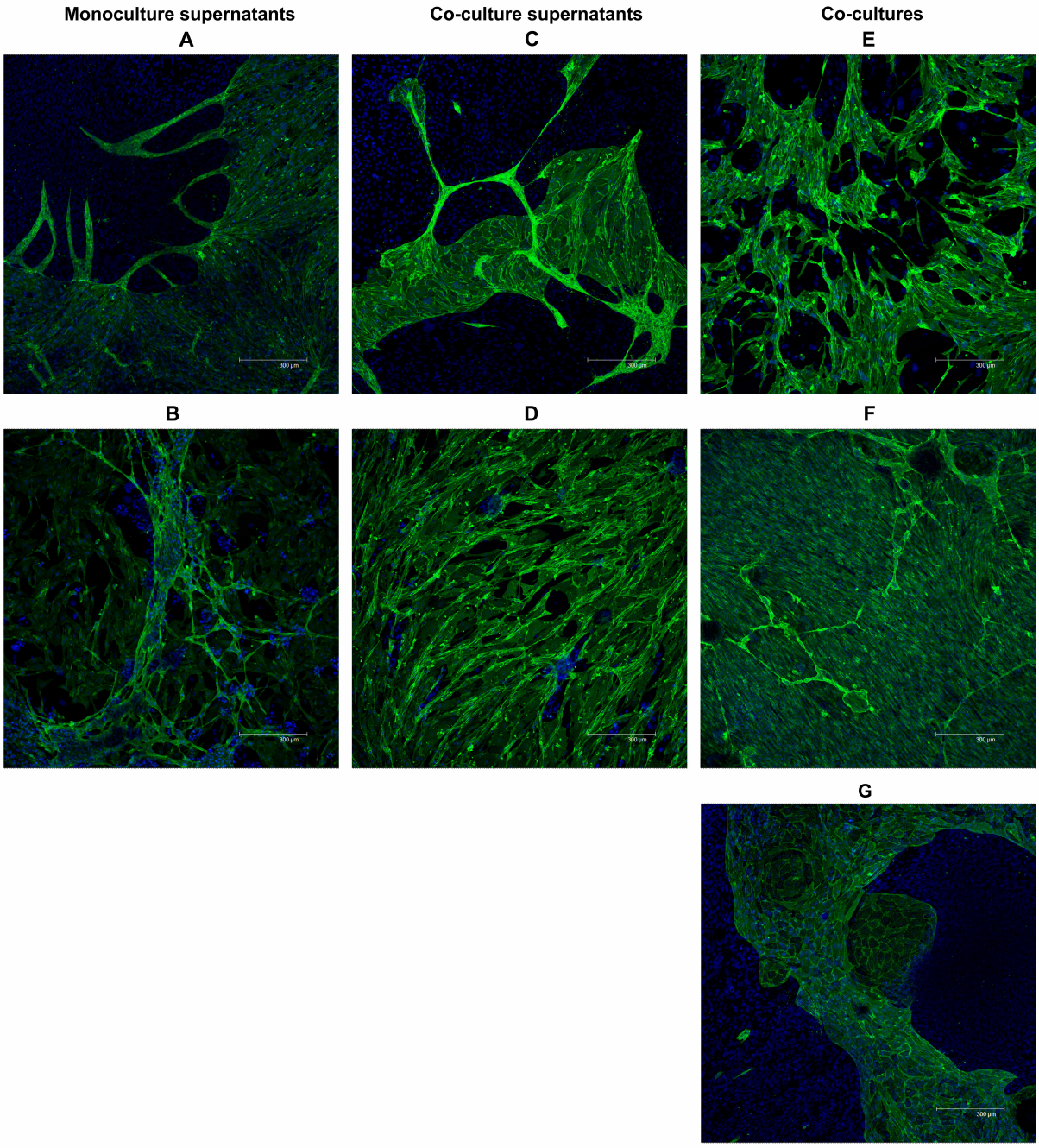

Figure A.52: **HDMEC and SaOS-2 co-cultures with cell culture supernatants**
Co-cultures of HDMEC and SaOS-2 with medium supernatants from **A** Cal-72 and **B** MG-63 monocultures, and from **C** HDMEC-Cal-72 and **D** HDMEC-MG-63 co-cultures after 28 days. Positive controls are co-cultures of HDMEC with **E** Cal-72 and **F** MG-63. The negative control **G** is a co-culture of HDMEC with SaOS-2. Cells were immunostained with CD31 antibody (green) and DAPI (blue) and visualised by laser scanning confocal microscopy.

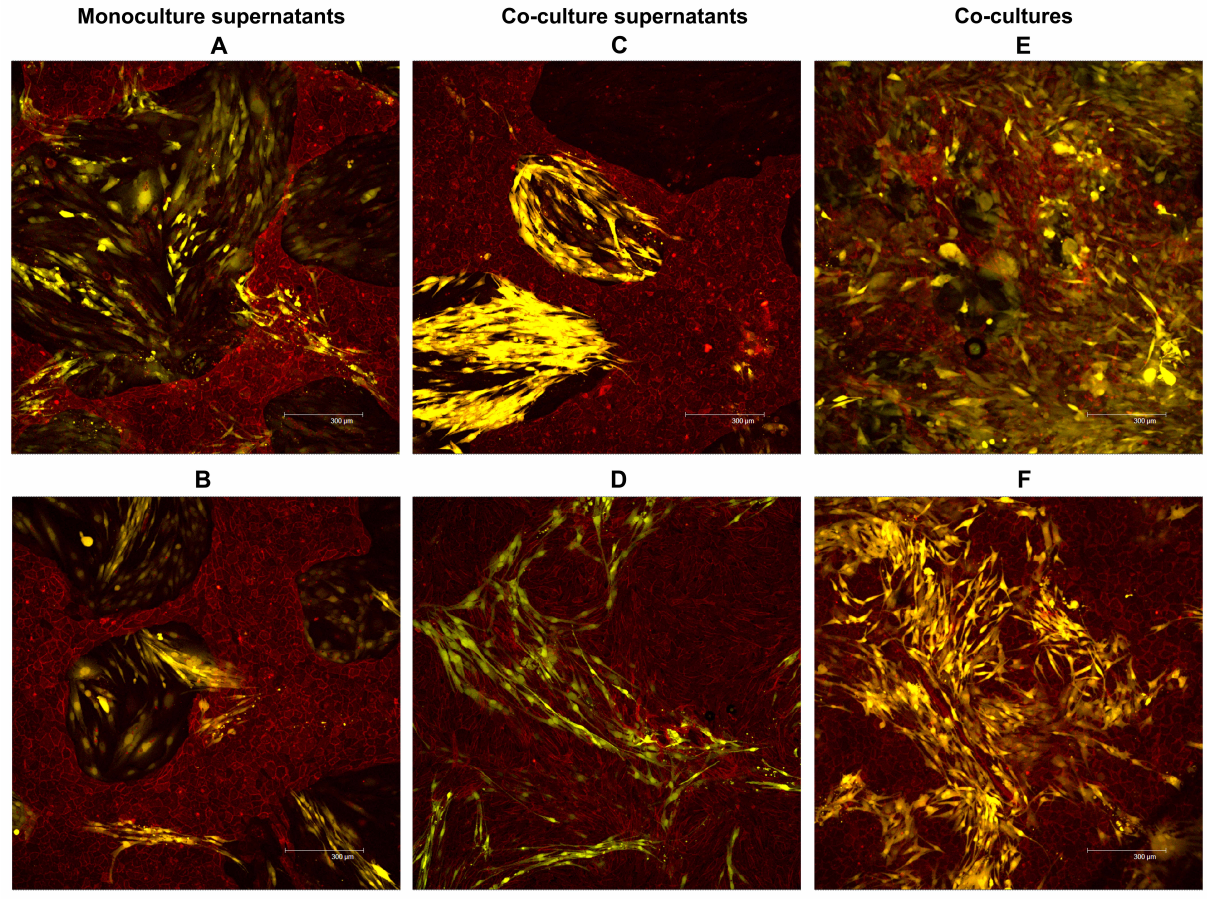

Figure A.53: **HUVEC and SaOS-2 GFP co-cultures with cell culture supernatants**
Co-cultures of HUVEC and gfp-transfected SaOS-2 with medium supernatants from **A** Cal-72 GFP and **B** MG-63 GFP monocultures, and from **C** HUVEC-Cal-72 GFP and **D** HUVEC-MG-63 GFP co-cultures after 28 days. Positive controls are co-cultures of HUVEC with **E** Cal-72 GFP and **F** MG-63 GFP. Cells were immunostained with CD31 antibody (red) and visualised by laser scanning confocal microscopy.

A.3 Effects of medium supernatants with bFGF on angiogenesis

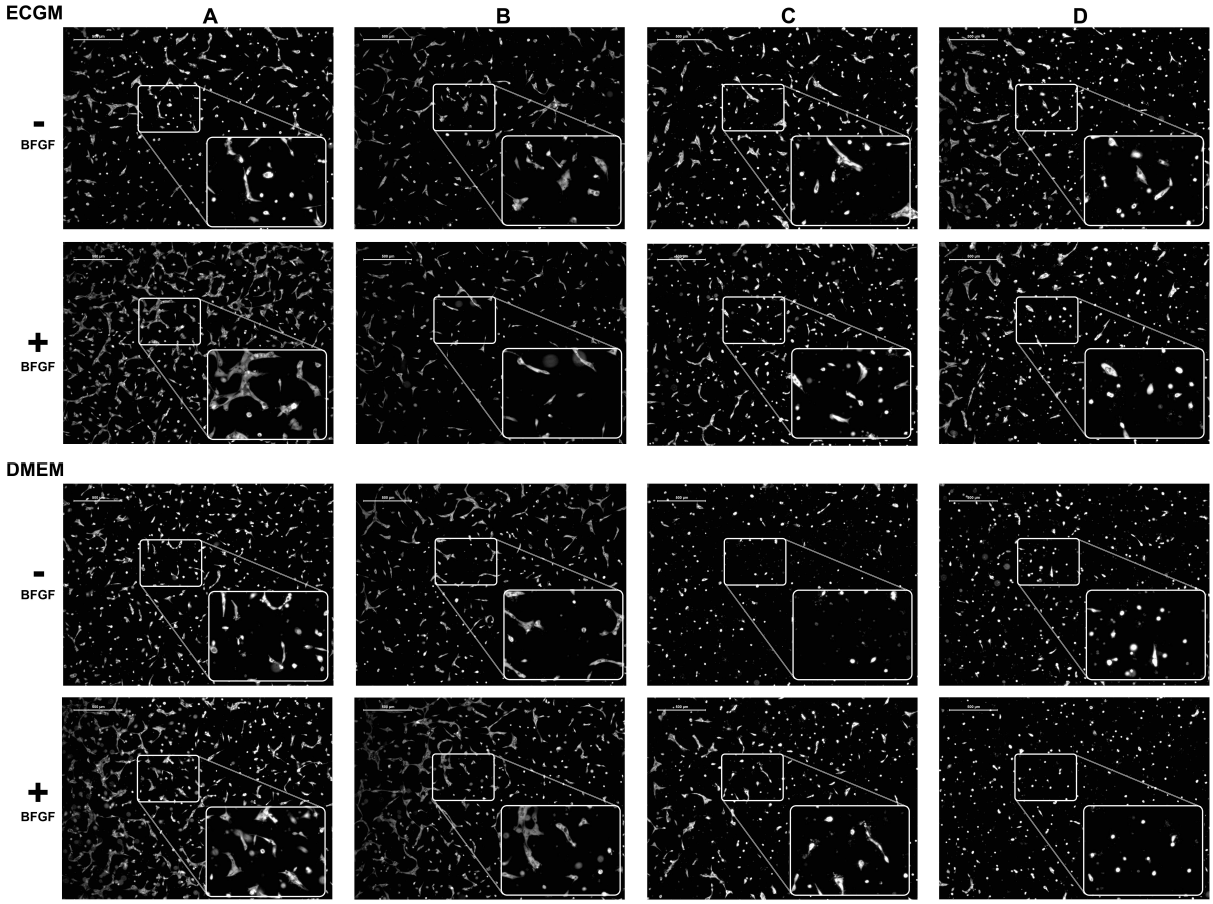

Figure A.54: **3-D culture of umbilical artery endothelial cells with medium supernatants and bFGF**
3-D collagen gel cultures of umbilical artery endothelial cells with medium supernatants from **A** Cal-72, **B** MG-63, **C** SaOS-2 and the negative control **D** umbilical artery endothelial cells supplemented with 20 ng/µl bFGF. Cultures were set up with ECGM and DMEM for 24 hours, stained with Calcein-AM and visualised by fluorescence microscopy.

A.4 Transcriptional analysis of angiogenesis-related factors

Table A.30: P value results of qPCR on osteosarcoma cell lines

Gene	MG-63 vs. SaOS-2		CAL-72 vs. SaOS-2		MG-63 vs. CAL-72	
	Log2FD	p Value	Log2FD	p Value	Log2FD	p Value
Akt1	-1.12	–	-0.99	–	-0.14	–
ANGPT1	0.08	0.88	-5.11	0.19	5.19	0.23
ANGPT2	0.04	–	-0.86	–	0.91	–
ANGPTL3	-3.6	0.024	-7.09	0.017	3.48	0.11
ANGPTL4	-0.95	0.23	-2.72	0.083	1.77	0.085
ANPEP	-3.06	0.13	-3.88	0.095	0.82	0.36
BAI1	-0.95	–	-4.54	–	3.59	–
CCL11	-0.17	0.96	2.16	0.076	-2.33	0.078
CCL2	-0.7	–	-1.66	–	0.96	0.39
CDH5	-3.89	0.042	-2.9	0.046	-0.99	0.68
COL18A1	-3	0.14	-5.94	0.045	2.94	0.29
COL4A3	-4.35	–	-4.5	–	0.15	0.82
CXCL1	-1.12	0.5	–	–	–	–
CXCL10	0.04	0.95	-5.25	0.072	5.28	0.03
CXCL3	-2.61	0.18	-1.26	–	-1.34	–
CXCL5	-3.18	0.13	-2.2	0.21	-0.98	0.37
CXCL6	-3.12	0.002	-0.97	0.13	-2.15	0.13
CXCL9	-1.21	0.63	-2.85	0.27	1.64	0.45
ECGF1	-2.1	0.12	-2.98	0.11	0.88	0.75
EDG1	-4.07	0.16	-2.04	0.2	-2.03	0.21
EFNA1	-3.19	0.081	-5.18	–	1.99	–
EFNA3	-3.49	–	-3.42	–	-0.06	0.57
EFNB2	-4.18	0.052	-4.89	0.053	0.72	0.99
EGF	-0.14	0.96	-5.15	0.083	5.01	0.12
ENG1	4.99	–	–	–	4.99	0.17
EPHB4	-0.26	0.7	-4.19	0.081	3.93	0.27
EREG	-3.25	0.21	-5.14	0.19	1.88	0.05
FGF1	0.38	0.67	-1.45	0.31	1.83	0.27
FGF2	-0.46	–	2.36	–	-2.81	0.28
FGFR3	-3.53	0.092	-3.38	0.1	-0.15	0.67
FIGF	-4.67	0.16	-5.98	–	1.32	–
FLT1	-4.31	–	-4.68	–	0.37	0.93
HAND2	-2.11	0.28	-3.9	0.14	1.79	0.25
HGF	-0.97	0.47	-3.8	0.12	2.83	0.19
HIF1A	-2.02	0.2	-2.39	0.27	0.37	0.76
HPSE	-2.05	0.069	-6.45	0.029	4.4	0.043
ID1	–	–	–	–	–	–
ID3	1.74	0.36	-0.09	–	1.83	–
IFNA1	0.03	0.93	-2.6	0.24	2.64	0.2
IFNB1	0.48	0.6	-1.07	0.58	1.55	0.31
IFNG	-2.44	0.12	-2.25	0.086	-0.19	0.68
IGF1	-4.15	–	-3.38	–	-0.77	0.45
IL1B	-3.03	0.11	-2.43	–	-0.59	–
IL6	-2.47	0.014	-2.75	0.033	0.28	0.92
IL8	-1.88	0.18	-3.3	0.092	1.42	0.18
ITGAV	-1.01	0.3	0.47	0.61	-1.48	0.36
ITGB3	–	–	–	–	-0.85	–
JAG1	-2.65	0.018	-4.12	0.013	1.47	0.46
KDR	–	–	–	–	–	–
LamA5	4.13	0.26	-2.44	0.086	6.57	0.25
LECT1	-2.59	–	-6.45	–	3.86	0.28
LEP	-6.46	0.036	-5.87	0.038	-0.59	0.44
MDK	-3.37	0.038	-3.78	0.038	0.4	0.93
MMP2	0.39	0.98	-0.1	0.62	0.5	0.48
MMP9	-3.62	0.2	-2.16	–	-1.47	–
Notch4	-2.4	0.11	-3.83	0.088	1.44	0.27

Continued on the following page

Table A.30 – Continued from the previous page

Gene	MG-63 vs. SaOS-2 Log2FD	MG-63 vs. SaOS-2 p Value	CAL-72 vs. SaOS-2 Log2FD	CAL-72 vs. SaOS-2 p Value	MG-63 vs. CAL-72 Log2FD	MG-63 vs. CAL-72 p Value
NRP1	2.64	–	1.94	–	0.71	0.36
NRP2	-2.04	0.13	-1.19	0.18	-0.85	0.33
PDGFA	–	–	–		2.12	0.28
PECAM1	–	–	–	–	–	–
PF4	3.68	–	–	–	–	–
PGF	–	–	–	–	0.82	0.41
PLAU	-0.28	0.75	0.83	0.21	-1.11	0.2
PLG	-3.55	0.18	-5.52	0.14	1.96	0.21
PLXDC1	-2.44	0.055	-2.63	–	0.19	–
PROK2	3.21	0.13	-1.49	0.17	4.7	0.1
PTGS1	-2.75	0.12	-1.94	0.17	-0.81	0.64
SERPINF1	4.15	–	0.97	–	3.18	0.13
SPHK1	-3.76	0.065	-3.19	0.099	-0.57	0.43
STAB1	-2.02	0.21	-4.99	0.13	2.97	0.16
TEK	-0.79	0.8	-4.41	0.018	3.62	0.23
TGFA	5.97	0.025	2.82	0.039	3.15	0.035
TGFB1	1.52	0.15	-5.91	–	7.43	–
TGFB2	2.23	0.19	-0.67	0.19	2.91	0.17
TGFBR1	-2.06	0.085	-2.68	0.077	0.62	0.69
THBS1	2.89	0.25	4.55	0.012	-1.65	0.2
THBS2	-3.98	0.1	-8.04	0.091	4.06	0.054
TIMP1	2.71	0.062	-0.06	0.88	2.77	0.061
TIMP2	2.13	0.04	2.12	0.036	0.01	1
TIMP3	-1.3	0.47	-3.78	0.2	2.49	0.33
TNF	-4.39	0.044	-3.62	–	-0.78	–
TNFAIP2	1	0.68	-0.95	0.34	1.96	0.12
VEGFA	1.81	0.028	1.61	0.029	0.2	0.56
VEGFC	5.94	0.093	-0.04	0.8	5.97	0.094

A.5 Mass spectroscopic analysis

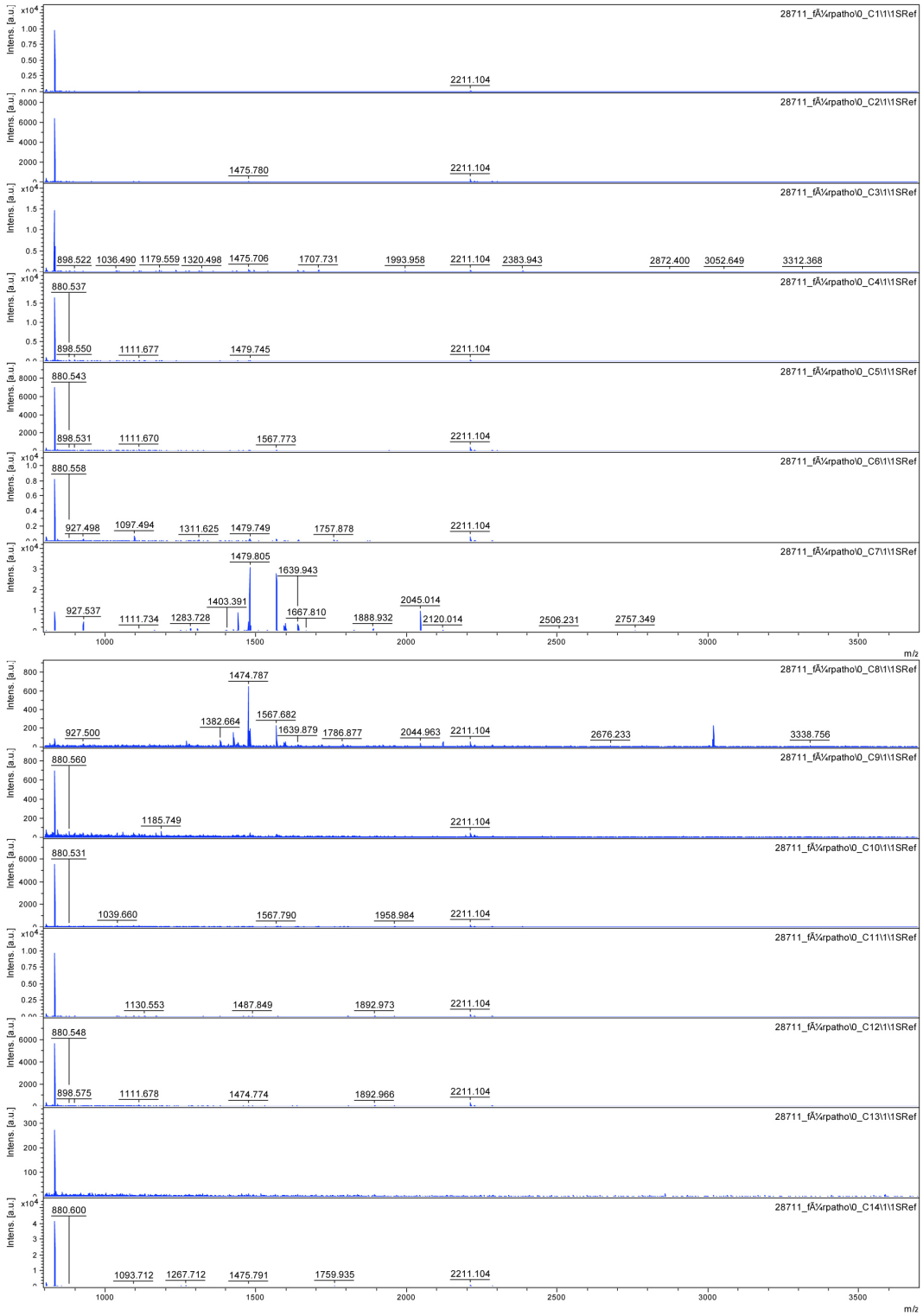

Figure A.55: **Mass spectroscopic analysis of cell culture supernatants**
Example plots of mass spectroscopic analysis.

Bibliography

Abdollahi, A., Hahnfeldt, P., Maercker, C., Grone, H. J., Debus, J., Ansorge, W., Folkman, J., Hlatky, L., and Huber, P. E. (2004). Endostatin's antiangiogenic signaling network. *Mol. Cell*, 13(5):649–663. [PubMed:15023336].

Akeno, N., Robins, J., Zhang, M., Czyzyk-Krzeska, M. F., and Clemens, T. L. (2002). Induction of vascular endothelial growth factor by IGF-I in osteoblast-like cells is mediated by the PI3K signaling pathway through the hypoxia-inducible factor-2alpha. *Endocrinology*, 143(2):420–425. [PubMed:11796494].

Albelda, S. M. and Buck, C. A. (1990). Integrins and other cell adhesion molecules. *FASEB J.*, 4(11):2868–2880. [PubMed:2199285].

Albert, A., Leemrijse, T., Druez, V., Delloye, C., and Cornu, O. (2006). Are bone autografts still necessary in 2006? A three-year retrospective study of bone grafting. *Acta Orthop Belg*, 72(6):734–740. [PubMed:17260612].

Alsalameh, S., Amin, R. J., Kunisch, E., Jasin, H. E., and Kinne, R. W. (2003). Preferential induction of prodestructive matrix metalloproteinase-1 and proinflammatory interleukin 6 and prostaglandin E2 in rheumatoid arthritis synovial fibroblasts via tumor necrosis factor receptor-55. *J. Rheumatol.*, 30(8):1680–1690. [PubMed:12913922].

Altschul, S. F., Gish, W., Miller, W., Myers, E. W., and Lipman, D. J. (1990). Basic local alignment search tool. *J. Mol. Biol.*, 215(3):403–410. [PubMed:2231712].

Ammit, A. J., Lazaar, A. L., Irani, C., O'Neill, G. M., Gordon, N. D., Amrani, Y., Penn, R. B., and Panettieri, R. A. (2002). Tumor necrosis factor-alpha-induced secretion of RANTES and interleukin-6 from human airway smooth muscle cells: modulation by glucocorticoids and beta-agonists. *Am. J. Respir. Cell Mol. Biol.*, 26(4):465–474. [PubMed:11919083].

Andaç, M., Baydemir, G., Yavuz, H., and Denizli, A. (2012). Molecularly imprinted composite cryogel for albumin depletion from human serum. *Journal of Molecular Recognition*, 25(11):555–563. [PubMed:23108615].

Andersson, A. K., Feldmann, M., and Brennan, F. M. (2008). Neutralizing IL-21 and IL-15 inhibits pro-inflammatory cytokine production in rheumatoid arthritis. *Scand. J. Immunol.*, 68(1):103–111. [PubMed:18482208].

Annaz, B., Hing, K. A., Kayser, M., Buckland, T., and Di Silvio, L. (2004). Porosity variation in hydroxyapatite and osteoblast morphology: a scanning electron microscopy study. *J Microsc*, 215(Pt 1):100–110. [PubMed:15230881].

Awwad, H. K., el Naggar, M., Mocktar, N., and Barsoum, M. (1986). Intercapillary distance measurement as an indicator of hypoxia in carcinoma of the cervix uteri. *Int. J. Radiat. Oncol. Biol. Phys.*, 12(8):1329–1333. [PubMed:3759554].

Balconi, G., Spagnuolo, R., and Dejana, E. (2000). Development of endothelial cell lines from embryonic stem cells: A tool for studying genetically manipulated endothelial cells in vitro. *Arterioscler. Thromb. Vasc. Biol.*, 20(6):1443–1451. [PubMed:10845856].

Baraldo, S., Faffe, D. S., Moore, P. E., Whitehead, T., McKenna, M., Silverman, E. S., Panettieri, R. A., and Shore, S. A. (2003). Interleukin-9 influences chemokine release in airway smooth muscle: role of ERK. *Am. J. Physiol. Lung Cell Mol. Physiol.*, 284(6):L1093–1102. [PubMed:12588703].

Beck, L. and D'Amore, P. A. (1997). Vascular development: cellular and molecular regulation. *FASEB J.*, 11(5):365–373. [PubMed:9141503].

Becker, S., Quay, J., Koren, H. S., and Haskill, J. S. (1994). Constitutive and stimulated MCP-1, GRO alpha, beta, and gamma expression in human airway epithelium and bronchoalveolar macrophages. *Am. J. Physiol.*, 266(3 Pt 1):L278–286. [PubMed:8166297].

Beresford, J. N., Gallagher, J. A., Poser, J. W., and Russell, R. G. (1984). Production of osteocalcin by human bone cells in vitro. Effects of 1,25(OH)2D3, 24,25(OH)2D3, parathyroid hormone, and glucocorticoids. *Metab Bone Dis Relat Res*, 5(5):229–234. [PubMed:6333574].

Beresford, J. N., Gallagher, J. A., and Russell, R. G. (1986). 1,25-Dihydroxyvitamin D3 and human bone-derived cells in vitro: effects on alkaline phosphatase, type I collagen and proliferation. *Endocrinology*, 119(4):1776–1785. [PubMed:3489608].

Bilbe, G., Roberts, E., Birch, M., and Evans, D. B. (1996). Pcr phenotyping of cytokines, growth factors and their receptors and bone matrix proteins in human osteoblast-like cell lines. *Bone*, 19(5):437–45. [PubMed:8922641].

Biltz, R. M. and Pellegrino, E. D. (1977). The nature of bone carbonate. *Clin. Orthop. Relat. Res.*, (129):279–292. [PubMed:608288].

Biosystems, A. (2010). *Relative Quantitation Using Comparative CT Getting Started Guide*. Invitrogen, part number 4347824 rev. f edition.

Bishop, E. T., Bell, G. T., Bloor, S., Broom, I. J., Hendry, N. F., and Wheatley, D. N. (1999). An in vitro model of angiogenesis: basic features. *Angiogenesis*, 3(4):335–344. [PubMed:14517413].

Blanco, R. and Gerhardt, H. (2013). VEGF and Notch in tip and stalk cell selection. *Cold Spring Harb Perspect Med*, 3(1):a006569. [PubMed:23085847].

Boldrini, L., Gisfredi, S., Ursino, S., Lucchi, M., Melfi, F., Mussi, A., Basolo, F., and Fontanini, G. (2006). Tumour necrosis factor-alpha: prognostic role and relationship with interleukin-8 and endothelin-1 in non-small cell lung cancer. *Int. J. Mol. Med.*, 17(5):887–892. [PubMed:16596276].

Borg, S. A., Kerry, K. E., Royds, J. A., Battersby, R. D., and Jones, T. H. (2005). Correlation of VEGF production with IL1 alpha and IL6 secretion by human pituitary adenoma cells. *Eur. J. Endocrinol.*, 152(2):293–300. [PubMed:15745939].

Bosetti, M., Leigheb, M., Brooks, R. A., Boccafoschi, F., and Cannas, M. F. (2010). Regulation of osteoblast and osteoclast functions by FGF-6. *J. Cell. Physiol.*, 225(2):466–471. [PubMed:20458746].

Bouis, D., Hospers, G. A., Meijer, C., Molema, G., and Mulder, N. H. (2001). Endothelium in vitro: a review of human vascular endothelial cell lines for blood vessel-related research. *Angiogenesis*, 4(2):91–102. [PubMed:11806248].

Breiteneder-Geleff, S., Soleiman, A., Kowalski, H., Horvat, R., Amann, G., Kriehuber, E., Diem, K., Weninger, W., Tschachler, E., Alitalo, K., and Kerjaschki, D. (1999). Angiosarcomas express mixed endothelial phenotypes of blood and lymphatic capillaries: podoplanin as a specific marker for lymphatic endothelium. *Am. J. Pathol.*, 154(2):385–394. [PubMed:10027397].

Brew, K., Dinakarpandian, D., and Nagase, H. (2000). Tissue inhibitors of metalloproteinases: evolution, structure and function. *Biochim. Biophys. Acta*, 1477(1-2):267–283. [PubMed:10708863].

Brown, K. L. and Cruess, R. L. (1982). Bone and cartilage transplantation in orthopaedic surgery. A review. *J Bone Joint Surg Am*, 64(2):270–279. [PubMed:7035461].

Brunius, G., Domeij, H., Gustavsson, A., and Yucel-Lindberg, T. (2005). Bradykinin upregulates IL-8 production in human gingival fibroblasts stimulated by interleukin-1beta and tumor necrosis factor alpha. *Regul. Pept.*, 126(3):183–188. [PubMed:15664665].

Burg, K. J., Porter, S., and Kellam, J. F. (2000). Biomaterial developments for bone tissue engineering. *Biomaterials*, 21(23):2347–2359. [PubMed:11055282].

Campbell, J. T. and Kaplan, F. S. (1992). The role of morphogens in endochondral ossification. *Calcif. Tissue Int.*, 50(3):283–289. [PubMed:1617504].

Caplan, A. I. and Goldberg, V. M. (1999). Principles of tissue engineered regeneration of skeletal tissues. *Clin. Orthop. Relat. Res.*, (367 Suppl):S12–16. [PubMed:10546632].

Carley, W. W., Niedbala, M. J., and Gerritsen, M. E. (1992). Isolation, cultivation, and partial characterization of microvascular endothelium derived from human lung. *Am. J. Respir. Cell Mol. Biol.*, 7(6):620–630. [PubMed:1333246].

Carmeliet, P. (2000a). Mechanisms of angiogenesis and arteriogenesis. *Nat. Med.*, 6(4):389–395. [PubMed:10742145].

Carmeliet, P. (2000b). VEGF gene therapy: stimulating angiogenesis or angioma-genesis? *Nat. Med.*, 6(10):1102–1103. [PubMed:11017137].

Carmeliet, P. (2005). Angiogenesis in life, disease and medicine. *Nature*, 438(7070):932–936. [PubMed:16355210].

Carmeliet, P. and Jain, R. K. (2011). Molecular mechanisms and clinical applications of angiogenesis. *Nature*, 473(7347):298–307. [PubMed:21593862].

Carpenter, T. O., Moltz, K. C., Ellis, B., Andreoli, M., McCarthy, T. L., Centrella, M., Bryan, D., and Gundberg, C. M. (1998). Osteocalcin production in primary osteoblast cultures derived from normal and hyp mice. *Endocrinology*, 139(1):35–43. [PubMed:9421395].

Cereseto, A. and Giacca, M. (2004). Integration site selection by retroviruses. *AIDS Rev*, 6(1):13–21. [PubMed:15168737].

Chalfie, M., Tu, Y., Euskirchen, G., Ward, W. W., and Prasher, D. C. (1994). Green fluorescent protein as a marker for gene expression. *Science*, 263(5148):802–805. [PubMed:8303295].

Chen, H. T., Tsou, H. K., Chang, C. H., and Tang, C. H. (2012). Hepatocyte growth factor increases osteopontin expression in human osteoblasts through PI3K, Akt, c-Src, and AP-1 signaling pathway. *PLoS ONE*, 7(6):e38378. [PubMed:22675553].

Chen, R. H., Chen, W. C., Wang, T. Y., Tsai, C. H., and Tsai, F. J. (2005). Lack of association between pro-inflammatory cytokine (IL-6, IL-8 and TNF-alpha) gene polymorphisms and Graves' disease. *Int. J. Immunogenet.*, 32(6):343–347. [PubMed:16313297].

Chim, S. M., Tickner, J., Chow, S. T., Kuek, V., Guo, B., Zhang, G., Rosen, V., Erber, W., and Xu, J. (2013). Angiogenic factors in bone local environment. *Cytokine Growth Factor Rev.* [PubMed:23611723].

Choi, K., Kennedy, M., Kazarov, A., Papadimitriou, J. C., and Keller, G. (1998). A common precursor for hematopoietic and endothelial cells. *Development*, 125(4):725–732. [PubMed:9435292].

Chung, U. I., Kawaguchi, H., Takato, T., and Nakamura, K. (2004). Distinct osteogenic mechanisms of bones of distinct origins. *J Orthop Sci*, 9(4):410–414. [PubMed:15278782].

Cines, D. B., Pollak, E. S., Buck, C. A., Loscalzo, J., Zimmerman, G. A., McEver, R. P., Pober, J. S., Wick, T. M., Konkle, B. A., Schwartz, B. S., Barnathan, E. S., McCrae, K. R., Hug, B. A., Schmidt, A. M., and Stern, D. M. (1998). Endothelial cells in physiology and in the pathophysiology of vascular disorders. *Blood*, 91(10):3527–3561. [PubMed:9572988].

Clover, J. and Gowen, M. (1994). Are mg-63 and hos te85 human osteosarcoma cell lines representative models of the osteoblastic phenotype? *Bone*, 15(6):585–91. [PubMed:7873286].

Cohen, M. M. (2006). The new bone biology: pathologic, molecular, and clinical correlates. *Am. J. Med. Genet. A*, 140(23):2646–2706. [PubMed:17103447].

Cook, K. M. and Figg, W. D. (2010). Angiogenesis inhibitors: current strategies and future prospects. *CA Cancer J Clin*, 60(4):222–243. [PubMed:20554717].

Cross, M. J. and Claesson-Welsh, L. (2001). FGF and VEGF function in angiogenesis: signalling pathways, biological responses and therapeutic inhibition. *Trends Pharmacol. Sci.*, 22(4):201–207. [PubMed:11282421].

Dallas, S. L. and Bonewald, L. F. (2010). Dynamics of the transition from osteoblast to osteocyte. *Ann. N. Y. Acad. Sci.*, 1192:437–443. [PubMed:20392270].

de Sa, A. R., Moreira, P. R., Xavier, G. M., Sampaio, I., Kalapothakis, E., Dutra, W. O., and Gomez, R. S. (2007). Association of CD14, IL1B, IL6, IL10 and TNFA functional gene polymorphisms with symptomatic dental abscesses. *Int Endod J*, 40(7):563–572. [PubMed:17511783].

Detsch, R., Uhl, F., Deisinger, U., and Ziegler, G. (2008). 3d-cultivation of bone marrow stromal cells on hydroxyapatite scaffolds fabricated by dispense-plotting and negative mould technique. *J Mater Sci Mater Med*, 19(4):1491–6. [PubMed:17990079].

Diaz-Rodriguez, L., Garcia-Martinez, O., Arroyo-Morales, M., Reyes-Botella, C., and Ruiz, C. (2009). Antigenic phenotype and phagocytic capacity of mg-63 osteosarcoma line. *Ann N Y Acad Sci*, 1173 Suppl 1:E46–54. [PubMed:19751414].

Diegelmann, R. F. and Evans, M. C. (2004). Wound healing: an overview of acute, fibrotic and delayed healing. *Front. Biosci.*, 9:283–289. [PubMed:14766366].

Dodds, R. A., Merry, K., Littlewood, A., and Gowen, M. (1994). Expression of mRNA for IL1 beta, IL6 and TGF beta 1 in developing human bone and cartilage. *J. Histochem. Cytochem.*, 42(6):733–744. [PubMed:8189035].

Dohle, E., Fuchs, S., Kolbe, M., Hofmann, A., Schmidt, H., and Kirkpatrick, C. J. (2011). Comparative study assessing effects of sonic hedgehog and VEGF in a human co-culture model for bone vascularisation strategies. *Eur Cell Mater*, 21:144–156. [PubMed:21305477].

Donovan, D., Brown, N. J., Bishop, E. T., and Lewis, C. E. (2001). Comparison of three in vitro human 'angiogenesis' assays with capillaries formed in vivo. *Angiogenesis*, 4(2):113–121. [PubMed:11806243].

Facchini, A., Borzi, R. M., Marcu, K. B., Stefanelli, C., Olivotto, E., Goldring, M. B., Facchini, A., and Flamigni, F. (2005). Polyamine depletion inhibits NF-kappaB binding to DNA and interleukin-8 production in human chondrocytes stimulated by tumor necrosis factor-alpha. *J. Cell. Physiol.*, 204(3):956–963. [PubMed:15828019].

Faggioli, L., Costanzo, C., Donadelli, M., and Palmieri, M. (2004). Activation of the Interleukin-6 promoter by a dominant negative mutant of c-Jun. *Biochim. Biophys. Acta*, 1692(1):17–24. [PubMed:15158360].

Ferrara, N. and Alitalo, K. (1999). Clinical applications of angiogenic growth factors and their inhibitors. *Nat. Med.*, 5(12):1359–1364. [PubMed:10581076].

Ferrara, N., Chen, H., Davis-Smyth, T., Gerber, H. P., Nguyen, T. N., Peers, D., Chisholm, V., Hillan, K. J., and Schwall, R. H. (1998). Vascular endothelial growth factor is essential for corpus luteum angiogenesis. *Nat. Med.*, 4(3):336–340. [PubMed:9500609].

Fiedler, W., Gehling, U., Mende, T., and Hossfeld, D. (2001). Neoangiogenese und tumorwachstum. *Deutsches Ärzteblatt*, 98(21):1392–1394.

Florczyk, S. J., Leung, M., Jana, S., Li, Z., Bhattarai, N., Huang, J. I., Hopper, R. A., and Zhang, M. (2012). Enhanced bone tissue formation by alginate gel-assisted cell seeding in porous ceramic scaffolds and sustained release of growth factor. *J Biomed Mater Res A*, 100(12):3408–3415. [PubMed:22767533].

Fogh, J., Fogh, J. M., and Orfeo, T. (1977). One hundred and twenty-seven cultured human tumor cell lines producing tumors in nude mice. *J. Natl. Cancer Inst.*, 59(1):221–226. [PubMed:327080].

Folkman, J. (1995). Angiogenesis in cancer, vascular, rheumatoid and other disease. *Nat. Med.*, 1(1):27–31. [PubMed:7584949].

Folkman, J. (1996). Fighting cancer by attacking its blood supply. *Sci. Am.*, 275(3):150–154. [PubMed:8701285].

Fraisl, P., Mazzone, M., Schmidt, T., and Carmeliet, P. (2009). Regulation of angiogenesis by oxygen and metabolism. *Dev. Cell*, 16(2):167–179. [PubMed:19217420].

Fredriksson, K., Lundahl, J., Palmberg, L., Romberger, D. J., Liu, X. D., Rennard, S. I., and Skold, C. M. (2003). Red blood cells stimulate human lung fibroblasts to secrete interleukin-8. *Inflammation*, 27(2):71–78. [PubMed:12797546].

Frisch, S. M. and Francis, H. (1994). Disruption of epithelial cell-matrix interactions induces apoptosis. *J. Cell Biol.*, 124(4):619–626. [PubMed:8106557].

Fuchs, S., Hofmann, A., and Kirkpatrick, C. (2007). Microvessel-like structures from outgrowth endothelial cells from human peripheral blood in 2-dimensional and 3-dimensional co-cultures with osteoblastic lineage cells. *Tissue Eng.*, 13(10):2577–2588. [PubMed:17655487].

Fuchs, S., Jiang, X., Schmidt, H., Dohle, E., Ghanaati, S., Orth, C., Hofmann, A., Motta, A., Migliaresi, C., and Kirkpatrick, C. J. (2009). Dynamic processes involved in the pre-vascularization of silk fibroin constructs for bone regeneration using outgrowth endothelial cells. *Biomaterials*, 30(7):1329–1338. [PubMed:19091396].

Gavard, J. and Gutkind, J. S. (2006). VEGF controls endothelial-cell permeability by promoting the beta-arrestin-dependent endocytosis of VE-cadherin. *Nat. Cell Biol.*, 8(11):1223–1234. [PubMed:17060906].

Geiger, F., Bertram, H., Berger, I., Lorenz, H., Wall, O., Eckhardt, C., Simank, H. G., and Richter, W. (2005). Vascular endothelial growth factor gene-activated matrix (VEGF165-GAM) enhances osteogenesis and angiogenesis in large segmental bone defects. *J. Bone Miner. Res.*, 20(11):2028–2035. [PubMed:16234976].

Giannona, S., Firkowska, I., Rojas-Chapana, J., and Giersig, M. (2007). Vertically aligned carbon nanotubes as cytocompatible material for enhanced adhesion and proliferation of osteoblast-like cells. *J Nanosci Nanotechnol*, 7(4-5):1679–1683. [PubMed:17450943].

Gitelis, S. and Saiz, P. (2002). What's new in orthopaedic surgery. *J. Am. Coll. Surg.*, 194(6):788–791. [PubMed:12081070].

Globus, R. K., Plouet, J., and Gospodarowicz, D. (1989). Cultured bovine bone cells synthesize basic fibroblast growth factor and store it in their extracellular matrix. *Endocrinology*, 124(3):1539–1547. [PubMed:2783905].

Glowacki, J., Rey, C., Glimcher, M. J., Cox, K. A., and Lian, J. (1991). A role for osteocalcin in osteoclast differentiation. *J. Cell. Biochem.*, 45(3):292–302. [PubMed:2066381].

Goad, D. L., Rubin, J., Wang, H., Tashjian, A. H., and Patterson, C. (1996). Enhanced expression of vascular endothelial growth factor in human SaOS-2 osteoblast-like cells and murine osteoblasts induced by insulin-like growth factor I. *Endocrinology*, 137(6):2262–2268. [PubMed:8641174].

Gotink, K. J. and Verheul, H. M. (2010). Anti-angiogenic tyrosine kinase inhibitors: what is their mechanism of action? *Angiogenesis*, 13(1):1–14. [PubMed:20012482].

Granger, J., Siddiqui, J., Copeland, S., and Remick, D. (2005). Albumin depletion of human plasma also removes low abundance proteins including the cytokines. *Proteomics*, 5(18):4713–4718. [PubMed:16281180].

Grellier, M., Bordenave, L., and Amedee, J. (2009). Cell-to-cell communication between osteogenic and endothelial lineages: implications for tissue engineering. *Trends Biotechnol*, 27(10):562–71. [PubMed:19683818].

Greten, F. R., Wagner, M., Weber, C. K., Zechner, U., Adler, G., and Schmid, R. M. (2001). TGF alpha transgenic mice. A model of pancreatic cancer development. *Pancreatology*, 1(4):363–368. [PubMed:12120215].

Gu, F., Amsden, B., and Neufeld, R. (2004). Sustained delivery of vascular endothelial growth factor with alginate beads. *J Control Release*, 96(3):463–472. [PubMed:15120902].

Guillotin, B., Bareille, R., Bourget, C., Bordenave, L., and Amedee, J. (2008). Interaction between human umbilical vein endothelial cells and human osteoprogenitors triggers pleiotropic effect that may support osteoblastic function. *Bone*, 42(6):1080–1091. [PubMed:18387350].

Guimaraes, A. L., Correia-Silva, J. d. e. F., Sa, A. R., Victoria, J. M., Diniz, M. G., Costa, F. d. e. O., and Gomez, R. S. (2007). Investigation of functional gene polymorphisms IL-1beta, IL-6, IL-10 and TNF-alpha in individuals with recurrent aphthous stomatitis. *Arch. Oral Biol.*, 52(3):268–272. [PubMed:17052682].

Günther, H. (2009). *Zelllinien in der Biomaterialforschung: Herstellung und Charakterisierung unterschiedlich gefärbter fluoreszenter Osteoblasten*. PhD thesis, Johannes Gutenberg Universität Mainz.

Ha, C. H., Bennett, A. M., and Jin, Z. G. (2008). A novel role of vascular endothelial cadherin in modulating c-Src activation and downstream signaling of vascular endothelial growth factor. *J. Biol. Chem.*, 283(11):7261–7270. [PubMed:18180305].

Hanahan, D. and Folkman, J. (1996). Patterns and emerging mechanisms of the angiogenic switch during tumorigenesis. *Cell*, 86(3):353–364. [PubMed:8756718].

Hannink, M. and Donoghue, D. J. (1989). Structure and function of platelet-derived growth factor (PDGF) and related proteins. *Biochim. Biophys. Acta*, 989(1):1–10. [PubMed:2546599].

Hao, Q., Wang, L., and Tang, H. (2009). Vascular endothelial growth factor induces protein kinase D-dependent production of proinflammatory cytokines in endothelial cells. *Am. J. Physiol., Cell Physiol.*, 296(4):C821–827. [PubMed:19176759].

Haq, M., Goltzman, D., Tremblay, G., and Brodt, P. (1992). Rat prostate adenocarcinoma cells disseminate to bone and adhere preferentially to bone marrow-derived endothelial cells. *Cancer Res.*, 52(17):4613–4619. [PubMed:1511429].

Hausser, H. J. and Brenner, R. E. (2005). Phenotypic instability of Saos-2 cells in long-term culture. *Biochem. Biophys. Res. Commun.*, 333(1):216–222. [PubMed:15939397].

He, X. M. and Carter, D. C. (1992). Atomic structure and chemistry of human serum albumin. [PubMed:1630489].

Heldin, C. H. (1992). Structural and functional studies on platelet-derived growth factor. *EMBO J.*, 11(12):4251–4259. [PubMed:1425569].

Hellmuth, M., Wetzler, C., Nold, M., Chang, J. H., Frank, S., Pfeilschifter, J., and Muhl, H. (2002). Expression of interleukin-8, heme oxygenase-1 and vascular endothelial growth factor in DLD-1 colon carcinoma cells exposed to pyrrolidine dithiocarbamate. *Carcinogenesis*, 23(8):1273–1279. [PubMed:12151344].

Henriksen, P. A., Hitt, M., Xing, Z., Wang, J., Haslett, C., Riemersma, R. A., Webb, D. J., Kotelevtsev, Y. V., and Sallenave, J. M. (2004). Adenoviral gene delivery of elafin and secretory leukocyte protease inhibitor attenuates NF-kappa B-dependent inflammatory responses of human endothelial cells and macrophages to atherogenic stimuli. *J. Immunol.*, 172(7):4535–4544. [PubMed:15034071].

Heremans, H., Billiau, A., Cassiman, J. J., Mulier, J. C., and de Somer, P. (1978). In vitro cultivation of human tumor tissues. II. Morphological and virological characterization of three cell lines. *Oncology*, 35(6):246–252. [PubMed:218153].

Hewett, P. W. and Murray, J. C. (1996). Coexpression of flt-1, flt-4 and KDR in freshly isolated and cultured human endothelial cells. *Biochem. Biophys. Res. Commun.*, 221(3):697–702. [PubMed:8630024].

Heyninck, K., De Valck, D., Vanden Berghe, W., Van Criekinge, W., Contreras, R., Fiers, W., Haegeman, G., and Beyaert, R. (1999). The zinc finger protein A20 inhibits TNF-induced NF-kappaB-dependent gene expression by interfering with an RIP- or TRAF2-mediated transactivation signal and directly binds to a novel NF-kappaB-inhibiting protein ABIN. *J. Cell Biol.*, 145(7):1471–1482. [PubMed:10385526].

Hirano, Y., Shichijo, M., Deguchi, M., Nagira, M., Suzuki, N., Nishitani, Y., Hattori, M., and Arimura, A. (2007). Synergistic effect of PGD2 via prostanoid DP receptor on TNF-alpha-induced production of MCP-1 and IL-8 in human monocytic THP-1 cells. *Eur. J. Pharmacol.*, 560(1):81–88. [PubMed:17307163].

Hoffmann, K. K., Kuhn, J. J., and Strasnick, B. (2003). Bone cements as adjuvant techniques for ossicular chain reconstruction. *Otol. Neurotol.*, 24(1):24–28. [PubMed:12544023].

Hofmann, A., Ritz, U., Verrier, S., Eglin, D., Alini, M., Fuchs, S., Kirkpatrick, C. J., and Rommens, P. M. (2008). The effect of human osteoblasts on proliferation and neovessel formation of human umbilical vein endothelial cells in a long-term 3D co-culture on polyurethane scaffolds. *Biomaterials*, 29(31):4217–4226. [PubMed:18692894].

Holewinski, R. J., Jin, Z., Powell, M. J., Maust, M. D., and Van Eyk, J. E. (2013). A fast and reproducible method for albumin isolation and depletion from serum and cerebrospinal fluid. *Proteomics*. [PubMed:23300121].

Holmes, K., Roberts, O. L., Thomas, A. M., and Cross, M. J. (2007). Vascular endothelial growth factor receptor-2: structure, function, intracellular signalling and therapeutic inhibition. *Cell. Signal.*, 19(10):2003–2012. [PubMed:17658244].

Hristov, M., Zernecke, A., Liehn, E. A., and Weber, C. (2007). Regulation of endothelial progenitor cell homing after arterial injury. *Thromb. Haemost.*, 98(2):274–277. [PubMed:17721606].

Huang, C. M., Huo, A. P., Tsai, C. H., Chen, C. L., and Tsai, F. J. (2006). Lack of association of interleukin-6 and interleukin-8 gene polymorphisms in Chinese patients with systemic lupus erythematosus. *J. Clin. Lab. Anal.*, 20(6):255–259. [PubMed:17115422].

Huang, S. P., Wu, M. S., Shun, C. T., Wang, H. P., Lin, M. T., Kuo, M. L., and Lin, J. T. (2004). Interleukin-6 increases vascular endothelial growth factor and angiogenesis in gastric carcinoma. *J. Biomed. Sci.*, 11(4):517–527. [PubMed:15153787].

Hutmacher, D. W. and Singh, H. (2008). Computational fluid dynamics for improved bioreactor design and 3D culture. *Trends Biotechnol.*, 26(4):166–172. [PubMed:18261813].

Ibbotson, K. J., Harrod, J., Gowen, M., D'Souza, S., Smith, D. D., Winkler, M. E., Derynck, R., and Mundy, G. R. (1986). Human recombinant transforming growth factor alpha stimulates bone resorption and inhibits formation in vitro. *Proc. Natl. Acad. Sci. U.S.A.*, 83(7):2228–2232. [PubMed:3485799].

Isfort, R. J., Cody, D. B., Lovell, G., and Doersen, C. J. (1995). Analysis of oncogenes, tumor suppressor genes, autocrine growth-factor production, and differentiation state of human osteosarcoma cell lines. *Mol. Carcinog.*, 14(3):170–178. [PubMed:7576109].

Jacome-Galarza, C. E., Lee, S. K., Lorenzo, J. A., and Aguila, H. L. (2011). Parathyroid hormone regulates the distribution and osteoclastogenic potential of hematopoietic progenitors in the bone marrow. *J. Bone Miner. Res.*, 26(6):1207–1216. [PubMed:21611963].

Jaffe, E. A., Nachman, R. L., Becker, C. G., and Minick, C. R. (1973). Culture of human endothelial cells derived from umbilical veins. Identification by morphologic and immunologic criteria. *J. Clin. Invest.*, 52(11):2745–2756. [PubMed:4355998].

Jahn, K., Richards, R. G., Archer, C. W., and Stoddart, M. J. (2010). Pellet culture model for human primary osteoblasts. *Eur Cell Mater*, 20:149–61.

Jin, H., Wyss, J. M., Yang, R., and Schwall, R. (2004). The therapeutic potential of hepatocyte growth factor for myocardial infarction and heart failure. *Curr. Pharm. Des.*, 10(20):2525–2533. [PubMed:15320761].

Jonsson, K. B., Frost, A., Nilsson, O., Ljunghall, S., and Ljunggren, O. (1999). Three isolation techniques for primary culture of human osteoblast-like cells: a comparison. *Acta Orthop Scand*, 70(4):365–373. [PubMed:10569267].

Kahn, H. J. and Marks, A. (2002). A new monoclonal antibody, d2-40, for detection of lymphatic invasion in primary tumors. *Lab Invest*, 82(9):1255–7. [PubMed:12218087].

Kai, H. S., Butler, G. S., Morrison, C. J., King, A. E., Pelman, G. R., and Overall, C. M. (2002). Utilization of a novel recombinant myoglobin fusion protein expression system to characterize the tissue inhibitor of metalloproteinase (TIMP)-4 and TIMP-2 C-terminal domain and tails by mutagenesis. The importance of acidic residues in binding the MMP-2 hemopexin C-domain. *J. Biol. Chem.*, 277(50):48696–48707. [PubMed:12374789].

Kaigler, D., Krebsbach, P. H., Polverini, P. J., and Mooney, D. J. (2003). Role of vascular endothelial growth factor in bone marrow stromal cell modulation of endothelial cells. *Tissue Eng.*, 9(1):95–103. [PubMed:12625958].

Kaigler, D., Krebsbach, P. H., West, E. R., Horger, K., Huang, Y. C., and Mooney, D. J. (2005). Endothelial cell modulation of bone marrow stromal cell osteogenic potential. *FASEB J.*, 19(6):665–667. [PubMed:15677693].

Kamer, A. R., El-Ghorab, N., Marzec, N., Margarone, J. E., and Dziak, R. (2006). Nicotine induced proliferation and cytokine release in osteoblastic cells. *Int. J. Mol. Med.*, 17(1):121–127. [PubMed:16328020].

Kazachkov, M. Y., Hu, P. C., Carson, J. L., Murphy, P. C., Henderson, F. W., and Noah, T. L. (2002). Release of cytokines by human nasal epithelial cells and peripheral blood mononuclear cells infected with Mycoplasma pneumoniae. *Exp. Biol. Med. (Maywood)*, 227(5):330–335. [PubMed:11976403].

Khetani, S. R. and Bhatia, S. N. (2006). Engineering tissues for in vitro applications. *Curr. Opin. Biotechnol.*, 17(5):524–531. [PubMed:16978857].

Kim, K. J., Li, B., Winer, J., Armanini, M., Gillett, N., Phillips, H. S., and Ferrara, N. (1993). Inhibition of vascular endothelial growth factor-induced angiogenesis suppresses tumour growth in vivo. *Nature*, 362(6423):841–844. [PubMed:7683111].

Kim, Y. M., Hwang, S., Kim, Y. M., Pyun, B. J., Kim, T. Y., Lee, S. T., Gho, Y. S., and Kwon, Y. G. (2002). Endostatin blocks vascular endothelial growth factor-mediated signaling via direct interaction with KDR/Flk-1. *J. Biol. Chem.*, 277(31):27872–27879. [PubMed:12029087].

Kimoto, M., Shima, N., Yamaguchi, M., Amano, S., and Yamagami, S. (2012). Role of hepatocyte growth factor in promoting the growth of human corneal endothelial cells stimulated by L-ascorbic acid 2-phosphate. *Invest. Ophthalmol. Vis. Sci.*, 53(12):7583–7589. [PubMed:23081981].

Kiran, M. S., Viji, R. I., Kumar, S. V., Prabhakaran, A. A., and Sudhakaran, P. R. (2011). Changes in expression of VE-cadherin and MMPs in endothelial cells: Implications for angiogenesis. *Vasc Cell*, 3(1):6. [PubMed:21349163].

Kirkpatrick, C. J., Fuchs, S., and Unger, R. E. (2011). Co-culture systems for vascularization–learning from nature. *Adv Drug Deliv Rev*, 63(4-5):291–9. [PubMed:21281686].

Kirkpatrick, C. J., Krump-Konvalinkova, V., Unger, R. E., Bittinger, F., Otto, M., and Peters, K. (2002). Tissue response and biomaterial integration: the efficacy of in vitro methods. *Biomol. Eng.*, 19(2-6):211–217. [PubMed:12202185].

Klein, S., Giancotti, F. G., Presta, M., Albelda, S. M., Buck, C. A., and Rifkin, D. B. (1993). Basic fibroblast growth factor modulates integrin expression in microvascular endothelial cells. *Mol. Biol. Cell*, 4(10):973–982. [PubMed:8298194].

Klinke, R., Kurtz, A., and Pape, H.-C. (2009). *Physiologie*. Thieme.

Knothe Tate, M. L., Adamson, J. R., Tami, A. E., and Bauer, T. W. (2004). The osteocyte. *The international journal of biochemistry and cell biology*, 36(1):1–8. [PubMed:14592527].

Kobayashi, H., Yoshida, R., Kanada, Y., Fukuda, Y., Yagyu, T., Inagaki, K., Kondo, T., Kurita, N., Yamada, Y., Sado, T., Kitanaka, T., Suzuki, M., Kanayama, N., and Terao, T. (2005). A soybean Kunitz trypsin inhibitor reduces tumor necrosis factor-alpha production in ultraviolet-exposed primary human keratinocytes. *Exp. Dermatol.*, 14(10):765–774. [PubMed:16176285].

Koch, C. M. and Wagner, W. (2011). Epigenetic-aging-signature to determine age in different tissues. *Aging (Albany NY)*, 3(10):1018–1027. [PubMed:22067257].

Kolek, O. I., Hines, E. R., Jones, M. D., LeSueur, L. K., Lipko, M. A., Kiela, P. R., Collins, J. F., Haussler, M. R., and Ghishan, F. K. (2005). 1alpha,25-Dihydroxyvitamin D3 upregulates FGF23 gene expression in bone: the final link in a renal-gastrointestinal-skeletal axis that controls phosphate transport. *Am. J. Physiol. Gastrointest. Liver Physiol.*, 289(6):G1036–1042. [PubMed:16020653].

Krump-Konvalinkova, V., Bittinger, F., Unger, R. E., Peters, K., Lehr, H. A., and Kirkpatrick, C. J. (2001). Generation of human pulmonary microvascular endothelial cell lines. *Lab. Invest.*, 81(12):1717–1727. [PubMed:11742042].

Kuhn, M. C., Willenberg, H. S., Schott, M., Papewalis, C., Stumpf, U., Flohe, S., Scherbaum, W. A., and Schinner, S. (2012). Adipocyte-secreted factors increase osteoblast proliferation and the OPG/RANKL ratio to influence osteoclast formation. *Mol. Cell. Endocrinol.*, 349(2):180–188. [PubMed:22040599].

Kwok, K., Yeung, K., and Cheung, N. (2007). Adsorption kinetics of bovine serum albumin on fused silica: Population heterogeneities revealed by single-molecule fluorescence microscopy. *Langmuir*, 23(4):1948–1952. [PubMed:17279679].

Laemmli, U. K. (1970). Cleavage of structural proteins during the assembly of the head of bacteriophage T4. *Nature*, 227:680–685. [PubMed:5432063].

Lahav, M., Levite, M., Bassani, L., Lang, A., Fidder, H., Tal, R., Bar-Meir, S., Mayer, L., and Chowers, Y. (2002). Lidocaine inhibits secretion of IL-8 and IL-1beta and stimulates secretion of IL-1 receptor antagonist by epithelial cells. *Clin. Exp. Immunol.*, 127(2):226–233. [PubMed:11876744].

Lamour, V., Detry, C., Sanchez, C., Henrotin, Y., Castronovo, V., and Bellahcene, A. (2007). Runx2- and histone deacetylase 3-mediated repression is relieved in differentiating human osteoblast cells to allow high bone sialoprotein expression. *J. Biol. Chem.*, 282(50):36240–36249. [PubMed:17956871].

Landi, S., Moreno, V., Gioia-Patricola, L., Guino, E., Navarro, M., de Oca, J., Capella, G., and Canzian, F. (2003). Association of common polymorphisms in inflammatory genes interleukin (IL)6, IL8, tumor necrosis factor alpha, NFKB1, and peroxisome proliferator-activated receptor gamma with colorectal cancer. *Cancer Res.*, 63(13):3560–3566. [PubMed:12839942].

Laurencin, C. T., Ambrosio, A. M., Borden, M. D., and Cooper, J. A. (1999). Tissue engineering: orthopedic applications. *Annu Rev Biomed Eng*, 1:19–46. [PubMed:11701481].

LeGeros, R. Z. (2002). Properties of osteoconductive biomaterials: calcium phosphates. *Clin. Orthop. Relat. Res.*, (395):81–98. [PubMed:11937868].

Leung, D. W., Cachianes, G., Kuang, W. J., Goeddel, D. V., and Ferrara, N. (1989). Vascular endothelial growth factor is a secreted angiogenic mitogen. *Science*, 246(4935):1306–9. [PubMed:2479986].

Li, M., Zhang, Y., Feurino, L. W., Wang, H., Fisher, W. E., Brunicardi, F. C., Chen, C., and Yao, Q. (2008). Interleukin-8 increases vascular endothelial growth factor and neuropilin expression and stimulates ERK activation in human pancreatic cancer. *Cancer Sci.*, 99(4):733–737. [PubMed:18307536].

Lin, D., Feng, J., and Chen, W. (2008). Bcl-2 and caspase-8 related anoikis resistance in human osteosarcoma mg-63 cells. *Cell Biol Int*, 32(10):1199–206. [PubMed:18675369].

Liu, F., Malaval, L., and Aubin, J. E. (1997). The mature osteoblast phenotype is characterized by extensive plasticity. *Exp Cell Res*, 232(1):97–105. [PubMed:9141626].

Liu, Y., Chan, J. K., and Teoh, S. H. (2012). Review of vascularised bone tissue-engineering strategies with a focus on co-culture systems. *J Tissue Eng Regen Med*. [PubMed:23166000].

Lockwood, C. J., Arcuri, F., Toti, P., Felice, C. D., Krikun, G., Guller, S., Buchwalder, L. F., and Schatz, F. (2006). Tumor necrosis factor-alpha and interleukin-1beta regulate interleukin-8 expression in third trimester decidual cells: implications for the genesis of chorioamnionitis. *Am. J. Pathol.*, 169(4):1294–1302. [PubMed:17003486].

Lottspeich, F., Engels, J., and Zettlmeier, L. (2008). *Bioanalytik*. Spektrum, Akad. Verl., 2. edition edition.

Lovett, M., Lee, K., Edwards, A., and Kaplan, D. L. (2009). Vascularization strategies for tissue engineering. *Tissue Eng Part B Rev*, 15(3):353–370. [PubMed:19496677].

Lu, W., Pan, K., Zhang, L., Lin, D., Miao, X., and You, W. (2005). Genetic polymorphisms of interleukin (IL)-1B, IL-1RN, IL-8, IL-10 and tumor necrosis factor alpha and risk of gastric cancer in a Chinese population. *Carcinogenesis*, 26(3):631–636. [PubMed:15579481].

Luecke, H. F. and Yamamoto, K. R. (2005). The glucocorticoid receptor blocks P-TEFb recruitment by NFkappaB to effect promoter-specific transcriptional repression. *Genes Dev.*, 19(9):1116–1127. [PubMed:15879558].

Ma, J., van den Beucken, J. J., Yang, F., Both, S. K., Cui, F. Z., Pan, J., and Jansen, J. A. (2011). Coculture of osteoblasts and endothelial cells: optimization of culture medium and cell ratio. *Tissue Eng Part C Methods*, 17(3):349–57. [PubMed:20932081].

Mackie, E. J., Abraham, L. A., Taylor, S. L., Tucker, R. P., and Murphy, L. I. (1998). Regulation of tenascin-C expression in bone cells by transforming growth factor-beta. *Bone*, 22(4):301–307. [PubMed:9556128].

Malviya, A., Kuiper, J. H., Makwana, N., Laing, P., and Ashton, B. (2009). The effect of newer anti-rheumatic drugs on osteogenic cell proliferation: an in-vitro study. *J Orthop Surg Res*, 4:17. [PubMed:19470170].

Marcet, B., Horckmans, M., Libert, F., Hassid, S., Boeynaems, J. M., and Communi, D. (2007). Extracellular nucleotides regulate CCL20 release from human primary airway epithelial cells, monocytes and monocyte-derived dendritic cells. *J. Cell. Physiol.*, 211(3):716–727. [PubMed:17295217].

Martin, D., Galisteo, R., and Gutkind, J. S. (2009). CXCL8/IL8 stimulates vascular endothelial growth factor (VEGF) expression and the autocrine activation of VEGFR2 in endothelial cells by activating NFkappaB through the CBM (Carma3/Bcl10/Malt1) complex. *J. Biol. Chem.*, 284(10):6038–6042. [PubMed:19112107].

Martini, F., Nath, J. L., and Bartholomew, E. F. (2011). *Fundamentals of anatomy & physiology*. Benjamin Cummings, 9th edition.

Matheson, M. C., Ellis, J. A., Raven, J., Walters, E. H., and Abramson, M. J. (2006). Association of IL8, CXCR2 and TNF-alpha polymorphisms and airway disease. *J. Hum. Genet.*, 51(3):196–203. [PubMed:16429233].

Mattioli, B., Straface, E., Quaranta, M. G., Giordani, L., and Viora, M. (2005). Leptin promotes differentiation and survival of human dendritic cells and licenses them for Th1 priming. *J. Immunol.*, 174(11):6820–6828. [PubMed:15905523].

Meijer, G. J., de Bruijn, J. D., Koole, R., and van Blitterswijk, C. A. (2007). Cell-based bone tissue engineering. *PLoS Med*, 4(2):e9. [PubMed:17311467].

Meikle, S. T., Bianchi, G., Olivier, G., and Santin, M. (2013). Osteoconductive phosphoserine-modified poly(varepsilon-lysine) dendrons: synthesis, titanium oxide surface functionalization and response of osteoblast-like cell lines. *J R Soc Interface*, 10(79):20120765. [PubMed:23193106].

Metzger, W., Schimmelpfennig, L., Schwab, B., Sossong, D., Dorst, N., Bubel, M., Gorg, A., Putz, N., Wennemuth, G., Pohlemann, T., and Oberringer, M. (2013). Expansion and differentiation of human primary osteoblasts in two- and three-dimensional culture. *Biotech Histochem*, 88(2):86–102. [PubMed:23210615].

Meyer, U. and Wiesmann, H. (2006). *Bone and Cartilage Engineering*. Springer.

Montero, A., Okada, Y., Tomita, M., Ito, M., Tsurukami, H., Nakamura, T., Doetschman, T., Coffin, J. D., and Hurley, M. M. (2000). Disruption of the fibroblast growth factor-2 gene results in decreased bone mass and bone formation. *J. Clin. Invest.*, 105(8):1085–1093. [PubMed:10772653].

Morelli, C., Barbanti-Brodano, G., Ciannilli, A., Campioni, K., Boriani, S., and Tognon, M. (2007). Cell morphology, markers, spreading, and proliferation on orthopaedic biomaterials. an innovative cellular model for the "in vitro" study. *J Biomed Mater Res A*, 83(1):178–83. [PubMed:17390321].

Morike, M., Schulz, M., Nerlich, A., Koschnik, M., Teller, W. M., Vetter, U., and Brenner, R. E. (1995). Expression of osteoblastic markers in cultured human bone and fracture callus cells. *J Mol Med (Berl)*, 73(11):571–5. [PubMed:8751141].

Morohoshi, M., Fujisawa, K., Uchimura, I., and Numano, F. (1996). Glucose-dependent interleukin 6 and tumor necrosis factor production by human peripheral blood monocytes in vitro. *Diabetes*, 45(7):954–959. [PubMed:8666148].

Mundy, G. R., Boyce, B., Hughes, D., Wright, K., Bonewald, L., Dallas, S., Harris, S., Ghosh-Choudhury, N., Chen, D., and Dunstan, C. (1995). The effects of cytokines and growth factors on osteoblastic cells. *Bone*, 17(2 Suppl):71S–75S. [PubMed:8579902].

Nakamura, A., Dohi, Y., Akahane, M., Ohgushi, H., Nakajima, H., Funaoka, H., and Takakura, Y. (2009). Osteocalcin secretion as an early marker of in vitro osteogenic differentiation of rat mesenchymal stem cells. *Tissue Eng Part C Methods*, 15(2):169–180. [PubMed:19191495].

Neufeld, G., Cohen, T., Gengrinovitch, S., and Poltorak, Z. (1999). Vascular endothelial growth factor (VEGF) and its receptors. *FASEB J.*, 13(1):9–22. [PubMed:9872925].

Newberry, E. P., Boudreaux, J. M., and Towler, D. A. (1996). The rat osteocalcin fibroblast growth factor (FGF)-responsive element: an okadaic acid-sensitive, FGF-selective transcriptional response motif. *Mol. Endocrinol.*, 10(8):1029–1040. [PubMed:8843419].

Nieters, A., Brems, S., and Becker, N. (2001). Cross-sectional study on cytokine polymorphisms, cytokine production after T-cell stimulation and clinical parameters in a random sample of a German population. *Hum. Genet.*, 108(3):241–248. [PubMed:11354638].

Niforou, K. M., Anagnostopoulos, A. K., Vougas, K., Kittas, C., Gorgoulis, V. G., and Tsangaris, G. T. (2008). The proteome profile of the human osteosarcoma U2OS cell line. *Cancer Genomics Proteomics*, 5(1):63–78. [PubMed:18359981].

Nishishita, T. and Lin, P. C. (2004). Angiopoietin 1, PDGF-B, and TGF-beta gene regulation in endothelial cell and smooth muscle cell interaction. *J. Cell. Biochem.*, 91(3):584–593. [PubMed:14755687].

Nissen, R. M. and Yamamoto, K. R. (2000). The glucocorticoid receptor inhibits NFkappaB by interfering with serine-2 phosphorylation of the RNA polymerase II carboxy-terminal domain. *Genes Dev.*, 14(18):2314–2329. [PubMed:10995388].

Oltmanns, U., Chung, K. F., Walters, M., John, M., and Mitchell, J. A. (2005). Cigarette smoke induces IL-8, but inhibits eotaxin and RANTES release from airway smooth muscle. *Respir. Res.*, 6:74. [PubMed:16029496].

Pap, E., Pallinger, E., Pasztoi, M., and Falus, A. (2009). Highlights of a new type of intercellular communication: microvesicle-based information transfer. *Inflamm. Res.*, 58(1):1–8. [PubMed:19132498].

Parfitt, A. M. (1976). The actions of parathyroid hormone on bone: relation to bone remodeling and turnover, calcium homeostasis, and metabolic bone diseases. II. PTH and bone cells: bone turnover and plasma calcium regulation. *Metab. Clin. Exp.*, 25(8):909–955. [PubMed:181659].

Pautke, C., Schieker, M., Tischer, T., Kolk, A., Neth, P., Mutschler, W., and Milz, S. (2004). Characterization of osteosarcoma cell lines MG-63, Saos-2 and U-2 OS in comparison to human osteoblasts. *Anticancer Res.*, 24(6):3743–3748. [PubMed:15736406].

Pawlik, A., Domanski, L., Rozanski, J., Florczak, M., Wrzesniewska, J., Dutkiewicz, G., Dabrowska-Zamojcin, E., and Gawronska-Szklarz, B. (2005). The cytokine gene polymorphisms in patients with chronic kidney graft rejection. *Transpl. Immunol.*, 14(1):49–52. [PubMed:15814282].

Petito, R. B., Amadeu, T. P., Pascarelli, B. M., Jardim, M. R., Vital, R. T., Antunes, S. L., and Sarno, E. N. (2013). Transforming growth factor-Î²1 may be a key mediator of the fibrogenic properties of neural cells in leprosy. *J. Neuropathol. Exp. Neurol.*, 72(4):351–366. [PubMed:23481710].

Pfaffl, M. (2004). Real-time rt-pcr: Neue ansätze zur exakten mrna quantifizierung. *BIOspektrum*, 1(04):92–95.

Pignochino, Y., Grignani, G., Cavalloni, G., Motta, M., Tapparo, M., Bruno, S., Bottos, A., Gammaitoni, L., Migliardi, G., Camussi, G., Alberghini, M., Torchio, B., Ferrari, S., Bussolino, F., Fagioli, F., Picci, P., and Aglietta, M. (2009). Sorafenib blocks tumour growth, angiogenesis and metastatic potential in preclinical models of osteosarcoma through a mechanism potentially involving the inhibition of ERK1/2, MCL-1 and ezrin pathways. *Mol. Cancer*, 8:118. [PubMed:20003259].

Pober, J. S. and Sessa, W. C. (2007). Evolving functions of endothelial cells in inflammation. *Nat. Rev. Immunol.*, 7(10):803–815. [PubMed:17893694].

Porta, C., Paglino, C., Imarisio, I., Ganini, C., Sacchi, L., Quaglini, S., Giunta, V., and De Amici, M. (2013). Changes in circulating pro-angiogenic cytokines, other than VEGF, before progression to sunitinib therapy in advanced renal cell carcinoma patients. *Oncology*, 84(2):115–122. [PubMed:23154434].

Prie, D. and Friedlander, G. (2010). Reciprocal control of 1,25-dihydroxyvitamin D and FGF23 formation involving the FGF23/Klotho system. *Clin J Am Soc Nephrol*, 5(9):1717–1722. [PubMed:20798257].

Puchacz, E., Lian, J. B., Stein, G. S., Wozney, J., Huebner, K., and Croce, C. (1989). Chromosomal localization of the human osteocalcin gene. *Endocrinology*, 124(5):2648–2650. [PubMed:2785029].

Qin, J. Y., Zhang, L., Clift, K. L., Hulur, I., Xiang, A. P., Ren, B. Z., and Lahn, B. T. (2010). Systematic comparison of constitutive promoters and the doxycycline-inducible promoter. *PLoS ONE*, 5(5):e10611. [PubMed:20485554].

Qu, G. and von Schroeder, H. P. (2006). Role of osterix in endothelin-1-induced downregulation of vascular endothelial growth factor in osteoblastic cells. *Bone*, 38(1):21–29. [PubMed:16126465].

Radonic, A., Thulke, S., Mackay, I. M., Landt, O., Siegert, W., and Nitsche, A. (2004). Guideline to reference gene selection for quantitative real-time PCR. *Biochem. Biophys. Res. Commun.*, 313(4):856–862. [PubMed:14706621].

Ramakers, C., Ruijter, J. M., Deprez, R. H., and Moorman, A. F. (2003). Assumption-free analysis of quantitative real-time polymerase chain reaction (PCR) data. *Neurosci. Lett.*, 339(1):62–66. [PubMed:12618301].

Ratcliffe, J. F. (1981). The arterial anatomy of the developing human dorsal and lumbar vertebral body. A microarteriographic study. *J. Anat.*, 133(Pt 4):625–638. [PubMed:7333964].

Rehn, M., Veikkola, T., Kukk-Valdre, E., Nakamura, H., Ilmonen, M., Lombardo, C., Pihlajaniemi, T., Alitalo, K., and Vuori, K. (2001). Interaction of endostatin with integrins implicated in angiogenesis. *Proc. Natl. Acad. Sci. U.S.A.*, 98(3):1024–1029. [PubMed:11158588].

Reilly, D. T. and Burstein, A. H. (1975). The elastic and ultimate properties of compact bone tissue. *J Biomech*, 8(6):393–405. [PubMed:1206042].

Reyes-Botella, C., Vallecillo-Capilla, M. F., and Ruiz, C. (2002). Effect of different growth factors on human cultured osteoblast-like cells. *Cell. Physiol. Biochem.*, 12(5-6):353–358. [PubMed:12438771].

Ricci-Vitiani, L., Pallini, R., Biffoni, M., Todaro, M., Invernici, G., Cenci, T., Maira, G., Parati, E. A., Stassi, G., Larocca, L. M., and De Maria, R. (2010). Tumour vascularization via endothelial differentiation of glioblastoma stem-like cells. *Nature*, 468(7325):824–8. [PubMed:21102434].

Richard, L., Velasco, P., and Detmar, M. (1998). A simple immunomagnetic protocol for the selective isolation and long-term culture of human dermal microvascular endothelial cells. *Exp. Cell Res.*, 240(1):1–6. [PubMed:9570915].

Risau, W. (1997). Mechanisms of angiogenesis. *Nature*, 386(6626):671–674. [PubMed:9109485].

Risau, W. and Flamme, I. (1995). Vasculogenesis. *Annu. Rev. Cell Dev. Biol.*, 11:73–91. [PubMed:8689573].

Rivron, N. C., Liu, J. J., Rouwkema, J., de Boer, J., and van Blitterswijk, C. A. (2008). Engineering vascularised tissues in vitro. *Eur Cell Mater*, 15:27–40.

Robey, P. G. (1995). Collagenase-treated trabecular bone fragments: a reproducible source of cells in the osteoblastic lineage. *Calcif. Tissue Int.*, 56 Suppl 1:S11–12. [PubMed:7719973].

Robey, P. G., Fedarko, N. S., Hefferan, T. E., Bianco, P., Vetter, U. K., Grzesik, W., Friedenstein, A., Van der Pluijm, G., Mintz, K. P., and Young, M. F. (1993). Structure and molecular regulation of bone matrix proteins. *J. Bone Miner. Res.*, 8 Suppl 2:S483–487. [PubMed:8122516].

Rochet, N., Dubousset, J., Mazeau, C., Zanghellini, E., Farges, M. F., de Novion, H. S., Chompret, A., Delpech, B., Cattan, N., Frenay, M., and Gioanni, J. (1999). Establishment, characterisation and partial cytokine expression profile of a new human osteosarcoma cell line (CAL 72). *Int. J. Cancer*, 82(2):282–285. [PubMed:10389764].

Rodan, S. B., Imai, Y., Thiede, M. A., Wesolowski, G., Thompson, D., Bar-Shavit, Z., Shull, S., Mann, K., and Rodan, G. A. (1987). Characterization of a human osteosarcoma cell line (saos-2) with osteoblastic properties. *Cancer Res*, 47(18):4961–6. [PubMed:3040234].

Ross, O. A., O'Neill, C., Rea, I. M., Lynch, T., Gosal, D., Wallace, A., Curran, M. D., Middleton, D., and Gibson, J. M. (2004). Functional promoter region polymorphism of the proinflammatory chemokine IL-8 gene associates with Parkinson's disease in the Irish. *Hum. Immunol.*, 65(4):340–346. [PubMed:15120188].

Rouwkema, J., de Boer, J., and Van Blitterswijk, C. A. (2006). Endothelial cells assemble into a 3-dimensional prevascular network in a bone tissue engineering construct. *Tissue Eng*, 12(9):2685–93. [PubMed:16995802].

Rudolf, M. and Kuhlisch, W. (2008). *Biostatistik: Eine Einfuehrung fuer Biowissenschaftler*. Cambridge University Press.

Rueger, J. M., Linhart, W., and Sommerfeldt, D. (1998). [Biologic reactions to calcium phosphate ceramic implantations. Results of animal experiments]. *Orthopade*, 27(2):89–95. [PubMed:9530665].

Ruoslahti, E. and Rajotte, D. (2000). An address system in the vasculature of normal tissues and tumors. *Annu. Rev. Immunol.*, 18:813–827. [PubMed:10837076].

SABiosciences (2013). Gncpro.

Sansone, P., Storci, G., Tavolari, S., Guarnieri, T., Giovannini, C., Taffurelli, M., Ceccarelli, C., Santini, D., Paterini, P., Marcu, K. B., Chieco, P., and Bonafe, M. (2007). IL-6 triggers malignant features in mammospheres from human ductal breast carcinoma and normal mammary gland. *J. Clin. Invest.*, 117(12):3988–4002. [PubMed:18060036].

Santos, M. I., Tuzlakoglu, K., Fuchs, S., Gomes, M. E., Peters, K., Unger, R. E., Piskin, E., Reis, R. L., and Kirkpatrick, C. J. (2008). Endothelial cell colonization and angiogenic potential of combined nano- and micro-fibrous scaffolds for bone tissue engineering. *Biomaterials*, 29(32):4306–4313. [PubMed:18706689].

Santos, M. I., Unger, R. E., Sousa, R. A., Reis, R. L., and Kirkpatrick, C. J. (2009). Crosstalk between osteoblasts and endothelial cells co-cultured on a polycaprolactone-starch scaffold and the in vitro development of vascularization. *Biomaterials*, 30(26):4407–4415. [PubMed:19487022].

Satoh, N., Yamada, Y., Kinugasa, Y., and Takakura, N. (2008). Angiopoietin-1 alters tumor growth by stabilizing blood vessels or by promoting angiogenesis. *Cancer Sci.*, 99(12):2373–2379. [PubMed:19018775].

Scapoli, C., Mamolini, E., and Trombelli, L. (2007). Role of IL-6, TNF-A and LT-A variants in the modulation of the clinical expression of plaque-induced gingivitis. *J. Clin. Periodontol.*, 34(12):1031–1038. [PubMed:17953695].

Schieker, M., Seitz, S., Gulkan, H., Nentwich, M., Horvath, G., Regauer, M., Milz, S., and Mutschler, W. (2004). [Tissue engineering of bone. Integration and migration of human mesenchymal stem cells in colonized contructs in a murine model]. *Orthopade*, 33(12):1354–1360. [PubMed:15551050].

Schlaeppi, J. M., Gutzwiller, S., Finkenzeller, G., and Fournier, B. (1997). 1,25-Dihydroxyvitamin D3 induces the expression of vascular endothelial growth factor in osteoblastic cells. *Endocr. Res.*, 23(3):213–229. [PubMed:9378108].

Schroeder, T. M., Kahler, R. A., Li, X., and Westendorf, J. J. (2004). Histone deacetylase 3 interacts with runx2 to repress the osteocalcin promoter and regulate osteoblast differentiation. *J. Biol. Chem.*, 279(40):41998–42007. [PubMed:15292260].

Seghezzi, G., Patel, S., Ren, C. J., Gualandris, A., Pintucci, G., Robbins, E. S., Shapiro, R. L., Galloway, A. C., Rifkin, D. B., and Mignatti, P. (1998). Fibroblast growth factor-2 (FGF-2) induces vascular endothelial growth factor (VEGF) expression in the endothelial cells of forming capillaries: an autocrine mechanism contributing to angiogenesis. *J. Cell Biol.*, 141(7):1659–1673. [PubMed:9647657].

Shevchenko, A., Tomas, H., Havlis, J., Olsen, J. V., and Mann, M. (2006). In-gel digestion for mass spectrometric characterization of proteins and proteomes. *Nat Protoc*, 1:2856–2860. [PubMed:17406544].

Siqueira, A. S., Carvalho, M. R., Monteiro, A. C., Freitas, V. M., Jaeger, R. G., and Pinheiro, J. J. (2010). Matrix metalloproteinases, TIMPs and growth factors regulating ameloblastoma behaviour. *Histopathology*, 57(1):128–137. [PubMed:20653784].

Smit, E. E., Sra, S. K., Grabowski, L. R., Ward, S. L., and Trocme, S. D. (2003). Modulation of IL-8 and RANTES release in human conjunctival epithelial cells: primary cells and cell line compared and contrasted. *Cornea*, 22(4):332–337. [PubMed:12792476].

Son, D. O., Satsu, H., and Shimizu, M. (2005). Histidine inhibits oxidative stress- and TNF-alpha-induced interleukin-8 secretion in intestinal epithelial cells. *FEBS Lett.*, 579(21):4671–4677. [PubMed:16107255].

Song, X., Liu, S., Qu, X., Hu, Y., Zhang, X., Wang, T., and Wei, F. (2011). BMP2 and VEGF promote angiogenesis but retard terminal differentiation of osteoblasts in bone regeneration by up-regulating Id1. *Acta Biochim. Biophys. Sin. (Shanghai)*, 43(10):796–804. [PubMed:21880603].

Stahl, A., Wenger, A., Weber, H., Stark, G. B., Augustin, H. G., and Finkenzeller, G. (2004). Bi-directional cell contact-dependent regulation of gene expression between endothelial cells and osteoblasts in a three-dimensional spheroidal coculture model. *Biochem. Biophys. Res. Commun.*, 322(2):684–692. [PubMed:15325284].

Stains, J. P. and Civitelli, R. (2005). Gap junctions in skeletal development and function. *Biochim. Biophys. Acta*, 1719(1-2):69–81. [PubMed:16359941].

Starr, C. and McMillan, B. (2011). *Human Biology*. Cengage Learning, 9th edition.

Staton, C. A., Reed, M. W., and Brown, N. J. (2009). A critical analysis of current in vitro and in vivo angiogenesis assays. *Int J Exp Pathol*, 90(3):195–221. [PubMed:19563606].

Stegmann, T. J. (1999). New approaches to coronary heart disease: induction of neovascularisation by growth factors. *BioDrugs*, 11(5):301–308. [PubMed:18031140].

Steinbrech, D. S., Mehrara, B. J., Saadeh, P. B., Greenwald, J. A., Spector, J. A., Gittes, G. K., and Longaker, M. T. (2000). VEGF expression in an osteoblast-like cell line is regulated by a hypoxia response mechanism. *Am. J. Physiol., Cell Physiol.*, 278(4):C853–860. [PubMed:10751333].

Storey, J. D. and Tibshirani, R. (2003). Statistical significance for genomewide studies. *Proc. Natl. Acad. Sci. U.S.A.*, 100(16):9440–9445. [PubMed:12883005].

Stuchbury, G. and Munch, G. (2010). Optimizing the generation of stable neuronal cell lines via pre-transfection restriction enzyme digestion of plasmid DNA. *Cytotechnology*, 62(3):189–194. [PubMed:20424915].

Sulpice, E., Ding, S., Muscatelli-Groux, B., Berge, M., Han, Z. C., Plouet, J., Tobelem, G., and Merkulova-Rainon, T. (2009). Cross-talk between the VEGF-A and HGF signalling pathways in endothelial cells. *Biol. Cell*, 101(9):525–539. [PubMed:19281453].

Sumpio, B. E., Riley, J. T., and Dardik, A. (2002). Cells in focus: endothelial cell. *Int. J. Biochem. Cell Biol.*, 34(12):1508–1512. [PubMed:12379270].

Sutherland, M. S., Rao, L. G., Muzaffar, S. A., Wylie, J. N., Wong, M. M., McBroom, R. J., and Murray, T. M. (1995). Age-dependent expression of osteoblastic phenotypic markers in normal human osteoblasts cultured long-term in the presence of dexamethasone. *Osteoporos Int*, 5(5):335–343. [PubMed:8800783].

Taichman, R., Reilly, M., Verma, R., Ehrenman, K., and Emerson, S. (2001). Hepatocyte growth factor is secreted by osteoblasts and cooperatively permits the survival of haematopoietic progenitors. *Br. J. Haematol.*, 112(2):438–448. [PubMed:11167845].

Takahashi, H., Numasaki, M., Lotze, M. T., and Sasaki, H. (2005). Interleukin-17 enhances bFGF-, HGF- and VEGF-induced growth of vascular endothelial cells. *Immunol. Lett.*, 98(2):189–193. [PubMed:15860217].

Takezawa, T. (2003). A strategy for the development of tissue engineering scaffolds that regulate cell behavior. *Biomaterials*, 24(13):2267–2275. [PubMed:12699663].

Tambur, A. R., Pamboukian, S., Costanzo, M. R., and Heroux, A. (2006). Genetic polymorphism in platelet-derived growth factor and vascular endothelial growth factor are significantly associated with cardiac allograft vasculopathy. *J. Heart Lung Transplant.*, 25(6):690–698. [PubMed:16730575].

Tammela, T., Petrova, T. V., and Alitalo, K. (2005). Molecular lymphangiogenesis: new players. *Trends in cell biology*, 15(8):434–41. [PubMed:16005628].

Tanaka, K., Waki, H., Ido, Y., Akita, S., Yoshida, Y., Yoshida, T., and Matsuo, T. (1988). Protein and polymer analyses up to m/z 100 000 by laser ionization time-of-flight mass spectrometry. *Rapid Communications in Mass Spectrometry*, 2(8):151–153.

Theodoropoulos, G., Papaconstantinou, I., Felekouras, E., Nikiteas, N., Karakitsos, P., Panoussopoulos, D., Lazaris, A. C. h., Patsouris, E., Bramis, J., and Gazouli, M. (2006). Relation between common polymorphisms in genes related to inflammatory response and colorectal cancer. *World J. Gastroenterol.*, 12(31):5037–5043. [PubMed:16937502].

Thiele, J. O., Lohrer, P., Schaaf, L., Feirer, M., Stummer, W., Losa, M., Lange, M., Tichomirowa, M., Arzt, E., Stalla, G. K., and Renner, U. (2003). Functional in vitro studies on the role and regulation of interleukin-6 in human somatotroph pituitary adenomas. *Eur. J. Endocrinol.*, 149(5):455–461. [PubMed:14585094].

Tremblay, P. L., Hudon, V., Berthod, F., Germain, L., and Auger, F. A. (2005). Inosculation of tissue-engineered capillaries with the host's vasculature in a reconstructed skin transplanted on mice. *Am J Transplant*, 5(5):1002–10. [PubMed:15816880].

Tsai, J. A., Rong, H., Torring, O., Matsushita, H., and Bucht, E. (2000). Interleukin-1beta upregulates PTHrP-mRNA expression and protein production and decreases TGF-beta in normal human osteoblast-like cells. *Calcif. Tissue Int.*, 66(5):363–369. [PubMed:10773106].

Tsaryk, R., Santin, M., Dohle, E., Unger, R. E., and Kirkpatrick, C. J. (2012). *Angiogenesis control in spine regeneration.* Biomaterials for spinal surgery. Woodhead Publishing.

Turner, C. H., Wang, T., and Burr, D. B. (2001). Shear strength and fatigue properties of human cortical bone determined from pure shear tests. *Calcif. Tissue Int.*, 69(6):373–378. [PubMed:11800235].

Tusher, V. G., Tibshirani, R., and Chu, G. (2001). Significance analysis of microarrays applied to the ionizing radiation response. *Proc. Natl. Acad. Sci. U.S.A.*, 98(9):5116–5121. [PubMed:11309499].

Ulbrich, C., Westphal, K., Baatout, S., Wehland, M., Bauer, J., Flick, B., Infanger, M., Kreutz, R., Vadrucci, S., Egli, M., Cogoli, A., Derradji, H., Pietsch, J., Paul, M., and Grimm, D. (2008). Effects of basic fibroblast growth factor on endothelial cells under conditions of simulated microgravity. *J. Cell. Biochem.*, 104(4):1324–1341. [PubMed:18253936].

Unger, R. E., Ghanaati, S., Orth, C., Sartoris, A., Barbeck, M., Halstenberg, S., Motta, A., Migliaresi, C., and Kirkpatrick, C. J. (2010). The rapid anastomosis between prevascularized networks on silk fibroin scaffolds generated in vitro with cocultures of human microvascular endothelial and osteoblast cells and the host vasculature. *Biomaterials*, 31(27):6959–6967. [PubMed:20619788].

Unger, R. E., Halstenberg, S., Sartoris, A., and Kirkpatrick, C. J. (2011). Human endothelial and osteoblast co-cultures on 3D biomaterials. *Methods Mol. Biol.*, 695:229–241. [PubMed:21042976].

Unger, R. E., Krump-Konvalinkova, V., Peters, K., and Kirkpatrick, C. J. (2002). In vitro expression of the endothelial phenotype: comparative study of primary isolated cells and cell lines, including the novel cell line HPMEC-ST1.6R. *Microvasc. Res.*, 64(3):384–397. [PubMed:12453433].

Unger, R. E., Peters, K., Wolf, M., Motta, A., Migliaresi, C., and Kirkpatrick, C. J. (2004). Endothelialization of a non-woven silk fibroin net for use in tissue engineering: growth and gene regulation of human endothelial cells. *Biomaterials*, 25(21):5137–46. [PubMed:15109837].

Unger, R. E., Sartoris, A., Peters, K., Motta, A., Migliaresi, C., Kunkel, M., Bulnheim, U., Rychly, J., and Kirkpatrick, C. J. (2007). Tissue-like self-assembly in cocultures of endothelial cells and osteoblasts and the formation of microcapillary-like structures on three-dimensional porous biomaterials. *Biomaterials*, 28(27):3965–3976. [PubMed:17582491].

Vailhe, B., Vittet, D., and Feige, J. J. (2001). In vitro models of vasculogenesis and angiogenesis. *Lab. Invest.*, 81(4):439–452. [PubMed:11304563].

Vandesompele, J., De Preter, K., Pattyn, F., Poppe, B., Van Roy, N., De Paepe, A., and Speleman, F. (2002). Accurate normalization of real-time quantitative RT-PCR data by geometric averaging of multiple internal control genes. *Genome Biol.*, 3(7):RESEARCH0034. [PubMed:12184808].

Viguet-Carrin, S., Garnero, P., and Delmas, P. D. (2006). The role of collagen in bone strength. *Osteoporos Int*, 17(3):319–336. [PubMed:16341622].

Villars, F., Bordenave, L., Bareille, R., and Amedee, J. (2000). Effect of human endothelial cells on human bone marrow stromal cell phenotype: role of VEGF? *J. Cell. Biochem.*, 79(4):672–685. [PubMed:10996857].

Villars, F., Guillotin, B., Amedee, T., Dutoya, S., Bordenave, L., Bareille, R., and Amedee, J. (2002). Effect of huvec on human osteoprogenitor cell differentiation needs heterotypic gap junction communication. *Am J Physiol Cell Physiol*, 282(4):C775–85. [PubMed:11880266].

Vohra, S., Hennessy, K. M., Sawyer, A. A., Zhuo, Y., and Bellis, S. L. (2008). Comparison of mesenchymal stem cell and osteosarcoma cell adhesion to hydroxyapatite. *J Mater Sci Mater Med*, 19(12):3567–74. [PubMed:18626747].

Walker, D. G. (1973). Osteopetrosis cured by temporary parabiosis. *Science*, 180(4088):875. [PubMed:4706681].

Walsh, C. (2006). *Posttranslational modification of proteins: expanding nature's inventory*. Roberts & Company.

Wang, R., Chadalavada, K., Wilshire, J., Kowalik, U., Hovinga, K. E., Geber, A., Fligelman, B., Leversha, M., Brennan, C., and Tabar, V. (2010). Glioblastoma stem-like cells give rise to tumour endothelium. *Nature*, 468(7325):829–33. [PubMed:21102433].

Wang, Y., Crisostomo, P. R., Wang, M., Markel, T. A., Novotny, N. M., and Meldrum, D. R. (2008). TGF-alpha increases human mesenchymal stem cell-secreted VEGF by MEK- and PI3-K- but not JNK- or ERK-dependent mechanisms. *Am. J. Physiol. Regul. Integr. Comp. Physiol.*, 295(4):R1115–1123. [PubMed:18685072].

Wei, L. H., Kuo, M. L., Chen, C. A., Chou, C. H., Lai, K. B., Lee, C. N., and Hsieh, C. Y. (2003). Interleukin-6 promotes cervical tumor growth by VEGF-dependent angiogenesis via a STAT3 pathway. *Oncogene*, 22(10):1517–1527. [PubMed:12629515].

Wei, Y. M., Li, X., Xiong, J., Abais, J. M., Xia, M., Boini, K. M., Zhang, Y., and Li, P. L. (2013). Attenuation by Statins of Membrane Raft-Redox Signaling in Coronary Arterial Endothelium. *J. Pharmacol. Exp. Ther.* [PubMed:23435541].

Widdermann, A. (2004). *Die Rolle von Parathormon und Kollagenasen im Knochenumbau*. PhD thesis, Orthopädische Universitätsklinik Würzburg.

Williams, M. A., Cave, C. M., Quaid, G., Robinson, C., Daly, T. J., Witt, D., Lentsch, A. B., and Solomkin, J. S. (2005). Interleukin 8 dimerization as a mechanism for regulation of neutrophil adherence-dependent oxidant production. *Shock*, 23(4):371–376. [PubMed:15803062].

Xie, H. and Gu, X. X. (2008). Moraxella catarrhalis lipooligosaccharide selectively upregulates ICAM-1 expression on human monocytes and stimulates adjacent naïve monocytes to produce TNF-alpha through cellular cross-talk. *Cell. Microbiol.*, 10(7):1453–1467. [PubMed:18363879].

Yamada, Y., Sawai, S., Misawa, S., Kanai, K., Shibuya, K., Mori, M., Moriya, J., Sogawa, K., Yamamoto, H., Beppu, M., Taniguchi, J., Nakaseko, C., Nomura, F., and Kuwabara, S. (2013). Multiple angiogenetic factors are upregulated in POEMS syndrome. *Ann. Hematol.*, 92(2):245–248. [PubMed:23053181].

Yamaguchi, S., Kazuki, Y., Nakayama, Y., Nanba, E., Oshimura, M., and Ohbayashi, T. (2011). A method for producing transgenic cells using a multi-integrase system on a human artificial chromosome vector. *PLoS ONE*, 6(2):e17267. [PubMed:21390305].

Yao, J. S., Zhai, W., Young, W. L., and Yang, G. Y. (2006). Interleukin-6 triggers human cerebral endothelial cells proliferation and migration: the role for KDR and MMP-9. *Biochem. Biophys. Res. Commun.*, 342(4):1396–1404. [PubMed:16516857].

Yaszemski, M. J., Payne, R. G., Hayes, W. C., Langer, R., and Mikos, A. G. (1996). Evolution of bone transplantation: molecular, cellular and tissue strategies to engineer human bone. *Biomaterials*, 17(2):175–185. [PubMed:8624394].

Yuan, J. S., Reed, A., Chen, F., and Stewart, Jr, C. N. (2006). Statistical analysis of real-time pcr data. *BMC Bioinformatics*, 7:85. [PubMed:16504059].

Zalewska, A., Glowacka, E., Wyczolkowska, J., Tchorzewski, H., Narbutt, J., and Sysa-Jedrzejowska, A. (2006). Interleukin 6 and 8 levels in plasma and fibroblast cultures in psoriasis. *Mediators Inflamm.*, 2006(1):81767. [PubMed:16864908].

Zambonin, G., Camerino, C., Greco, G., Patella, V., Moretti, B., and Grano, M. (2000). Hydroxyapatite coated with heaptocyte growth factor (HGF) stimulates human osteoblasts in vitro. *J Bone Joint Surg Br*, 82(3):457–460. [PubMed:10813189].

Zarkesh-Esfahani, H., Pockley, A. G., Wu, Z., Hellewell, P. G., Weetman, A. P., and Ross, R. J. (2004). Leptin indirectly activates human neutrophils via induction of TNF-alpha. *J. Immunol.*, 172(3):1809–1814. [PubMed:14734764].

Zhang, X. Y., Guckian, M., Nasiri, N., Lovell, P. A., Dalgleish, A. G., and Barton, D. P. (2002). Normal and SV40 transfected human peritoneal mesothelial cells produce IL-6 and IL-8: implication for gynaecological disease. *Clin. Exp. Immunol.*, 129(2):288–296. [PubMed:12165085].

Zisch, A. H., Lutolf, M. P., Ehrbar, M., Raeber, G. P., Rizzi, S. C., Davies, N., Schmokel, H., Bezuidenhout, D., Djonov, V., Zilla, P., and Hubbell, J. A. (2003). Cell-demanded release of VEGF from synthetic, biointeractive cell ingrowth matrices for vascularized tissue growth. *FASEB J.*, 17(15):2260–2262. [PubMed:14563693].

List of Figures

1.1. Structure and blood supply of a mature long bone 5
1.2. Types of bone cells 7
1.3. Functions of resting endothelial cells 9
2.4. Density gradient centrifugation of human peripheral blood 31
3.5. DNA quantification in pOB cultures 54
3.6. Quantification of osteogenic differentiation markers in pOB cultures 56
3.7. Quantification of osteogenic differentiation markers in osteosarcoma cell lines 59
3.8. ALP activity and collagen quantification in pOB cultures 60
3.9. Calcium and matrix mineralisation quantification in pOB cultures 61
3.10. WST-1 assay on osteosarcoma cell line cultures 62
3.11. Quantification of osteogenic differentiation markers in GFP-expressing and normal osteosarcoma cell lines 63
3.12. Quantification of growth factors, ALP and DNA in GFP-expressing and normal osteosarcoma cell lines 64
3.13. HDMEC monolayer 67
3.14. Endothelial cell types and ratio of D2-40 positive to D2-40 negative cells . 67
3.15. 2-D co-culture of HDMEC and osteoblasts 69
3.16. 2-D co-culture of HDMEC and GFP-expressing osteosarcoma cell lines . . 70
3.17. 2-D co-culture of umbilical endothelial cells with osteosarcoma cell lines . . 71
3.18. Co-cultures of HDMEC and osteoblasts in collagen gel 72
3.19. HDMEC and SaOS-2 GFP co-cultures with medium supernatants 73
3.20. HDMEC and SaOS-2 co-cultures with cell culture supernatants 74
3.21. HUVEC and SaOS-2 GFP co-cultures with medium supernatants 75
3.22. HDMEC in collagen gel with medium supernatants 76
3.23. HUVEC in collagen gel with medium supernatants 77
3.24. Comparative results of qPCR on osteosarcoma cell lines 78
3.25. Regulation network model in SaOS-2 79
3.26. 3-D culture of HDMEC with medium supernatants and bFGF 81
3.27. 3-D culture of HUVEC with medium supernatants and bFGF 82
3.28. Quantification of HGF and VEGF in medium supernatants 83
3.29. Quantification of HGF and endostatin in medium supernatants 84
3.30. 2D co-cultures of HDMEC fractions with pOB 85
3.31. Cloning of podoplanin into pEGFP-N1 86
3.32. VEGF quantification in osteoblasts and SaOS-2_PDPN 87
3.33. 2-D co-culture of HDMEC and SaOS-2_PDPN 87
3.34. 3-D co-culture of HDMEC and SaOS-2_PDPN 88
3.35. SDS-PAGE of cell culture supernatants 89
3.36. Quantification of the BSA standard sample 90
3.37. Representative MALDI-TOF spectra 90

4.38. Schematic overview of osteoblastic differentiation markers in human osteosarcoma cell lines . . . 97
4.39. Schematic overview of growth factors in human osteosarcoma cell lines . . 99
4.40. Changes in key markers between GFP-expressing and parental osteosarcoma cell lines . . . 101
A.41. FACS analysis of CD31 in different HDMEC donors . . . II
A.42. FACS analysis of CD31 and D2-40 in different HDMEC donors . . . II
A.43. FACS analysis of D2-40 in different HUVEC donors . . . II
A.44. FACS analysis of CD31 and D2-40 in ST1 cultures . . . III
A.45. FACS analysis of CD31 and D2-40 in HCMEC cultures . . . III
A.46. FACS analysis of CD31 and D2-40 in HPMEC cultures . . . III
A.47. FACS analysis of D2-40 in oral mucosa endothelial cell cultures . . . IV
A.48. FACS analysis of D2-40 in OEC donors . . . IV
A.49. HDMEC and SaOS-2 GFP co-cultures with cell culture supernatants . . . V
A.50. HDMEC and SaOS-2 co-cultures with cell culture supernatants . . . VI
A.51. HDMEC and SaOS-2 co-cultures with cell culture supernatants . . . VII
A.52. HDMEC and SaOS-2 co-cultures with cell culture supernatants . . . VIII
A.53. HUVEC and SaOS-2 GFP co-cultures with cell culture supernatants . . . IX
A.54. 3-D culture of umbilical artery endothelial cells with medium supernatants and bFGF . . . X
A.55. Mass spectroscopic analysis of cell culture supernatants . . . XIII

List of Tables

1.1. Primary functions of the skeletal system . . . 3
1.2. A selection of the most important angiogenic factors . . . 12
2.3. Instruments and microscopes . . . 21
2.4. Consumables . . . 22
2.5. Chemicals . . . 22
2.6. Buffers . . . 24
2.7. Solutions and cell culture media . . . 25
2.8. Enzymes . . . 26
2.9. Antibodies . . . 26
2.10. Oligonucleotides . . . 27
2.11. Kit systems . . . 27
2.12. Bacteria, primary cells and cell lines . . . 28
2.13. Software . . . 28
2.14. Cell culture media for different cell types . . . 33
2.15. SaOS-2 transfection . . . 35
2.16. Growth factor concentrations . . . 35
2.17. ELISA standard dilutions . . . 38
2.18. Antibodies for immunofluorescent staining . . . 40
2.19. FACS antibodies and isotypes . . . 43
2.20. SDS-PAGE buffer and gel composition for two gels . . . 44
2.21. Acrylamide gel staining solution . . . 44
2.22. Elution buffers for trypsin restriction of gel samples . . . 46
2.23. RT-PCR scheme and program . . . 49
2.24. Pipetting scheme and PCR program . . . 49
2.25. Blunt-end subcloning . . . 50
2.26. Restriction . . . 50
2.27. Ligation . . . 51
3.28. Significant p-value results of qPCR on osteosarcoma cell lines . . . 79
3.29. Pathway and regulation network references . . . 80
A.30. Significant p value results of qPCR on osteosarcoma cell lines . . . XI